MINISTRY OF PUBLIC WORKS

****

MINISTÈRE DES TRAVAUX PUBLICS

****

Ecole Nationale Supérieure des Travaux Publics

****

DEPARTEMENT DE GENIE CIVIL
DEPARTMENT OF CIVIL ENGINEERING

MINISTRY OF HIGHER EDUCATION

****

MINISTERE DE L'ENSEIGNEMENT SUPÉRIEUR

****

UNIVERSITÀ DEGLI STUDI DI PADOVA

****

DEPARTMENT OF CIVIL, ARCHITECTURAL AND ENVIRONMENTAL ENGINEERING

THE INFLUENCE OF THE SOIL INTERACTION FOR THE MEDIUM TALL CONCRETE STRUCTURE IN STATIC AND DYNAMIC DESIGN: CASE OF A SIX-STOREY BUILDING WITH TWO BASEMENTS IN YAOUNDE

A thesis submitted in partial fulfilment of the requirements for the degree

Of Master of Engineering (MEng) in Civil Engineering

Curriculum: **Structural Engineering**

Presented by:

FOTSA YEMFAK Armel

Student number: 16TP21194

Supervised by:

Pr. Carmelo MAJORANA

Co-supervised by:

Eng. Giuseppe CARDILLO

Dr.Eng Guillaume Hervé POH'SIE

Academic year: 2020/2021

DEDICATION

I dedicate this endeavor work to my lovely mother DJENTA Flolette Menozette

ACKNOWLEDGMENTS

This thesis is the fruit of the combined efforts of several individuals who contributed either directly or indirectly to its elaboration. It is therefore with gratitude that I address my sincere thanks to:

- The President of the jury**, Pr. NKENG George ELAMBO** for the honour of accepting to preside this jury;
- The Examiner of this jury, Pr**. TALLA Andre** for accepting to bring his criticisms and observations to ameliorate this work.
- My supervisors Prof. Eng. **Carmelo MAJORANA,** Eng. **Giuseppe CARDILLO** and Dr Eng. **Guillaume Hervé POH'SIE** for all the guidance, the advices and the patience provided to me during this work;
- Dr **BWEMBA Charles** for all his academic and administrative support during these five years spent at NASPW in this MEng program in partnership with University of Padova;
- Pr. **MBESSA Michel,** the Head of Department of Civil Engineering for tutoring and valuable advices;
- All **the teaching and administrative staff** of University of Padova and NASPW for their good quality of teaching and the motivation they developed in us to continue our studies;
- **All my classmates and my friends** of the 7th batch of Meng in The NASPW who were source of motivation and tenacity;
- To my parents**,** Mr **YEMFAK** and Mrs **DJENTA** for the trust they placed in me and all the efforts made in the accomplishment of this degree;
- To my family, especially to Mr **FOUEKENG Berlin** for its encouragement, devotion and financial support during all these years;
- To my brother and sister **Rosianine, Arolle, Erika, Gildas, Sonita, Manuella, Denis, Yvann, Kris-Nell, Joyce, Favour, Melvis.**
- To my friends **Armel, Evita, Leslie, Kelyane, Philippe, Rostand, Tedy, Igor**
- To engineer **SONNA DONKO Mael**
- Also, I really thank those who directly or indirectly contributed and supported me in the accomplishment of this work;

ABSTRACT

The main objective of this work was to show the influence of soil-structure interaction (SSI) in the static and dynamic design of mid-rise concrete structures. In order to achieve this objective, an evaluation of the behaviour of an elevated building resting on two different types of foundations, namely (i) the base embedment, which excludes SSI, and (ii) two rafts resting respectively on wet clay and an embankment of humus, sand and gravel, was carried out. A literature review was carried out to highlight the basic principles of soil-structure interaction, the methods of consideration and their effects on the static and dynamic requirements of mid-rise buildings. The methodology used started with the identification of the site and the collection of the geometric data of the building. The case study, which is a multi-use building of type R+Mezzanine+4 with two (02) basements that has been elevated to six floors, was then analysed and designed under static loads according to European standards. The underlying soil was modelled using the Winkler spring approach to describe soil flexibility. Then, the building was subjected to the Palermo earthquake, recorded in Italy using the SAP 2000 (Structural Analysis Program) version 22 software. The results were presented and compared in terms of settlement, solicitation in the structure, natural vibration period, lateral deformation, inter-storey displacement, and base shear for the different soil types. The results showed that as the stiffness of the foundation soil decreases, the effects of soil-structure interaction become more dominant and detrimental to the structure. The SSI leads to an increase in the solicitation in the structural elements except for the axial force in the column, which decreases. The increase in soil flexibility also leads to an increase in the period of natural vibration, lateral deformation, inter-storey drift, base shear in the superstructure and foundation deformation. The results lead to a criteria indicating that the consideration of SSI in the static and dynamic design of concrete structures is extremely important.

Key words: soil-structure interaction, displacement, settlement, inter-storey drift, solicitations.

RESUME

L'objectif principal de ce travail était de montrer l'impact de l'interaction sol-structure (ISS) dans le dimensionnement statique et dynamique des structures de moyenne hauteur en béton Pour atteindre cet objectif, une évaluation du comportement d'un bâtiment surélevé reposant sur deux différents types de fondation à savoir (i) l'encastre à la base qui exclut l'ISS (ii) deux radiers reposant respectivement sur l'argile humide et un remblai d'humus, sable et gravier, a été faite. Une revue de la littérature a été effectuée pour mettre en évidence les principes de base liés à l'interaction sol-structure, les méthodes de prise en compte de cette dernière et ses effets sur les exigences statiques et dynamique des bâtiments de moyenne hauteur. La méthodologie adoptée a consisté d'abord en une reconnaissance du site et la collecte de données géométriques du prototype de bâtiment. Ensuite, le cas d'étude, qui est un immeuble à multi-usage de type sous-sol (2) +R+Mezzanine+4 surélevé à 6 étages, a été analysé et conçu sous des charges statiques selon les normes européennes. Le sol sous-jacent a été modélisé en utilisant l'approche des ressorts de Winkler pour décrire la flexibilité du sol. Ensuite, le bâtiment a été soumis au tremblement de terre de Palerme enregistré en Italie en utilisant le logiciel SAP 2000 (Structural Analysis Program) version 22. Les résultats ont été présentés et comparés en termes de tassement, sollicitation, période de vibration propre, de déformation latérale, de déplacement inter-étage, du cisaillement de base pour les différents types de sol. Les résultats ont montré que lorsque la rigidité du sol de fondation diminue, les effets de l'interaction sol-structure deviennent plus dominants et nuisibles pour la structure. L'ISS conduit à une augmentation des sollicitations dans les éléments structuraux exception faite pour l'effort axial dans le poteau qui diminue. L'augmentation de la flexibilité du sol induit aussi une augmentation de la période de vibration propre, de la déformation latérale, de la dérive inter-étage, du cisaillement de base dans la superstructure et les déformations en fondation. Les résultats ont conduit à un critère indiquant que la prise en compte de l'ISS dans la conception statique et dynamique des structures en béton est très importante

Mot clés : interaction sol structure, déplacement, tassement, dérive inter-étage, sollicitations

SUMMARY

LIST OF ABREVIATIONS AND SYMBOLS

EC	Eurocode
RC	Reinforced Concrete
SAP	Structural Analysis Program
SLS	Serviceability Limit State
SSI	Soil-Structure-Interaction
ULS	Ultimate Limit State
A	Area of the cross section (mm^2)
A_c	Area of the concrete cross section (mm^2)
A_{min}	Minimum section area (mm^2)
A_{net}	Net area of the cross section (mm^2)
A_s	Area of the steel reinforcement section (mm^2)
A_{sw}	Cross sectional area of the shear reinforcement (mm^2)
B	Foundation half width (mm)
C	Modulus of subgrade reaction of the soil (KN/m^3)
Cu	Undrained shear strength (KN)
C_{min}	Minimum concerte cover (mm)
$C_{min,b}$	Minimum cover due to bond requirement (mm)
$C_{min,dur}$	Minimum cover due to environmental conditions (mm)
Cs	Ordinate obtained from the design spectrum at period T
D	Embedment depth (mm)
$F_{Ed,Sup}$	Design support reaction (kN)

F_b	Shear force (kN)
G	Shear modulus (kN)
G_{1k}	Structural load of the building (kN/m^2)
G_{2k}	Non-structural load apply on the building (kN/m^2)
L	Foundation half length (m)
N_c	Bearing capacity factor (Mpa)
N_q	Bearing capacity factor (Mpa)
M_{sd}^{+}	Positive moment at mid-span in hyperstatic condition (kN.m)
M_{sd}^{-}	Negative moment at support in hyperstatic condition (kN.m)
M_{Ed}	Bending moment at support (kN.m)
M_{Rd}	Resisting moment (kN.m)
M_{Sd}	Soliciting bending moment (kN.m)
T	Period of the structure with fixed base (s)
$\tilde{T}$	Period of the structure with flexible base (s)
T_B	Lower limit of the period of the constant spectral acceleration branch (s)
T_C	Upper limit of the period of the constant spectral acceleration branch (s)
T_D	Value defining the beginning the constant displacement response range (s) of the spectrum
T_x	Fictitious period along x (s)
T_{yy}	Fictitious period along y (s)
V_{app}	Apparent velocity (m/s)
V_s	Shear velocity (m/s)
W	Weight of the structure (KN/m^3)
a_g	Design ground acceleration
a_i	Shifting distance (mm)

a_0^k	Dimensionless frequency
b	Width of the element (mm)
b_t	Mean width of the tension zone (mm)
b_w	Smallest width of the cross section in the tensile area (mm^2)
c	Concrete cover (mm)
d	Effective height of the section (mm)
d_r	Design inter-storey drift (mm)
e_x	Eccentricity along x axis (mm)
e_y	Eccentricity along x axis (mm)
fcd	Design resisting strength of the concrete (Mpa)
f_{ctm}	Tensile strength of the concrete (Mpa)
f_y	Design yielding strength of the steel (Mpa)
f_{yd}	Design yielding strength of the steel (Mpa)
f_{yk}	Characteristic yield strength (Mpa)
f_{ywd}	Design yield strength of the shear reinforcement (Mpa)
h	Structure height or the effective structure height (m)
h_i	Height of the level I (m)
h_{wi}	height of the wall i; (m)
k	Stiffness of the fixed base structure (kN/m)
k_x	Lateral stiffness of the foundation(kN/m)
k_{yy}	Rotational stiffness of the foundation(kN/m)

k_w	the factor reflecting the prevailing failure mode in structural systems with walls
k_z^i	Individual spring stiffness(kN/m)
l	is the span length of the beam (m)
l_o	Effective length of the element (m)
l_{wi}	is the length of the section of the wall i (m)
m	Mass of the structure (kg)
n_r	Number of surfaces in contact
n_s	Exponent that is equal to 2 for linear viscous damping and 3 otherwise
n_x	Exponent that is equal to 2 for linear viscous damping and 3 otherwise
n_{yy}	Exponent that is equal to 2 for linear viscous damping and 3 otherwise
q	Behavior factor
q_0	Basic value of the behavior factor
q_a	Allowable bearing pressure (Mpa)
$s_{l,max}$	Maximum longitudinal spacing (mm)
$s_{t,max}$	Maximum transversal spacing (mm)
$S_d(T_1)$	Design spectral accélération (m/s^2)
$S_e(T_{is}, \xi_{is})$	Spectral acceleration corresponding to the isolated period on the elastic spectrum of the project (m/s^2)
$\Delta C_{dur\ add}$	Add reduction of minimum cover for use of additional protection (mm)
$\Delta C_{dur,st}$	Reduction of minimum cover for use of stainless steel (mm)
$\Delta C_{dur,\gamma}$	Additive safety element (mm)

$\emptyset_{l,min}$	Minimum diameter of the longitudinal bars (mm)
σ	Contact pressure (Mpa)
σ_{adm}	Admissible pressure on the soil (Mpa)
σ_{VL}	Vertical stress at the base of the pile dimensions (Mpa)
φ_{ef}	Effective creep ratio
γ	Specific weight (KN/m^3)
γ_c	Partial factor for concrete
γ_s	Partial safety factor for steel
$\Psi_{E,i}$	Combination coefficient for variable action
λ	Slenderness
λ_{lim}	Limit value of slenderness
ν	Poisson's ratio
ν_1	Reduction factor for concrete cracked on shear
θ	Angle of concrete compression struts to the beam axis
ρ_w	Shear reinforcement ratio
$\rho_{w,min}$	Minimum shear reinforcement ratio
σ_c	Stress in the concrete (Mpa)
σ_s	Stress in the reinforcement (Mpa)

LIST OF FIGURES

LIST OF TABLE

GENERAL INTRODUCTION

Due to increasing demography and a lack of available land, engineers are forced to build taller and taller structures in areas with poor geotechnical characteristics (very soft soils) and sometimes subject to dynamic actions of high magnitude, such as earthquakes, wind, etc. Thus, many structures that can be considered medium-sized structures have been built in areas that can be classified as risk zones.

In the past, these structures were designed with the hypothesis of a base embedment, Thus, neglecting the flexibility of the soil by considering it to be infinitely rigid. However, the catastrophic consequences of several recent earthquakes in different parts of the world have posed a serious problem for engineers in understanding the seismic behaviour of structures. As structures are founded on soils through which seismic loads are transmitted, it was therefore essential to know how the soil-structure system works. i.e., taking into account the effect of soil-structure interaction (SSI). Thus, Veletsos and Meek (1974) proposed formulas for determining the fundamental period (a very important parameter in a dynamic analysis) of a building-type structure by considering the flexibility of the foundation. In the same order of idea, numerical simulations by Jeremi (2004)have shown that soil-structure interaction can have beneficial or detrimental effects on the behaviour of structures depending on soil characteristics. Poh'sie* and al. (2021) have shown that SSI can change the magnitude of stresses in a structure. Hence, neglecting the flexibility of the soil can lead to poor design of the structure.

The objective of this work is to show the influence of soil interaction on the static and dynamic design of mid-rise concrete structures. To do this, the work will be divided into three main parts. The first one will be the literature review, which will detail the methods of analysis of the soil-structure interaction, the specificities and the structural systems of mid-rise buildings. The second part will present the methodology used to achieve the goal, and the third part will present the obtained results.

CHAPTER 1: LITERATURE REVIEW

Introduction

The solution of any mechanical problem requires a good knowledge of its boundary conditions. In order to understand this, we can imagine that a slender structure such as a beam embedded at one end behaves in a totally different way than a beam whose embedding is replaced by a kneecap with a spring. Its stiffness and natural frequencies are reduced, while its displacements can be amplified. The same reasoning can be applied to a building resting on any foundation. The knowledge of the foundation and the underlying soil is essential to determine the actual behaviour of the structure. At the same time, it can be shown that the presence of the structure also influences the behaviour of the soil, i.e., the behaviour it would have in a free field(Grange, 2008). Thus, there is an influence of both the soil on the structure and the structure on the soil. This is why we speak of interactions between the soil and the structure.

1.1. Soil-structure interaction

1.1.1. Definition

Soil-structure interaction is a phenomenon that refers to the interaction that occurs between the structure, its foundation and the soil on which it rests. Under dynamic loading, the soil and the superstructure vibrate simultaneously and interact with each other. The vibration of the superstructure leads forces on the foundation which are transmitted to the ground, changing its response. This phenomenon is a combination of two physical phenomena, the inertial interaction and the kinematic interaction(Uildings et al., 1999). The analysis of the soil-structure interaction is carried out by various methods including the direct method, the substructure method and the hybrid method.

1.1.2. Components of soil-structure interaction

a. Kinematic interaction

The kinematic interaction is caused by the fact that the foundations are much stiffer than the soil in which they are located. This relatively high stiffness of the foundation compared to the soil causes a deviation of the response recorded in the free field (soil without the foundation and the superstructure) to that applied to the foundation. Thus, the kinematic interaction results

only from the difference in stiffness between the soil and the foundation, which prevents the structure from following the movements imposed by the soil. To understand this phenomenon, it is possible to imagine that in the absence of the structure the maximum soil acceleration in the structure's envelope would have been greater in the free field (Murugananthan, 2018). In his studies, Housner (1955) concludes that another cause of this deviation is the filtration of wavelengths smaller than the size of the foundation.

b. Inertial interaction

The inertial interaction refers to the inclusion of the mass of the structure which will induce additional inertial forces and moments at the base of the structure and therefore in the soil, which will again modify the displacement field. The inertial forces obtained from an analysis with a fixed foundation differ from an analysis considering a flexible foundation supported by a system of springs and dampers. Thus, the flexible foundation modifies the response of the structure to seismic excitation in two ways. On the one hand, the vibration period of the structure is lengthened. On the other hand, the damping is increased.

These two effects, as shown in the following figure, result in increased displacements in the structure and damping of the response by plasticization of the soil beneath the foundation. As a limit is imposed on the displacements of a structure in a dynamic analysis, the latter can be critical depending on the characteristics of the soil.

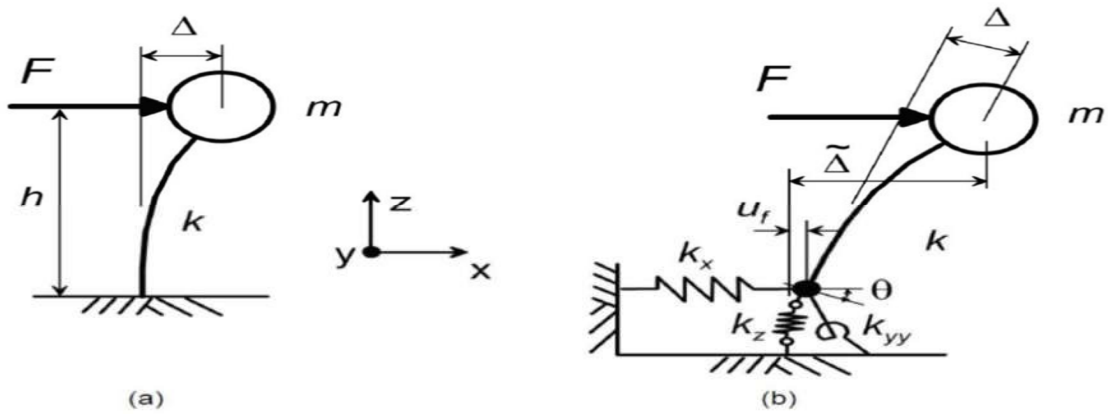

Figure 1.1. Illustration of the deflection caused to a structure with 1 DDL by a force applied to : (a) a fixed-base structure (b) a flexible-base structure supported on springs. (Murugananthan, 2018)

To appreciate the inertial interaction effect, a non-dimensional parameter has been proposed by (Bielak, 1974) as shown in expression 1.1.

$$\frac{h}{V_s T} \qquad 1.1$$

Where:

h: is the structure height

V_s: is the shear wave velocity

T: is the period of the structure

The term in relation 1.11 represents the structure-to-soil stiffness ratio and is the most important parameter controlling the significance of inertial interaction. Studies done by (Stewart et al., 1999) showed that the SSI effects are generally negligible for $h/(VsT) < 0.1$, which occurs in flexible structures (e.g., moment frame buildings) located on competent soil or rock. For typical building structures on soil and weathered rock sites, $h/(V_sT)$ is less than 0.1 for moment frame structures, and between approximately 0.1 and 0.5 for shear wall and braced frame structures.

1.1.3. Numerical methods in the soil structure interaction analysis

Different methods exist to take into account the issue, among which, we distinguish the global methods, which solve, as their name indicates, the global problem and those which are based on a decomposition of the system in subsystems. they are called method of the substructures

a. Direct approach

Also known as global methods, direct methods treat the soil-structure interaction problem as a whole in such a way that the responses of the soil and the structure are obtained simultaneously. Here, the soil and the structure are modelled by finite elements. This method has the advantage of being able to take into account in the numerical model, the heterogeneities of the soil and the structure, the geometrical singularities of the problem, and the behaviour laws well adapted to take into account the non-linearities in the soil or at the soil-foundation interface of the system.

However, the global numerically solved formulation method faces the problem of taking into account the wave propagation in a semi-infinite medium such as soil. Thus, it requires a more extensive discretisation of the soil mass supporting the foundation in order to minimise the numerical reflection on the boundary which again stresses the structure (Zhang, 2012). Indeed, a wave hitting the boundary of the foundation may numerically reflect and re-load the structure, whereas in reality, this wave goes to infinity and takes with it part of the energy of the structure

and the soil (Grange, 2008). Absorbing boundaries will therefore have to be added to the limits of the soil mass to take account of this damping.

The implementation of this method remains a generally numerically expensive operation, especially for three-dimensional problems, and requires the mastery of specialised computational software such as ABAQUS, ANSYS, and LS-DYNA or any other finite element software that can perform a non-linear analysis using a direct method while considering the soil-structure interaction.

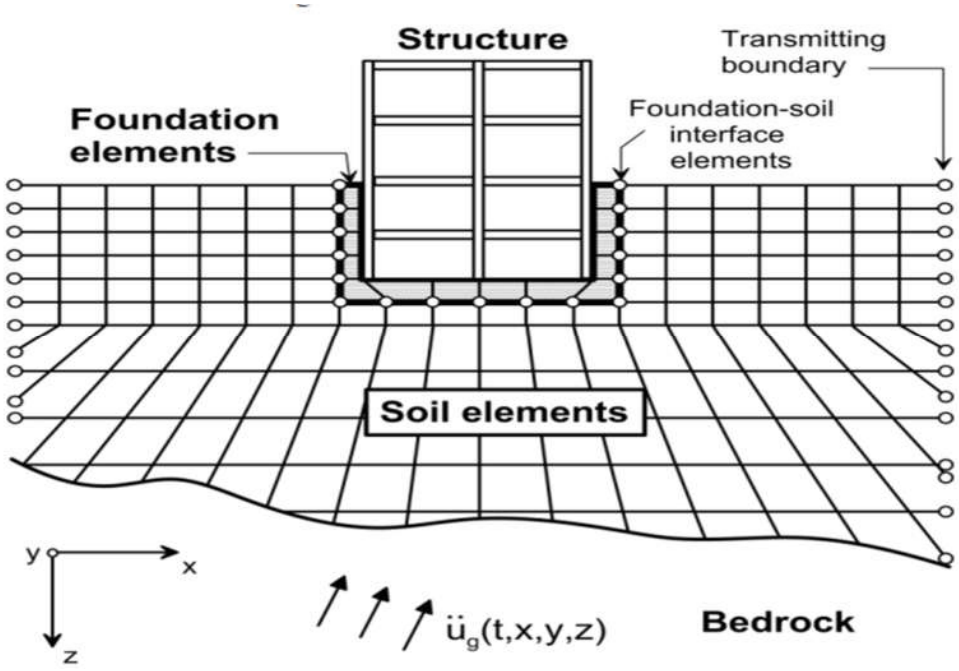

Figure 1.2. Schematic illustration of a direct analysis of soil-structure interaction(NIST,2012)

Although complex, this method is still the most realistic. However, it is essential to formulate easier and simpler methods.

b. Substructure approach

This method is based on the principle of decomposing problems into successive stages. It aims to decompose the problem into the sum of sub-problems that are simpler to solve than the overall problem, both from a modelling and a computational point of view. This approach is illustrated by the Figure 1.3

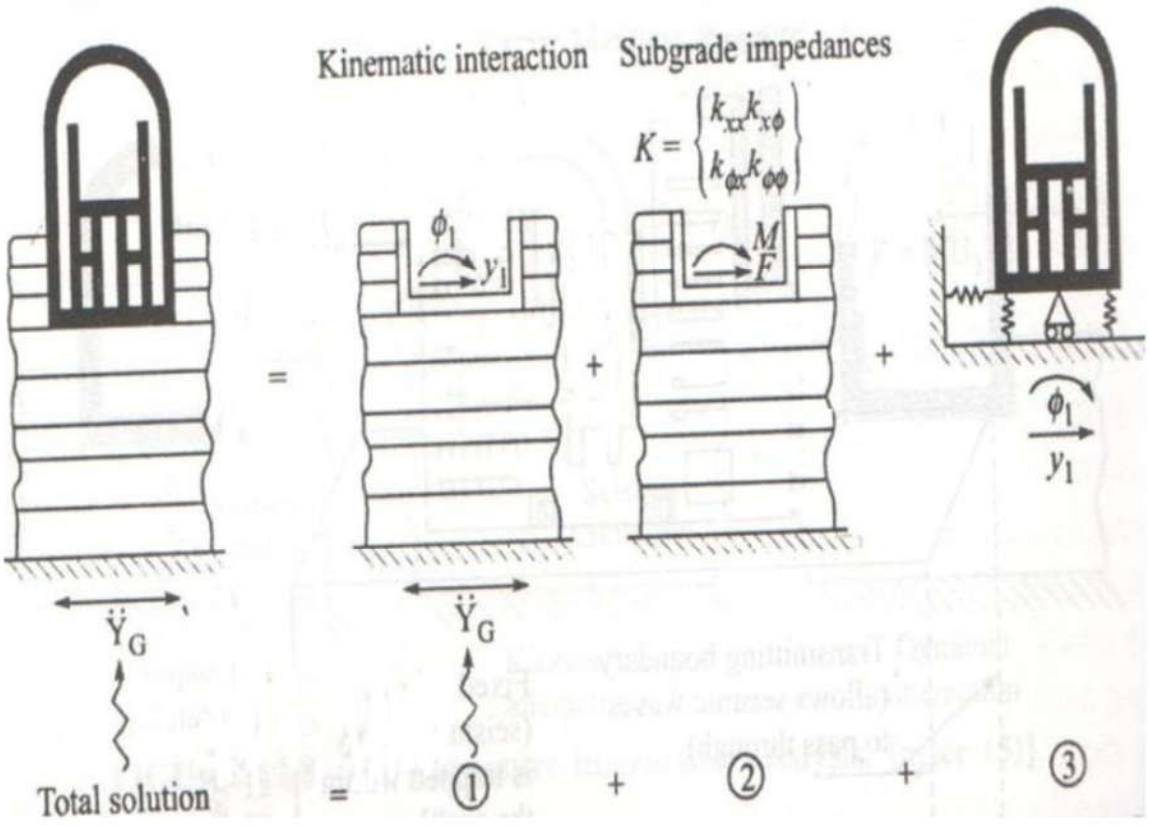

Figure 1.3. Soil-structure interaction analysis by substructure Methods.(Ghalimath et al., 2015)

- The first step is the determination of the movement of the sub-structure including the geotechnical profile and the massless foundation. Many methods exist to solve this step, notably the integral equation method (Aubry, 1986)or the boundary element method (Chebli et al., 2008).
- The second step is the determination of the foundation impedance matrix. Here, the dynamic impedances of the foundation are evaluated and assembled into the impedance matrix [K]. This matrix represents the dynamic response (in terms of forces) of the massless foundation, placed on the heavy soil mass and subjected to a harmonic type of loading of unit amplitude, characterised by its pulsation. Analytical results for all types of foundations are given in (Gazetas, 1991) and (Pecker, 1984)
- The last step consists of the calculation of the dynamic response of the structure linked to springs corresponding to the impedances of the foundation. This step is usually solved with the finite element method which solves the dynamic equation of a structure linked to the ground by a system of springs and dampers.

1.1.4. Physical representations of the interaction phenomenon

To represent soil-structure interaction problems (Figure1.4) methods such as the Modulus of Reaction Method and the Finite Element or Finite Difference Method, which are the most widely used, have been developed to take into account the relative deformations of the structure and the ground when designing. However, several researchers have tried to create a more convenient model to represent the physical behaviour of the soil in a more real way.

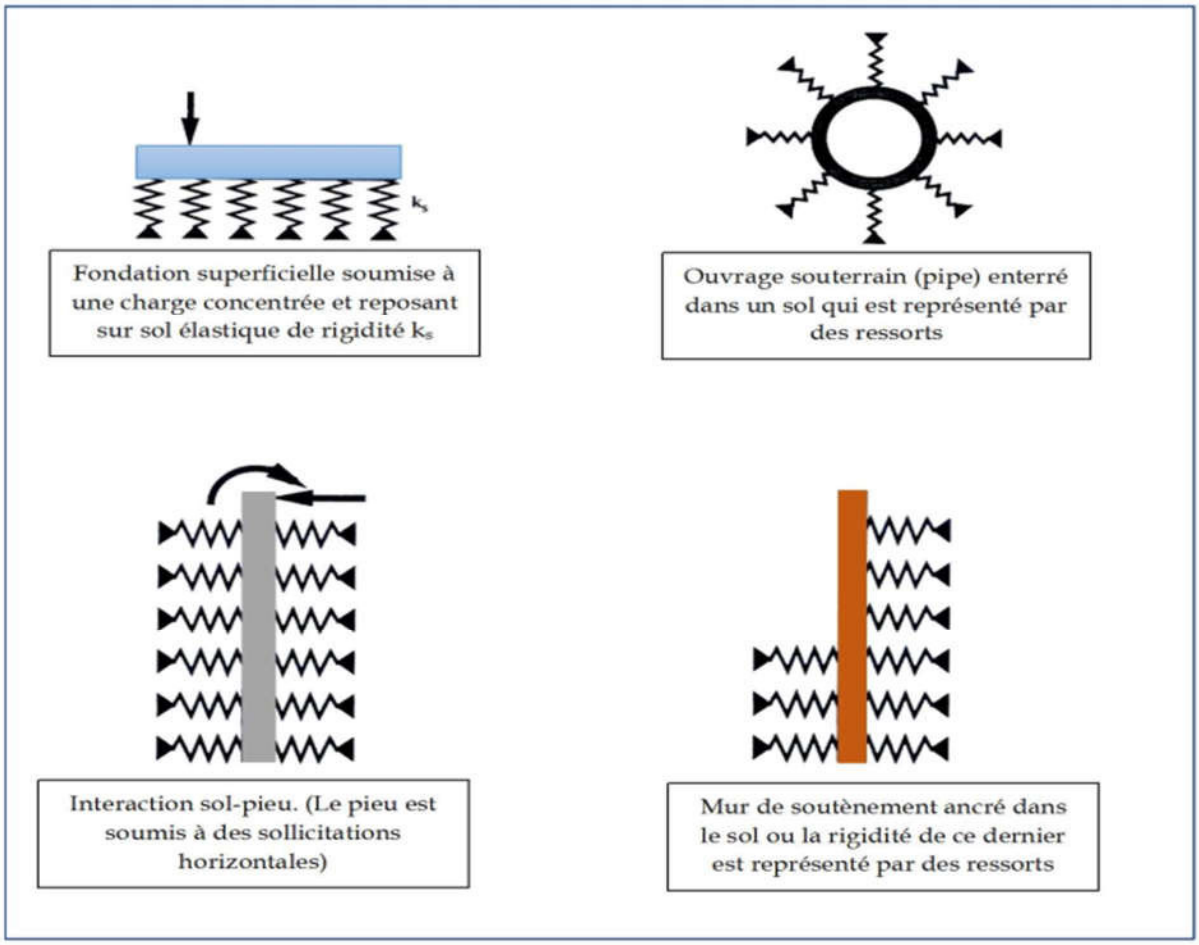

Figure 1.4. type of soil-structure interaction problems (**https://www.scirp.org**)

a. Winkler's model

Winkler's foundation model is the best known and most widely used model for the analysis of soil-structure interaction. Indeed, Winkler defined the soil as a stack of independent slices and each soil slice is modelled by a vertical spring on which the foundation is supported.

To calculate the stresses under a foundation, Winkler assumed that the soil reaction at each point under the foundation is proportional to the deflection of the foundation. In effect the

characteristic vertical deflection of the foundation is thus defined by the use of identical, independent, closely spaced, linearly elastic springs. The proportionality constant of these springs is known as the soil reaction coefficient. This model is defined by the following formula:

$$\boldsymbol{P(x) = k\,s.b.w(x)}$$

Where p(x) is the foundation reaction (pressure), ks is the soil reaction coefficient,

b is the width of the foundation and w(x) is the vertical displacement.

The model defined by Winkler was first used by Zimmerman, (1888) to calculate the behaviour of wooden sleepers supporting the rails and resting on ballast. The method was later used by other researchers (Rifaat, (1935); Bauman(1935); Delattre (2000)for the study of other types of foundations such as raft, retaining walls While, the insufficiency of the Winkler model has been proven by several researchers such as (Terzaghi, 1955) Indeed, the disadvantage of this model is that it does not take into account the interaction between the springs, which amounts to neglecting the vertical shear in the soil. As a result, a displacement discontinuity is created between the loaded and unloaded area under the foundation, but in reality, the surface shows no discontinuity. Therefore, researchers have proposed modifications to Winkler's model to make it more efficient and logical by introducing certain forms of interaction between the springs such as bending elements Hetenyi (1946)), shear layers (Pasternak 1954), membranes under constant tension (Filonenko-Borodich,1940). These models have another parameter that characterises the interaction between the springs.

The differential deflection equation, w(x) of an elastic beam resting on a Winkler foundation and subjected to a continuous transverse load q(x), can be written as follows:

$$\boldsymbol{Ec.I\frac{d^4W(x)}{dx^4} + K_s.b.W(x) = q(x)} \qquad 1.2$$

Where Ec and I are the Young's modulus and moment of inertia of the concrete respectively.

b. Hetenyi's model

In the model proposed by Hetenyi (1946), the interaction between the independent springs of Winkler's model is done through an elastic plate. He assumed that the beam or plate deforms only in bending and that the bending stiffness of a beam or plate characterises the interaction between the spring elements of the Winkler model. The relationship between the pressure p and the deflection of the foundation surface w for this model is defined by the following equation

$$\boldsymbol{P(x) = k_s.b.W(x) + D.\nabla^4 W(x)} \qquad 1.3$$

∇^4 is the Laplacian operator with $\nabla^4 = \frac{\partial^4}{\partial x^4} + \frac{\partial^4}{\partial y^4} + 2\frac{\partial^4}{\partial x^2 \partial y^2}$ and D is the bending stiffness of an elastic plate. $D = \frac{Eh^3}{12(1-\nu^2)}$

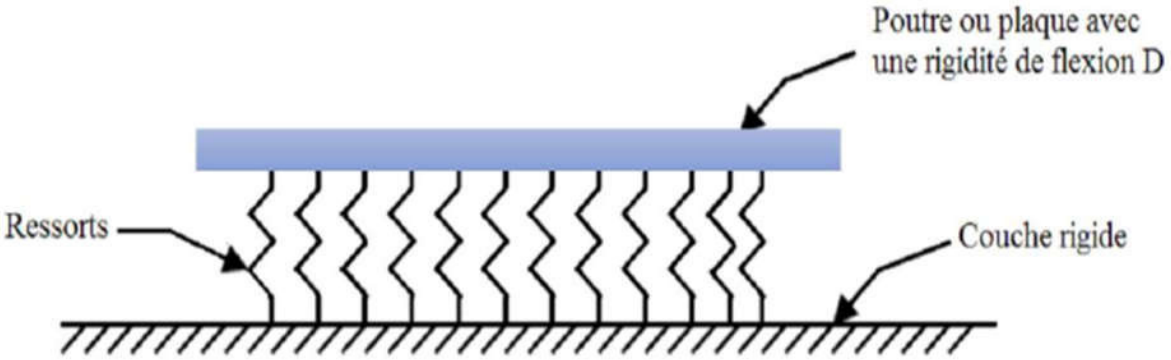

Figure 1.5. Hetenyi model (Hetenyi, 1946)

c. Filonenko-borodich model

This foundation model includes in the Winkler model a thin elastic membrane under constant tension (Figure 1.6). This membrane takes into account the interaction between adjacent spring elements. The relationship between the surface stress field p and the corresponding deflection w is defined for a rectangular or circular foundation by the following expression

$$\boldsymbol{P(x) = K_s.b.w(x) + T.\nabla^2 w(x)} \qquad 1.4$$

And for a spinning sole

$$\boldsymbol{P(X) = K_s.b.W(x) - T\frac{d^2W(x)}{dx^2}} \qquad 1.5$$

∇^2 is the Laplacian operator with $\nabla^2 = \frac{\partial^2}{\partial x^2} + \frac{\partial^2}{\partial y^2}$ and T is the tension or tensile force which is considered to be constant.

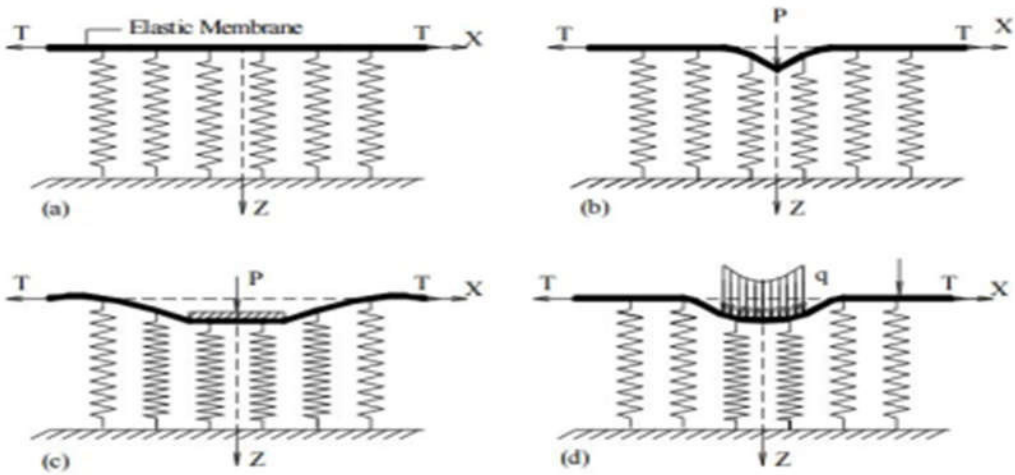

Figure 1.6 Filonenko-borodich model (Filonenko-Borodich,1940).

d. Pasternak's model

Based on Winkler's model, Pasternak assumed that there would be a shear interaction between the springs, which can be achieved by connecting the springs to a horizontal incompressible plate that deforms only in the transverse shear direction. Based on this assumption, Pasternak defined the relationship between pressure p and deflection w by the following equation:

$$\boldsymbol{P(x) = K_s.b.w(x) + G.\nabla^2 w(x)} \qquad 1.6$$

∇^2 is the Laplacian operator with $\nabla^2 = \frac{\partial^2}{\partial x^2} + \frac{\partial^2}{\partial y^2}$ and G represents the shear modulus where its neglect leads to the formulations adopted for the Winkler foundation type.

e. Kerr's model

Also based on Winkler's foundation model, Kerr introduced a shear layer and assumed that the springs above and below this layer are different.

The following figure shows the foundation model introduced by kerr (1964) and the response of the foundation to a uniformly distributed load P(x) is given by the differential equation below.

$$\left(\mathbf{1} + \frac{K_2}{K_1}\right).\boldsymbol{P(x)} = \frac{G}{K_1}.\nabla^2 \boldsymbol{P} + \boldsymbol{K_2 W(x)} - \boldsymbol{G.\nabla^2.W(x)} \qquad 1.7$$

Where K1 and K2 are the reaction modulus of the first and second layer respectively and G is the shear modulus

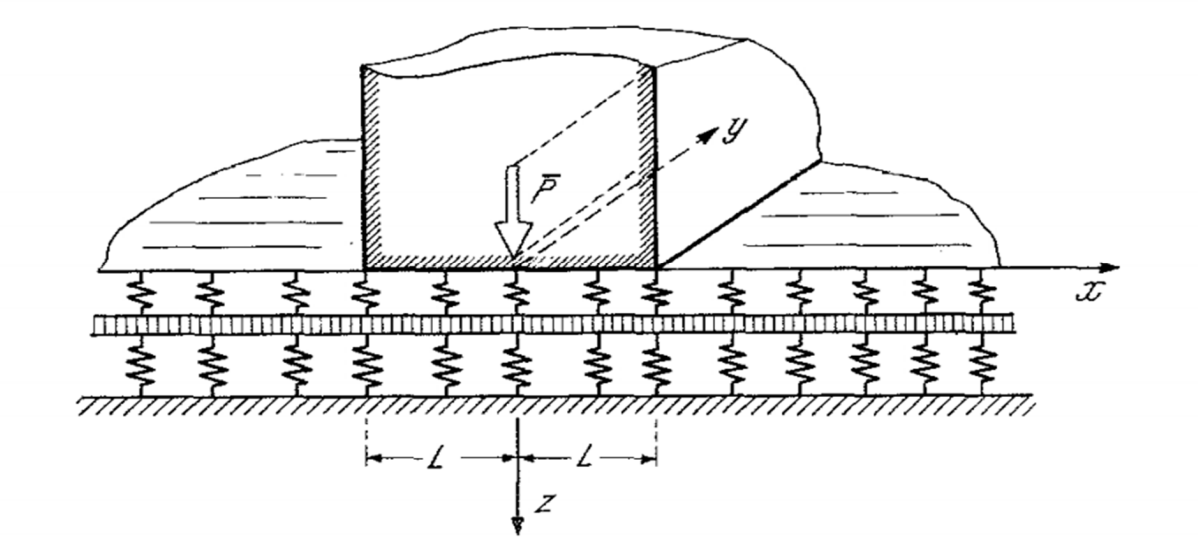

Figure 1.7 Kerr foundation model (kerr, 1964)

1.1.5. Effects of the ISS on building performance

a. Period lengthening

For a system with one degree of freedom, the ratio of the period extension, defined as the period of a system on a flexible base (Figure 1.1) divided by the period of the system on a fixed base, can be calculated from the classical expression developed by Veletsos and Meek (1974):

$$\frac{\tilde{T}}{T} = \sqrt{1 + \frac{k}{k_x} + \frac{kh^2}{k_{yy}}} \qquad 1.8$$

Where:

T: is the fundamental period of the fixed base structure

k: is the stiffness of the fixed base structure

k_x: is the lateral stiffness of the foundation

k_{yy}: is the rotational stiffness of the foundation

h: is the effective height of the structure is equal to 2/3 of the total height

From the above equation, it is clear that it is the stiffness ratio between the structure and the soil that contributes to the lengthening of the period. Furthermore, when the stiffness of the soil tends to infinity (fixed base), the equation shows that the elongation ratio will tend to 1. Thus,

it can be concluded that the impact of soil-structure interaction will be reduced for a soil categorised as rigid. Furthermore, the equation can be applied to multi-degree of freedom systems where the fundamental mode of vibration is dominant by taking the height, h, as the height of the centre of mass of the first mode (NEHRP, 2012)

b. System damping

The change in damping is one of the effects of the inertial interaction. There are two main sources of foundation damping that are the hysteric and radiation damping. Hysteretic damping is caused by the hysteric behaviour of soil under seismic excitation while radiation damping is originated by the radiation of the reflected wave-field away from the foundation. The damping of a flexible base system is greater compared to the structural damping due to the contribution of the foundation damping.

NIST (2012) presents works done by many researchers to develop analytical models for the evaluation of the foundation damping. Most of these models are frequency-dependent. One exception is the expression suggested by (Wolf, 1989) using a circular foundation resting on a half-space, which ignores the frequency dependence of the foundation stiffness terms and assumes a linear foundation radiation damping. Similar to a previous study presented by Roësset (1980) considering frequency dependence, the expression initially suggested by Wolf's can be expressed as:

$$\boldsymbol{\beta_f} = \left[\frac{(\tilde{T}/T)^{n_s}-1}{(\tilde{T}/T)^{n_s}}\right]\boldsymbol{\beta_s} + \frac{1}{(\tilde{T}/T_x)^{n_x}}\boldsymbol{\beta_x} + \frac{1}{(\tilde{T}/T_{yy})^{n_{yy}}}\boldsymbol{\beta_{yy}} \qquad 1.9$$

Where:

β_s: is the hysteric damping evaluated from information in the literature

β_x: is the translational damping

β_{yy}: is the rotational damping

n_s, n_x, n_{yy} are exponents that are equal to 2 for linear viscous damping and 3 otherwise

T_x *and* T_{yy} are the fictitious period defined as:

$$\boldsymbol{T_x = 2\pi\sqrt{\frac{m}{k_x}}} \qquad \boldsymbol{T_{yy} = 2\pi\sqrt{\frac{mh^2}{k_{yy}}}} \qquad 1.10$$

From the increase in the damping, it is obvious that when using a general acceleration response spectrum, consideration of SSI effects will reduce the response of the flexible base system.

c. Lateral deformation and inter-storey drift

Overall lateral deformation and inter-story drift are the most used damage parameters in the performance-based seismic design approach. The increase in the lateral deformation of the building can change the performance level of the structure and is particularly important in tall, slender, and closely spaced structures that can be subjected to pounding when relative displacements are large (Kramer 1996). Moreover, increase in the total deformation of the structure, and in turn secondary P-Δ effect, influences the total stability of the structure as well as the performance of the non-structural elements. Storey drift ratio is the maximum relative displacement of each floor divided by the height of the same floor and is strictly connected to the damage suffered by both structural and non-structural elements.

1.2. Medium tall building

Globally, there is no unambiguous classification of buildings according to their height. In fact, there are no strict rules for classifying a structure as low-rise, medium-rise, high-rise or tall, as this depends on the context, the country, the use, the building proportion. For example, in Toronto, on the narrower downtown streets, 20 meters wide, an average building is 5 or 6 storeys high. On the wider streets outside the city centre, an average building can be taller, up to a maximum of 11 storeys on the wider avenues. In France, any building for residential use between 28 and 50 metres in height is considered to be a mid-rise building (Elan, 2018)

In general, mid-rise buildings represent the intermediate scale of buildings, they are larger than houses but smaller than high-rise buildings.

1.2.1. Structural System of Medium Tall Buildings

1.2.1.1. Resisting loads system

a. Gravity resisting loads

The main components associated with vertical load-resisting systems for mid-rise buildings are the frame system, columns, beams, and shear walls. These vertical loads remain relatively similar in tall, medium and short buildings.

The vertical loads considered are permanent structural loads, permanent non-structural loads, and construction loads. The permanent non-structural loads are actually the weight of the load-bearing elements of the structure. The permanent non-structural loads consist of the weight of

the walls, partitions, and infill elements. In addition to these loads, the load-bearing structure must also support another load called the operating load, which is the weight of the occupants, goods, and equipment of the structure.

b. Lateral Loads Systems

A good design must consider the configuration of the building's lateral load resisting system. There are many lateral load resisting systems for mid-rise buildings, including the braced frame structure, shear wall, rigid frame structure. The first two are often found in areas of high wind and seismic activity, such as earthquakes and hurricanes. These vertical elements help prevent a structure from tipping over or collapsing.

It is obvious that choosing a lateral load-resisting system for a particular building is an essential design choice. There isn't a single system that works best for all buildings, though.

1.2.2. Specificity of medium tall buildings

The design of a mid-rise building takes into account parameters that might be overlooked in the design of lower buildings.

1.2.2.1. Natural frequencies of the structure

All structures have specific frequencies called natural frequencies. The lowest natural frequency is called the fundamental frequency. These parameters are very important in the dynamic analysis of a structure. These natural frequencies are described by modes associated with the forms of vibration.

In the calculation of the frequency, the mass and Stiffness at each stage is required. Normally, the mass includes all permanent loads plus 10–30% of the live load. There is no rule about how much live load to include, and the coefficient is based on the use of the building and the opinion of the structural engineer. Thus, it is important to include all mass as it will have a significant effect on the natural frequency.

1.2.2.2. Comfort requirement

One of the most important aspects to consider in the design process of a slender structure is the serviceability limit state. The design for comfort is carried out with two main parameters in mind: the horizontal deflection and the building movement. Lateral building motions include

maximum building deflection and storey drift. Storey drift is the difference in deflection between consecutive storeys and is of interest because of the possibility of damage to non-structural elements such as cladding.

When considering building movements, acceleration is the factor that is evaluated. Comfort due to movement will be discussed in more detail due to its complex nature (Ferrareto et al.2015), as found by Viktor and Stefan (2016).

1.3. Analysis method of concrete structure

Concrete structures are made up of load-bearing elements (beams, columns, walls, etc.) which form a skeleton. When buildings are analysed, it is this skeleton that is analysed.

Depending on the importance of the structure and the actions to which it is or will be subjected, there are various approaches to its analysis. The most common of these approaches is linear analysis. Certain approximations are made during this analysis:

- The deformations remain in the elastic domain (small deformation)
- The stiffness of elements is constant;
- The changes of geometry due to displacement are assumed to be small and therefore, can be ignored;
- Original or undeformed state is use as the reference state.

Depending on the actions, a static or dynamic analysis can be performed.

1.3.1.1. Linear static analysis

Linear static analysis (LSA) is the most basic type of analysis used to study a building's response. A linear relationship exists between the applied forces and displacements in this analysis. In practise, this applies to structural problems where the stresses remain within the material's linear elastic range. The stiffness matrix of the model is constant in a linear static analysis, and the solution process is relatively short compared to a non-linear analysis on the same model. The structural analysis incorporates only linear elastic materials and small deformation theory, and buckling phenomena are assessed through examination of the output. Inertial forces are not taken into account.

Linear static analysis is used in structural design to determine the stresses on structural elements when they are subjected to loads, typically static loads. Static analysis is critical because it serves as the foundation for all other analyses and is simple to perform. Before performing a

full non-linear analysis, linear static analysis is frequently used for a first estimation, and linear dynamic analysis is also frequently used.

1.3.1.2. Linear dynamic analysis

When a structure is likely to be loaded by a dynamic action, such as an earthquake or wind action, dynamic analysis is performed. Depending on the characteristics of the system under study and the external environment of the system, the vibration can be damped or undamped. In reality, there is no such thing as an undamped system. Due to this damping, all vibrations are in fact damped to some degree. Reinforced concrete buildings are damped systems, and their damping factor is about 5%. This analysis can be performed by lateral force or modal response spectrum analysis.(CEN, 2005)

Conclusion

In this first chapter, the basic concepts of soil-structure interaction were detailed, followed by the characteristics of mid-rise buildings, and the methods of linear analysis. It was found that the dynamic response of a structure resting on a flexible soil differs from that of a structure resting on a flexible base due to the interactions between the structure, the foundation, and the soil underlying and surrounding the foundation. There are several numerical methods for studying the behaviour of structures on soft soil. However, in practical SSI problems, simple methods, such as the Winkler approach, are preferred over the direct method. The effects of SSI can be summarised as follows: an increase in the system's natural period, an increase in damping, an increase in the rate of lateral displacement, and a change in the structure's force demands.

CHAPTER 2: METHODOLOGY

Introduction

The methodology is a part that establishes the procedure of the research in order to achieve the set objectives. In other words, it will describe the different elements of our research. In this work, the first step consists of a reconnaissance of the site through a literature search followed by data collection. Then, the standards used and the design procedure of the elements such as beam, column, retaining wall, and foundation will be presented. The ground motion selection and the numerical simulation procedure will also be discussed. Finally, the parameters such as foundation deformation, loads in structural elements, period, lateral displacement, storey drift, and base shear used as comparison criteria will be highlighted and explained.

2.1. Site recognition

The site recognition will be carried out from documentary research whose essential goal is to know the location of the site, the climate, the hydrology and socio-economic parameters in the region.

2.2. Site visit

The purpose of this activity is the building description results from the observation and the presentation of the use category, the dimension, the floor plans and elevation configuration.

2.3. Data collection

Architectural, structural plans and geotechnics data's will be the main data collected. These plans define the geometry of the building and highlight the distribution of structural elements. geotechnics data give the characteristics of soil on site.

2.4. Codes

A construction project has to respect a specific norm depending on where the construction is done. In the world, there are many types of norms like China code, American code, Eurocode, etc. Depending on the site of construction, on the material used and the type of structure to be built, different parts of Eurocodes are used.

For this case study the parts used are:

- Eurocode 0: Basis of structural design
- Eurocode 1: Actions on the structures, part 1: general actions
- Eurocode 2: Design of concrete structure, part 1: general rules and rules for buildings
- Eurocode 7: geotechnical design
- Eurocode 8: Design of structures of earthquake resistance, part 1: general rules, seismic action rules for building.

2.5. Actions and combination of actions

2.5.1. Actions

The different loads that shall be applied to this case study are the permanent and the variable loads (imposed loads).

2.5.1.1. Permanent loads

They are constituted by actions which have negligible variation with time although the structure lifespan.it can either be structural or non-structural.

- Structural loads (G1k): self-weight of slabs, beams, pillars
- non-structural loads (G2k): weight of wall, Ceramic stone ware, sand layers, etc

2.5.1.2. Variables loads

a. Imposed loads (Qk)

These are arising from occupancy. It includes the normal use by persons, the furniture and moveable objects, vehicles and other. The value of the imposed loads is defined in the Eurocode according to the category of use of the building.

b. Seismic action

This action is due to earthquake ground motions. It is accounted in the analysis by the definition of the elastic response spectrum defined in the Eurocode 8 by the following's expressions:

$$\mathbf{0 \le T \le T_B : S_e(t) = a_g S \left[1 + \frac{1}{T_B}(2.5\eta - 1)\right]} \qquad 2.1$$

$$\boldsymbol{T_B \leq T \leq T_c : S_e(t) = 2.5 a_g S \eta} \quad 2.2$$

$$\boldsymbol{T_c \leq T \leq T_D : S_e(t) = 2.5 a_g S \eta (\frac{T_c}{T})} \quad 2.3$$

$$\boldsymbol{T_D \leq T : S_e(t) = 2.5 a_g S \eta (\frac{T_c T_D}{T^2})} \quad 2.4$$

Where:

$S_e(t)$ is the elastic response spectrum

T: is the vibration period of a linear single degree of freedom system

a_g: is the design ground acceleration on type A ground

T_B: is the lower limit of period of the constant spectral acceleration branch

T_C: is the upper limit of the period of the constant spectral acceleration branch

T_D: is the value defining the beginning the constant displacement response range of the spectrum

S: is the soil factor that depends on the ground type

η: is the correction factor given by $\eta = \sqrt{10/(5 + \xi)}$

ξ: is the viscous damping ratio depends on the material used and the structural type of the building. For a concrete building, the Eurocode 8 uses a default damping ratio ξ of 5%.

2.5.2. Combination of actions

Combination of actions is a set of design values used for the verification of the structural reliability for a limit state under the simultaneous influence of different actions. In the case of a building, they are defined by the fundamental combination, used for the Ultimate Limit State (ULS) associated with collapse or other similar forms of structural failure. this combination is presented in equation below.

$$\boldsymbol{\sum_{j \geq 1} \gamma_{G,j} G_{k,j} + \gamma_{Q;1} Q_{k,1} + \sum_{i>1} \gamma_{Q;1} \psi_{0.i} Q_{k,i}} \quad 2.5$$

Where the coefficients $\gamma G,j$ and $\gamma Q,i$ are partials factors which minimize the action which tends to reduce the solicitations and maximize the one which tends to increase it. The recommended values preconized by the Eurocode 0 for the structural and geotechnical (STR and GEO) verifications are:

$\gamma G, jsup$ = 1.35 and $\gamma G, jinf$ = 1

γQ,1, sup = 1.50 and γQ,1, sup = 0

γQ, i, sup = 1.50 and γQ, i, inf = 0

The Characteristic combination (rare), used for non-reversible serviceability limit states (SLS) to be used in the verifications with the allowable stress method is presented below.

$$\sum_{j\geq 1} G_{k,j} + Q_{k,1} + \sum_{i>1} \psi_{0,i} Q_{k,i} \qquad 2.6$$

The seismic combination, used for the ultimate and serviceability limit state related to the seismic action is presented

$$\sum_{j\geq 1} G_{k,j} + E + \sum_{i\geq 1} \psi_{2,i} Q_{k,i} \qquad 2.7$$

Gk,j is the characteristic value of the permanent action j

Qk,i is the characteristic value of the accompanying variable action i

E is combination of the effects of the horizontal component of the seismic action

ψ is the combination factors that is function of the use category of the building. The recommended values are found in Eurocode 0

2.6. static design

Static analysis consists of determining the action of static loads on different part of the structure. It starts from the durability verifications to the design of beams, columns and a retaining wall at the basement The interaction between the soil and the structure is also defined in other to take into account the soil properties in the design of the foundation.

2.6.1. Durability and concrete cover

Durability can be defined as the conservation of the physical and mechanical characteristics of the structure and the materials with which the structures are constructed; this conservation must have a duration equal to the design life of the building. The protection and conservation of material of building can be ensured good concrete cover which guarantees the protection of steel against corrosion, the safe transmission of bond forces and an adequate fire resistance.

concrete cover can be defined as the distance between the surface of the reinforcement closest to the nearest concrete surface (including links and stirrups and surface reinforcement where relevant) and the nearest concrete surface

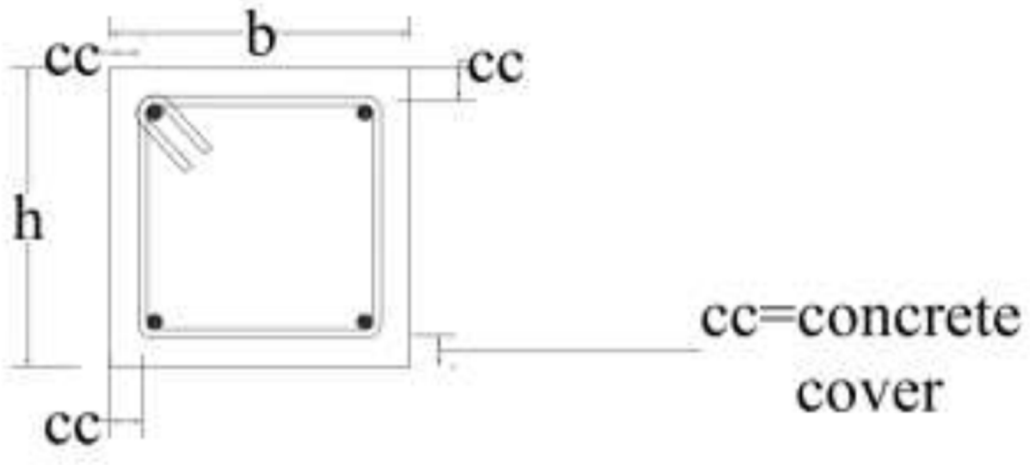

Figure 2.1. illustration of concrete cover

The nominal cover is defined as a minimum cover, Cmin, plus an allowance in design for deviation, Δcdev

$Cnom = Cmin + \Delta Cdev$

With

$Cmin = \max(Cmin, b; Cmin, dur + \Delta Cdur, \gamma - \Delta Cdur, st - \Delta Cdur\ add; 10mm)$

Where:

Cmin: the minimum cover

ΔCdev: the allowance in design for deviation with a recommended value of 10 mm

Cmin,b is the minimum cover due to bond requirement equal to the diameter of the bars or the equivalent diameter in the case of bundled bar

Cmin,dur is minimum cover due to environmental conditions

ΔCdur,ɣ additive safety element

ΔCdur,st reduction of minimum cover for use of stainless steel

ΔCdur,add reduction of minimum cover for use of additional protection

2.6.2. Beam design

beam design is composed of an Ultimate Limit State (ULS) design and a Serviceability Limit State verification (SLS).

2.6.2.1. Ultimate limit state

ULS design of this element will be done for the bending moment and the shear force solicitations since there is not axial force inside the elements.

a. Bending moment design

The design of the beam for bending moment is done by using the bending moment solicitation obtained from the envelop curve. For this solicitation, Eurocode 2 prescribe a reduction at the support. The value of this reduction is a function on the connection between the elements.

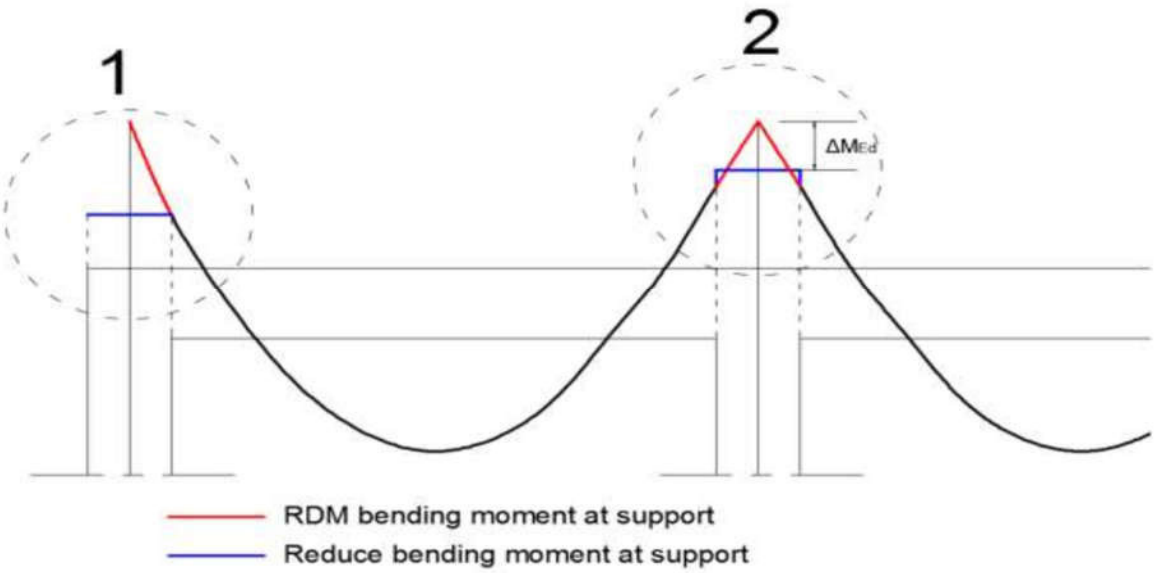

Figure 2.2. Reduction of the bending moment at support (Djeukoua, 2019)

i. Longitudinal steel reinforcement

Knowing the envelop solicitation curve of the moment, section of steel reinforcement of the rectangular beam at each point of that beam is estimate using the formula 2.1

$$As = \frac{M_{ED}}{0.9d * f_{yd}} \qquad 2.8$$

The section of reinforcement obtained has to verify the prescription given by the Eurocode2 which defines the maximum and the minimum reinforcement areas by the equations

$$A_{s,min} = \max\left(0.26\frac{f_{ctm}}{f_{yk}} b_t d; 0,0013 b_t d\right) \qquad 2.9$$

$$A_{s,max} = 0.04Ac \qquad 2.10$$

Where:

bt is the Mean width of the tension zone;

d is the is the effective depth of the section;

$fctm$ is the tensile strength of the concrete.

ii. Verification of the steel reinforcement

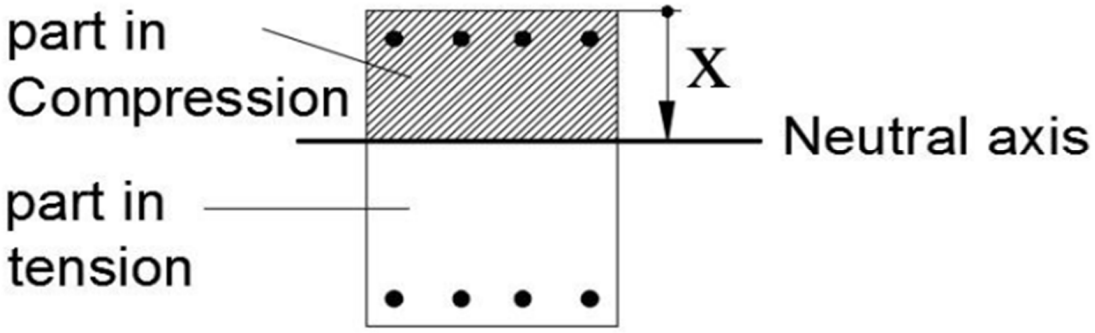

Figure 2.3. Neutral axis position inside a section

The verification of the design beam section is done by calculating the resisting bending moment and comparing with the design moment value to order to assure that the section can resist to the oncoming bending moment solicitations. The resisting bending moment is calculated using the position of the neutral axis inside the section. This neutral axis is obtained from the equation 2.11

$$\boldsymbol{x = \frac{d}{2\beta_2} - \sqrt{(\frac{d}{2\beta_2})^2 - \frac{M_{ED}}{\beta_1\beta_2 b f_{cd}}}} \qquad 2.11$$

Where:

is the effective depth of the section b is the width of the section;

fcd is the design compressive strength of the concrete;

$\beta 1\ and\ \beta 2$ is a correction factor equal to 0.81 and 0.41 respectively.

This resisting moment is then given by the relation

$$\boldsymbol{M_{Rd} = A_{s\,p}.f_{yd}.(d - \beta_2.x)} \qquad 2.12$$

Where:

Asp: is the effective area of the steel section

fyd: is the design yielding strength of the steel

b. Shear verification

As bending moment, Shear solicitation are equally obtained from the envelop curve solicitation. Transversal steel reinforcement has to be insert inside the section in order to take over the shear force inside the beam.

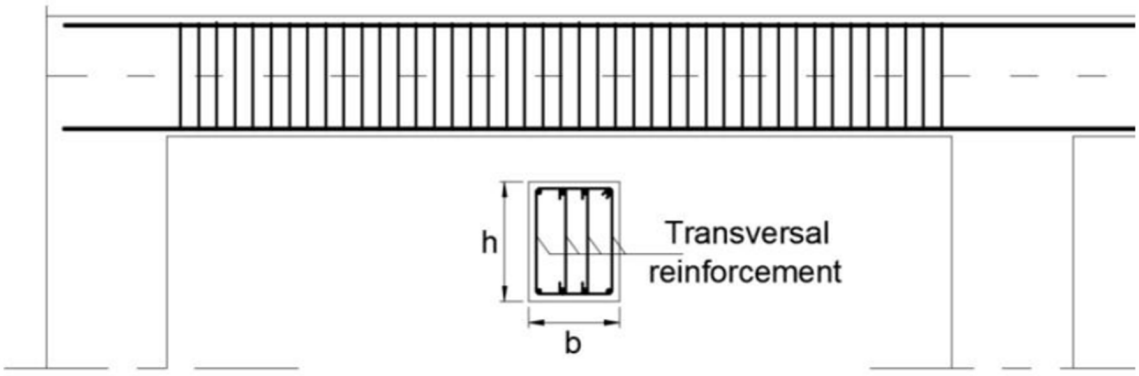

Figure 2.4. Longitudinal and transversal beam section with transversal reinforcement

shear reinforcement is verified by comparing the acting shear VEd to the design shear resistance of the member without shear reinforcement VRd, C which is defined by equation 2.13

$$\boldsymbol{V_{RDC} = \max\{\left[C_{RD,C}K(100\rho f_{ck})^{\frac{1}{3}} + K_1\sigma_{CP}\right]b_w d; (v_{min} + K_1\sigma_{CP})b_w}\text{d}\} \qquad 2.13$$

Where:

fck is the characteristic strength of the reinforcement;

d is the is the effective depth of the section;

bw is the smallest width of the cross section in the tensile area

$$\boldsymbol{\sigma_{cp} = \frac{N_{ED}}{Ac} \leq 0.2 f_{cd}} \quad [\text{N/mm}^2] \qquad 2.14$$

N_{Ed} is the axial force in the cross section due to loading or prestressing (in N);

AC is the area of the concrete cross section

$$\boldsymbol{K = 1 + \sqrt{\frac{200}{d}} \leq 2.0} \text{ with d in mm} \qquad 2.15$$

If no design shear reinforcement is required, the minimum shear reinforcement is applied according to the detailing of that member.

For members where the design shear reinforcement is required, the shear resistance is the minimum of $Vrds$ and $Vrdmax$

$$V_{RD,max} = \alpha_{CW} b_w z v_1 f_{cd} / (cot\theta + tan\theta) \quad 2.16$$

$$V_{Rd,s} = \frac{A_{sw}}{S} Z f_{yd} cot\theta \quad 2.17$$

Where:

$fywd$ is the design yield strength of the shear reinforcement;

$v1$ is a reduction factor for concrete cracked in shear ($v1 = 0.6$ for $fck \leq 60N/mm^2$);

αcw is a coefficient taking account of the state of stress in the compression cord;

$\alpha cw = 1$ for non-prestressed structures;

S is the spacing of the stirrups.

Asw is the cross-sectional area of the shear reinforcement

2.6.2.2. Serviceability Limit State Verification

The common serviceability limit states are the stress limitation, the crack and the deflection control. Only the stress limitation is presented on this work.

The verification of the allowable stress on the beam is done at the characteristic (rare) combination and permits to avoid inelastic deformation of the reinforcement and longitudinal cracks in concrete. The stress value is function of the modular ratio in short terms and long terms expressed in equation

$$n_0 = \frac{Es}{Es} \quad 2.18$$

$$n_\infty = n_0(1 + \varphi_L . \rho_\infty) \quad 2.19$$

Where $\varphi L = 0.55$ for shrinkage of concrete and the parameter $\rho\infty = 2 \div 2.5$

The neutral axis position is computed for an uncracked concrete using 2.20

$$x = \frac{-n(As+As') + \sqrt{[n(As+As')^2 + 2bn(As.d + As'd')}}{b} \quad 2.20$$

Where

$A's$: is the area of the compressive steel reinforcement inside the section

As: is the area of the tensile steel reinforcement inside the section

b, d' and d are the geometrical characteristics of the section as presented in Figure 2.5

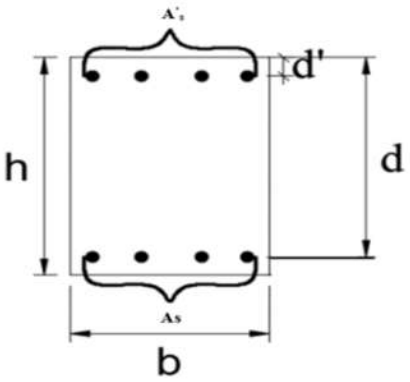

Figure 2.5. Geometric characteristic of the transversal section of a beam

The moment of inertia of the uncracked section is given by equation

$$J_{cr} = \frac{bx^3}{3} + nAs(d-x)^2 + nAs'(x-d')^2 \qquad 2.21$$

The stress in the concrete and in the steel reinforcement in tension are then obtained using respectively the equation below

$$\sigma_c = \frac{M_{ED}}{J_{cr}} \qquad 2.22$$

$$\sigma_s = \frac{M_{ED}\, n(d-x)}{J_{cr}} \qquad 2.23$$

Eurocode 2 preconizes a limitation of the stresses as presented in expressions below

$$\sigma_c \leq K_1 . f_{ck} \qquad 2.24$$

$$\sigma_S \leq k_3 . f_{yk} \qquad 2.25$$

With $k_1 = 0.6$ and $k_3 = 0.8$

2.6.3. Column design

For the column design, 3D frame of structure is modelling in the software SAP 2000. The solicitations required for the design are obtained from this 3D model by applying different loads and load combinations on the structure. The preliminary design is done and the design at ULS

for the axial force, the bending moment and the shear and the verification is done for the slenderness.

2.6.3.1. Preliminary design

In a seismic area, the preliminary design of the column considers that 60% of the concrete resistance is used to take over the axial force. the formulation used for the preliminary design is represented by equation 2.26

$$N_{rd} = 0.6\, f_{cd} A_c \geq qS_r n \qquad 2.26$$

With

n: number of stories above the considered column

Ac: concrete section area

q: uniform distributed load at each floor at ULS

Sr: recovery area of a column

Nsd: axial load computed using the recovery area of a column

2.6.3.2. Bending moment-axial force verification

Design for bending moment and axial force solicitations is carried out through an M-N interaction diagram. The maximum value of solicitations obtained from the envelop curve have to belong on M-N interaction diagram of the section considered. This diagram is computed by determining some significant points.

a. First point

The section is completely subjected to tension; hence, the concrete is not reacting. We impose $\varepsilon s = \varepsilon su$, $\varepsilon s' = \varepsilon syd$ then $\sigma s = \sigma s' = fyd$. The limit axial force and bending moment are obtained from the equations 2.19 and 2.20

$$N_{RD} = f_{yd} A_s + f_{yd} A'_s \qquad 2.27$$

$$M_{RD} = f_{yd} A_s \left(\frac{h}{2} - d'\right) + f_{yd} A'_s \left(\frac{h}{2} - d'\right) \qquad 2.28$$

b. Second point

The section is completely subjected to tension; hence, the concrete is not reacting. We impose $\varepsilon s = \varepsilon su$, $\varepsilon c = 0$. The upper steel has to be verified if yielded or not. The value of the limit axial force and bending moment at this point are computed using equation 2.27 and 2.28

c. Third point

Here, failure is due to concrete and the lower reinforcements have yielded. Assume $\varepsilon s \geq \varepsilon syd$, $\varepsilon c = \varepsilon cu$. Then, computing the neutral axis, NRd and MRd can be computed using respectively equations 2.21 and 2.22

$$N_{RD} = -\beta_1 b x f_{cd} + f_{yd} As - f_{yd} A's \qquad 2.29$$

$$M_{rd} = f_{yd} As \left(\frac{h}{2} - d'\right) + f_{yd} A's \left(\frac{h}{2} - d'\right) + \beta_1 b x f_{cd} \left(\frac{h}{2} - \beta_2 x\right) \qquad 2.30$$

d. Fourth point

The failure is due to concrete and the lower reinforcement reaches exactly $\varepsilon s = \varepsilon syd$. As for the previous point, we determine the neutral axis position, NRd and MRd are determined using the equations 2.21 and 2.22

e. Fifth point

The failure is still due to concrete and the lower reinforcement reaches exactly $\varepsilon s = 0$. Then, the neutral axis position is equal to the effective depth of the section. The limit axial force and bending moment are obtained from the equations 2.23 and 2.24

$$N_{RD} = -\beta_1 b x f_{cd} + f_{yd} As - f_{yd} A's \qquad 2.31$$

$$M_{rd} = f_{yd} As \left(\frac{h}{2} - d'\right) + f_{yd} A's \left(\frac{h}{2} - d'\right) + \beta_1 b x f_{cd} \left(\frac{h}{2} - \beta_2 x\right) \qquad 2.32$$

f. Sixth point

Here, concrete is uniformly compressed and assume the strains $\varepsilon_s = \varepsilon_c \geq \varepsilon_{c2}$. Limit values of axial force and bending moment are computed by using equations

$$N_{RD} = -b h f_{cd} - f_{yd} A_s - f_{yd} A'_s \qquad 2.33$$

$$M_{RD} = f_{yd} A_s \left(\frac{h}{2} - d'\right) - f_{yd} A'_s \left(\frac{h}{2} - d'\right) \qquad 2.34$$

The steel reinforcement of the column is provided by some limitation given in Eurocode 2 as presented in equations below.

$$\boldsymbol{As_{min} = \max(\frac{0.1\,NED}{f_{yd}}; 0.002Ac)} \quad 2.35$$

$$\boldsymbol{As_{max} = 0.04\,Ac} \quad 2.36$$

With

N_{ED}: design axial compressive force

f_{yd}: design yield strength

2.6.3.3. Shear design

Unlike the beam as early explained above, shear design of column follows the same procedures however, the detailing of members prescribed by Eurocode 2 imposed a minimum diameter of 8 mm or one quarter the maximum diameter of the longitudinal bars. The maximum spacing of the transverse reinforcement is given by the equation 2.37

$$\boldsymbol{S_{cl\,max} = \min(20\emptyset_{l,min}; b; 400mn)} \quad 2.37$$

Where:

$\emptyset$ is the minimum diameter of the longitudinal bars;

b is lesser dimension of the column.

The factor of 0.6 is used to reduce the maximum spacing in sections within a distance equal to the larger dimension of the column bars.

2.6.3.4. Slenderness verification

The need for slenderness verification arises from whether or not second order effects are to be accounted for. It consists in verifying if the slenderness of the element is below a limit value, defined by the Eurocode 2 as expressed in equation 2.38.

$$\boldsymbol{\lambda_{lim} = 20ABC/\sqrt{n}} \quad 2.38$$

Where:

$A = \frac{1}{1+2\varphi_{ef}}$ (φef is the effective creep ratio; A=0.7 if φef is unknown)

$B = \sqrt{1 + 2\omega}$ ($\omega = Asfyd/Acfcd$, is the mechanical reinforcement ratio)

$C = 1.7 - rm$ (rm is the moment ratio, $r_m = M_{01}/M_{02;}$ equal to 1 for unbraced system)

$n = NED/Acfcd$ (relative normal force)

The slenderness of an element is computed using equation

$$\boldsymbol{\lambda = \frac{l_0}{i}} \qquad 2.39$$

Where

l_0: is the effective length of the element ($l_0 = 0.7l$)

$i = \sqrt{(I/A)}$ (i, I, and A represent the gyration radius of the uncracked section, the moment of inertia and the area of the section respectively).

2.6.4. Retaining wall design process

Retaining wall is a structure designed and constructed to resist the lateral pressure of soil or hold back soil material. There are many types of retaining walls like gravity wall, reinforced retaining wall, buttressed retaining wall, cantilevered wall and so on.

reinforced concrete wall will be considered in this work. geotechnical analysis and structural design of wall will be done after determining lateral earth pressures by using equations 2.40 and 2.41. The total lateral earth pressure is given by equation 2.42

$$\boldsymbol{Sk, surcharge = K_a WH} \qquad 2.40$$

$$\boldsymbol{Sk, ground = 0.5 k_a \gamma H^2} \qquad 2.41$$

$$\boldsymbol{Lateral\ earth\ pressure = Sk, surcharge + Sk, ground} \qquad 2.42$$

Where:

Sk,ground is Ground horizontal force;

Sk, surcharge is Surcharge horizontal force provided by the surcharge on the embankment;

W is the uniform surcharge load;

H is the height of the embedded part of the wall.

Ka is factor of horizontal active earth pressure which is compute by using equation

$$Ka = \frac{1-sin\phi}{1+sin\phi} \quad 2.43$$

Notice that Φ is the angle of shearing resistance

Geotechnical analysis consists to verify sliding and overturning. In the other side structural design permits to get the required steel reinforcement and to check the resistance of the concrete wall against normal force using equation 2.52

$$N_{rd} = \frac{\alpha B_r f_{cd}}{0.9} \quad 2.44$$

Where

$\alpha = \frac{0.65}{1+\frac{0.2\lambda}{30}}$ with λ the slenderness ratio of the wall

The required steel is get after the computation of the bending moment in the longitudinal and in the transverse direction of the wall by using equation 2.1

2.6.5. Foundation design

The foundation adopted is an invert foundation. This can be defined as a reinforced concrete slab spread over the structure's footprint. It is used when the supporting soil has a low bearing capacity and is compressible. There are many types of invert foundations. For a heavily loaded invert, it is necessary that the foundation be reinforced with beams and footings to form a ribbed slab. The choice of mat size depends on the geotechnical conditions. The slab floor and the reinforcing beams are designed as inverted elements, as explained above. the footings are designed as rigid footings.

a. Preliminary design of the raft

The surface area of the raft is considered to be equal to that of the whole building. The thickness of the slab, H, can be estimated using equation

$$H \geq \frac{L_{max}}{20} \quad 2.45$$

Where, $lmax$ is the maximum distance between two columns. The effective depth of the slab can be obtained using equations 2.39 and 2.40

$$dx = H - Cnom - \frac{\emptyset}{2} \quad 2.46$$

$$dy = H - Cnom - \emptyset - \frac{\emptyset}{2} \quad 2.47$$

b. Geotechnical design of raft foundation

The slab is designed by the conventional rigid method. The pressure developed by the total vertical load of applied on the raft should less than the allowable pressure of the soil as expressed in relation 2.38

$$\sigma_{adm} \geq \frac{Q}{A} = \sigma \quad 2.48$$

Where:

is the contact pressure;

σ_{adm} is the admissible pressure on the soil;

Q is the total vertical loads arriving at the foundations;

A is the surface of the mat.

The position of the resulting vertical load is computed along x and y axis as shown in relation 2.80 and 2.81, respectively

$$X = \sum \frac{P_i x_i}{Pi} \quad 2.49$$

$$Y = \sum \frac{P_i y_i}{Pi} \quad 2.50$$

If there is an eccentricity between the resultant vertical load and the center of gravity of the raft the contact pressure distribution is obtained as expressed in equation

$$\sigma_{max} = \frac{Q}{A} \pm \frac{Q\, e_X}{I_y} \pm \frac{Q\, e_y}{I_x} \quad 2.51$$

Where:

ex: is the eccentricity along x axis

ey: is the eccentricity along y

Ix: is the moment of inertia of the section along x axis

Iy: is the moment of inertia of the section along y axis

x and y: are the position of a given point along x and y axis respectively

c. Structural design of the slab

The panel are designed as a Shell thick element. The panels will be modelled in SAP2000 as a shell resting on Winkler's springs. The stiffness of the springs is obtained from the modulus of subgrade reaction of the soil times the area of the meshing square using relation 2.52. The modulus of subgrade reaction is obtained using the table presented in Annex

$$\boldsymbol{K = C * A} \qquad 2.52$$

Where:

C: is the modulus of subgrade reaction of the soil

A: is the mesh area

The computation of the reinforcement area is done for one-meter. The strengthening beams are designed as inverted beams. The depth of the beam H follows the relation 2.46

$$\boldsymbol{H \geq \frac{L}{10}} \qquad 2.53$$

d. Design of the rigid footing

The design will be done using the shoring and anchorage model, where the footing is designed for the axial force only. It is assumed that the transmission of the axial force from the superstructure is provided by a succession of struts (at an angle of 45° to the horizontal) balanced by the soil pressure and the bottom reinforcement. The soil pressure and the bottom reinforcement of the footing, as shown in Figure 2.10 below. t and c in the diagram represent tension in the steel and compression in the concrete, respectively.

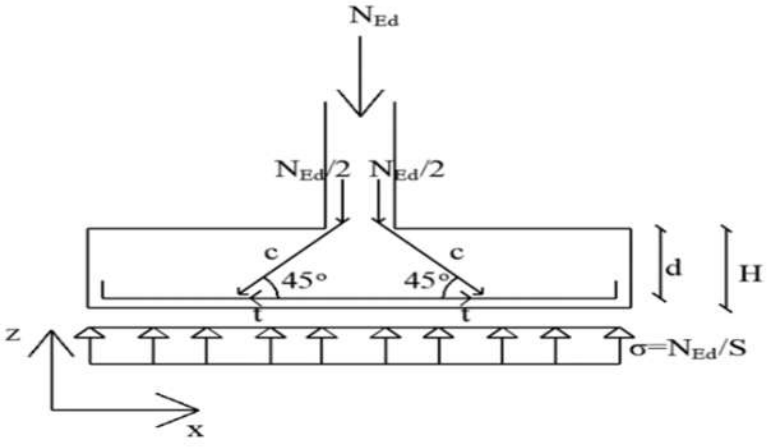

Figure 2.6. Strut and tie model of the footing

the value of t is obtained as follows:

$$t = \frac{Ned}{2tan\,45°} \qquad 2.54$$

$$tan\,45° = \frac{4d}{(A-a)} \qquad 2.55$$

$$t = \frac{Ned(A-a)}{8d} \qquad 2.56$$

T can also express as:

$$t = Asfyd \qquad 2.57$$

From these equations is deduced the expression 2.58 to find the required steel sections in the footing.

$$As = \frac{Ned\,(A-a)}{8dfyd} \qquad 2.58$$

Where

Ned: is the axial force solicitation obtained from the envelop curve at Ultimate Limit State.

A: is the width of the footing in the x direction

a: is the corresponding side of the column

d: is the corresponding effective depth of the footing. it is calculated as above

2.6.6. Numerical modelling of the structure

The structural model of building will be modelled with the software SAP 2000 (Structural Analysis Program) version 22, which is a software based on the finite element method and structural design. It allows the modelling of structures by the finite element method with the possibility to perform several types of analysis: from static analysis to dynamic or linear

analysis and nonlinear analysis. Modelling shall consist of creating the appropriate material, section properties, loads and combinations. The loads induced by the slabs will be distributed and directly applied on the beams as well as the linear loads provided by the external walls, imposed loads as distributed frame loads. The beams and the columns of the structure are modelled as frame elements according to the plan. The connection between these elements is done through the insertion of joints between the two elements.

six models will be developed, the first two model with a fixed base and the other four integrates soil-structure interaction through the insertion of linear springs with translational stiffness at the base of the structure.

2.6.7. Analysis criteria

The study's findings will be analysed using four parameters: settlement, shear force, bending moment, and axial force solicitations.

2.6.7.1. Structural deformation and foundation settlement

Foundation settlement is an important parameter to consider when designing a foundation because exceeding the limit of settlement may affect the intended function of the building. is the absolute value of the vertical deformation of the structure. The limit set by Eurocode 7 is 50 mm.

2.6.7.2. Bending moment and shear forces on Beam

The most important parameters used in the design of beams are moment and shear force. As these parameters depend on the stiffness of the structure and the support conditions, the change in soil type and foundation type can affect their values. The variation of these values will help to determine whether the design of structural elements should be considered under different support conditions.

2.6.7.3. Axial force and bending moment on column

The axial force and moment are parameters that govern the design of the column in the static analysis, and their values are strongly influenced by the support conditions at the base of the building. As for the beam, the verification of the variation of these values will allow us to know if the design of the column should be reconsidered for these solicitations according to the different support conditions.

2.7. Dynamic analysis

This section will focus on linear dynamic analysis. An earthquake will be applied to the different models studied through a response spectrum to study the response of the structure.

2.7.1. Modal analysis

The structural response is the combination of several modes. A modal analysis is performed on 3D models of the structure (one with a fixed base and one with a flexible base) to determine the frequency and vibration modes of the structure. Since there are Since there are several vibration modes, the selection of the vibration modes to be treated is important and must comply with the conditions indicated by Eurocode 8 section 4.3.3.3.1.

2.7.2. Ground motion selection

The structural model will be subjected to the 2002 Palermo earthquake. The design response spectrum of this earthquake is inserted into the software as a function and its application to the structure is done by defining load cases that use the response spectrum function and the direction of the action. The software allows for the eccentricity of the seismic force and then the effect of accidental torsion is taken into account, as recommended in Eurocode 8, by defining three seismic load cases in each direction and the seismic force considered is the envelope of these load cases.

2.7.3. Analysis criteria

The results of the study will be analysed on four parameters including the period of the different vibration modes of the structure, lateral deformation, inter-storey drift, base shear and storey shear.

2.7.3.1. Vibration period

The fundamental period of a building is an intrinsic property of the structure. It's mainly affected by the mass, the stiffness, the height and the column orientation. Some empirical formulas permit to estimate this period. It's the case of the one defined by the Eurocode 8 for buildings with heights up to 40m as expressed in equation 2.41

$$\boldsymbol{T = C_t H^4} \qquad 2.59$$

Where:

c_t is a coefficient that depends on the moment resisting type of the structure;

H is the total height of the building above the foundations in meter.

The real values of this property of the building can be obtained through a modal analysis of the structure. It is the first step for the dynamic studying of a structure. For this work, modal analysis will be computed directly from the structural analysis program SAP2000 for models under fixed base and modelled foundation.

2.7.3.2. Lateral displacement

Resulting from horizontal forces (seismic load in this case) and p-delta effects for tall buildings, the storey lateral displacement is the absolute value of the horizontal displacement of the storey. It also allows a correct estimation of the separation distance between buildings. In the case of this study, the p-delta effects (second order) will be neglected. Figure 2.7 shows the displacement of the storey of a building.

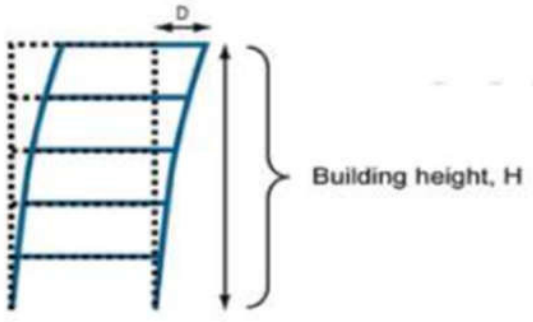

Figure 2.7. illustration of storey displacement of the building

In seismic design, this displacement can affect the structural elements of the building. This parameter is best assessed through the inter-storey drift ratio.

2.7.3.3. Inter-storey drift

The storey drift ratio is the maximum relative displacement of each stage divided by the height of the same stage. It is an important parameter that will be evaluated. The inter-storey drift is the most important parameter to be analysed as it is strictly related to the damage to the structural and non-structural elements of the building. The inter-storey drift has been used as an indicator to evaluate the deformation capacity of buildings and to determine their performance.

This parameter is evaluated as the difference between the average lateral displacements. For a correct design, Eurocode 8 sets some limits according to this parameter, as defined in the following equations.

$$d_r V = 0.005h \quad (2.60)$$

$$d_r = d_{i+1} - d_i \quad (2.61)$$

dr is the inter-storey drift at (i+1) level

di+1 is displacement at (i+1) level

di is displacement at (i) level

v is reduction factor

h is Storey height

The storey drift in the model with fixed base will be compared to the soil structure interaction models.

2.7.3.4. Base shear

Base shear is an estimate of the maximum expected lateral force on the base of the structure due to seismic activity. It is an output of overall behaviour of the structure. The base shear is further distributed to each storey as storey shear. both foundations models. the shear forces in the model with fixed base will be compared the soil structure interaction models.

2.7.3.5. Solicitation on structural element

The study's findings will be analysed using two parameters: bending moment on reference beam and column.

Conclusion

The objective of this chapter was to present the different codes, the different procedures that will be used in this work, the analysis criteria and the seismic performance on which the analyses will be based, which will be carried out with the help of the structural analysis software SAP 2000 version 22, while the different designs will be carried out manually with the help of the Excel software by applying the European standards. After the different procedures have been well described, the case study will be presented, analysed in the SAP 2000 software, and designed statically following the process presented in this section.

CHAPTER 3: PRESENTATION AND INTERPRETATION OF RESULTS

Introduction

3.1. General presentation of the site

Here, the study area through its location, geology, relief and soil, and climate are presented.

3.1.1. Geographic location

the case study is located in the nlongkak district of Yaoundé 1, in the city of Yaoundé in Cameroon, the political capital and headquarters of the Centre region. This city is situated at 3.87° (3.50°) north latitude and 11.52° (11.31°) east longitude, at an altitude of 760 meters above sea level.

Figure 3.1.localisation of case study

3.1.2. Geology and relief

The bedrock in Yaoundé is mainly composed of gneiss. This rock is neither porous nor soluble, but it is its discontinuities (faults, diaclases) that give fissure permeability to the formation. The hydrogeology is characterized by continuous aquifers, approximately exploitable overlying water bearing fissures or fracture aquifers in the bedrock; these types of aquifers are superimposed or isolated. Concerning the relief, the land rises gently in escarpments from the southwestern coastal plain before joining the Adamawa Plateau via depressions and granite massifs. The field is characterized by rolling, forested hills, the tallest of which have bare, rocky tops.

3.1.3. Climate and hydrology

Yaoundé's climate is tropical, it is characterized by an almost constant temperature of around

24°C and very heavy rainfall. this city has a long rainy season that lasts for nine months, from March to November. However, there is a noticeable decrease in rainfall during the rainy season, observed in the months of July and August. The rainfall in the months of July and August gives the impression that the city has two rainy seasons and two dry seasons. The average rainfall is 1650mm per year and the average humidity is 80%.

Yaounde has a dense hydrographic network, with permanent rivers such as the Mfoundi, which crosses the city from north to south, as well as some streams and lakes. Yaoundé is located on the western plateau of southern Cameroon. Gentle rolling hills characterize the landscape. A series of hills, valleys, and wetlands, this diverse physical landscape allows for a variety of rivers.

3.1.4. Population and economic activities

The total population of Yaoundé was estimated at 4.1 million in 2020. Yaoundé is a cosmopolitan city with a large population from several other regions of the country (west, far north, etc.). The majority of Yaoundé's economy revolves around the administrative structure of civil and diplomatic services. Due to these factors, Yaoundé enjoys a higher standard of living and security than the rest of Cameroon. On the other hand, Yaoundé is a tertiary city with some industries, including breweries, sawmills, carpentry, tobacco, paper mills, machinery, and construction materials.

3.2. Presentation of the project

This part, we will present and describe the case study and present the general characteristics of the materials to be used.

3.2.1. Building configuration

The case study is a multi-usage building. It is a structure of 06 floors plus a mezzanine above the ground floor with two basement levels. The building is 31.675 m high above ground level. The area of the basement floors is 636.15 m², while the area of the other floors (above level 0) is smaller. The horizontal force resistance system consists of a reinforced concrete shear wall core and a concrete retaining wall. The gravity system consists of cast-in-place concrete mushroom slabs supported by concrete columns. The picture of the building is shown in the figure 3.3 while the plan view of the mezzanine is shown in figure 3.2.

This structure was designed in two phases. initially it was to be composed of 4 floors and a mezzanine, but during the construction phase it was redesigned and two more floors were added on top.

Figure 3.2. axonometric view of the building

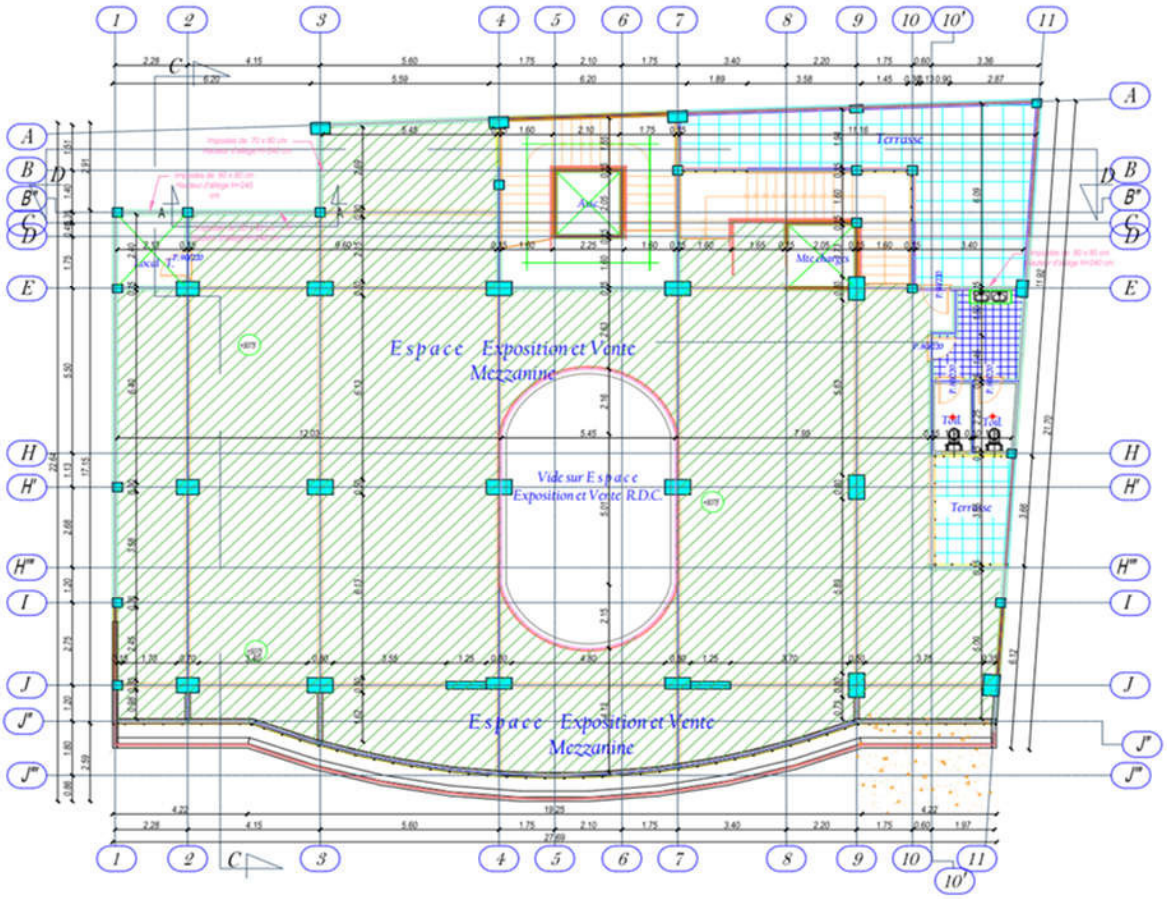

Figure 3.3. Plan view of mezzanine

The cross-section of the building is presented in the annexe.

3.2.2. Geotechnical characteristics

Soil information was obtained by geotechnical testing at the construction site. The test pits revealed relatively soft soil conditions, consisting of a reddish lateritic gravel on the surface, varying in thickness from 0.00 m to 2.5 m, overlying a layer of reddish clay with a bearing capacity of 0.20 MPa. This layer will be considered as wet clay in the rest of this work. The water table was not detected on this site.

3.2.3. Material properties

the concrete class adopted for the structure is C25/30 and the longitudinal steel reinforcement is Fe500B. For the transverse reinforcement, Fe400B is considered. The main characteristics of these materials for the linear analysis and design of the structure are given in Table 3.1 for the concrete and Table 3.2 for the steel reinforcement.

Table 3.1. Characteristics of concrete for the structure

Property	Value	Unit	Definition
Class	C25/30	-	Concrete class
R_{ck}	30	N/mm^2	Characteristic cubic compressive strength
f_{ck}	25	N/mm^2	Characteristic compressive strength of concrete at 28 days
$f_{cm} = f_{ck} + 8$	33	N/mm^2	Mean value of concrete cylinder compressive strength
γ_c	1.5	-	Partial factor for concrete
$f_{cd} = \alpha_{cc} f_{ck}/\gamma_c$	14.16	N/mm^2	Design value of concrete compressive strength
$f_{ctm} = 0.3 \times (f_{ck})^{2/3}$	2.56	N/mm^2	Mean value of axial tensile strength of concrete
$f_{ctk,0.05} = 0.7 \times f_{ctm}$	1.79	N/mm^2	Concrete tensile strength 5% fractile
$f_{ctd} = \alpha_{ct} f_{ctk,0.05}/\gamma_c$	1.2	N/mm^2	Design tensile strength
$E_{cm} = 22000 \times (f_{cm}/10)^{0.3}$	31476	N/mm^2	Secant modulus of elasticity
υ	0.2	-	Poisson's ratio
$G = E_{cm}/2(1 + \upsilon)$	13115	N/mm^2	Shear modulus
γ	25	kN/m^3	Specific weight of concrete

Table 3.2. longitudinal Steel reinforcement characteristics

Property	Value	Unit	Definition
class	Fe500B	-	Steel class
f_{yk}	500	N/mm^2	Characteristic yield strength
f_{yd}	434.78	N/mm^2	Design yield strength
γ_s	1.15	-	Partial safety factor for steel
γ	78.5	kN/m^3	Specific weight of steel
υ	0.3	-	Poisson's ratio

Table 3.3. Transversal Steel reinforcement characteristics

Property	Value	Unit	Definition
class	Fe400B	-	Steel class
f_{yk}	400	N/mm^2	Characteristic yield strength
$f_{wd} = 0.8f_{yk}$	320	N/mm^2	Design yield strength
γ_s	1.15	-	Partial safety factor for steel
γ	78.5	kN/m^3	Specific weight of steel
υ	0.3	-	Poisson's ratio

3.3. Loads on the building and load combination

3.3.1. Loads

Loads acting on the building are presented as follows

a. Permanent loads

The loads applied on the building are divided into two structural and non-structural the self-weight of the slab is a structural permanent loads G1 and others are non-structural load G2.

In this case, the slab is 20 cm thick so G1K is 5 KN/m2. For permanent non-structural load the value is the same from basements to floor 6 and decreases at the roof floor as presented in table 3.4 and table 3.5.

Table 3.4. Permanent non-structural loads for floors 1 to 6 and basements

Nature	Description	Value	Unit
G2k	Screed (5 cm thick)	1,16	kN/m^2
G2k	Tiles	0,6	kN/m^2
G2k	False sealing	0,5	kN/m^2
G2k	Partition wall	1.35	kN/m^2
TOTAL		3,61	KN/m^2

Table 3.5. Permanent non-structural loads for the roof floor

Nature	Designation	Value	Units
G2K	Waterproof	0.12	kN/m2
G2K	Concrete in the form of slope	2.2	kN/m2
G2K	False sealing	0.5	kN/m2
Total	2.82	kN/m2	kN/m2

Linear load provided by external wall of the building with of 15 cm thickness the load Gk for each floor is provided in table 3.6

Table 3.6 loads provided by external wall

Nature	Height of the floor	value	units
Gk-ground floor	5.075	12.8	kN/m
Gk-mezzanine	3.60	8.93	kN/m
Gk-level 1 to level 6	3.00	7.8	KN/m

b. Variable action

i. Imposed loads

for this case study, Eurocode 2 recommends a load of 5 KN/m^2 (category D) for the ground floor to level 1, qk=2.5 KN/m^2 for the parking area for light vehicles (category F) and qk =2.5 kN/m^2 for level to level 6 (category B). the last floor is accessible (use category A) so the imposed load can be taken as 1.5 kN/m^2

ii. Seismic Loads

The seismic load applied in this work will be applied as a ground acceleration corresponding to the horizontal component of the elastic response spectrum. The properties of the spectrum is defined in table 3.7

Table 3.7. Seismic parameters

Ground	Type D
Horizontal response Spectrum	Type 1
Building class	Commercial building
Peak ground acceleration (a_{gR})	0.74g
Importance factor	3.6
Damping ratio	5%

3.3.2. Load combinations

The load combination in the equation below provides for the verification of the structure at Ultimate Limit State

$$F_{ED} = 1.3\,Gk + 1.5Qk \quad (3.1)$$

$$G_k = G_{1K} + G_{2k} \quad (3.2)$$

Where, $G1k$ is the self-weight of the element to design

For non-reversible Serviceability Limit State (characteristic and quasi permanent), the verification is done using equations 3.3 and 3.4

$$FEd = Gk + Qk \quad (3.3)$$

$$FEd = Gk + 0,3Qk \quad (3.4)$$

The combination used for the seismic analysis is:

$$Gk + E + 0.3Qk \quad (3.5)$$

Where E is action effect due to the combination of the effects of the horizontal component of the seismic action

3.4. Static design of the case study

The static design of the building is done under the vertical static action considering only the permanent and imposed loads. It consists of the design of a beam, a column a part of the retaining wall and the foundation. The selected beam and column elements are considered representative of the other elements of the structure.

The structure will be studied in two phases. Firstly, it will be designed as initially planned, i.e., 2 basements + G +Mezzanine +4 (G for ground floor). Secondly, the columns and foundations will be checked after its extension to G+Mezzanine+6. Before the design phase of these structural elements, the concrete cover must be defined in order to meet the durability requirements of the structure.

3.4.1. Durability and concrete cover

For a structure of class S4 and exposure class XC1, following the procedure described in section 2.6.1, the nominal concrete cover is given by

$Cmin$ = max (20,15,10) = $20mm$

$Cnom$ = $20mm$ + $10mm$ = $30mm$

Thus, the concrete cover considered will be 30 mm for the designs.

3.4.2. Design of beam

The horizontal structural elements of the considered building are composed of the beams which support the slab. The principal beam chosen for the design is highlighted in the figure 3.4 and has same influence area according to the span.

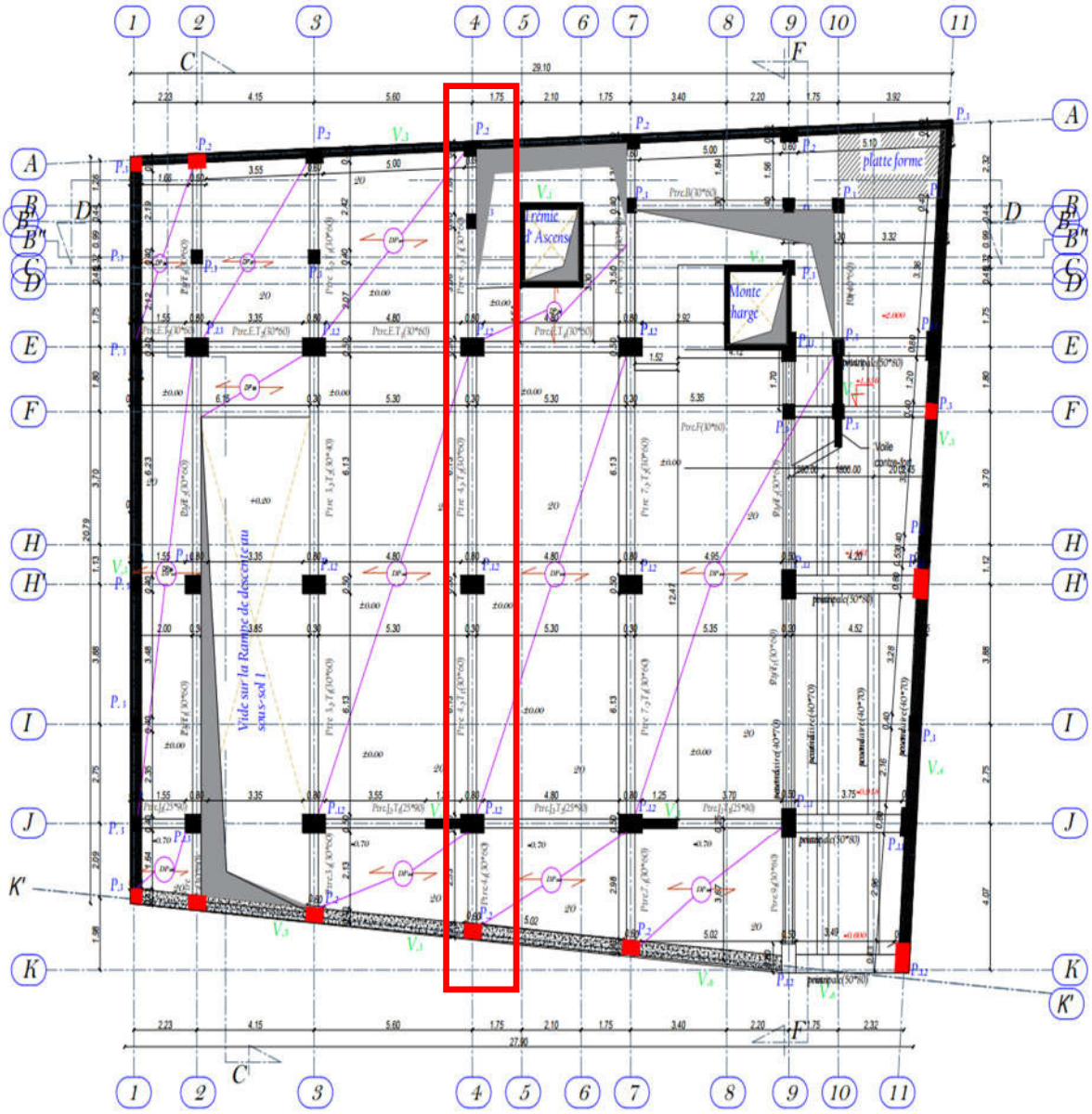

Figure 3.4 chosen beam

the preliminary dimensions for the design are obtained to satisfy the conditions $h \geq \frac{L}{14} = \frac{663}{14} = 47.35\ cm$ and $0.3h \leq b \leq 0.5h$ thus, the dimensions h=60cm and b=30cm can be considered for the design.

From this model, six loads arrangements are defined for the design of the beam and are presented in the Figure3.5

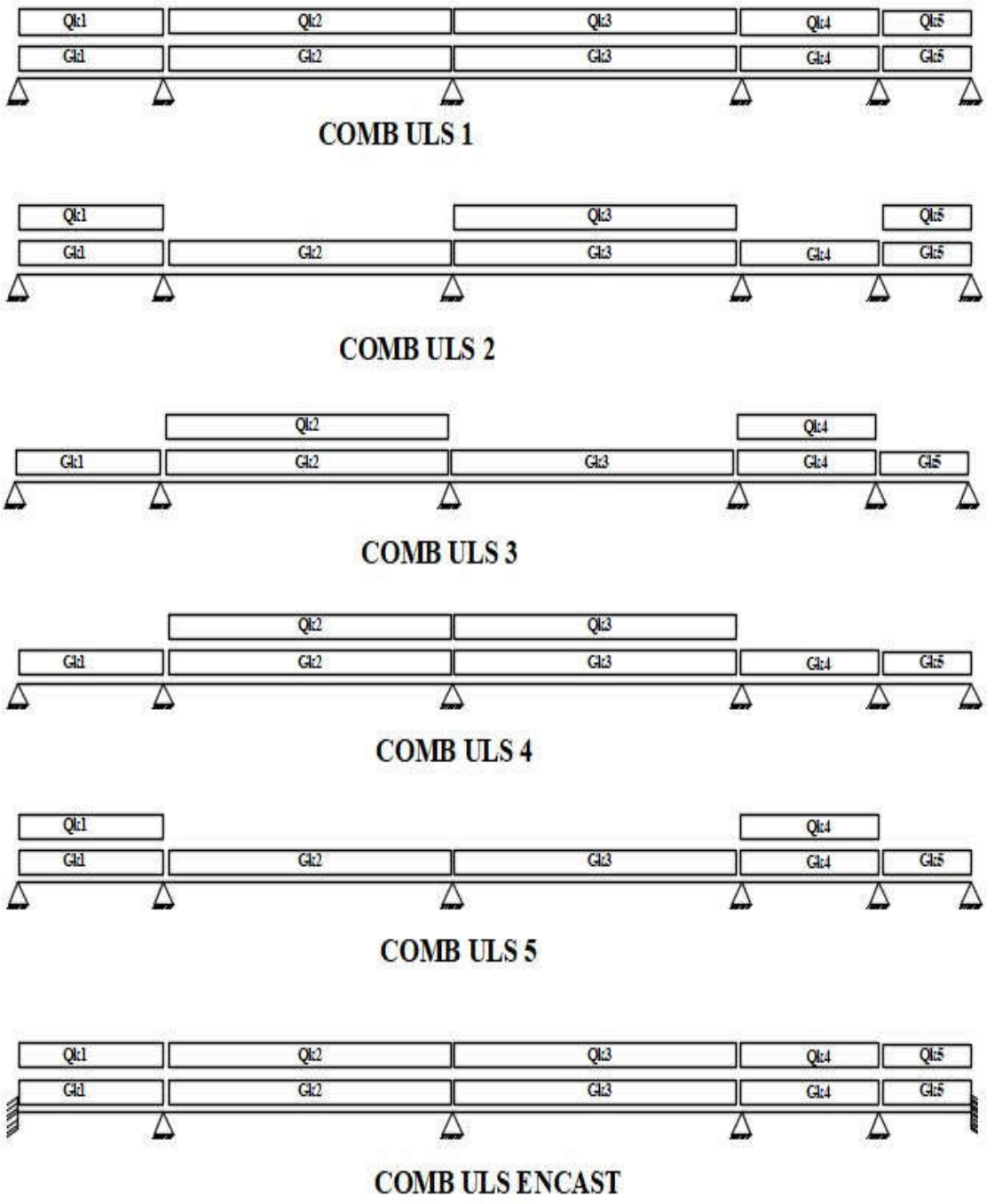

Figure 3.5. Loads combinations on the beam.

3.4.2.1. Ultimate limit state design

The loads arrangement inserted in the software SAP 2000 permit to obtain solicitations curves along the beam for the bending moment and the shear force as represented in figure

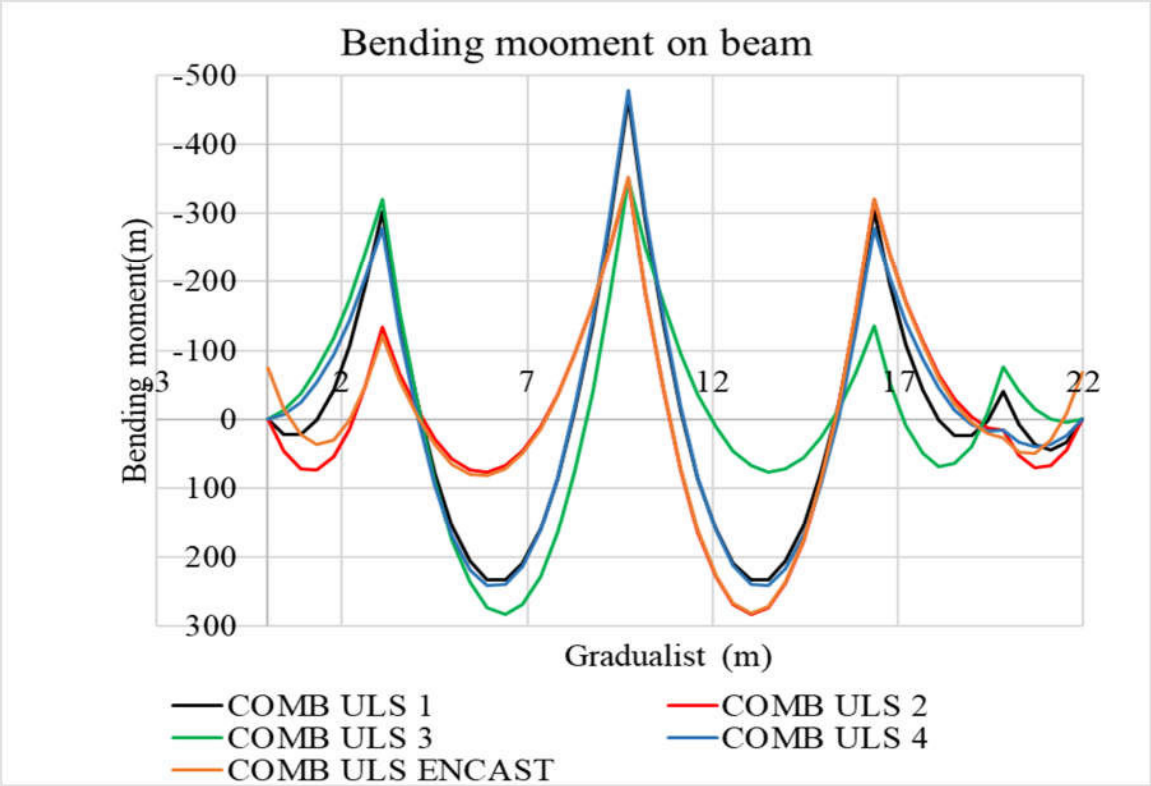

Figure 3.6. Bending moment curves on the beam.

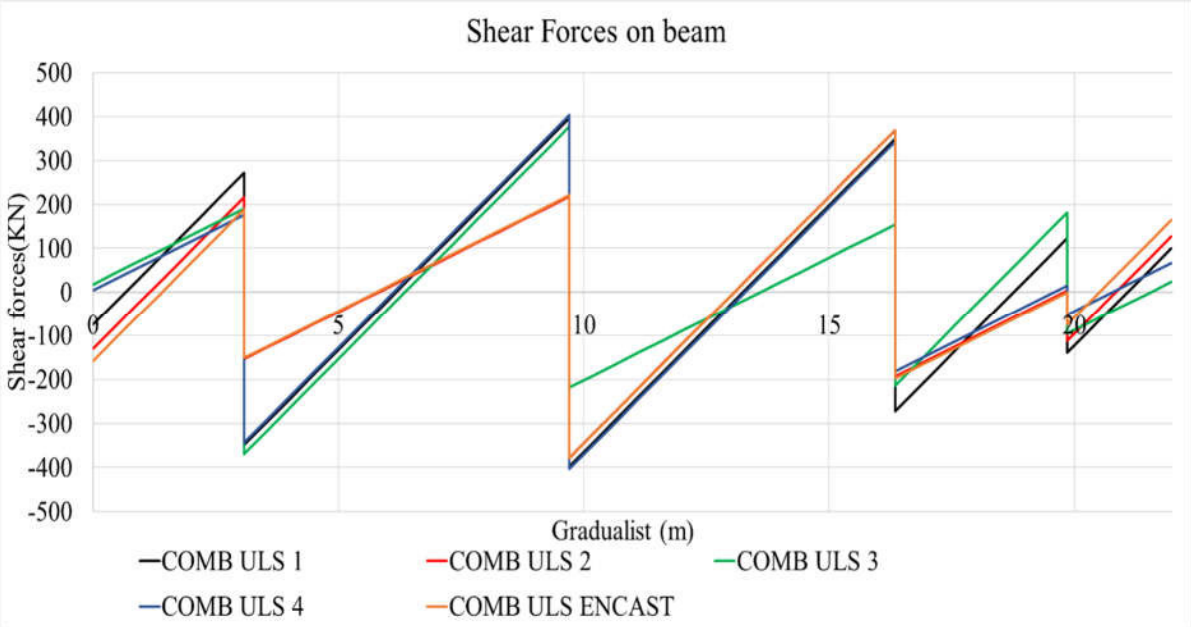

Figure 3.7. Shear solicitations curves on the beam.

both bending moment and shear forces curve permit to obtain the envelope curve of these solicitation as represented in figure.

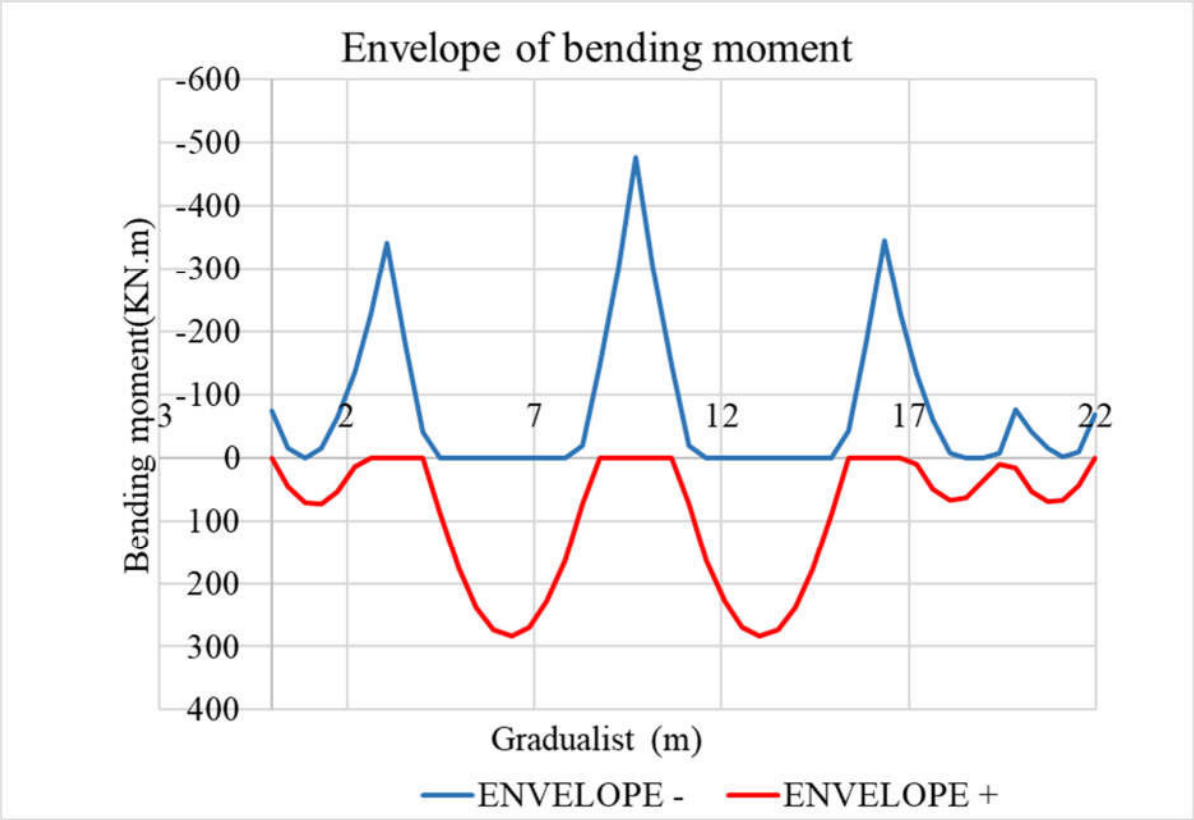

Figure 3.8. Envelope curve of bending moment on the beam

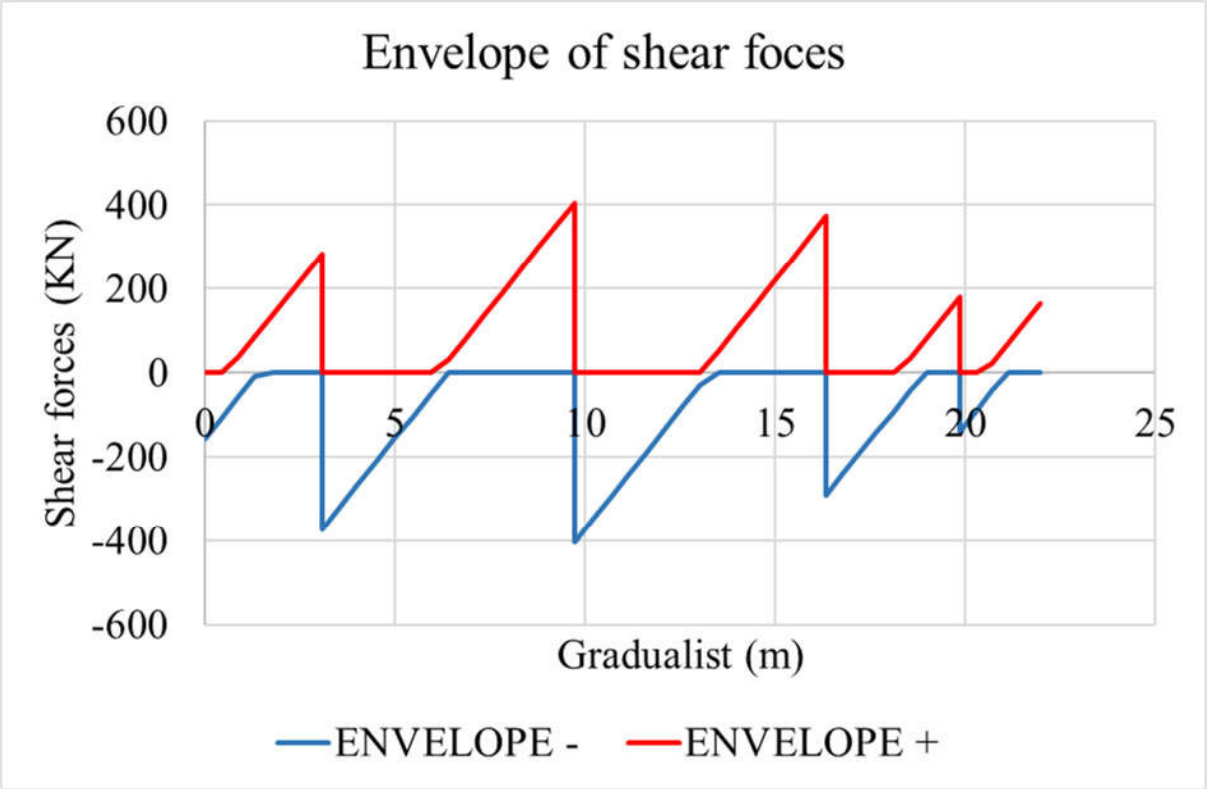

Figure 3.9 . Envelope curve of shear on the beam

the reinforcement cross-sections are calculated using Equation 2.1. verifications are performed on the element using Equations 2.2 and 2.3. Finally, the steel sections are checked for a beam section of 350× 700 mm. Figure 3.10 below shows the reinforcement obtained from the previous calculations.

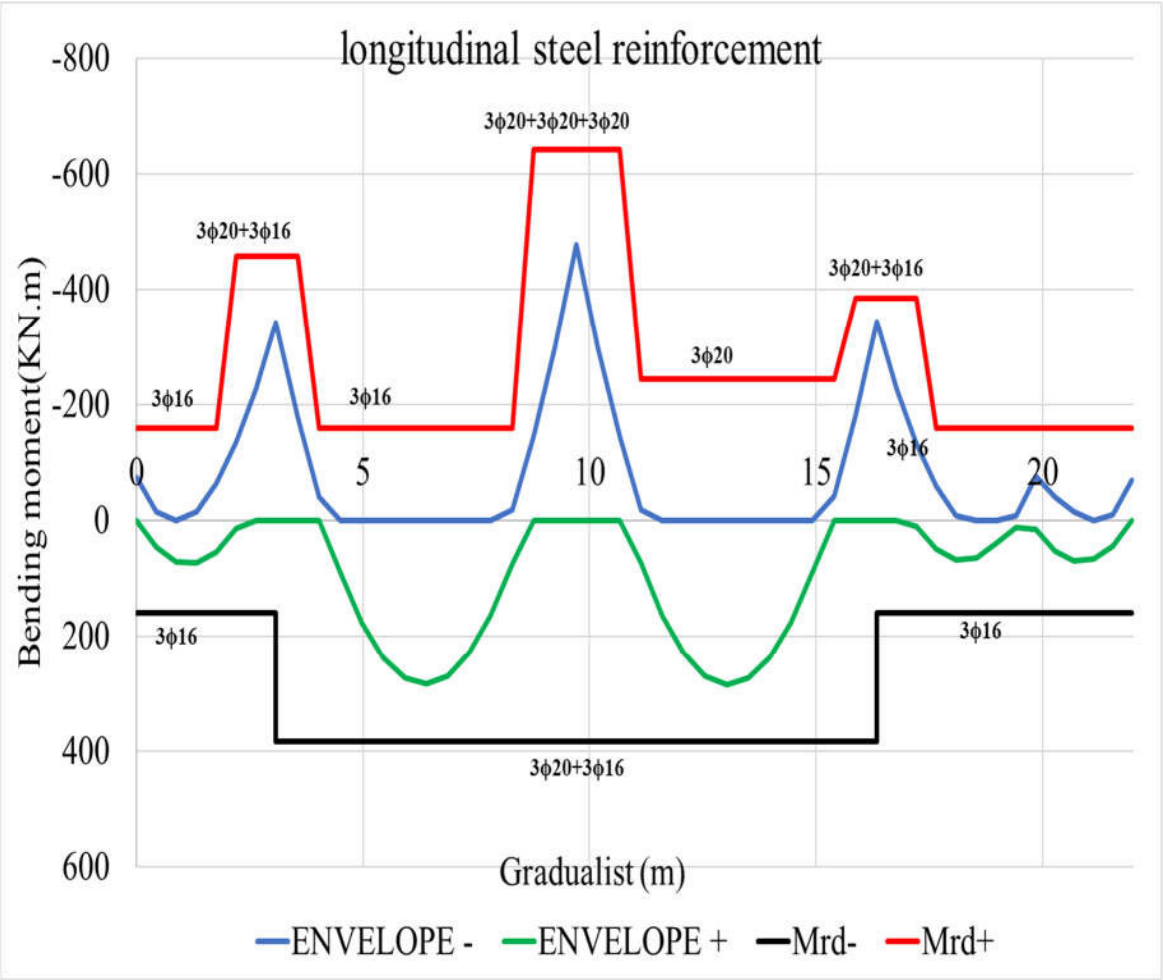

Figure 3.10 . Recapitulative curve of the bending moment verification of the beam

For the transversal reinforcement, considering a diameter of 6 mm the design procedure presented on the section 2.6.2.1.b permits to obtain the spacing of the stirrups necessary to resist to the envelope of the shear solicitations. Figure 3.11 presents a recapitulative of these stirrups spacing along the beam.

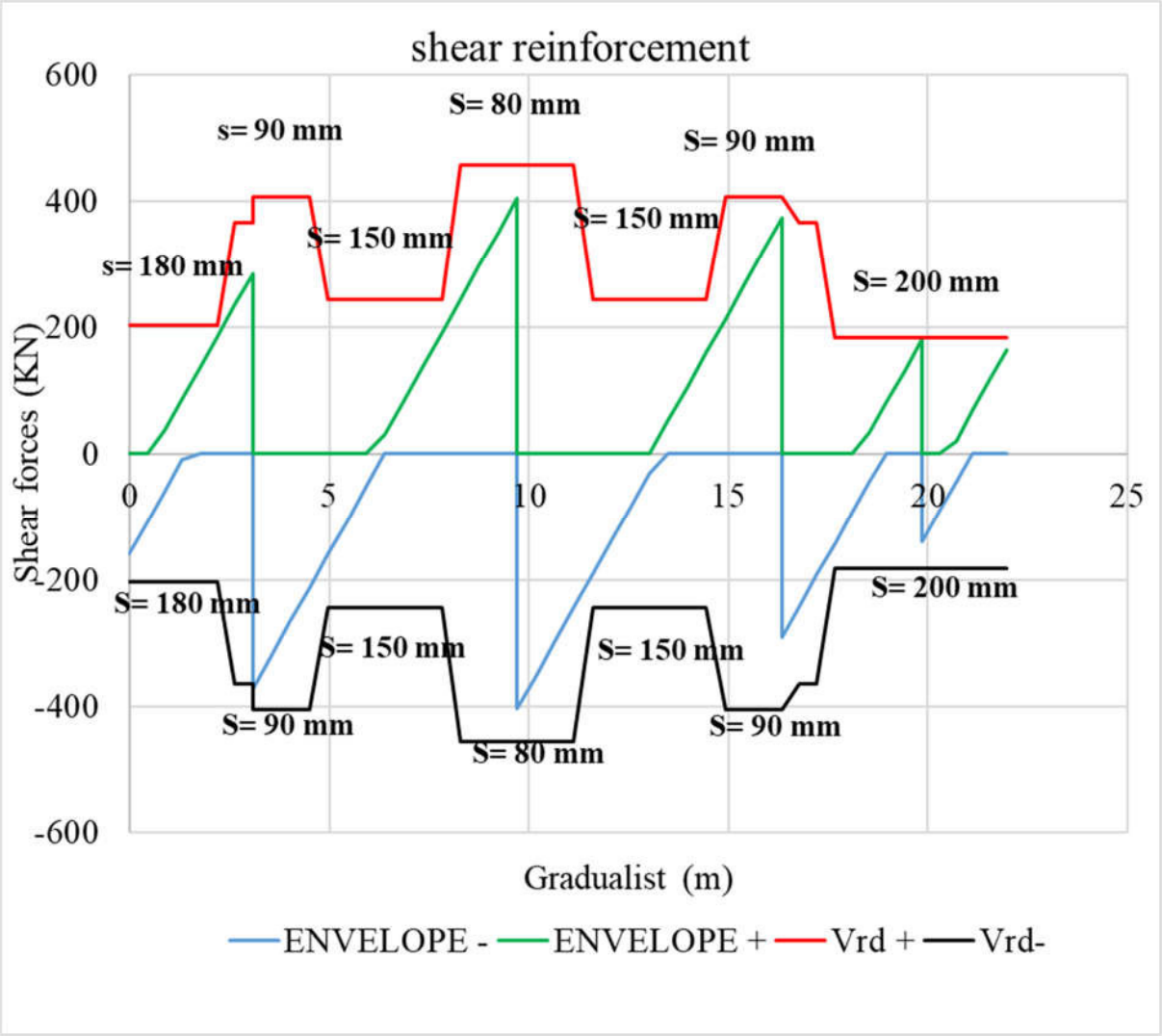

Figure 3.11. Recapitulative curve of the shear verification of the beam.

3.4.2.2. Serviceability limit state

The seven load arrangements inserted in SAP 2000 at the characteristic (rare) combination permit to obtain the solicitation curves presented in the figure 3.12.

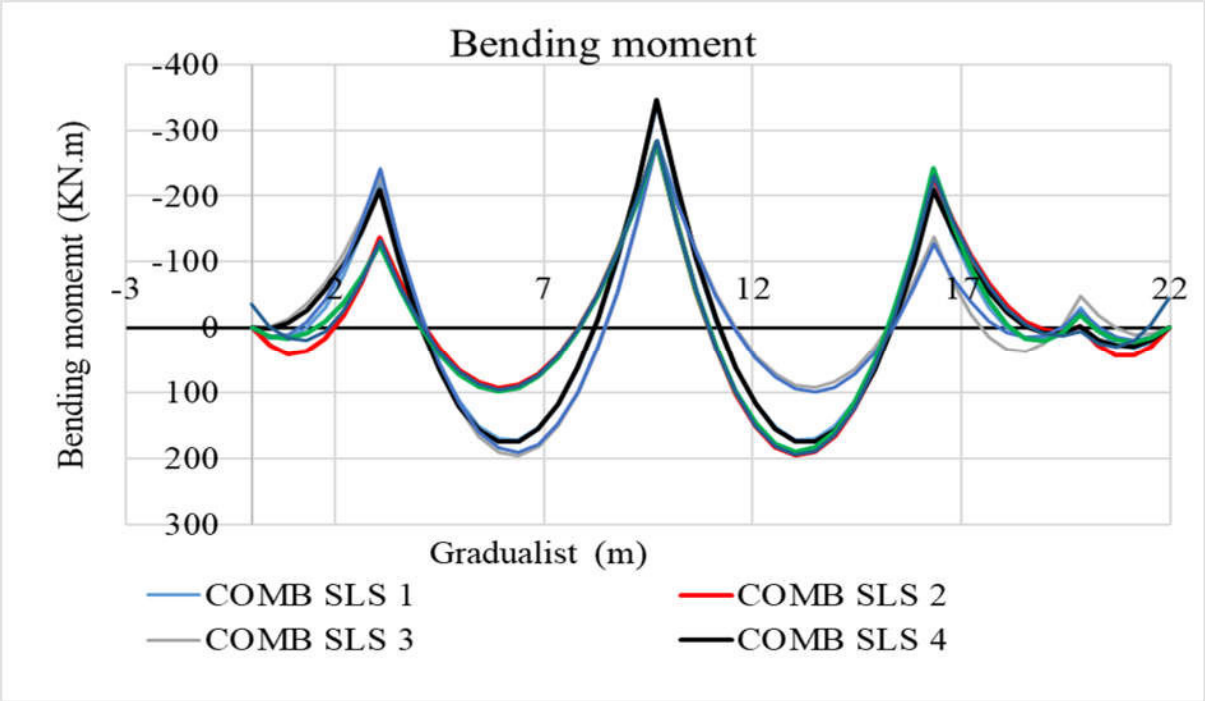

Figure 3.12. Bending moment curves on the beam at SLS

These solicitations permit to obtain the envelope curve presented in the figure 3.15

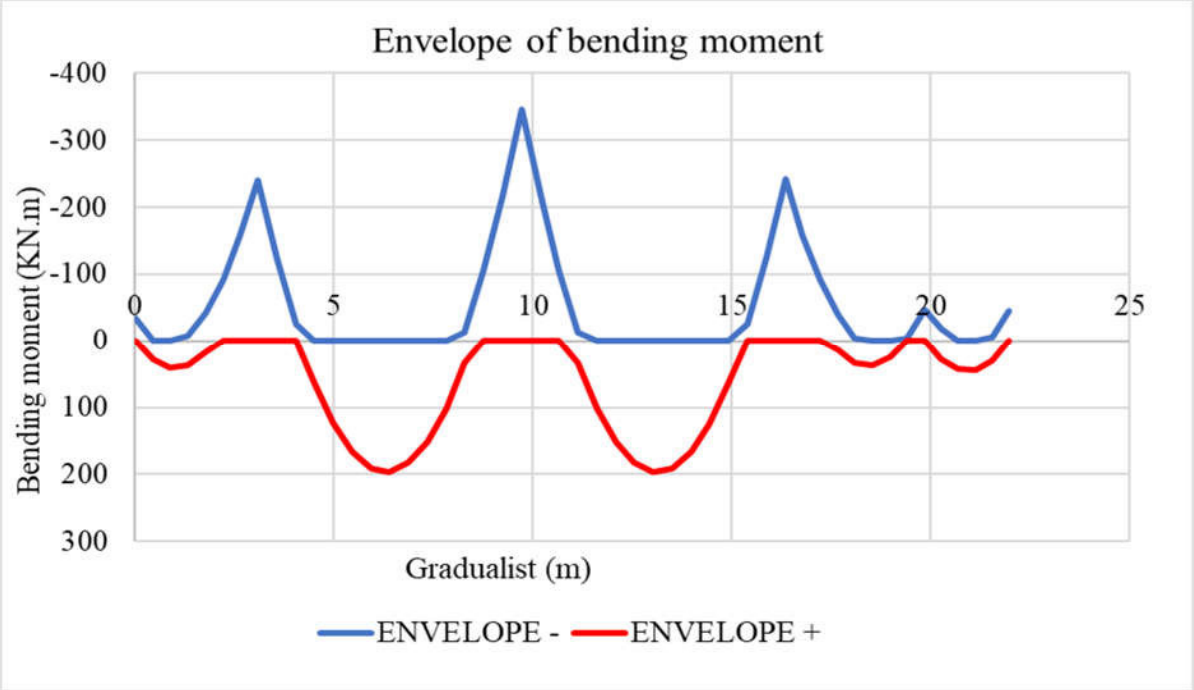

Figure 3.13. Envelope curve of the bending moment solicitation at serviceability limit

using this envelope curve for bending moment at serviceability limit state the stress in the concrete and steel are obtained using the equations 2.30 and 2.31.

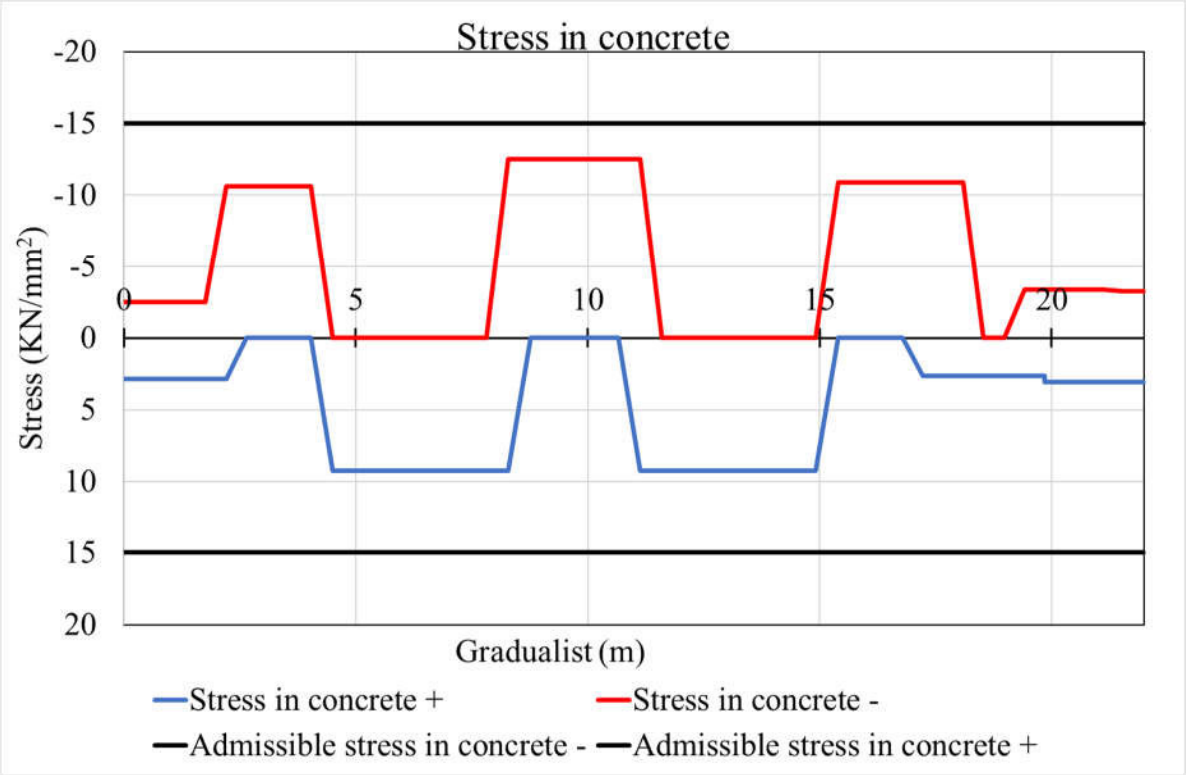

(a)

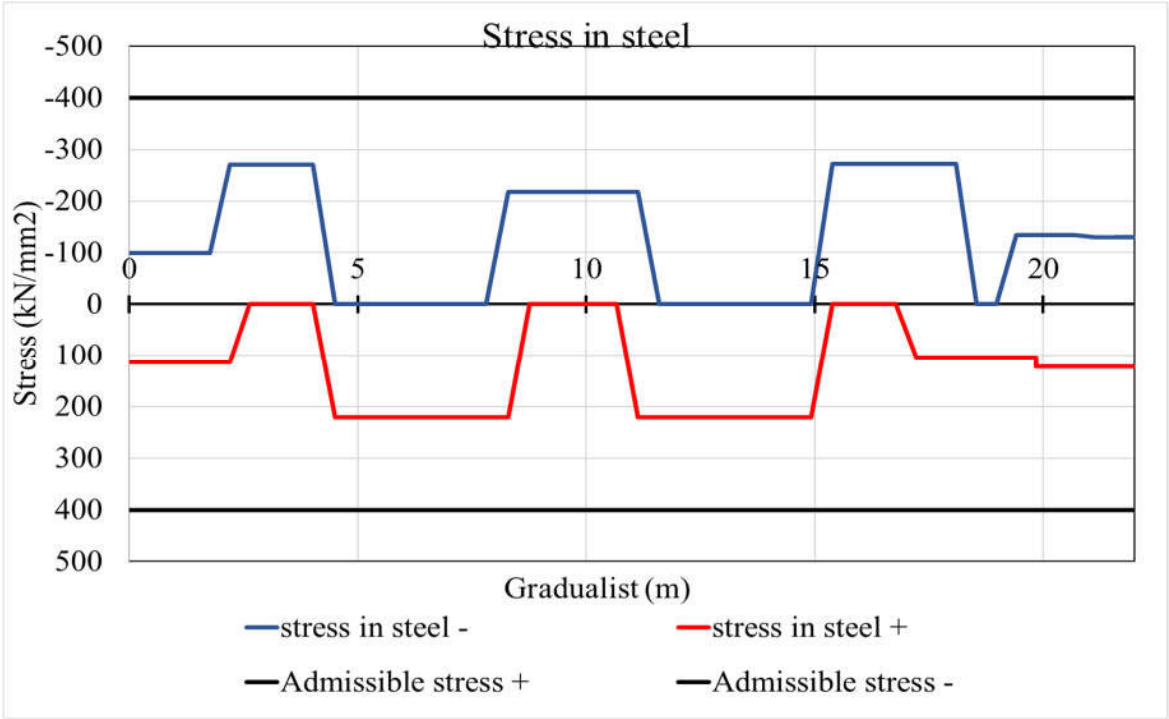

(b)

Figure 3.14. Recapitulative curve of stress verification of the beam: (a) in the concrete;(b) in the steel.

The structural detailing of the beam is presented on the Annex

3.4.3. Design of columns row

The preliminary design, the M-N verification, the shear verification and slenderness are presented.

3.4.3.1. Preliminary design

The columns chosen for the design are P1 and P2, shown in Figure 3.15. The vertical elements as well as the horizontal elements are modelled as frame elements. Column P1 has the largest axial force while P2 has the largest bending moment in both directions.

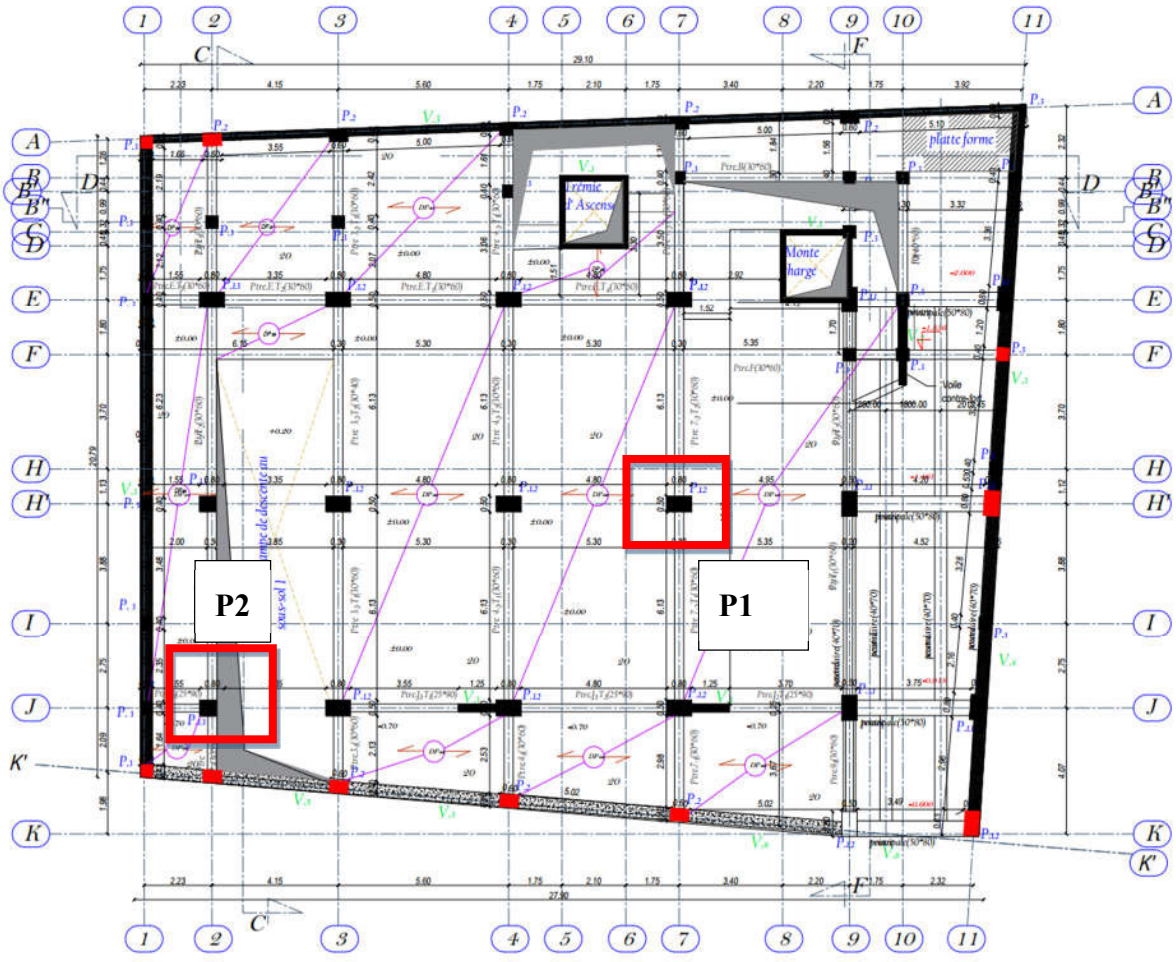

Figure 3.15. chosen column

column p1 is the one with the highest axial force and p2 the one with the highest bending moments

Using equations 2.19, the section of columns for basement to level 1 has to be Ac ≥ 573627.6 mm^2 for column P1. The same section can be used for P2

Considering a rectangular section, the dimensions can be a = 800 mm and b = 500 mm from basement to level 1. Repeating the procedure, dimensions can be a=500mm and b=400 mm for level 1 to level 4.

The structural model of the building is modelled using SAP 2000 software with frame elements for beams and columns, shell tick elements for walls. The cross-sectional dimensions of the beams are 35 cm wide and 70 cm high. The cross-sections of the columns are as pre-dimensioned above. Figure 3.16 shows the numerical model of the structure after modelling

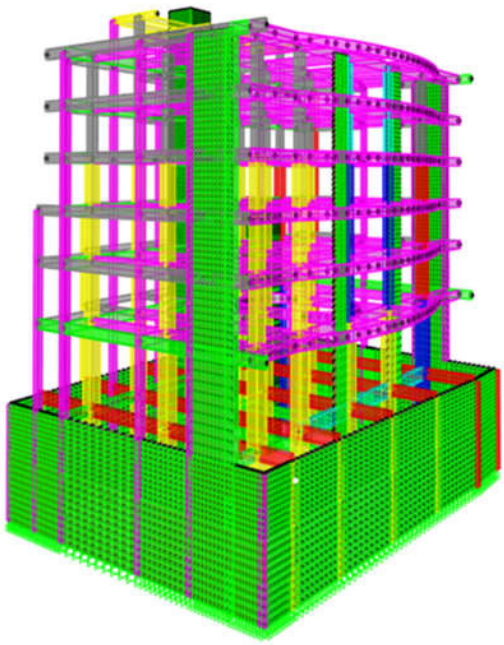

Figure 3.16. Numerical model of the building

3.4.3.2. Column with maximum axial forces

a. Axial and bending moment verification

Columns are designed for the six previous loads combinations. This permit to obtain different solicitation envelope curves for the axial loads and bending moment presented in figure 3.17, figure 3.18 and figure 3.19 respectively.

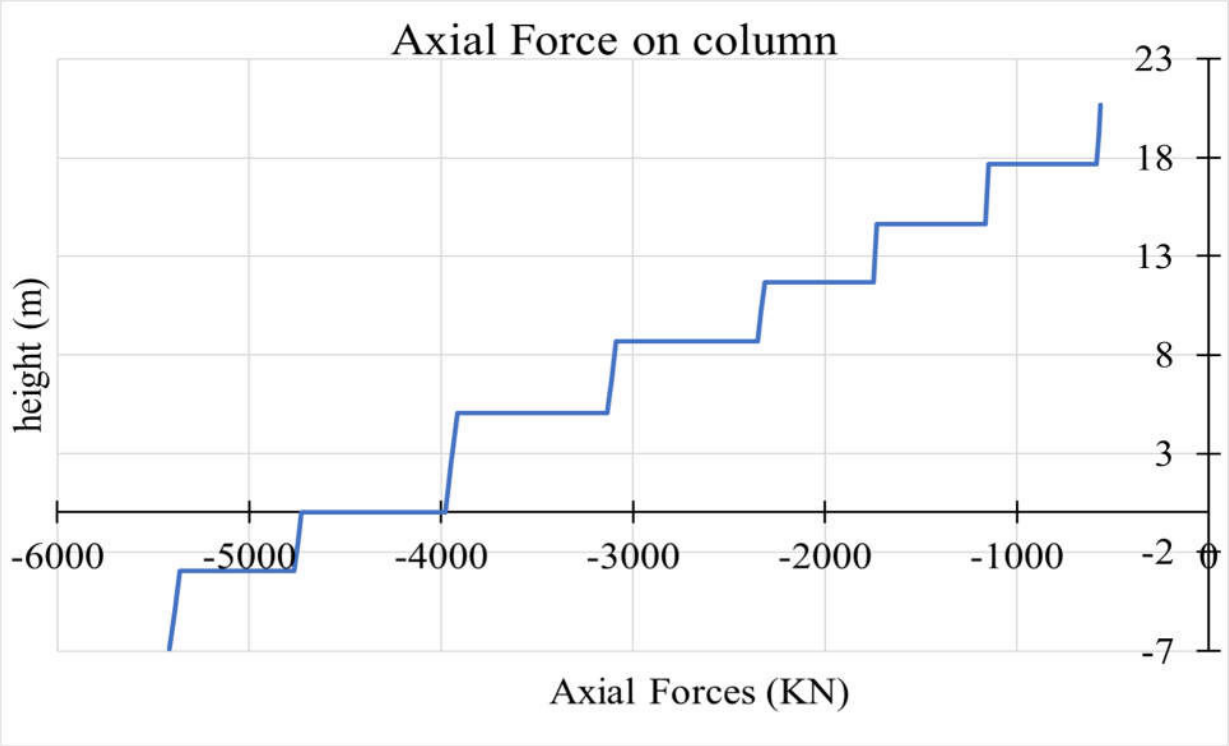

Figure 3.17 . Axial load envelope curve.

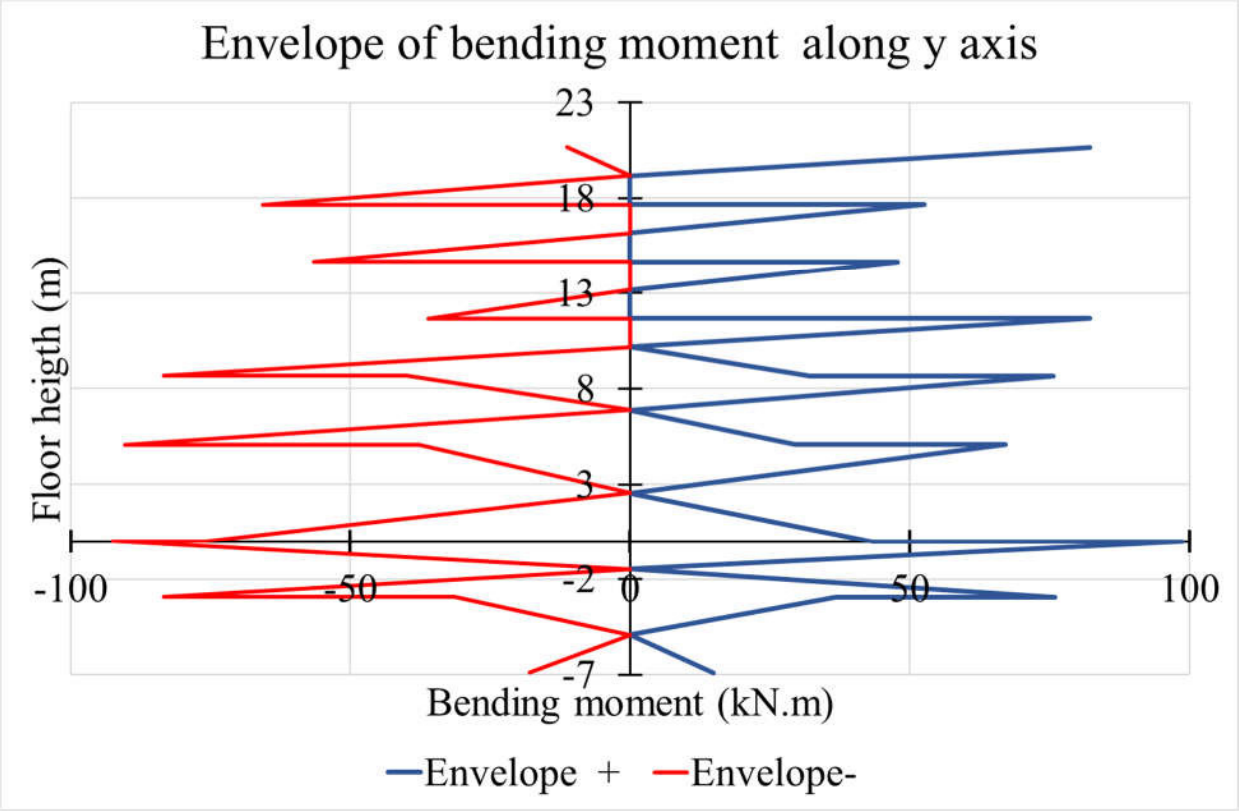

Figure 3.18. Bending moment curve around the x-axis in the column.

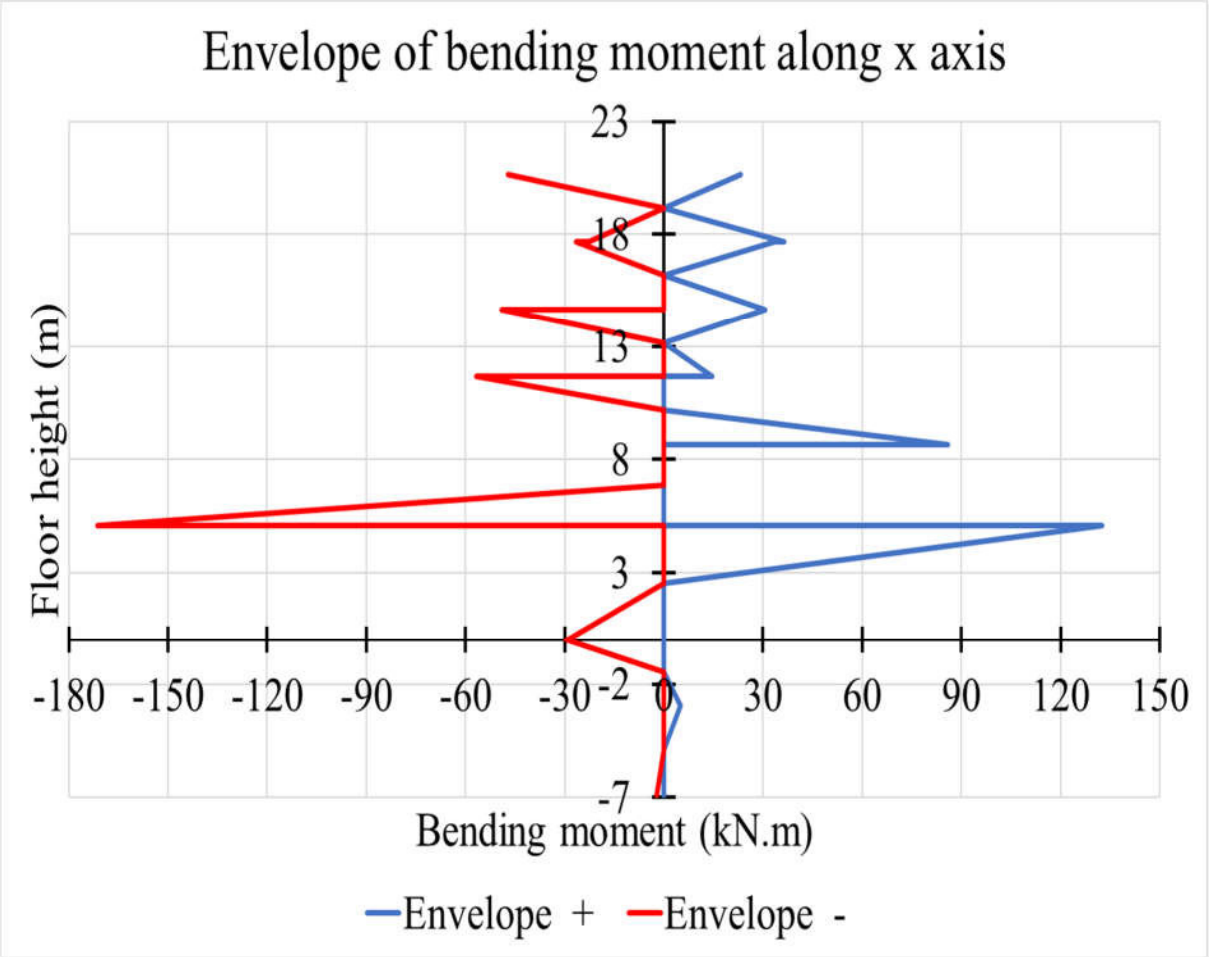

Figure 3.19. Bending moment curve around the y-axis in the column.

The verification of the axial loads and the bending moment is done through the interaction diagram as presented in the paragraph 2.4.3.2. In this case study, considering all concrete sections for different levels, the limitations prescribed in the equations 2.45 and 2.46 the reinforcement in the columns are presented in table 3.8

Table 3.8. Column renforcement.

	Section		As, min(mm2)	As max(mm2)	Reinforcement	As,provided (mm2)
	b(cm)	h(cm)				
Basements to level 1	50	80	800	16000	12 Ø14	1847.25
Level 2 TO 4	40	50	400	8000	4Ø14+6Ø12	1294 .33

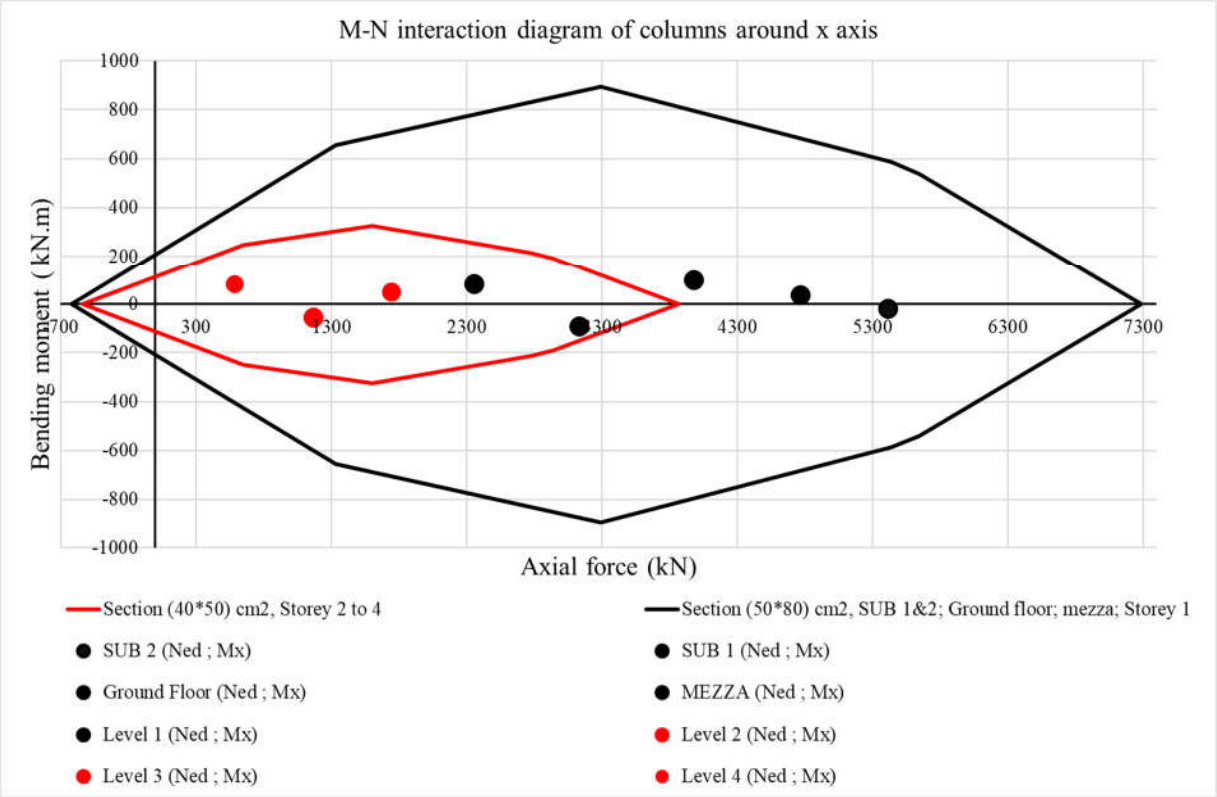

Figure 3.20 . Interaction diagram of column P1 in x direction

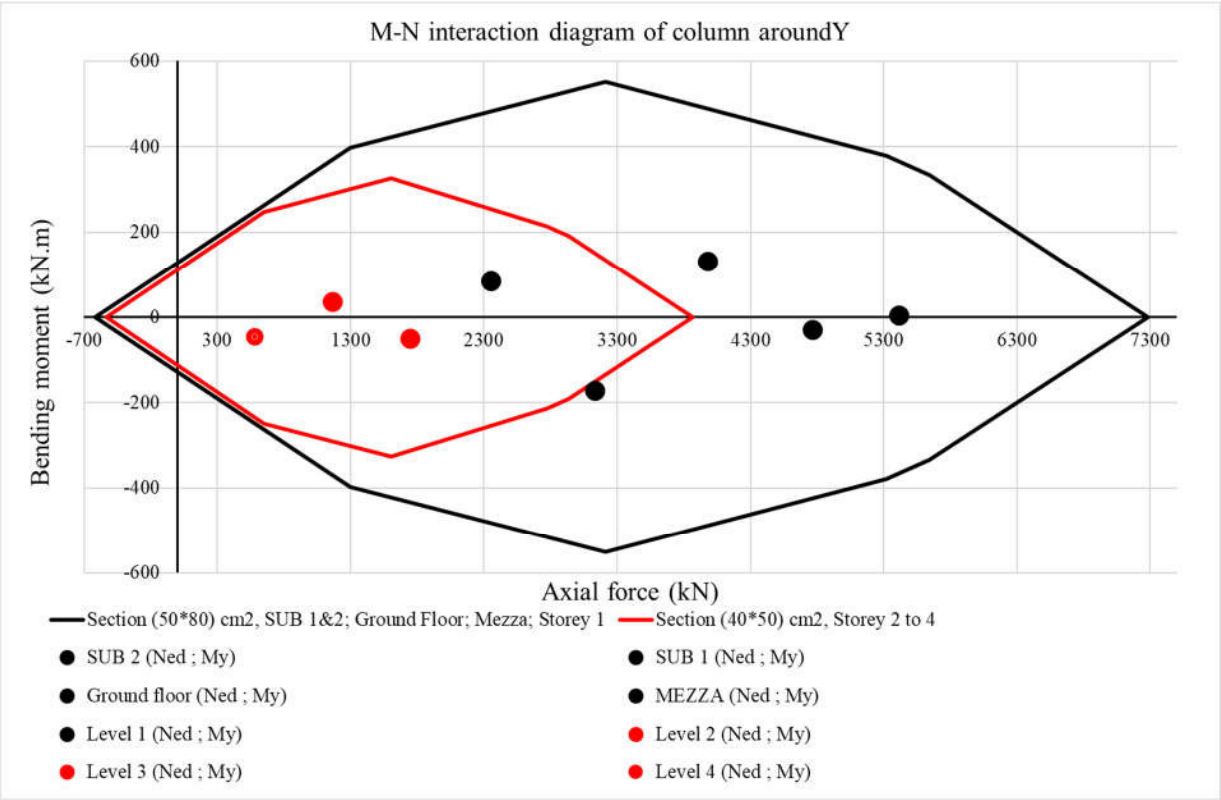

Figure 3.21. Interaction diagram of column P1 in y direction

b. Shear verification

The different load arrangements permit to obtain envelope curves of shear forces in the x and y-direction presented in Figure 3.22

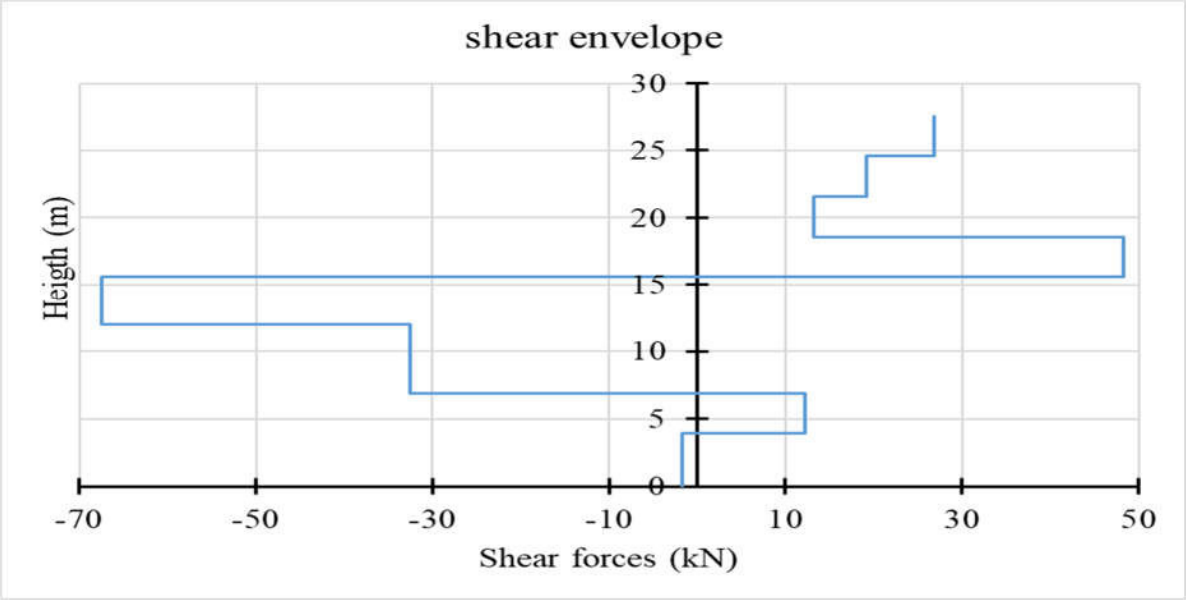

(a)

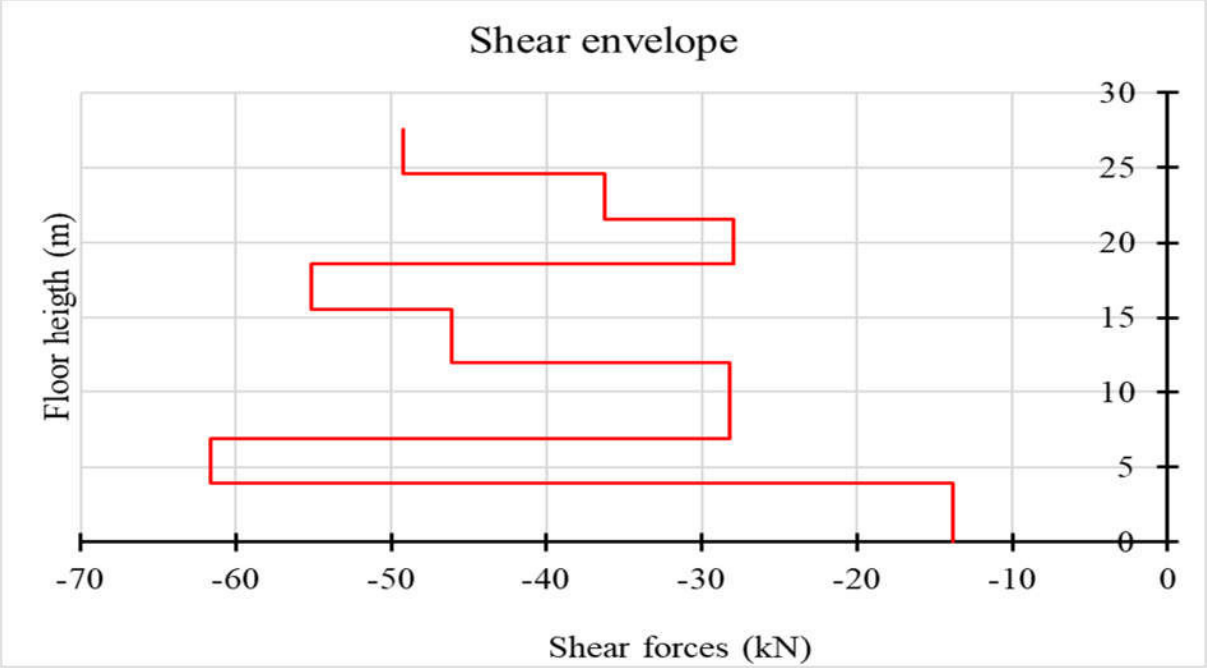

(b)

Figure 3.22. Shear force envelope curve on the column:(a) in x direction, (b) in the y direction

Applying the procedure presented in the section 2.6.2.1.b, shear resistance of the section without shear reinforcement is greater than the maximum shear solicitation on the column so the detailing of members has to be applied to have the spacing. In this case, a diameter of 8 mm is consider and the maximum spacing of the transverse reinforcement is given by:

$S_{cl,\,max}$ = min (280,500,400) = 280 mm

So, applying the prescriptions of the section 2.6.2.1.b, the space of the shear reinforcement of: 15 cm within 0.55 cm above and below the beams and 20 cm for the rest of the column.

c. Slenderness verification

Following the procedure presented on the section 2.4.3.3, the different parameters are evaluated and presented in table 3.9

Table 3.9 . Parameter for slenderness verification.

Level	λx	λy	λlimx	λlim y
Basement 2	18.67	9.01	26.74	26.74
Basement 1	15.28	7.37	28.50	28.50
Ground level	24.61	11.87	31.19	31.19
Mezza	17.46	10.91	35.15	35.15
Storey 1	14.55	9.09	40.58	40.58
Storey 2	18.19	6.43	35.14	35.14
Storey 3	18.19	13.01	43.03	43.03
Storey 4	18.19	13.01	60.85	60.85

Table 3.9 shows that $\lambda < \lambda_{lim}$, so the slenderness of the column is verified.

The structural detailing of the column is presented on the Annex

Column with maximum bending moment

3.4.3.3. Column with maximum bending moment

a. Axial forces and bending moment verification

The envelope of solicitation of this column is also done through the six previous loads combinations that was done for the beam.

Theses envelope curve are presented in the figure 3.23 and 3.24 for the axial, and bending moment respectively.

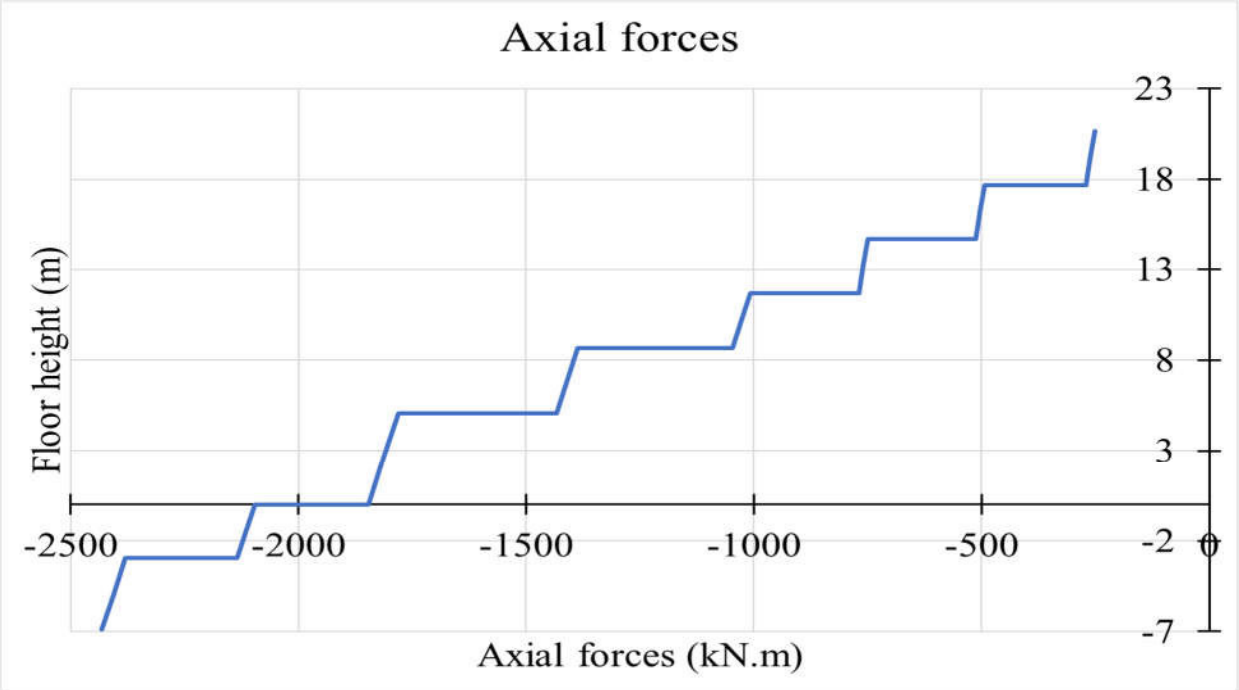

Figure 3.23. Axial load envelope curve

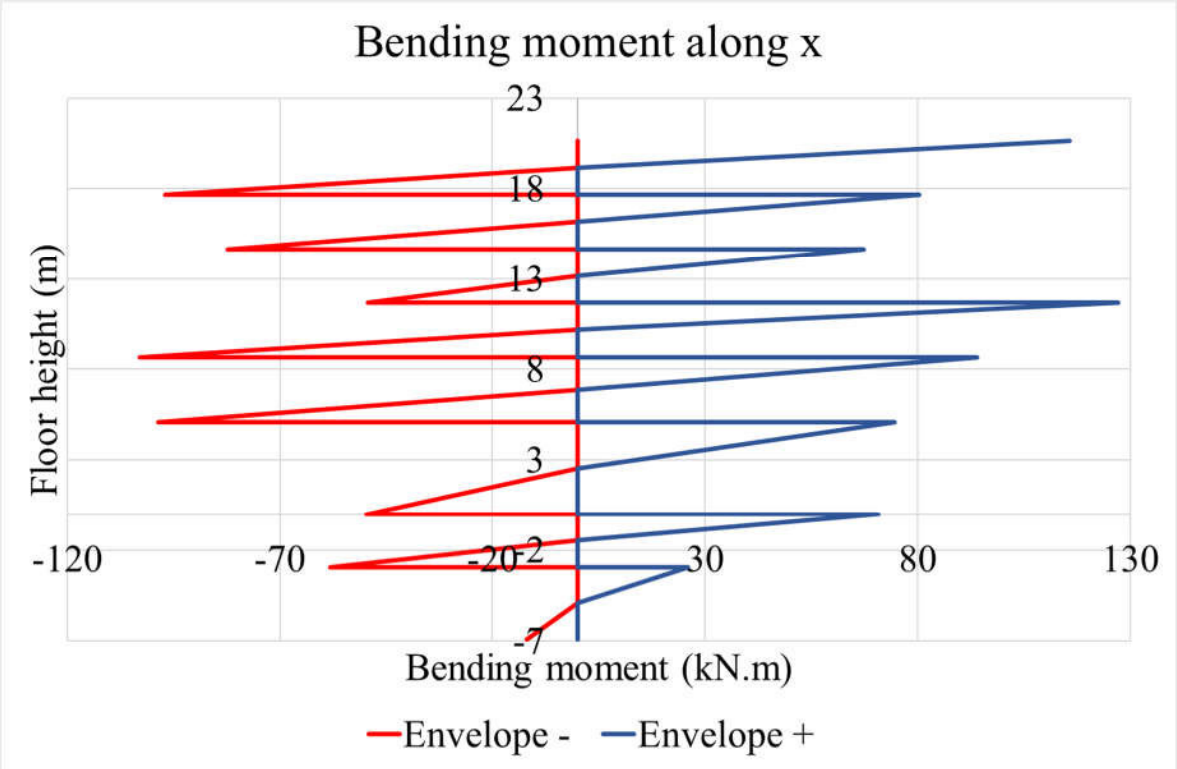

(a)

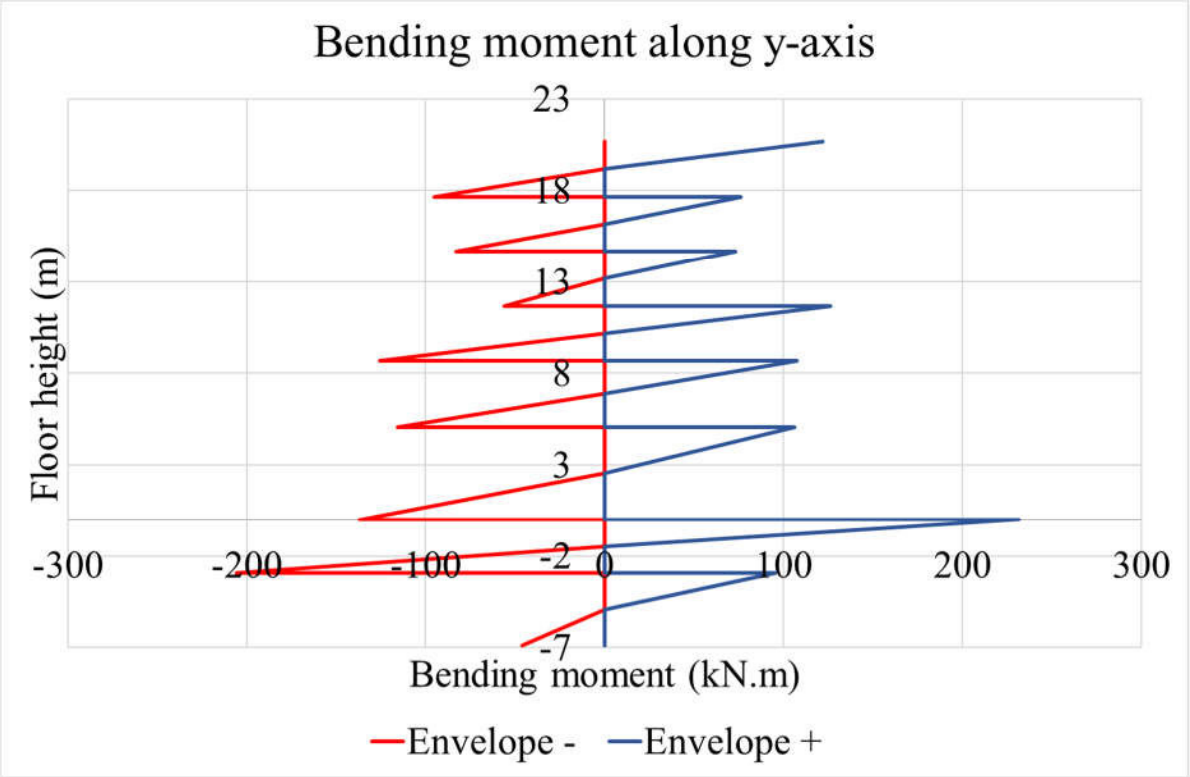

(b)

Figure 3.24. Bending moment curve along: (a) x-axis and (b) y-axis

verification of the axial loads and the bending moment is done through the interaction diagram the reinforcement in the columns are presented in table 3.10

Table 3.10. Columns reinforcement

	Section (cm×cm)	As, min(mm2)	As max(mm2)	Reinforcement	As,provided (mm2)
Basements to level 1	50×80	800	16000	12 Ø14	1420
Level 2 TO 4	40*50	400	8000	4Ø14+6Ø12	1294,33

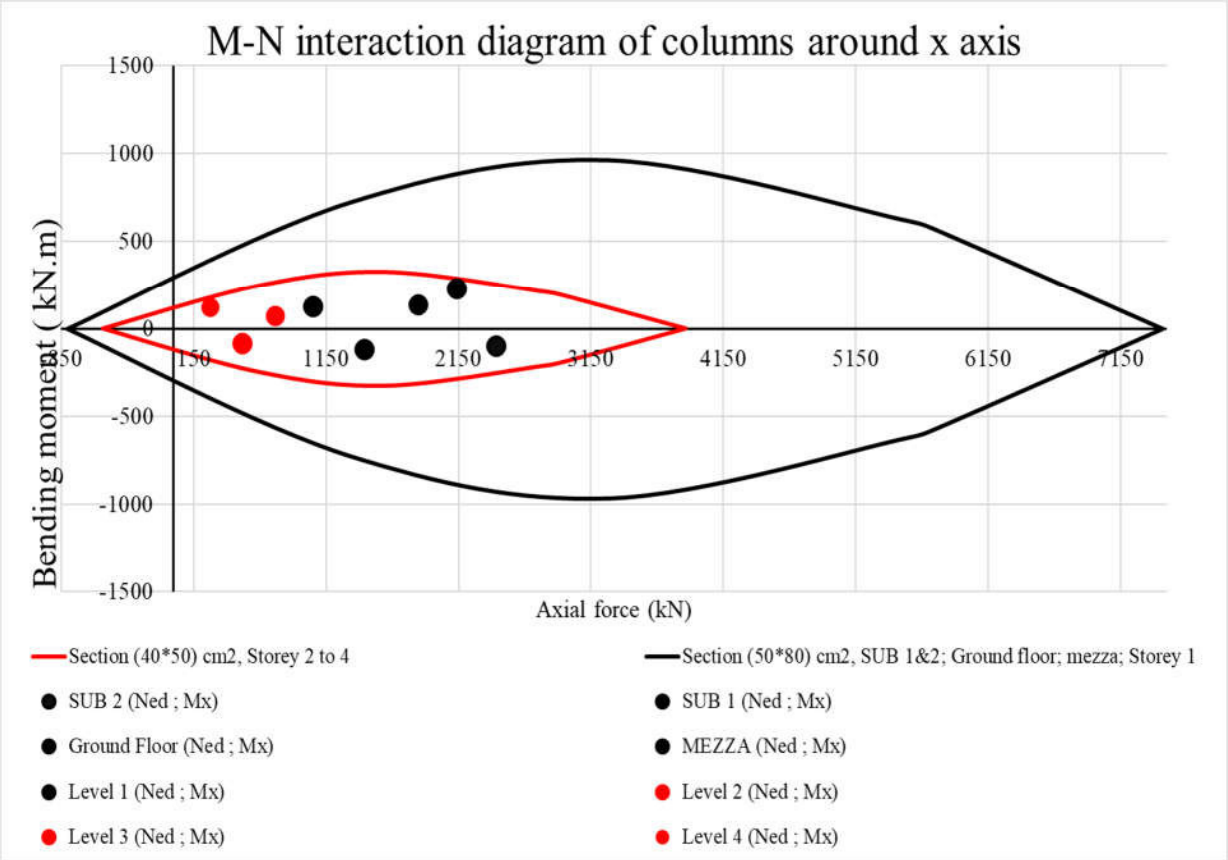

(a)

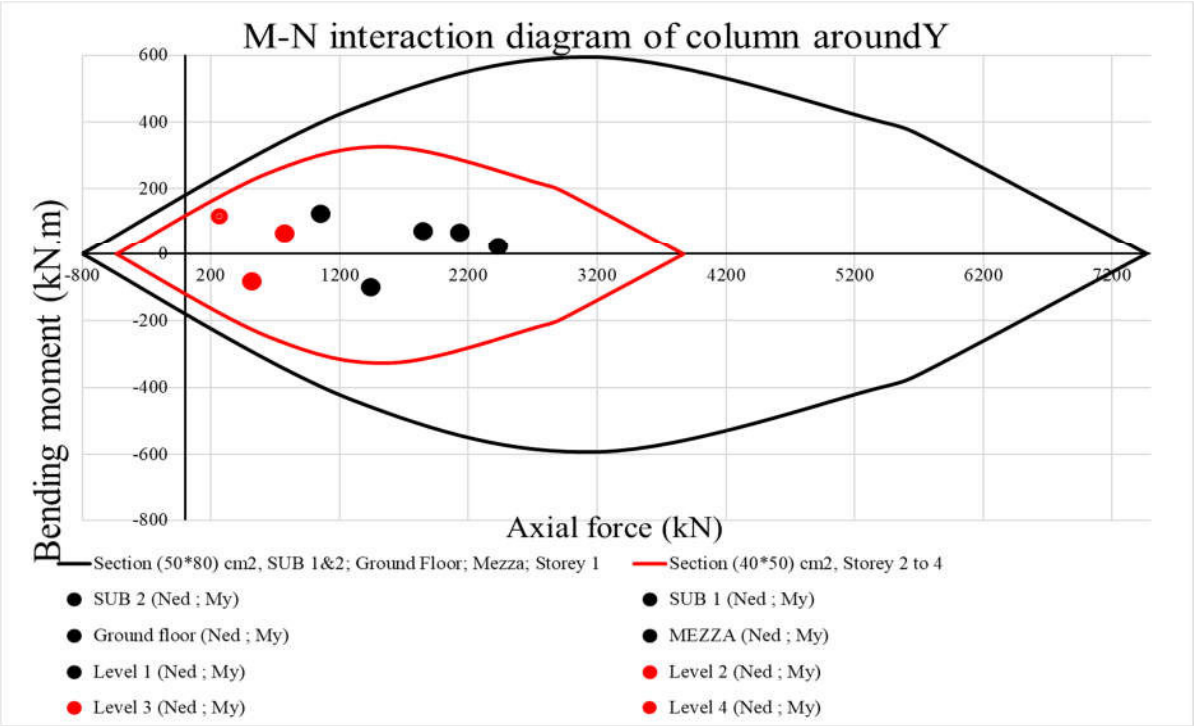

(b)

Figure 3.25. Interaction diagram of column P2 (a) around x-axis (b) around y-axis

b. Shear verification

The different load arrangements permit to obtain curves in the x and y-direction as presented in the figure 3.26

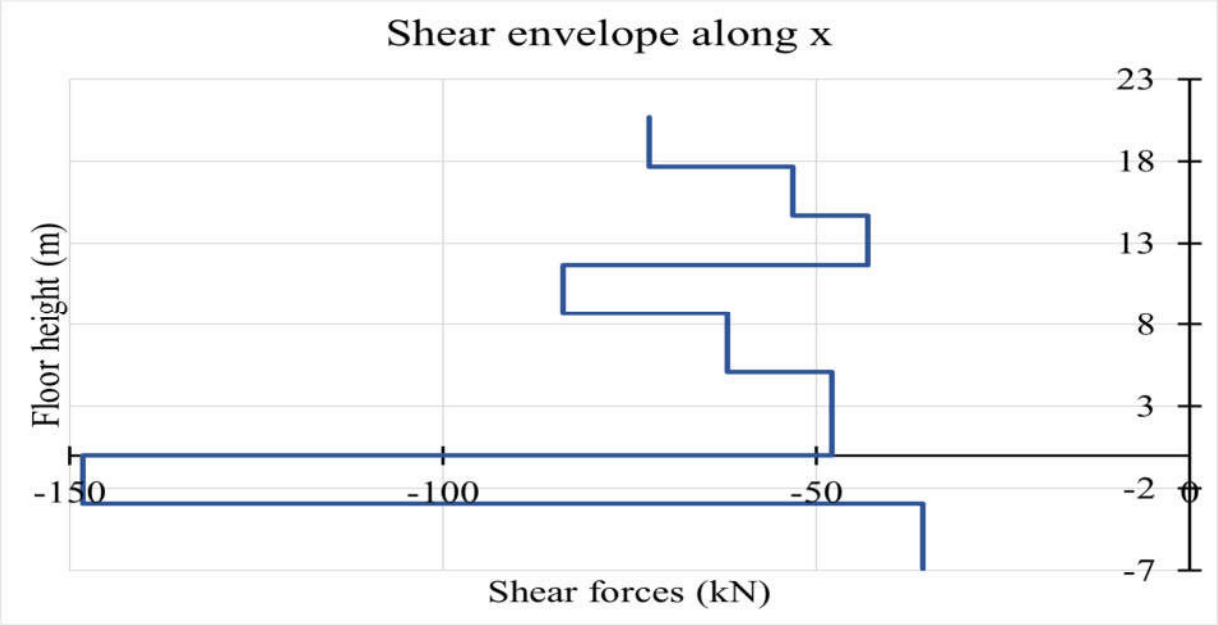

(a)

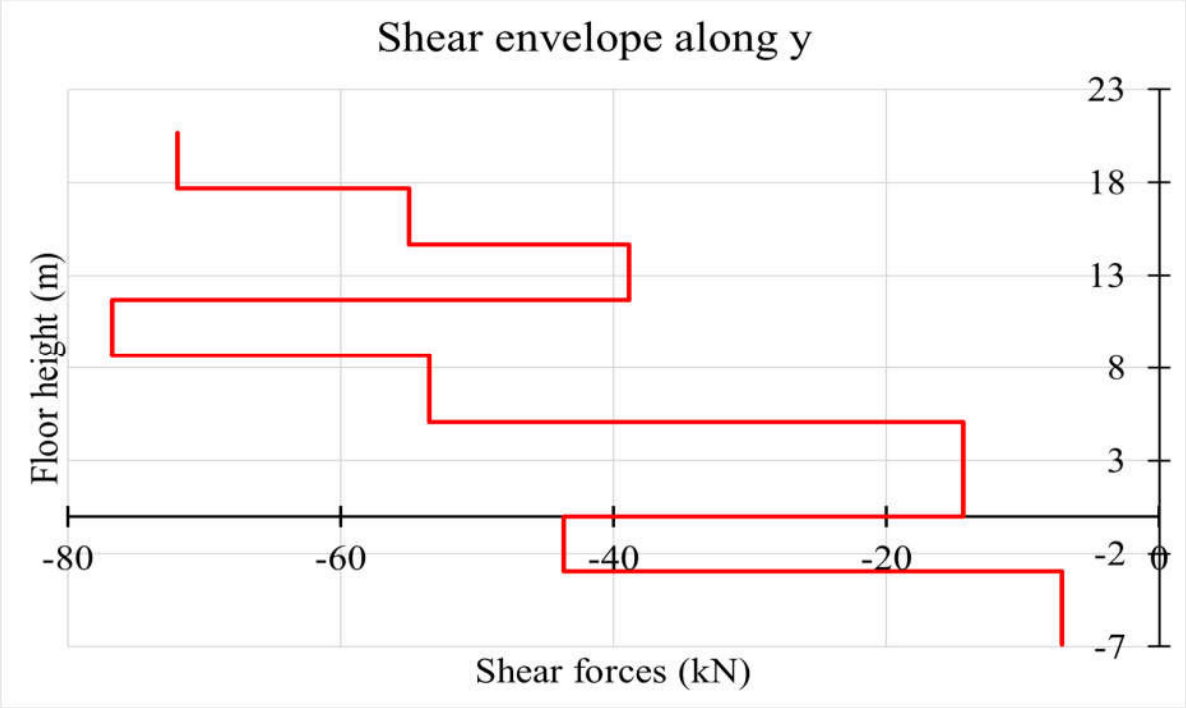

(b)

Figure 3.26. Shear force envelope curve on the column:(a) in x direction, (b) in the y direction

Applying the procedure presented in the section 2.6.2.1.b, shear resistance of the section without shear reinforcement is greater than the maximum shear solicitation on the column so the detailing of members has to be applied to have the spacing. In this case, a diameter of 8 mm is consider and the maximum spacing of the transverse reinforcement is given by:

$S_{cl,\,max}$ = min (280,500,400) = 280 mm

So, applying the prescriptions of the section 2.6.2.1.b, the space of the shear reinforcement of: 15 cm within 0.55 cm above and below the beams and 20 cm for the rest of the column.

c. Slenderness verification

Following the procedure presented on the section 2.4.3.3, the different parameters are evaluated and presented in table 3.11

Table 3.11 . Parameter for slenderness verification.

Level	λx	λy	λlimx	λlim y
Basement 2	18.67	9.01	26.74	26.74
Basement 1	15.28	7.37	28.50	28.50
Ground level	24.61	11.87	31.19	31.19
Mezza	17.46	10.91	35.15	35.15
Storey 1	14.55	9.09	40.58	40.58
Storey 2	18.19	6.43	35.14	35.14
Storey 3	18.19	13.01	43.03	43.03
Storey 4	18.19	13.01	60.85	60.85

Table 3.11 shows that $\lambda < \lambda_{lim}$, so the slenderness of the column is verified.

The structural detailing of the column is presented on the Annex

Column with maximum bending moment

3.4.4. Retaining wall design

This part concerns the study of the retaining wall at the basement levels of the structure. A preliminary design and structural analysis will be presented. The sliding and overturning verifications are not necessary, due to the fact that the wall is directly linked to the whole structure.

3.4.4.1. Preliminary design

The plan view and the typical cut section of the chosen retaining wall for the design are highlighted in the figure 3.18 and 3.19 respectively.

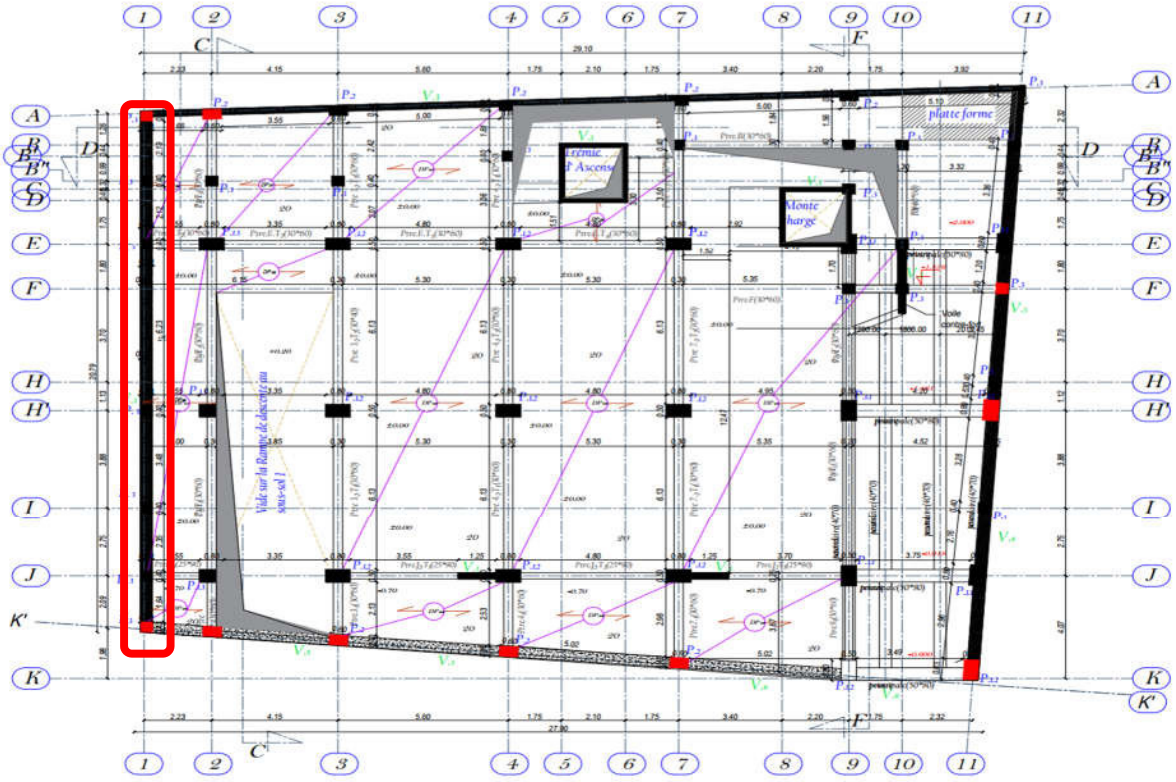

Figure 3.27. Chosen part of the retaining wall

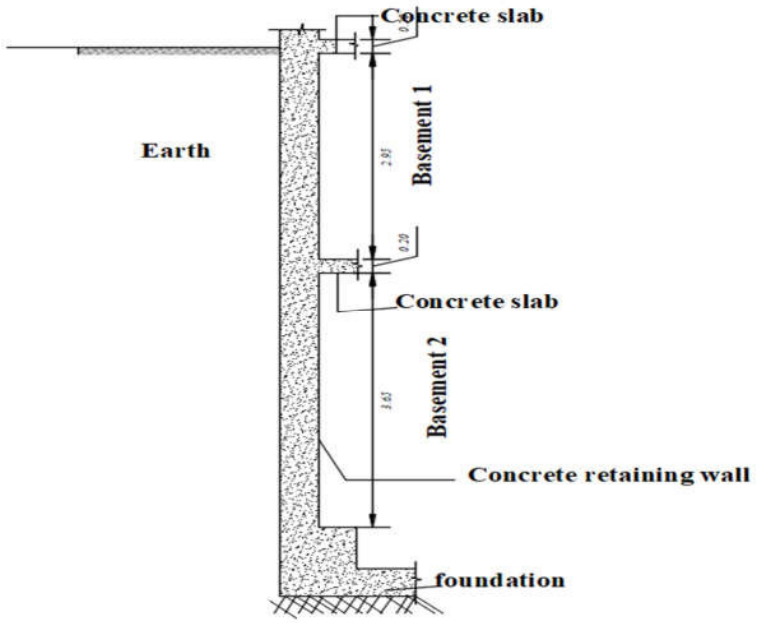

Figure 3.28. cut section of the chosen retaining wall.

The retaining wall thickness is determined using certain criterion.

$$\begin{cases} t \geq 15\ cm \\ t \geq \dfrac{h}{200} = 18{,}25cm \end{cases} \qquad Choose\ t = 40\ cm$$

3.4.4.2. Loads and loads combination

The different type of loads which are acting on the wall are summarize in figure 3.31

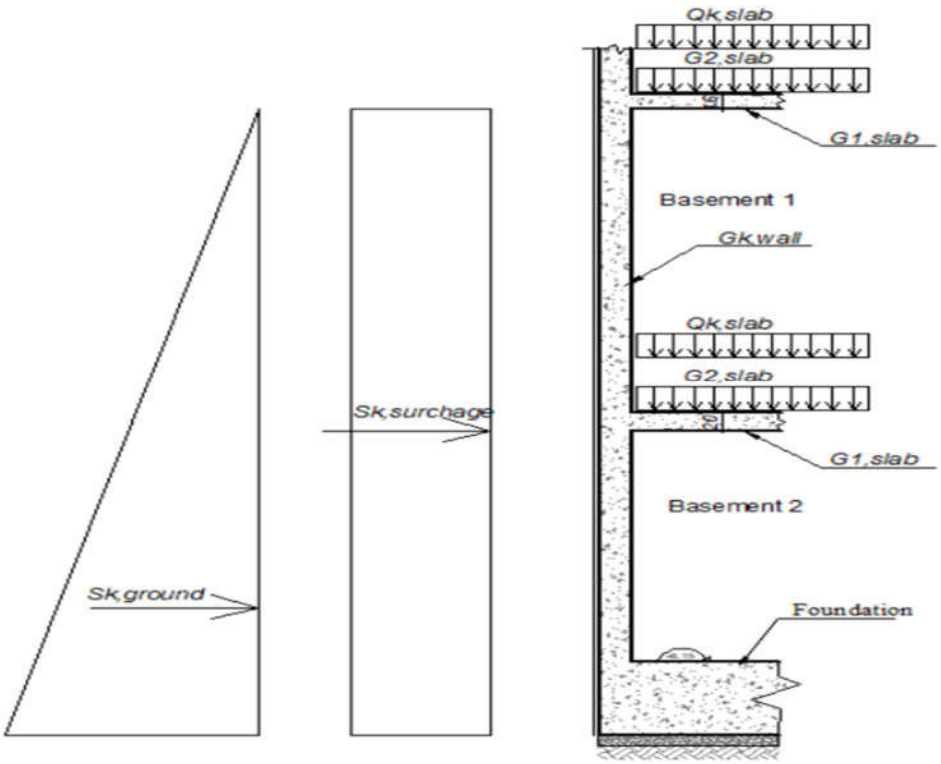

Figure 3.29. loads acting on the retaining Wall.

With:

Sk,ground is Ground horizontal force;

Sk,surcharge is Surcharge horizontal force provided by the surcharge on the embankment;

Gk,wall is the self-weight of wall;

Qk,slab is the imposed load acting on the slab;

G1,slab is the self-weight of the slab;

G2,slab is the surcharge load acting on the slab;

Based on the geotechnical data which are presented in table 3.9, Sk,ground and the load

Sk,surcharge can be computed.

Table 3.12. Geotechnical data of the soil

Geotechnical data	Symbols	Values
Soil weight density	γ	18KN/m³
Angle of shearing resistance	Φ	17.4°
Factor of horizontal active earth pressure	Ka	0.54
Wall-ground interface friction angle	δ	0

Based on the equation 2.33 and 2.35 the value of Sk,ground and Sk,surcharge are obtained. So Sk, surcharge =20.77 kN/m and Sk, ground=139.24 kN/m.

The wall will be designed under the load combination presented in equation 3.6.

$$ULS_{,wall}=1.35xSk_{,ground}+1.5xSk_{,surcharge}+1.35xGk_{,wall}+1.35xG1_{,slab}+1.35xG2_{,slab}+1.5xQk_{,slab} \quad 3.6$$

3.4.4.3. Bending moment design

The 3D modelling of the building in SAP 2000 with a flexible base is used to extract the required solicitations. The 3D view of the retaining wall is presented in figure 3.30

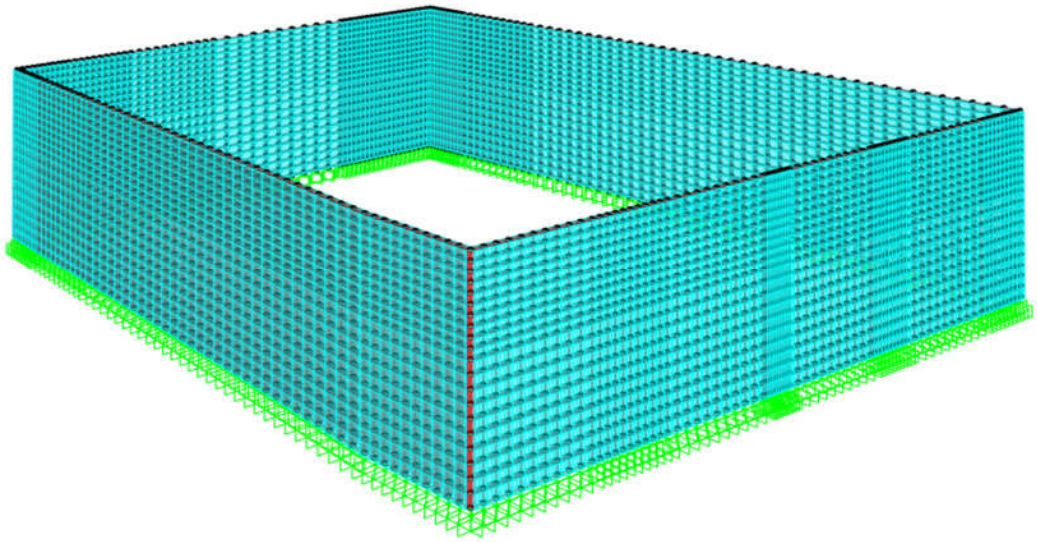

Figure 3.30. 3D view of the retaining wall in the numerical model

The bending moment along the y-axis and the z-axis are cartography in figure 3.31.

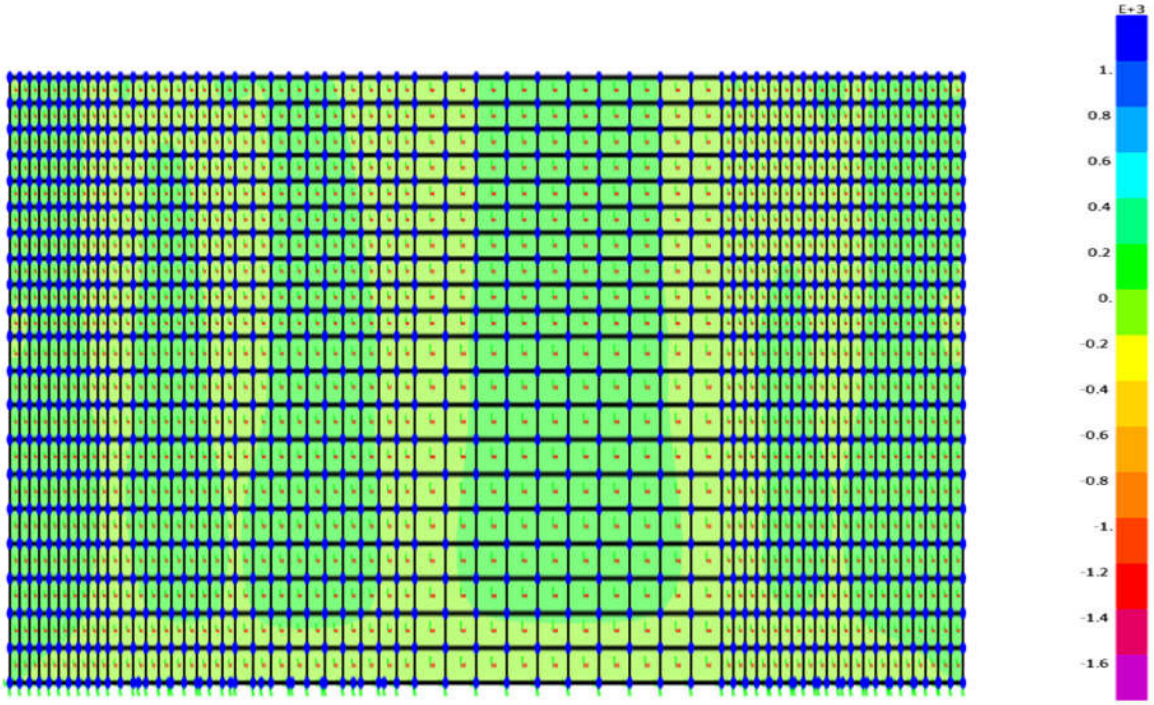

(a)

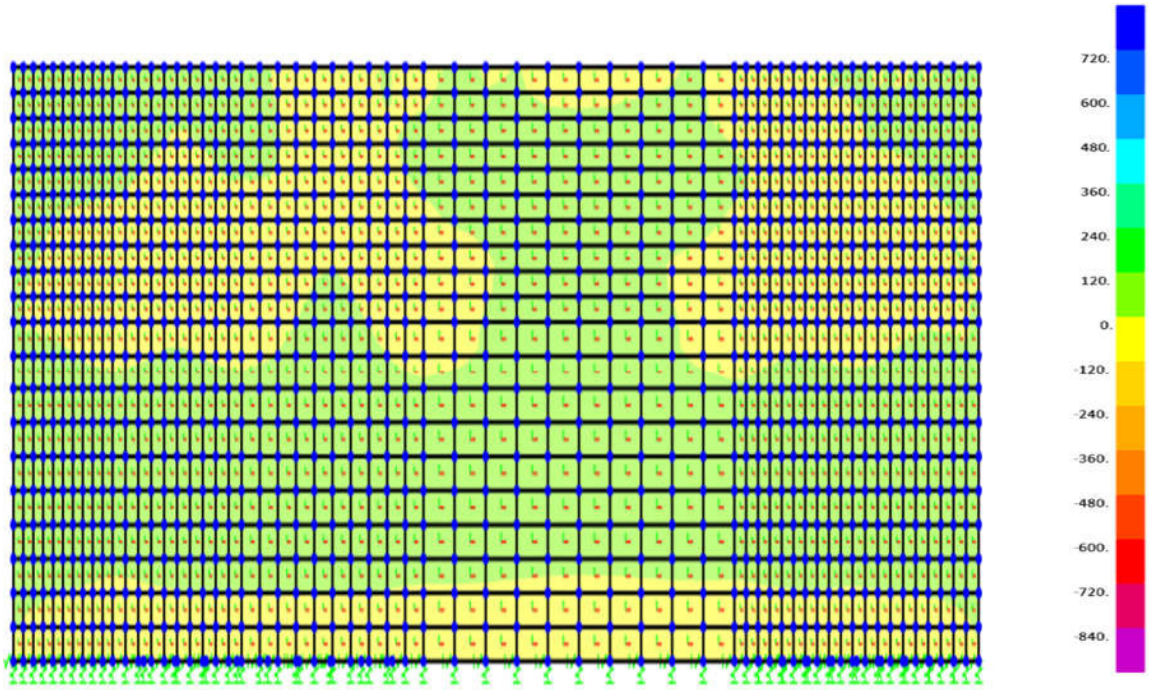

(b)

Figure 3.31 . Moment distribution (a) along Y ;(b) along Z

Table 3.13 below present the design moment

Table 3.13. Moment values inside the chosen panel

	Y direction	Z direction	Units
Positive moment	108	52	KN.m
Negative moment	-60	-120	KN.m

From there, the reinforcement for each side of the wall is calculated as a beam with a width of 1 m. results are presented in tables 3.14 and 3.15

Table 3.14. steel reinforcement of retaining wall (interior)

	Theoretical reinforcement (mm^2 /m)	Provided reinforcement per meter	Spacing (mm)
Y direction	904.78	8Φ12	150
Z direction	628.32	8Φ10	150

Table 3.15. steel reinforcement of retaining wall (exterior)

	Theoretical reinforcement (mm^2 /m)	Provided reinforcement per meter	Spacing (mm)
Y direction	628.32	8Φ10	150
Z direction	1,017.88	9Φ12	120

3.4.4.4. Axial forces verification

The axial force solicitation through the retaining wall under the ULS, wall combination is represented in figure 3.34

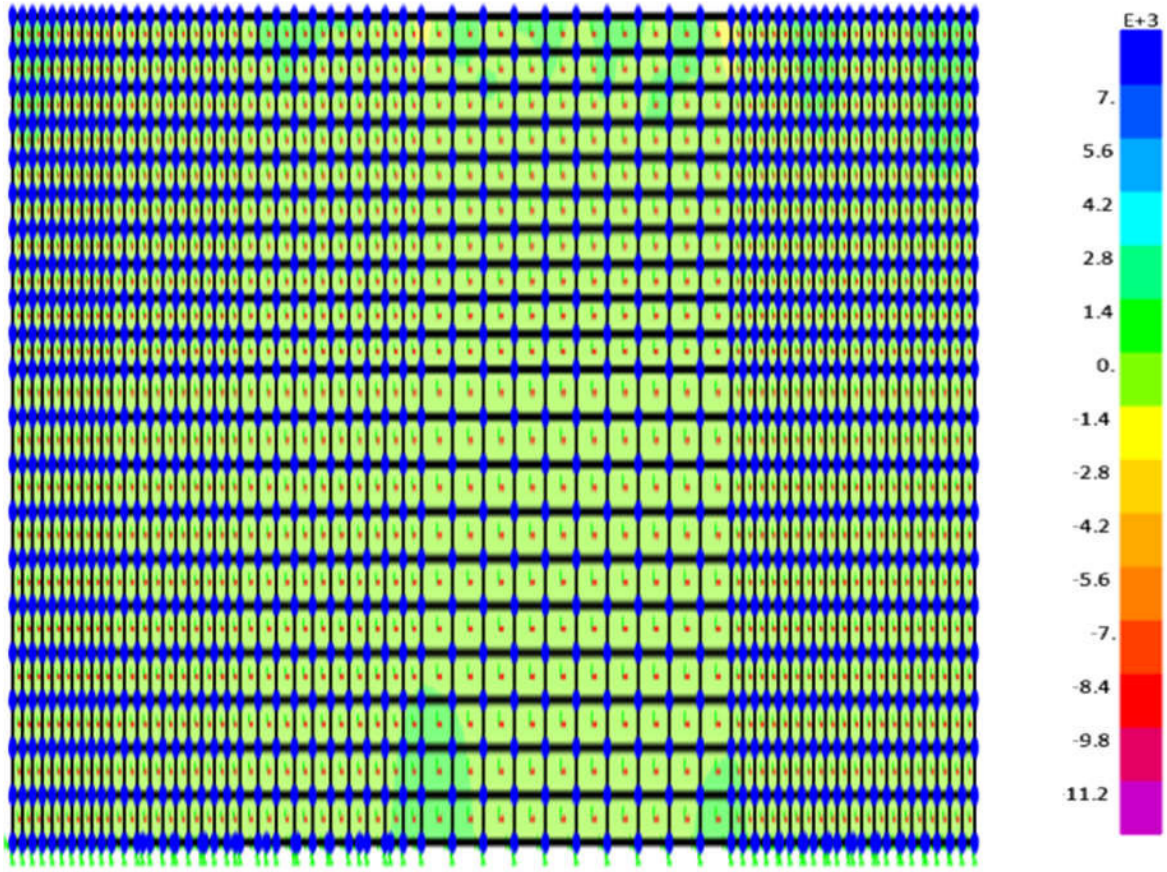

Figure 3.32. Axial forces distribution inside the wall

the design axial force is Ned=-649 KN

The resisting axial force provided by one meter length of the concrete part of the wall is calculated using equation 2.37.

Nrd= 4167,33 KN > Ned

So the wall can resist to the axial force only using its concrete resistance. The detailing of the retaining wall is shown in figure 3.33.

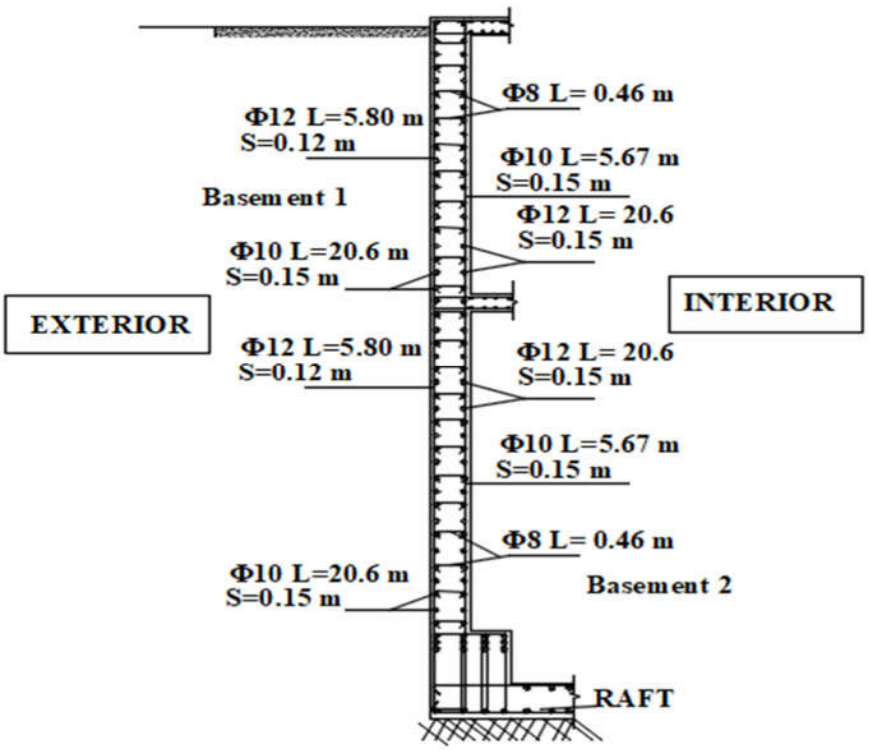

Figure 3.33 . Detailing of the study part of the retaining wall

3.4.5. Foundation design

The foundation is made by a raft with strengthening beams. Using equation 2.38 the depth of the slab can be taken equal to 40 cm and for strengthening beams, it is considered a section of 80cmx100cm. the cut section of the raft is present in figure 3.27.

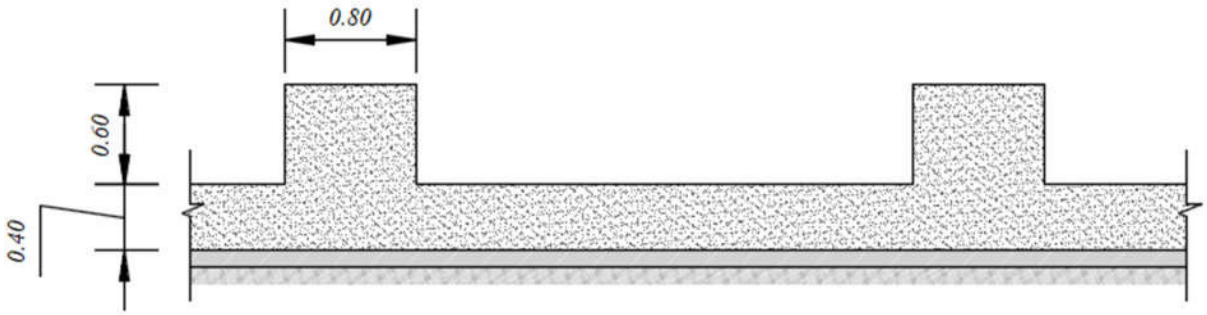

Figure 3.34. cut section of the raft

The raft has been modelled in sap 2000 by using shell thick element and strengthening beams as a frame element. The subgrade modulus of the soil Ks=39240 KN/m² /m which is given by the geotechnical report of the site of the project, have been used to implement the raft like a linear area spring object. the spring stiffness along Z is obtained taken the meshing area equal to 0,163 m^2 as: Kz = C x A=6396.12 kN/m

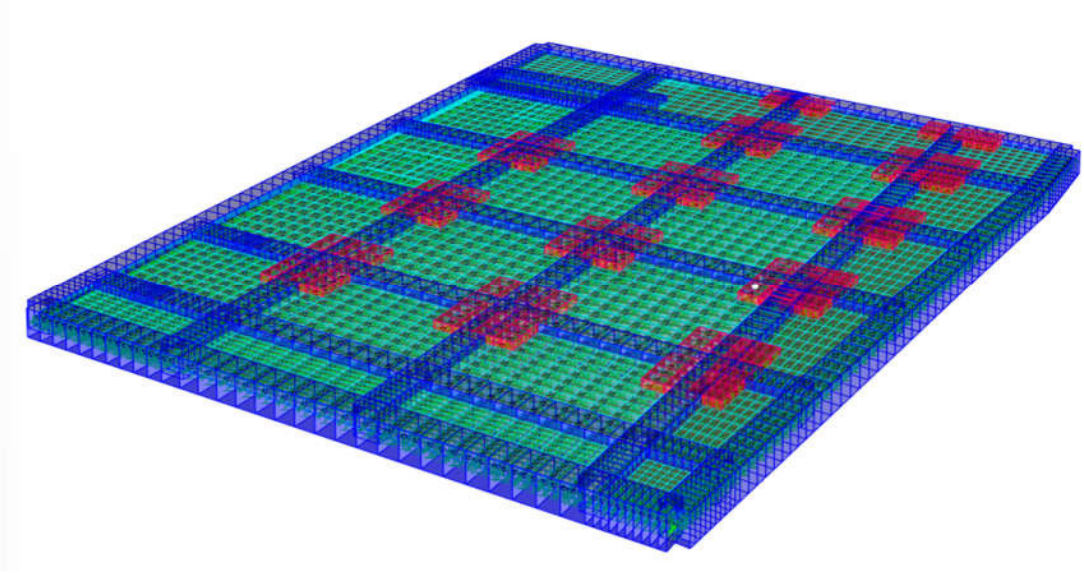

Figure 3.35. numerical model of raft foundation

The slab of this raft has been modelled with shell tick elements and the ribs with frame elements.

3.4.5.1. Admissible soil stress verification

Using the numerical model, the soil pressure under the raft can be obtained for the load combination SLS. So, the applied uniform pressure under the building area is given by:

$$\sigma = \frac{90814.4671X10^3}{636X\ 10^6} = 0{,}142 < 0.2\ MPa$$

Bearing capacity of the soil provided by the geotechnical study of the site is 0.2 MPa. It can be observed that the bearing pressure beneath the raft is less than the admissible bearing capacity, thus, the mat section is conserved. The position of the resultant force is given as

X= 11.4 m and Y= 10.57 m

The eccentricities between the position of the resultant vertical load and the center of gravity of the raft along x and y are equal to

$$e_x = 3.022\ m\ \ and\ e_y = 1.31\ m$$

Using equation 2.44, the maximal soil pressure under the raft is:

$$\sigma_{max} = 0.154\ Mpa < 0.2\ MPa = \sigma_{adm}$$

3.4.5.2. Slab design

The slab will be design in flexion. The moment distribution along x and y direction in slab are presented in the figure 3.36

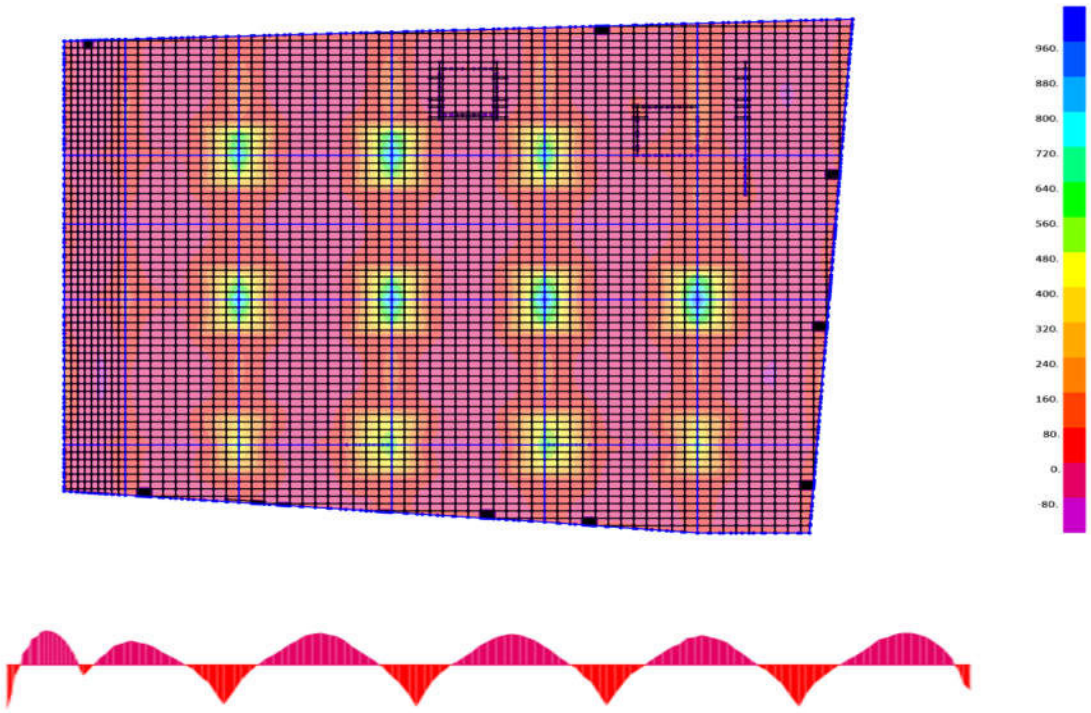

(a)

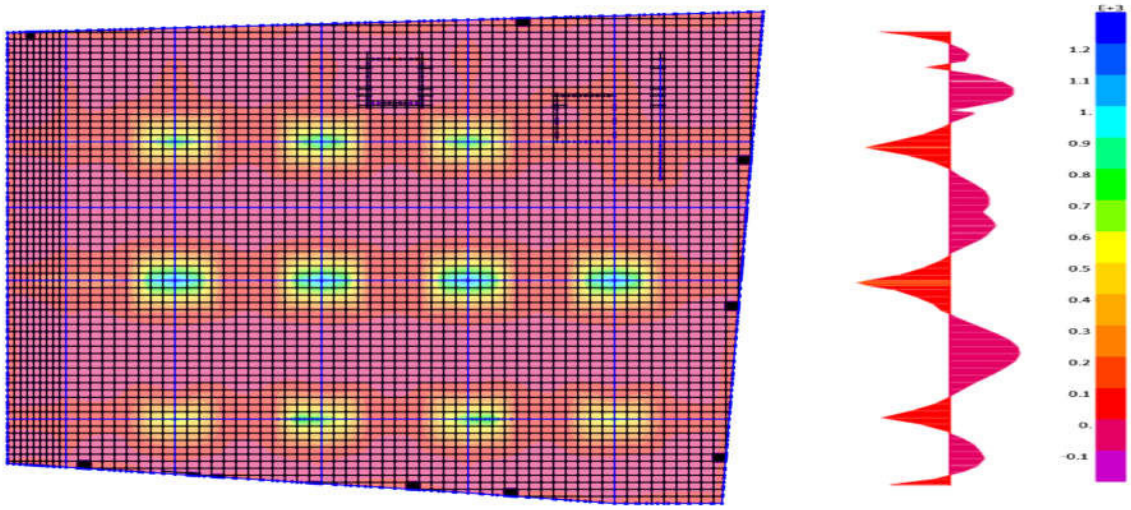

(b)

Figure 3.36 . Moment distribution in the foundation mesh (a) along X; (b) along Y

The designed moments are presented in table 3.16

Table 3.16. Design moment in the raft

	X direction	Y direction	Units
Maximum positive moment	242.78	280 .77	kN.m
Maximum negative moment	-167.53	-180.52	kN.m

Assuming a 16 mm diameter bars to be used and a concrete cover of 40 mm. as describe in part 2.6.5, the effective depth of the outer layer to be used in the design for moments in the short span direction is

$$dy = 400 - 40 - \frac{16}{2} = 352\,mm$$

And the effective depth of the inner layer to be used in the design for moments in the long span direction is:

$$dx = 400 - 40 - 16 - \frac{16}{2} = 336\,mm$$

Table 3.17. Reinforcement at the bottom of the raft

Bottom				
	Theoretical reinforcement (mm^2 /m)	Provided reinforcement per meter		Spacing (mm)
		At support	At mid-span	
X direction	1762.60	8Φ12+8Φ16	8Φ12	150
Y direction	2038.41	8Φ12+8Φ16	8Φ12	150
Top				
X direction	1216.28	8Φ16		150
Y direction	1310.59	8Φ16		150

3.4.5.3. Design of footing

The footing chosen is the one under the most solicited column. It's considered area is 2.8m*2.8 m for a thickness equal to 1m

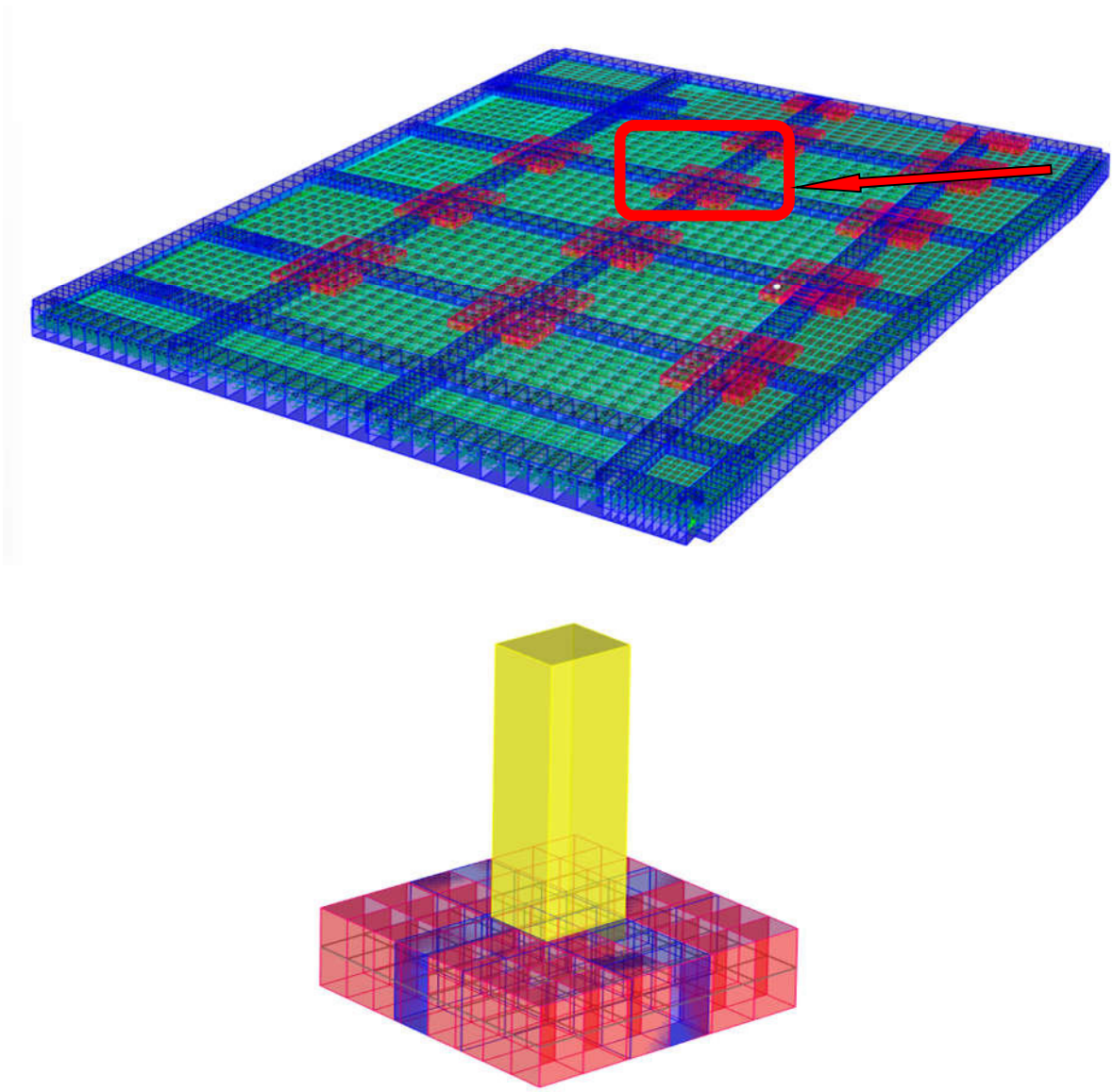

Figure 3.37. selected footing

this component is designed as described in section 2.6.5. the axial force arriving on this footing is Ned=5414 kN. considering the footing of area 2,8m*2,8 m and thickness 1m, the section of steel required for this footing using the equations described in section 2.6.5 is given by Asy= 3977.78 mm^2 in y direction and Asx=3458.94 mm^2 in x direction.

Table 3.18. Steel reinforcement on the footing

	Theoretical reinforcement (mm^2)	Provided reinforcement	Spacing (mm)
X direction	3458.94	20Φ16	12.5
Y direction	3977.78	20Φ16	12.5

3.4.5.4. Strengthening beam design

After simulation, the most solicited rib was chosen to be dimensioned. The chosen strengthening beam is highlighted in figure 3.38

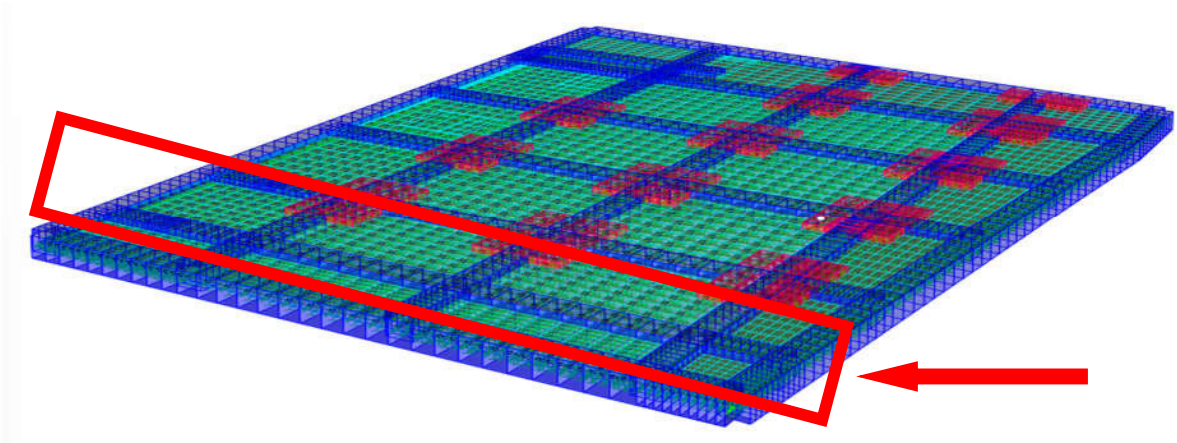

Figure 3.38.chosen beam

the choice of this beam is justified by Figure 3.31 which shows the solicitations in the beams

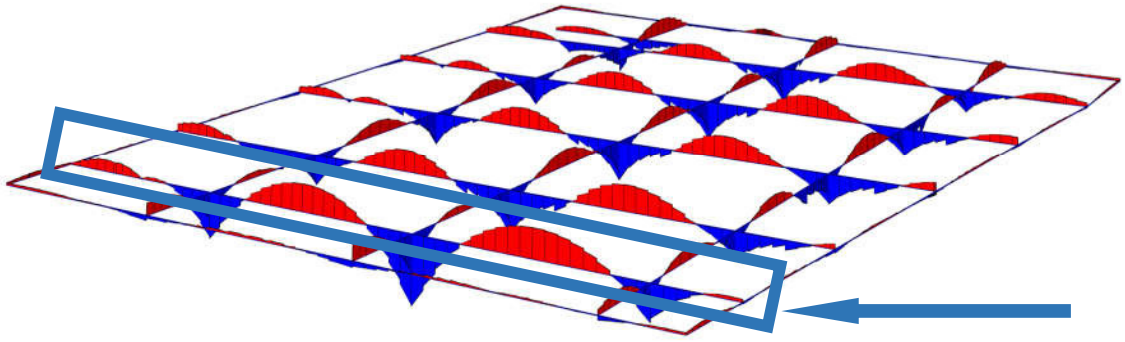

(a)

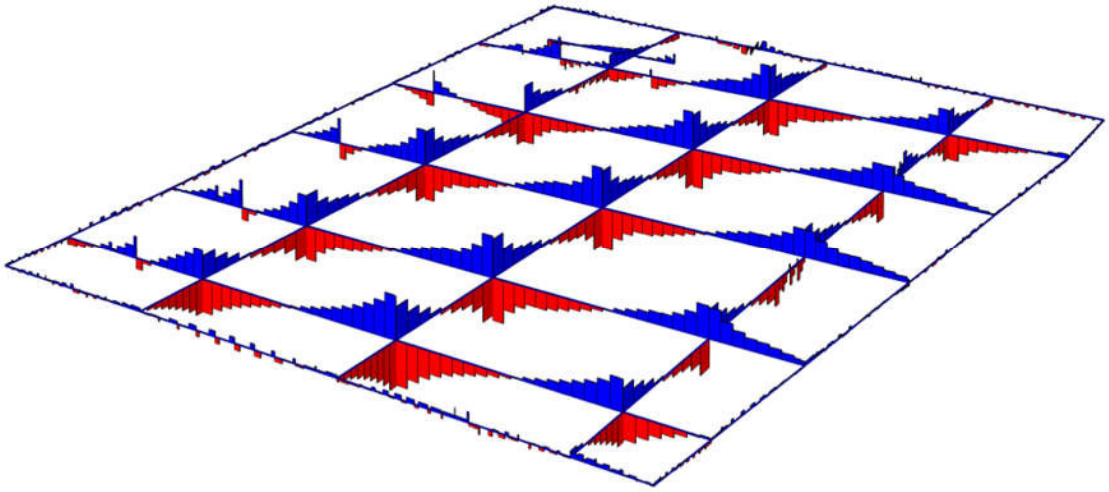

(b)

Figure 3.39. 3D View of solicitation on strengthening beam (a) Bending moment (b) shear forces

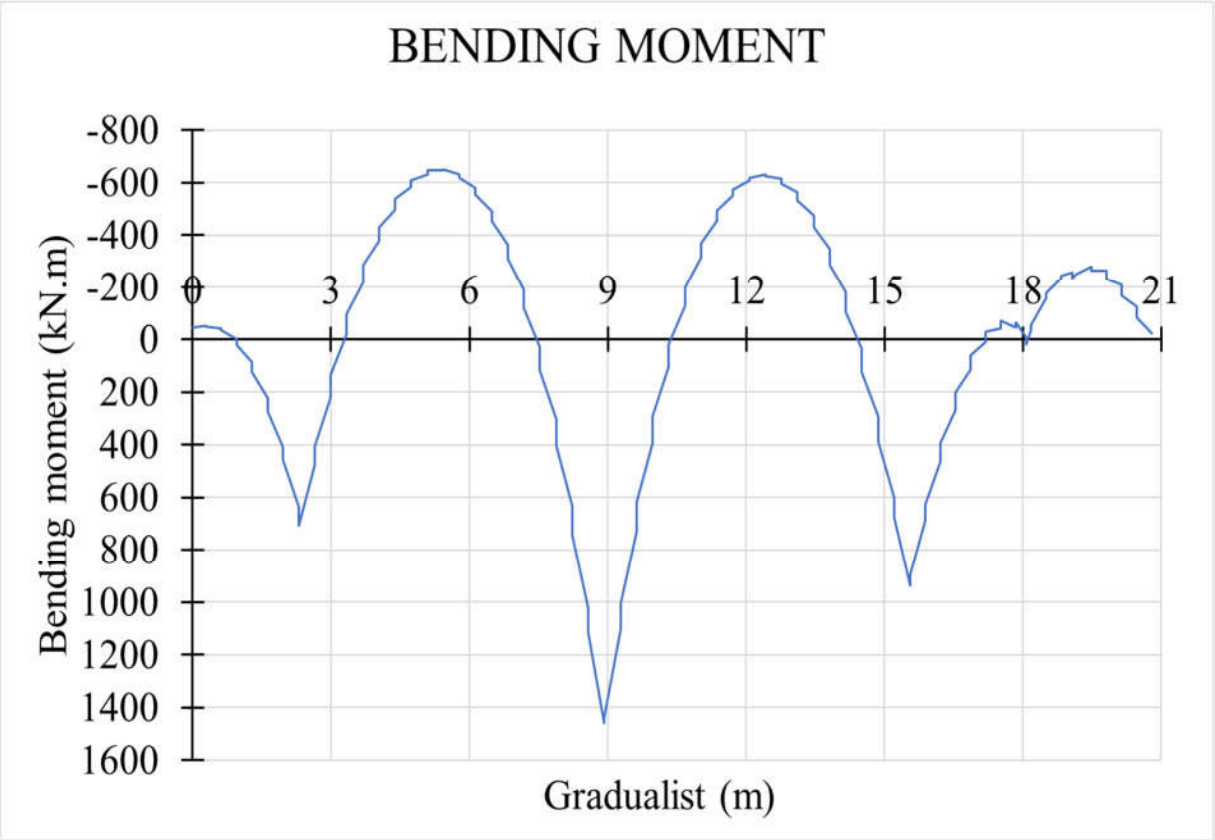

Figure 3.40. Bending moment on strengthening beam

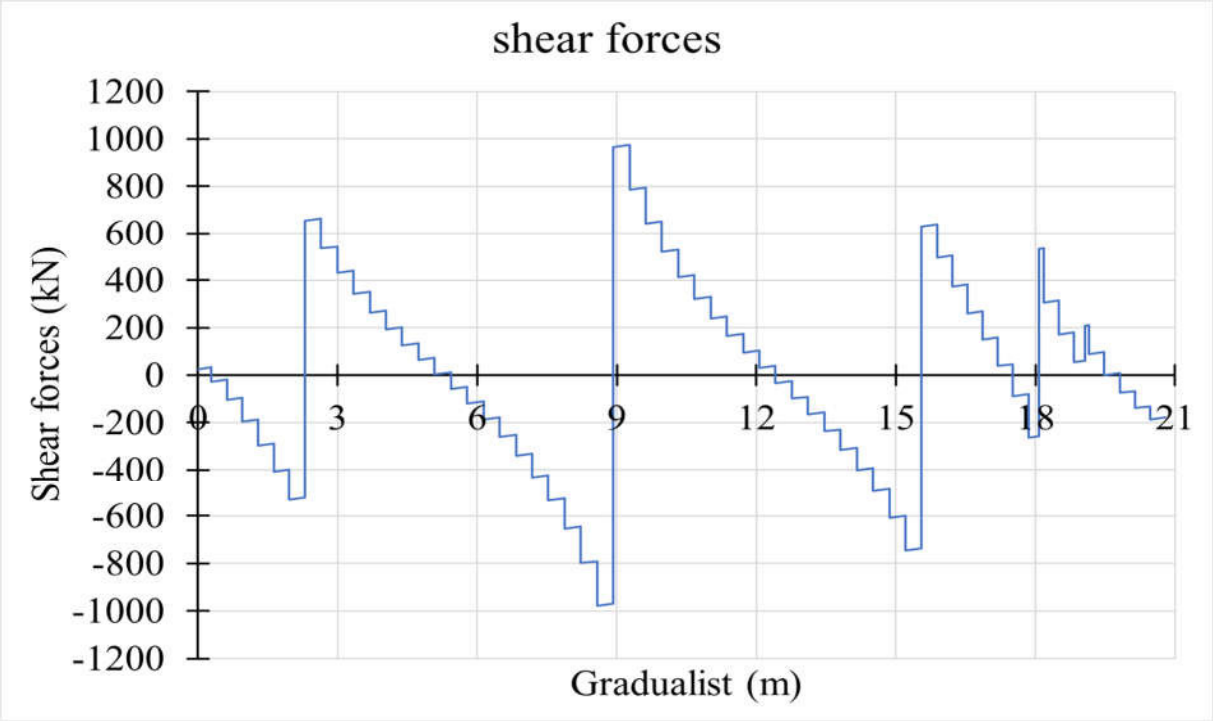

Figure 3.41. shear forces on strengthening beam

The strengthening beam will be designed in flexion and for the shear forces. Flexural reinforcements are design using equation 2.11 and the required shear reinforcement is provided by the procedure described in section 2.4.2.1.b. The recapitulative of the flexural design and the shear design are presented in figure 3.30 and 3.31.

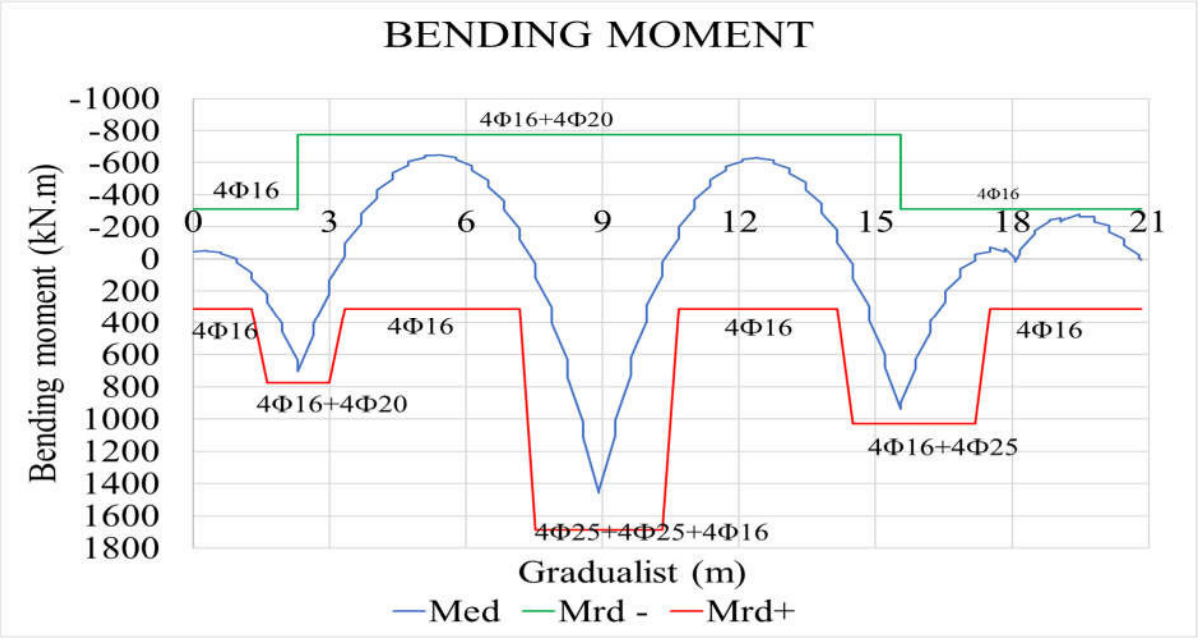

Figure 3.42. bending moment verification of the strengthening beam

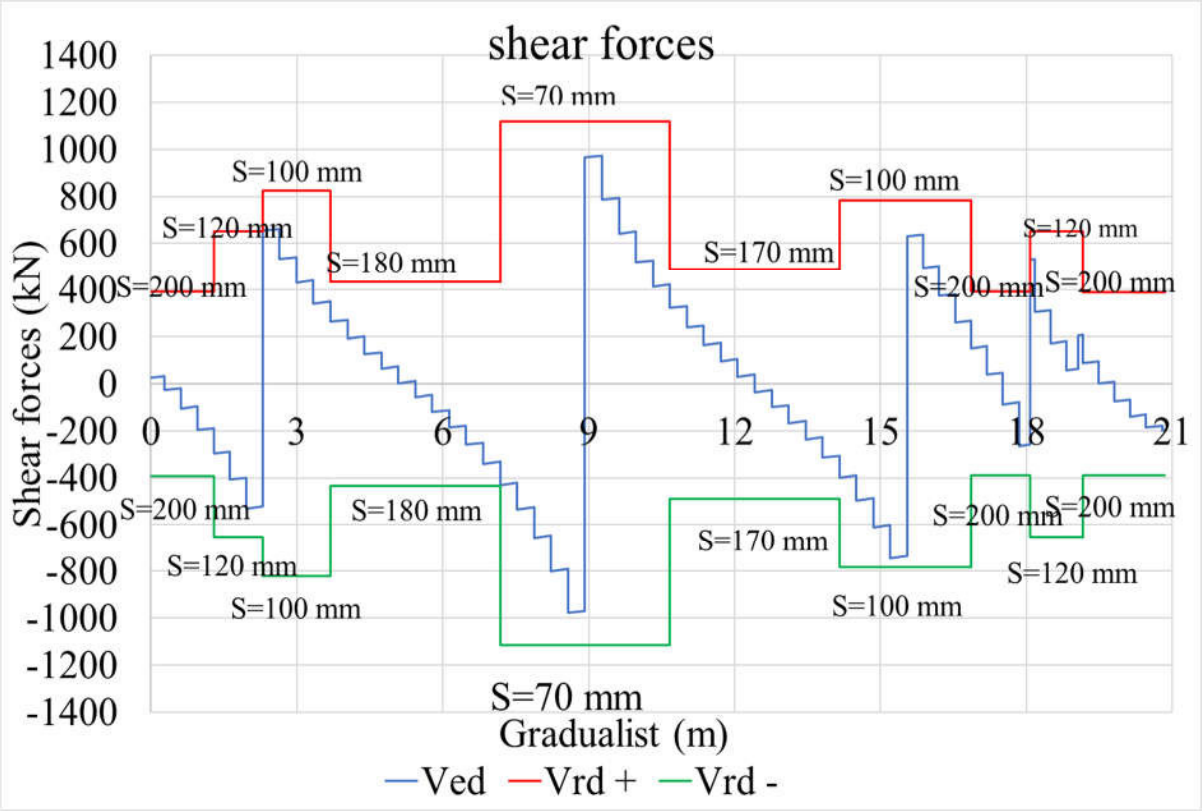

Figure 3.43. shear verification of the strengthening beam

Detailing of the raft foundation is represented in annex

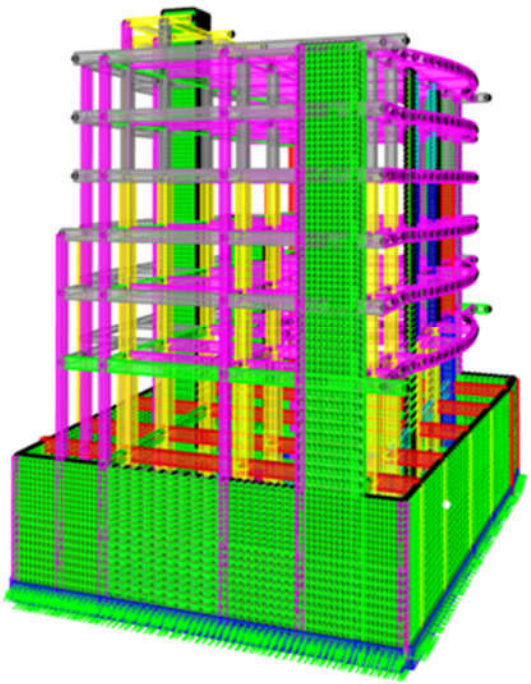

Figure 3.44. numerical model before over-elevation: h=25.675 m above the ground level

3.4.6. Verification of column and foundation after over-elevation

3.4.6.1. Verification of column

a. Column with maximum axial forces

Here, the verification is done as before. figures 3.42 to 3.44 show the new solicitation on the chosen column.

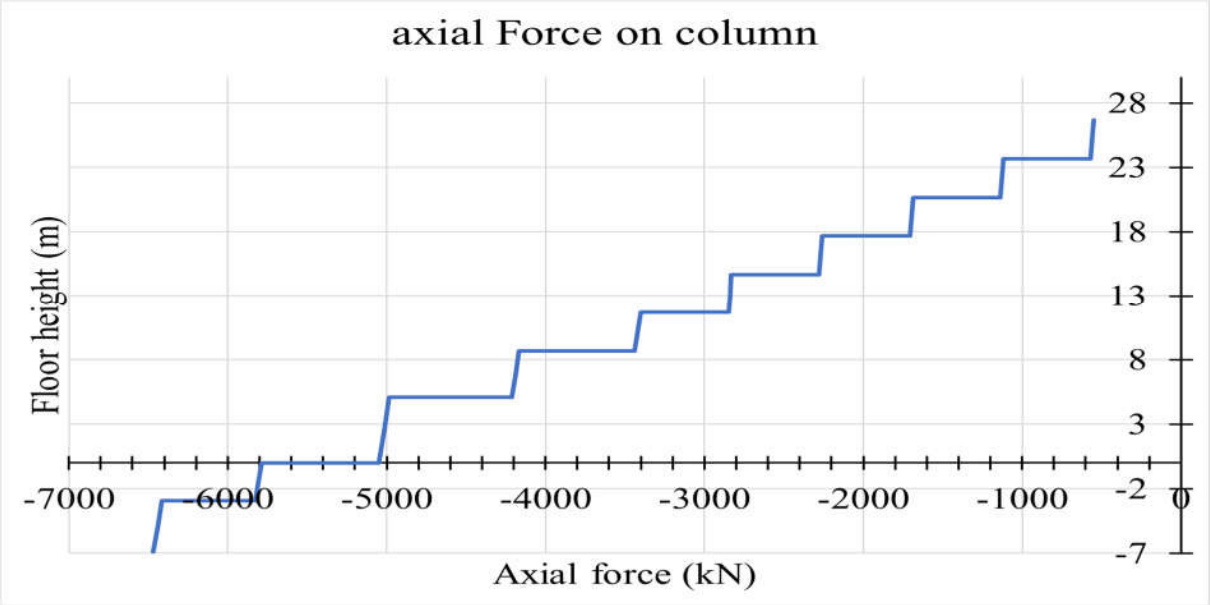

Figure 3.45 : New values of axial force on column

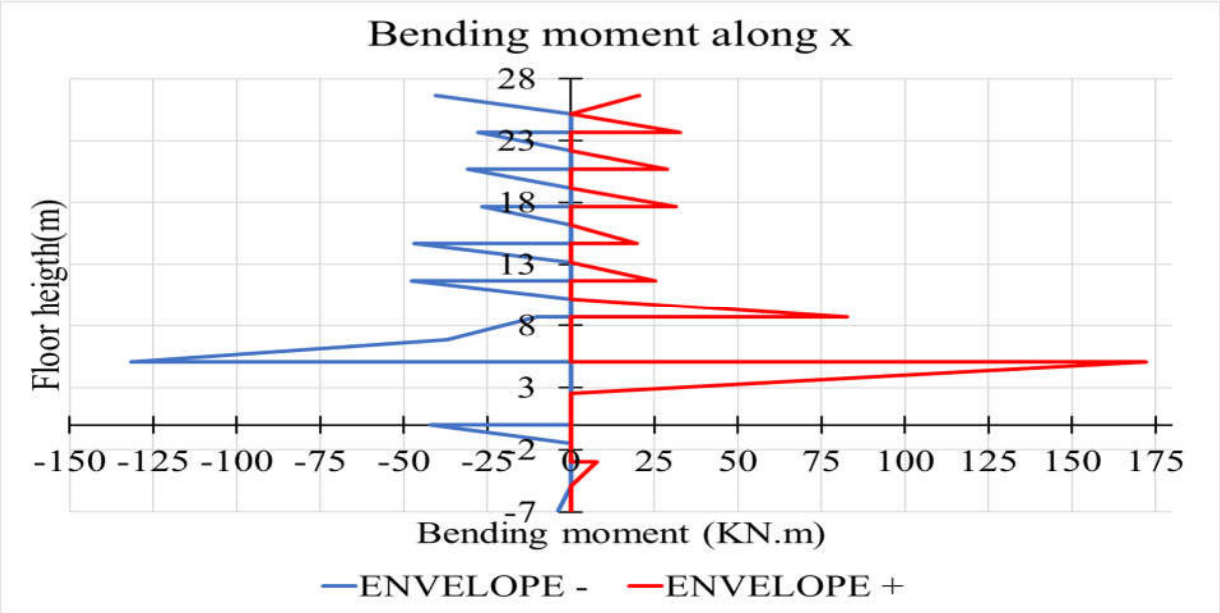

Figure 3.46. new values of bending moment Along x

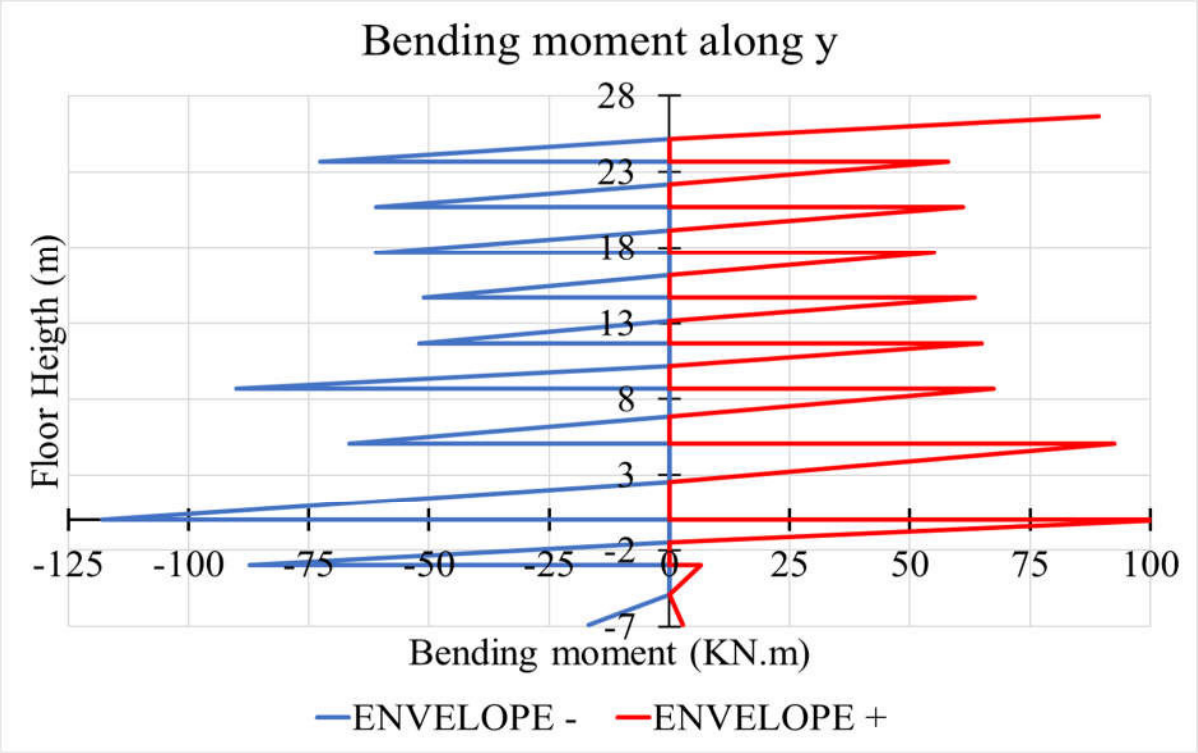

Figure 3.47. new values of bending moment Around y

The verification of the axial loads and the bending moment is done by means of the interaction diagram as before with the same steel and concrete sections.so, the section of column remain the same for basements to storey 1 and storey 2 to storey 6.

Table 3.19. values of resisting moment and axial forces on column in around y axis

	Nrd (kN)	Mrd(kN.m)
Section 50*80 cm^2		
1st point	-751.3	0
2nd point	-751.3	0
3rd point	1,330.9	704.04
4th point	3,290.6	944.53
5'th point	5,509.0	611.25
5th point	5,711.6	564.68
6th point	7,417.9	0
Section 40*50 cm^2		
1st point	- 535.43	0
2nd point	-535.43	0
3rd point	649.88	248.59
4th point	1,606.84	325.86
5'th point	2,774.38	214.31
5th point	2,938.58	191.31
6th point	3,868.77	0

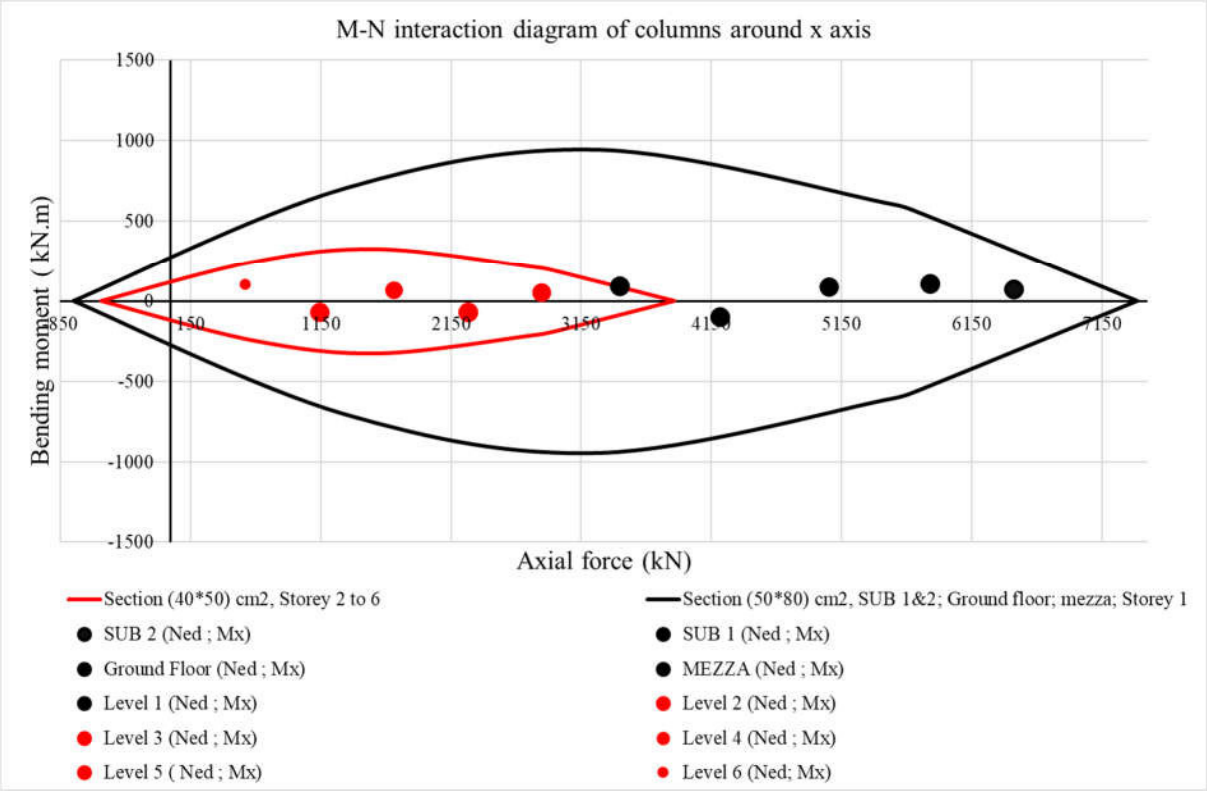

Figure 3.48. New Interaction diagram of column P1 around x

Table 3.20. values of resisting moment and axial forces on column in around y axis

	Nrd (kN)	Mrd(kN.m)
Section 50x80cm^2		
1st point	- 617.39	0
2nd point	- 617.39	0
3rd point	1,299.75	397.41
4th point	3,213.68	551.96
5'th point	5,322.03	378.74
5th point	5,646.23	333.66
6th point	7,284.06	0
Section 40x50 cm^2		
1st point	- 294.78	0
2nd point	- 294.78	0
3rd point	690.49	203.82
4th point	1,707.26	285.92
5'th point	2,810.72	197.55
5th point	2,984.92	173.17
6th point	3,836.45	0

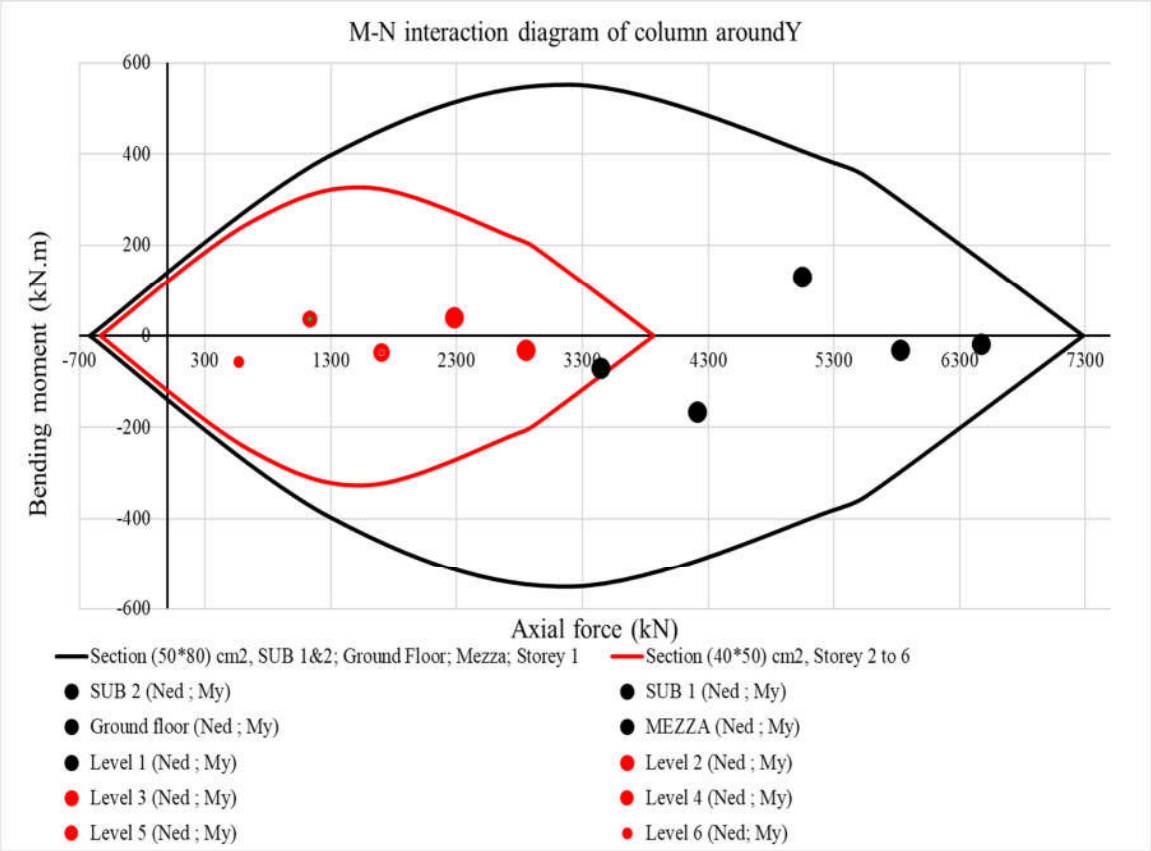

Figure 3.49. new Interaction diagram of column P1 around y

from these graphs it is clear that this column does not need to be reinforced. therefore, the same steel sections can a priori be used. however, the slenderness must be checked.

Table 3.21. slenderness values of the column

Level	λx	λy	$\lambda limx$	λlim y
Basement 2	18.67	13.05	24.47	24.47
Basement 1	15.28	10.67	25.78	25.78
Ground level	24.61	17.20	27.69	27.69
Mezza	17.46	12.20	30.31	30.31
Storey 1	14.55	10.17	33.54	33.54
Storey 2	18.19	14.55	27.52	27.52
Storey 3	18.19	14.55	30.78	30.78
Storey 4	18.19	14.55	35.55	35.55
Storey 5	18.19	14.55	43.53	43.53
Storey 6	18.19	14.55	61.46	61.46

Table 3.8 shows that $\lambda < \lambda lim$, so the slenderness of the column is verified.

b. Column with maximum bending moment

After over-elevation, new solicitation on the column P2 are obtain and presented in figures 3.50 and 3.51 for axial forces and bending moment respectively.

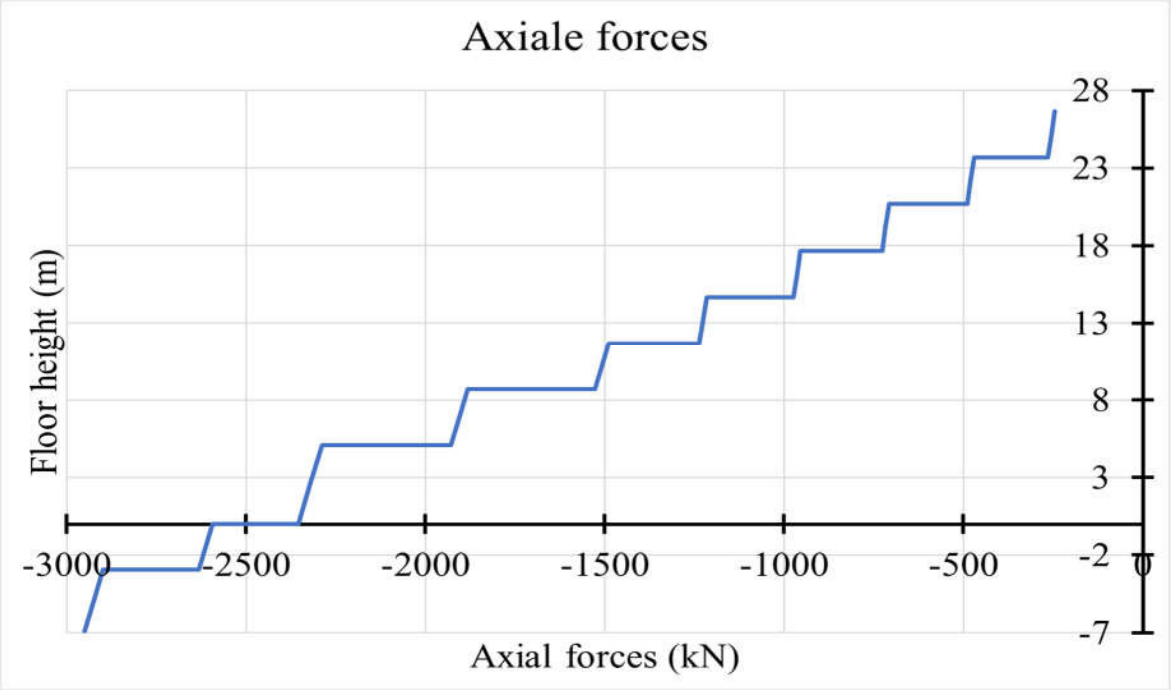

Figure 3.50. new axial forces on column P2

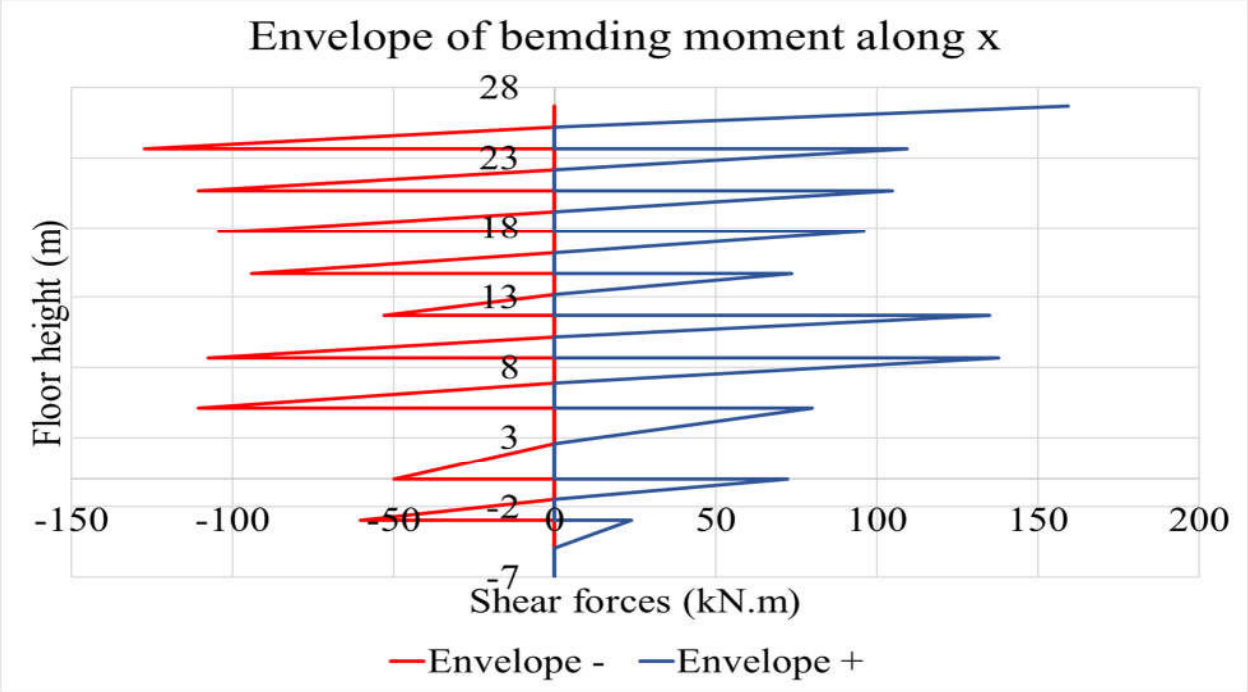

(a)

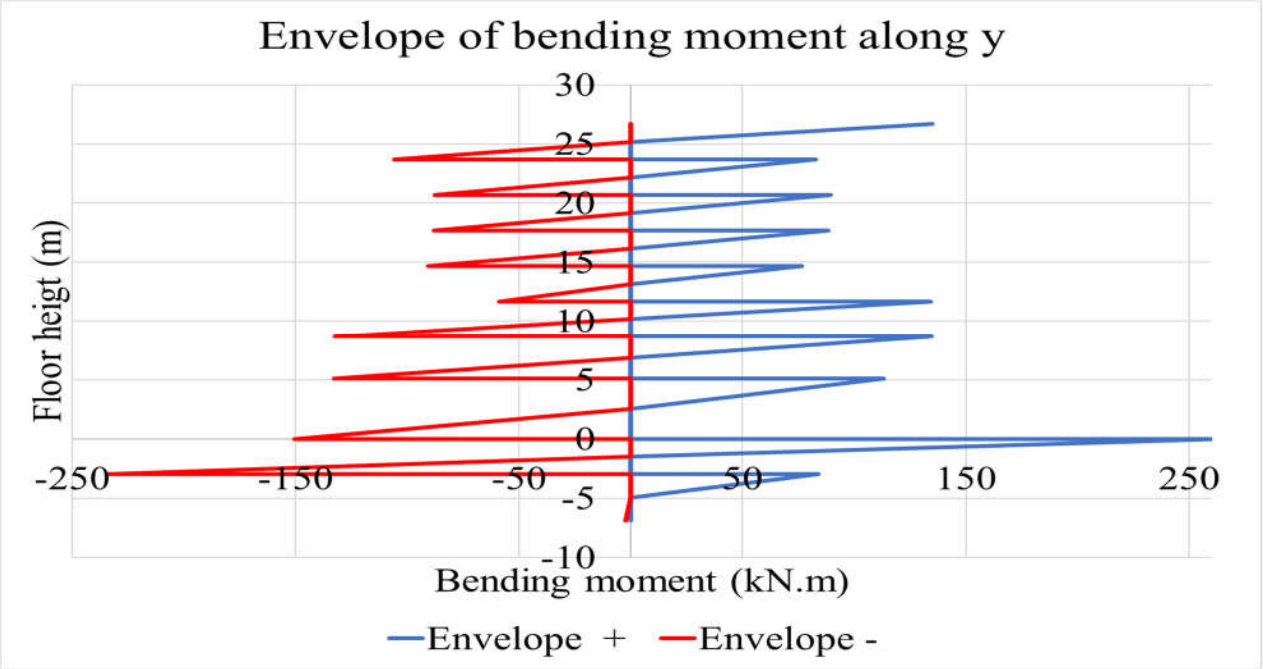

(b)

Figure 3.51. New bending moment on column P2 along :(a) x-axis and (b) y-axis

The M-N interaction diagram is drawn using the same steel sections and column sections as above. The dimensions of column remain a=500mm and b=400 mm for storey 1 to storey 6. The M-N diagram is represented by figure 3.52

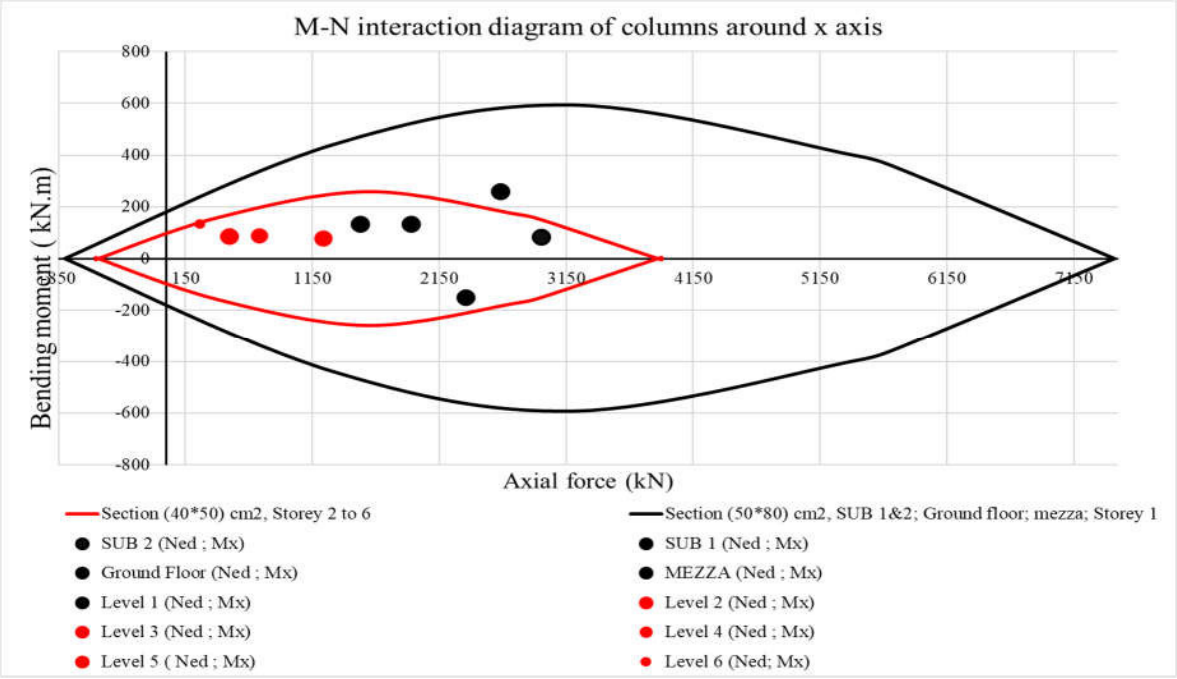

(a)

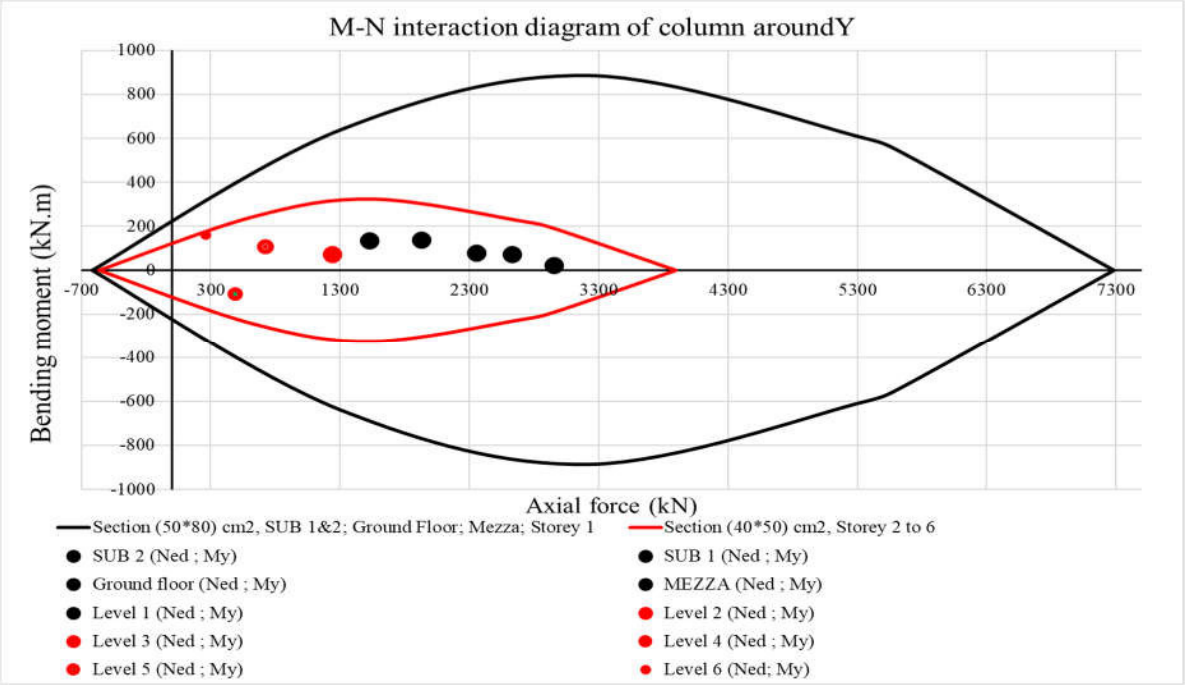

(b)

Figure 3.52. Interaction diagram of column P2 (a) around x-axis (b) around y-axis

So, according to this diagram, the column is verified. As this column has the same concrete section and steel sections as column p1, the slenderness does not need to be checked.

3.4.6.2. Verification of raft

a. Verification of slab

Using the numerical model, the soil pressure under the raft can be obtained for the load combination SLS. So, the applied uniform pressure under the building area is given by:

$$\sigma = \frac{106332.9251X10^3}{636X\ 10^6} = 0{,}167 < 0.20\ MPa$$

as done in section 3.4.5.1, бmax=0.18 MPa ≤ 0.2 MPa

table 3.22 present the new solicitation on raft foundation

Table 3.22 New solicitation on the slab

	X direction	Y direction	Units
Maximum positive moment	286.13	325	kN.m
Maximum negative moment	-191.35	-220	kN.m

The steel sections required for this raft are calculated as above and are grouped in table 3.23

Table 3.23. steel reinforcement of the raft foundation

Bottom				
	Theoretical reinforcement (mm^2 /m)	Provided reinforcement per meter		Spacing (mm)
		At support	At mid-span	
X direction	1762.60	8Φ12+8Φ16	8Φ12	150
Y direction	2038.41	8Φ12+8Φ16	8Φ12	150
Top				
X direction	1216.28	8Φ16		150
Y direction	1310.59	8Φ16		150

From these results, and compare with those found above, it appears that raft not need to be reinforced

b. Verification of strengthening beam and footing

After the over-elevation, the new demands in the rib are found with the help of the sap 2000 software and are presented in the figures.

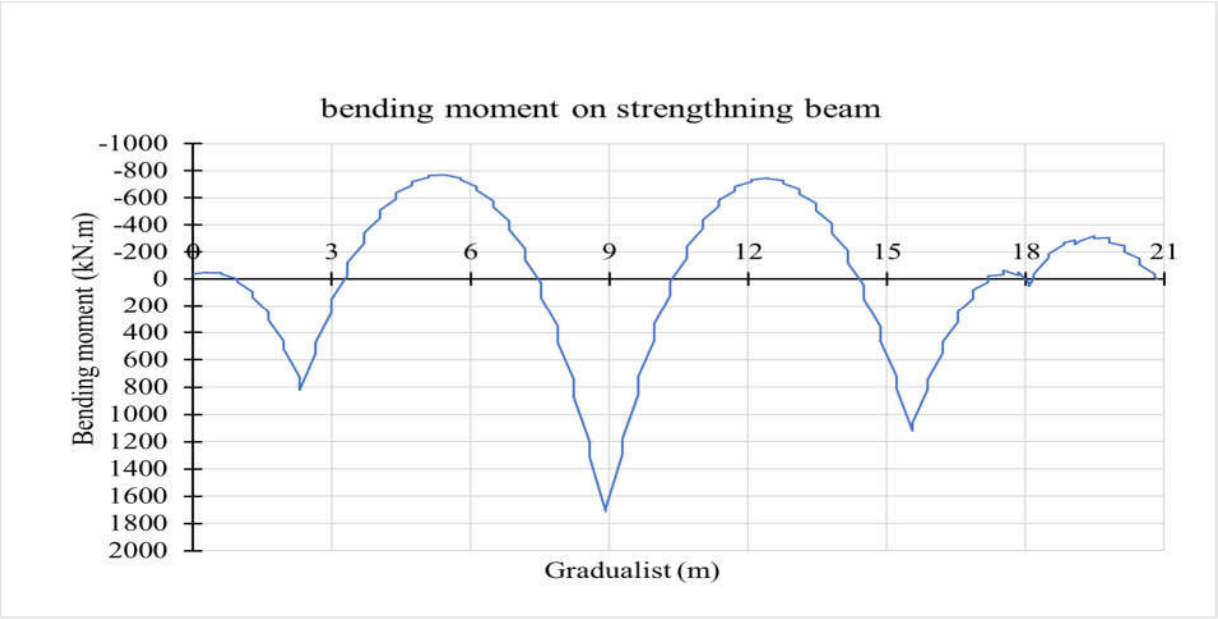

Figure 3.53 new bending moment on strengthening beam

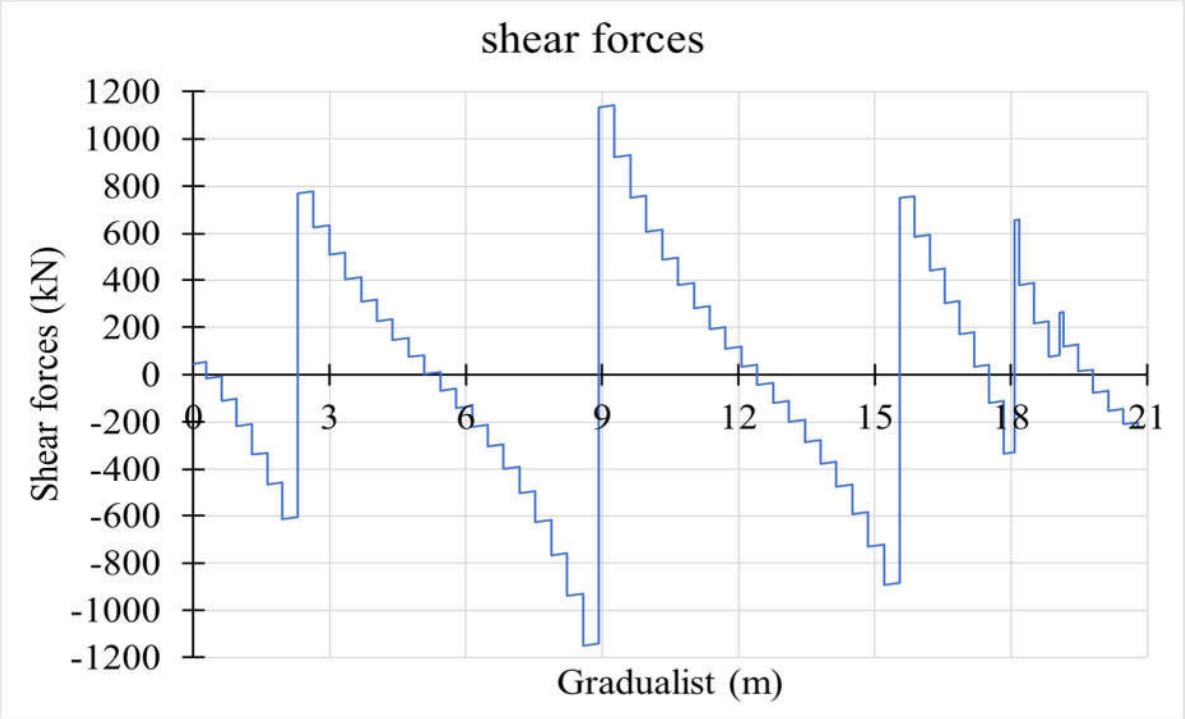

Figure 3.54. new shear forces on strengthening beam

the reinforcement steel sections are calculated as before and presented in figures 3.2

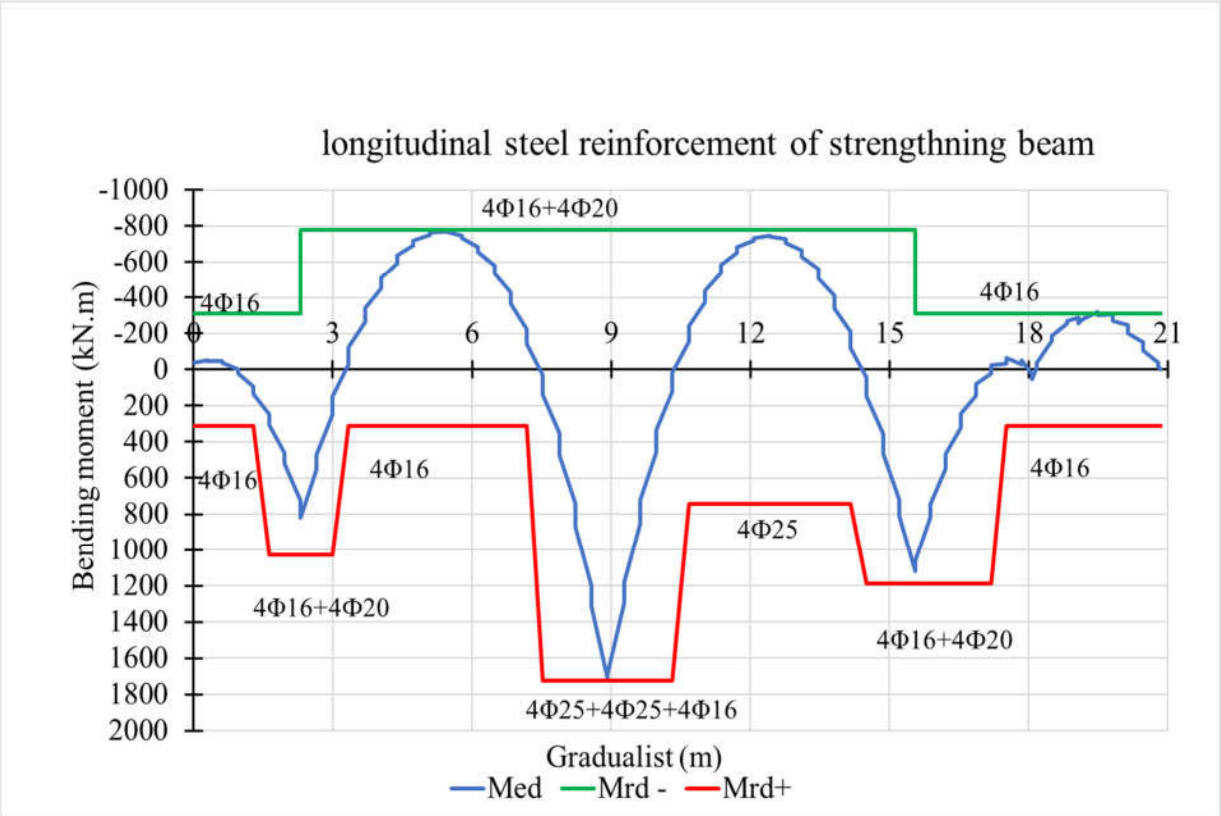

Figure 3.55. bending moment verification of the strengthening beam

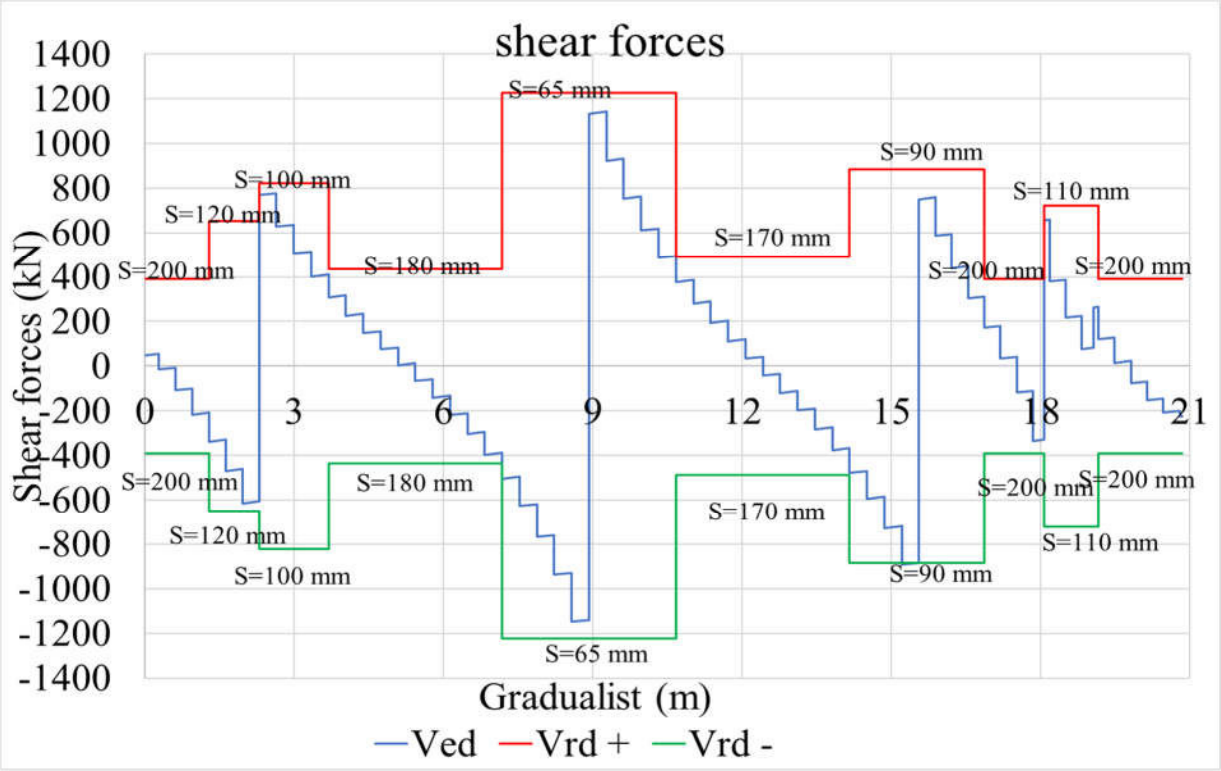

Figure 3.56. shear verification of the strengthening beam

so this rib does not need to be reinforced. concerning the footing, it is also checked as before.

The axial force arriving on the base is N=6468 KN and the section of steel necessary for this footing is Asy= 4492.61 mm^2 in y direction and Asx=3973.39 mm^2 in x direction. Theses steel are recapitulated in table 3.24

Table 3.24. steel reinforcement of footing (

	Theoretical reinforcement (mm^2)	Provided reinforcement	Spacing (mm)
X direction	3973.39	20Φ16	125
Y direction	4492.61	23Φ16	105

Thus, referring to the table, no reinforcement in the x-direction and an increase in steel in the y-direction.

The numerical 3D Of the building after over-elevation are presented in figure 3.57

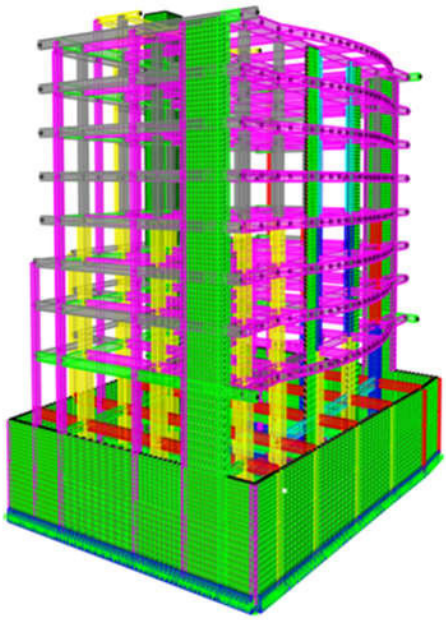

Figure 3.57. 3d model after over-elevation: h=31.675 m above the ground level

3.4.7. Numerical modelling of the structure

In this section, another much softer soil is taken into account in order to better appreciate the behaviour of the structure under static load. The reaction modulus of the soils used are shown in the table 3.25. Six models are used, three of them have a height of 25.675 m and are supported on a fixed base, a wet clay, and a humus, sand and gravel fill, respectively. The other three models have a height of h = 31.675 m and are supported under the same conditions as the others.

The beams and columns are modelled using frame elements while the shear walls are modelled using thick shell elements. The soil is represented by springs of stiffness ks (presented in table 3.25) using the Winkler method.

Figure 3.58 presents the analysed models.

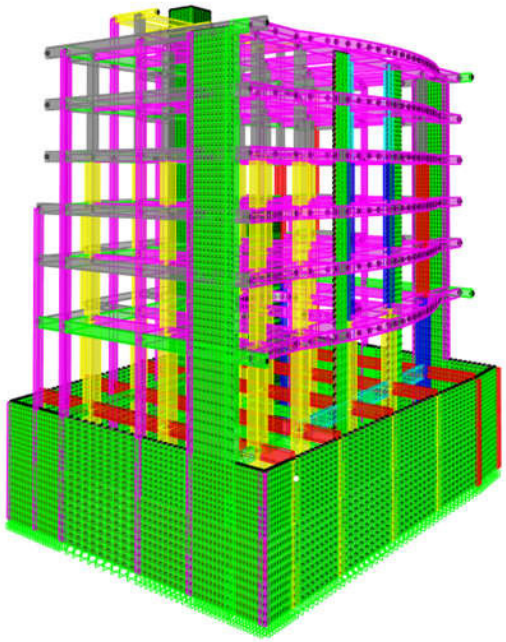

Model with fixed and h= 25.675 m

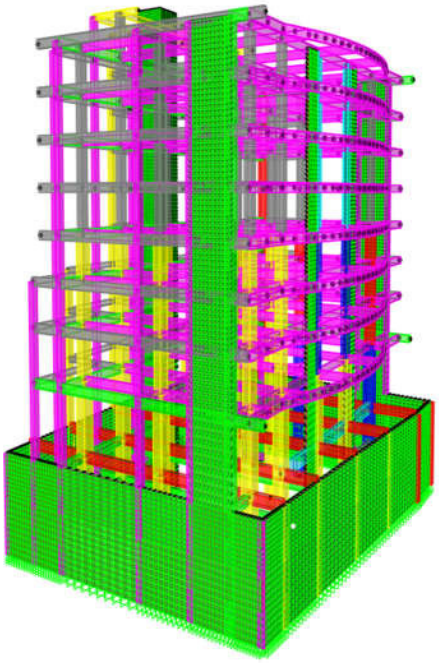

Model with fixed base and h= 31.675 m

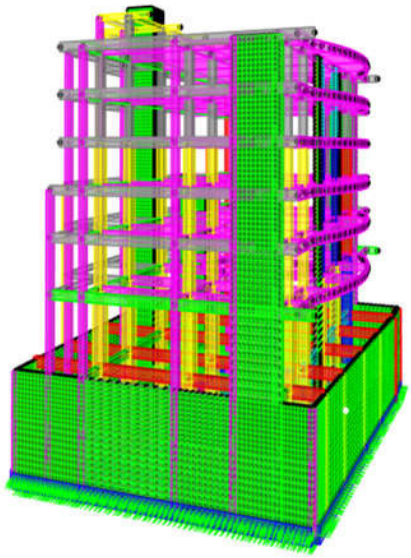

Model with flexible base and h= 25.675 m

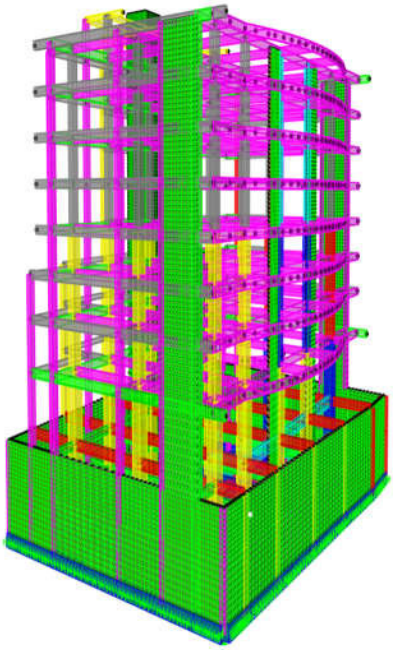

Model with flexible base and h= 31.675 m

Figure 3.58. Studied models

Table 3.25. Values of the modulus of subgrade reaction for different soil types((Forni, sd)

Soil type	Subgrade reaction	unit
Wet clay	39240	kN/m^3
Embankment of humus, sand and gravel	9810	kN/m^3

3.4.8. Analysis criteria

This section presents the deformations in the foundation and the variation of the solicitations in the structure according to the support conditions.

3.4.8.1. Settlement and deformation

In this section, six models that differ in height and support conditions are studied. The first three models have a height of 31.675 m, while the other three have a height of 25,675 m.

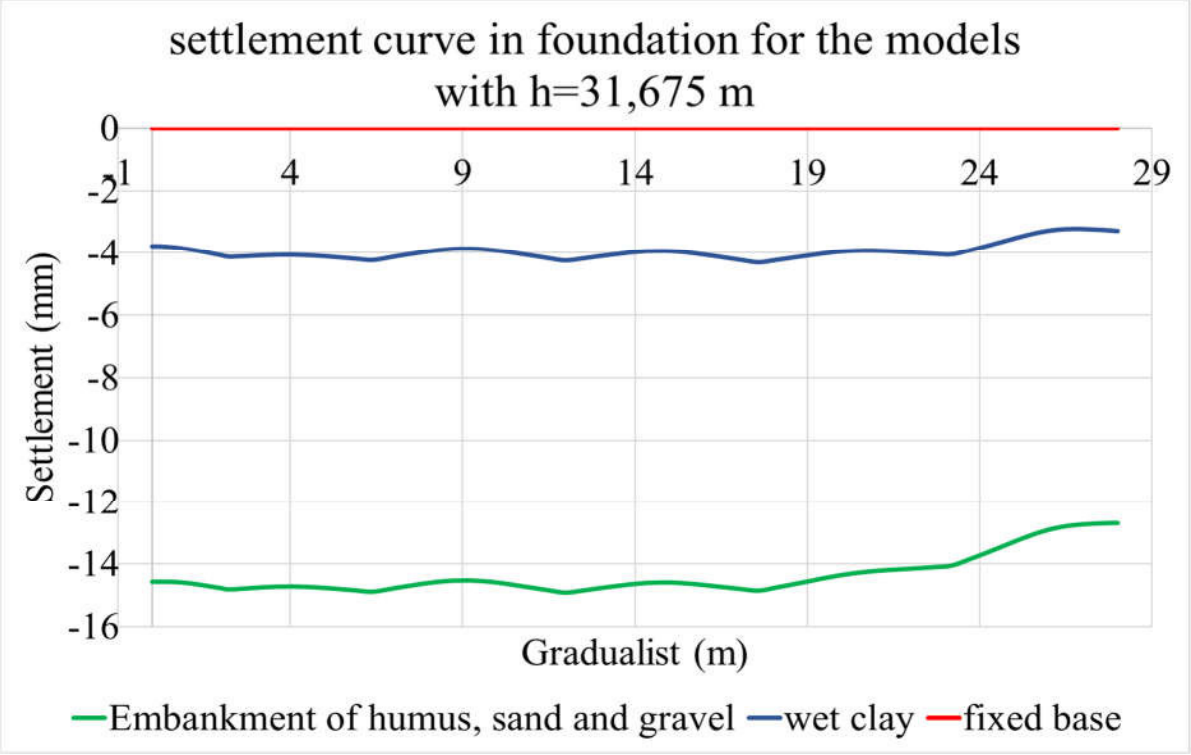

Figure 3.59. Settlement curve in foundation of the models with height h=31.675 m considering different soil type

The maximum values of displacement in foundation are presented in table 3.26

Table 3.26 maximum values of displacement in foundation of the models with h =31.675 m

Model	Maximum displacement Uz	unit
Fixed base	0	mm
Wet Clay	4.297	mm
Embankment of humus and sand	17.59	mm

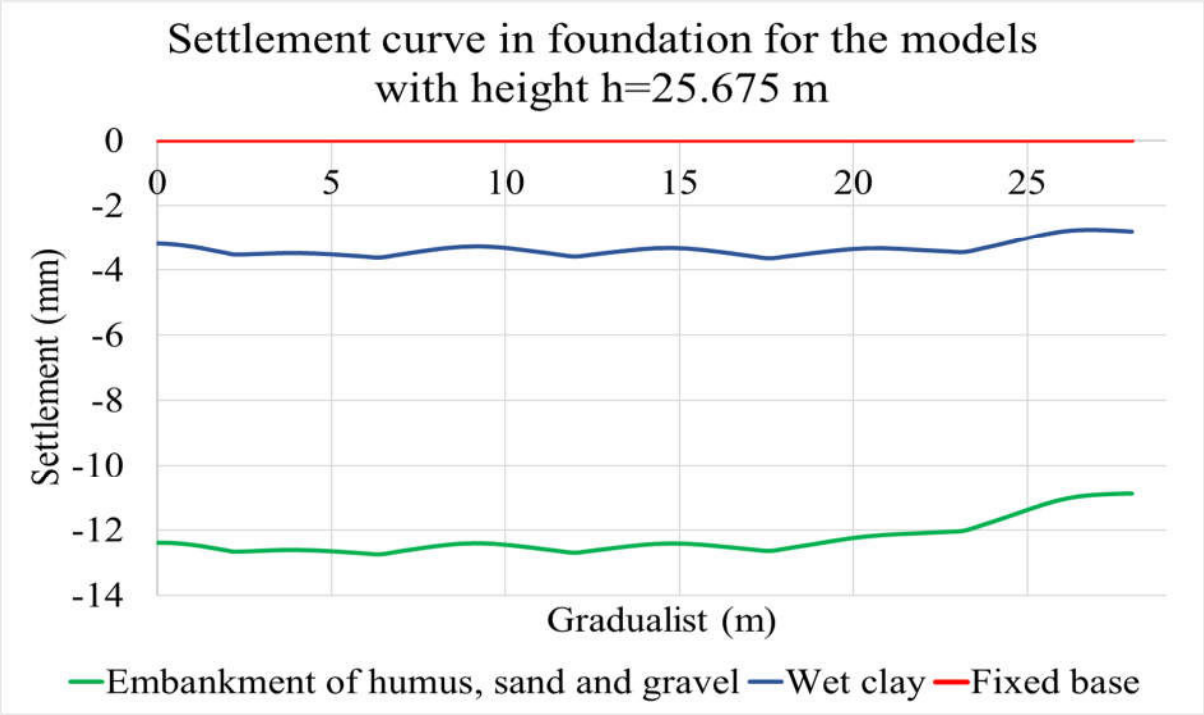

Figure 3.60. Settlement curve in foundation of the models with height h=26.675 m considering different soil type

Table 3.27. maximum values of displacement in foundation of the models with h =25.675 m

Model	Maximum displacement Uz	Unit
Fixed base	0	mm
Wet Clay	3.649	mm
Embankment of humus and sand	12.649	mm

Figures 3.59 and 3.60 show the settlement curves for each model studied. These settlements have a maximum value below the Eurocode recommended limit value of 50 mm. However, it

can be seen that the settlement increases with the softness of the soil and the size of the building, except in the case of the fixed base models, where it remains constant and equal to zero whatever the height of the building.

These deformations are due to the flexibility conditions introduced by the soil-structure interaction, which in reality materializes the real behaviour of the soil. These deformations can modify the response of the structure.

3.4.8.2. Solicitation on beam

The solicitation on the main beam designed in subsection 3.2.4 for the building with fixed supports and with the raft foundation on different types of soil is presented in Figure 3.61

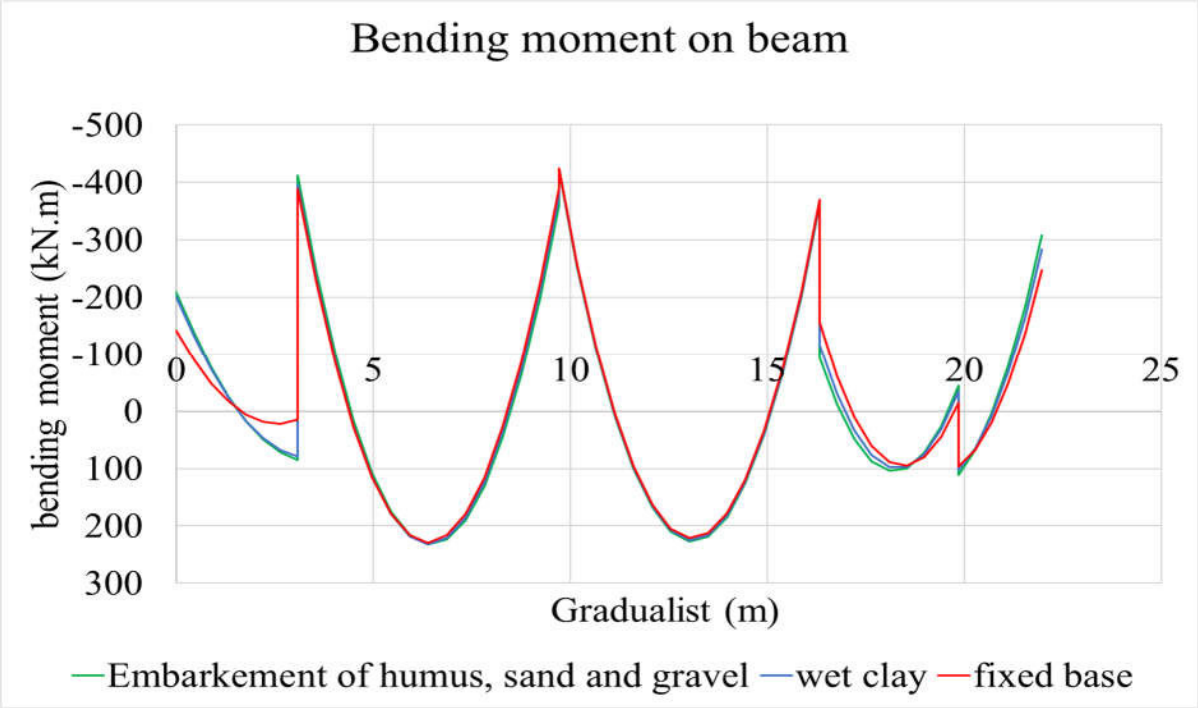

Figure 3.61. bending moment of the beam for the building resting on different base and soil type

Table 3.28 Maximum values of bending moment on reference beam considering different soil type

	MAXIMUM BENDING MOMENT (kN.m)		
	Fixed base	Wet clay	Embarkment of humus, sand and gravel
MID SPAN	229.2283	232.5735	232.7773
SUPPORT	-424.6917	-423.2505	-420.2206

The results show a slight variation of the loads on the beam. However, it is shown that the increased flexibility of the foundation soil leads to a reduction of the bending moment at the beam supports except for the first and last two supports and to an increase of the bending moment at the mid-span of the beam. thus, in general, the moment increases with the soil flexibility.

the same thing happens for the shear force shown in figure 3.62

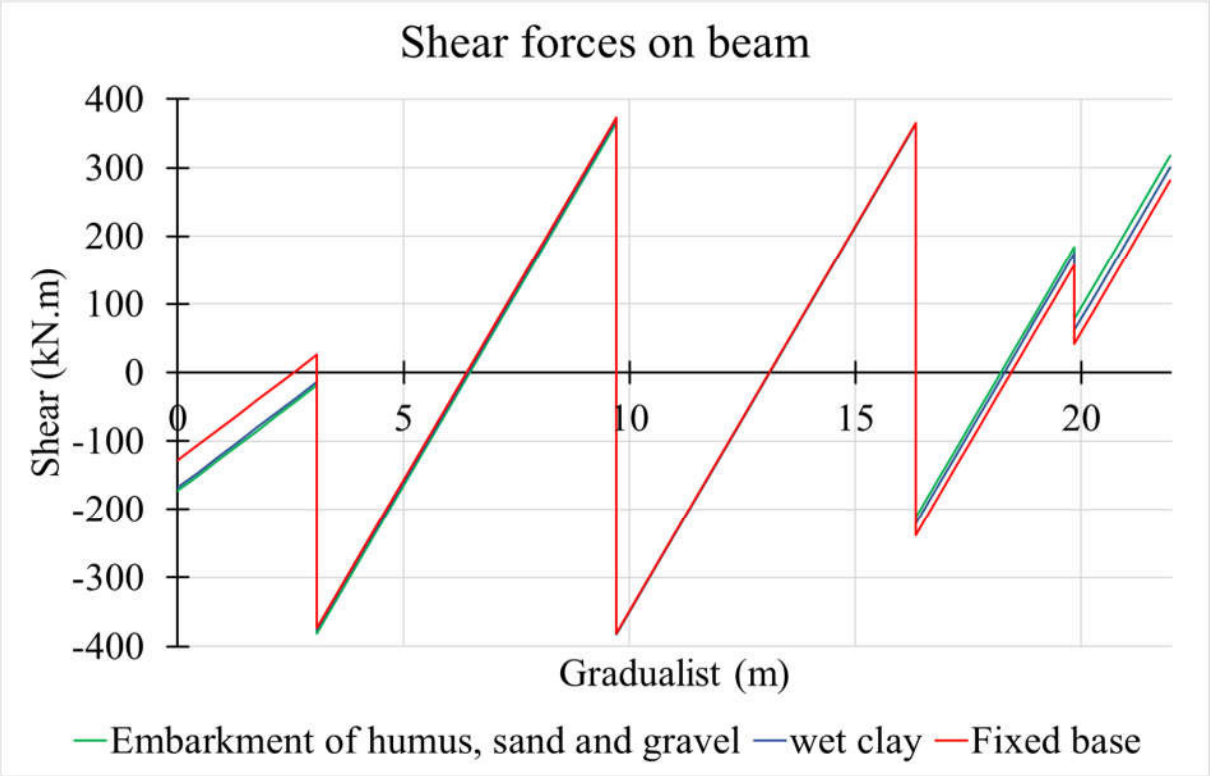

Figure 3.62. shear force on the main beam

From Figure 3.62, it is observed a reduction in shear force solicitation at the beam's midspan and an increase at the support of the beam

3.4.8.3. Solicitation on column

The variation of the axial forces and bending moment solicitation in the column for the building with fixed and flexible base on different soil types are presented in Figure 3.63 and 3.64 respectively.

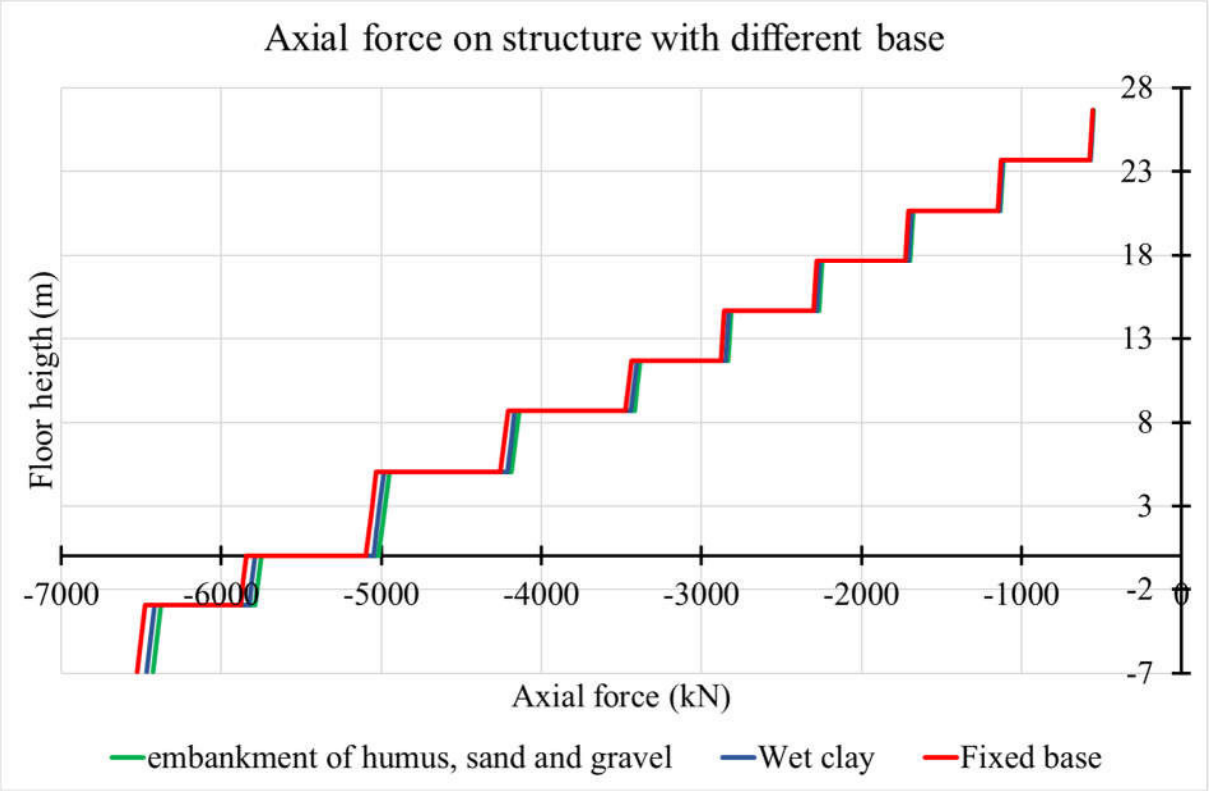

Figure 3.63. axial force for the column of building on different soil type

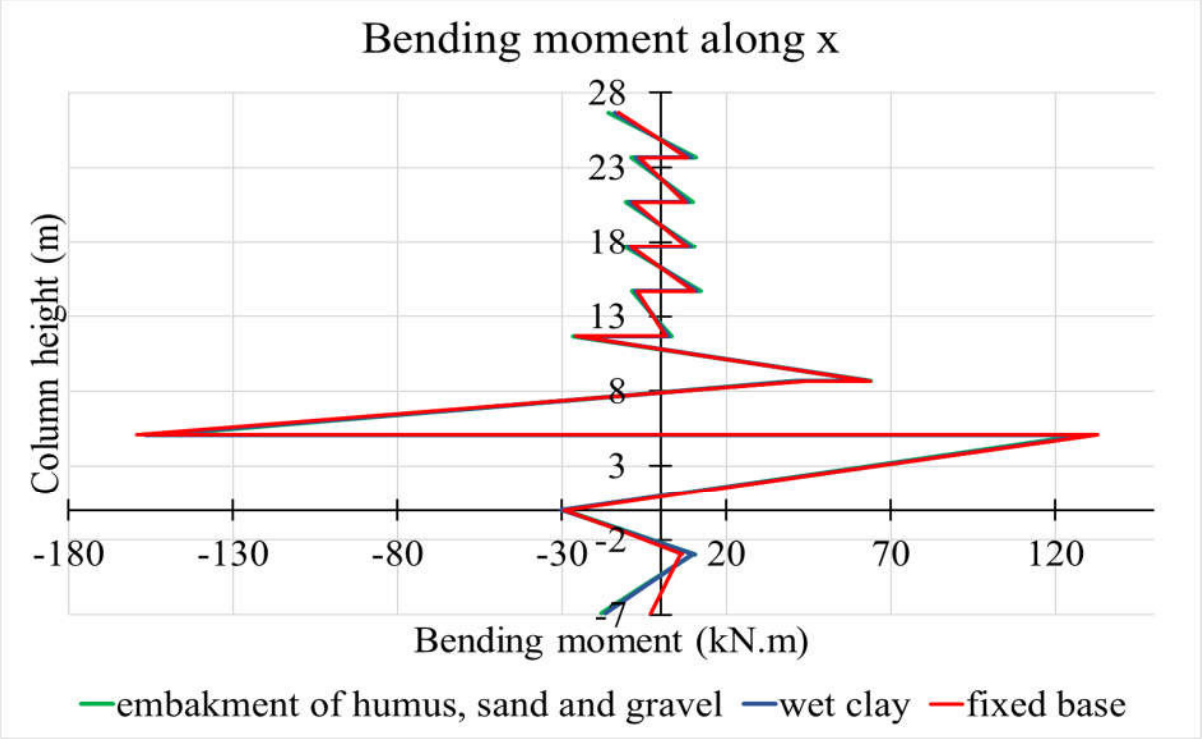

(a)

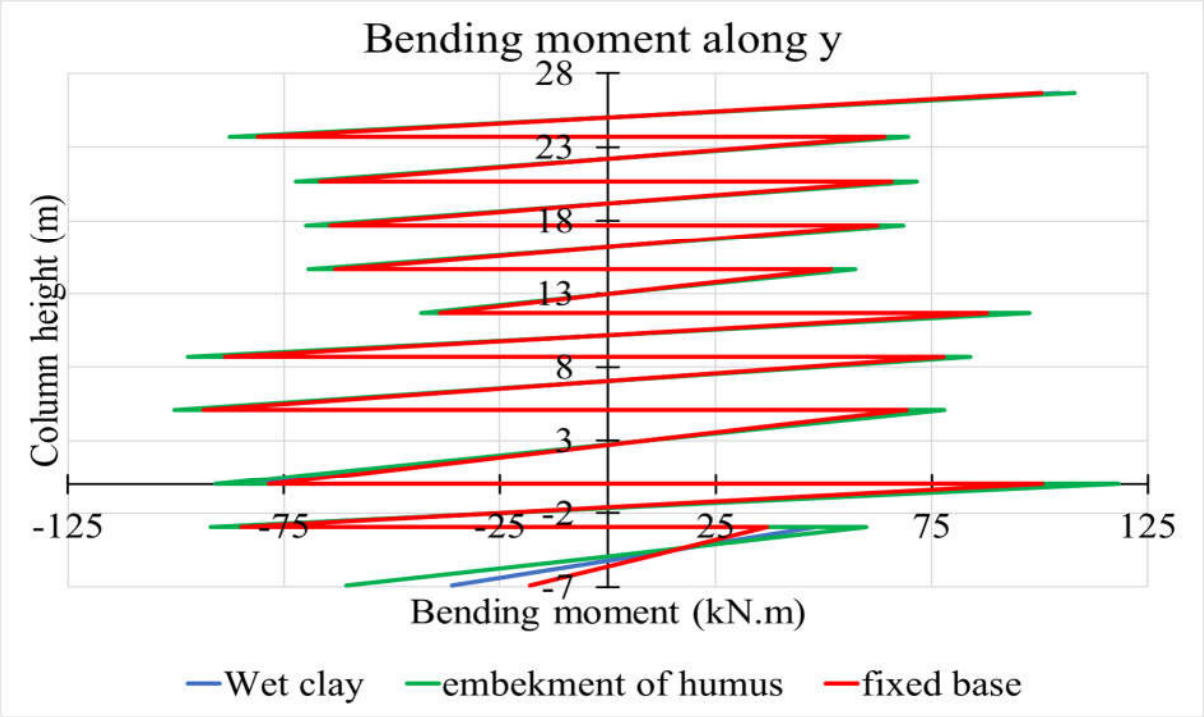

(b)

Figure 3.64. Bending moment for the column p1 of building on different soil type in: (a) x-axis and (b) y-axis

Figures above show that the flexibility introduced by the SSI increases the solicitations in the column except for the axial force, which decreases the maximum value of the moment along the x-axis, which is given by the model on fixed support.

Table 3.29. maximum values of bending moment on the column

Maximum bending moment(kN.m)			
direction	Fixed base	Wet clay	embankment of humus, sand and gravel
X	159.31	156.51	152.71
Y	100.4433	110.9792	118.1954

3.5. Dynamic analysis

For this study, the six preview models that differ in foundation type, height, and soil support are compared. The first two models have a fixed base, while the other four models have a flexible base resting on two types of soil: wet clay and an embankment of humus, sand, and gravel.

This study carries out the response of those models in terms of the period, the lateral deformation of the building, the inter-story drift, the shear force, displacement of foundation and solicitation in beam and column

3.5.1. Modal analysis

From the modelling of this structure, it is possible to have thousands or millions of degrees of freedom, which means that it is possible to find several natural frequencies, but it is not necessary to determine all of them. for this analysis, only the data extracted from the modes that have an influence on the dynamic behaviour of the structure will be used. These modes are those for which the sum of the effective modal masses is greater than or equal to 90% of the total mass of the structure. Figures 3.65 to 3.71 show respectively the deformation shape of the first three modes of vibration of each models studied and the cumulation of masses participation ratio of the vibrations along x and y directions and around the z axis.

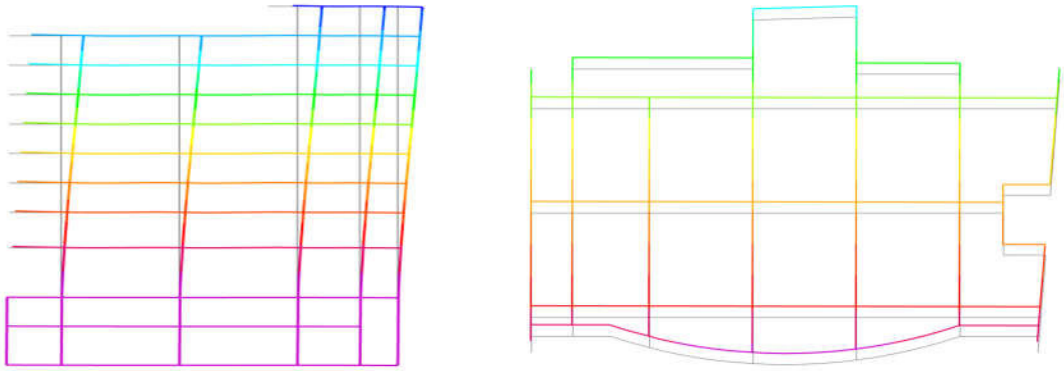

(a)

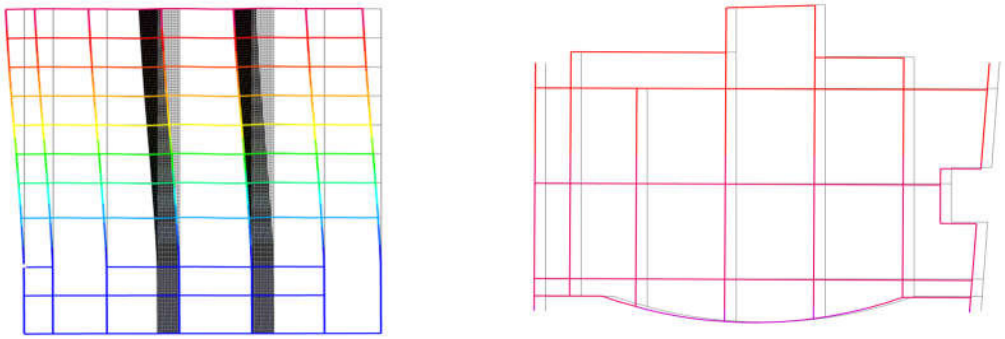

(b)

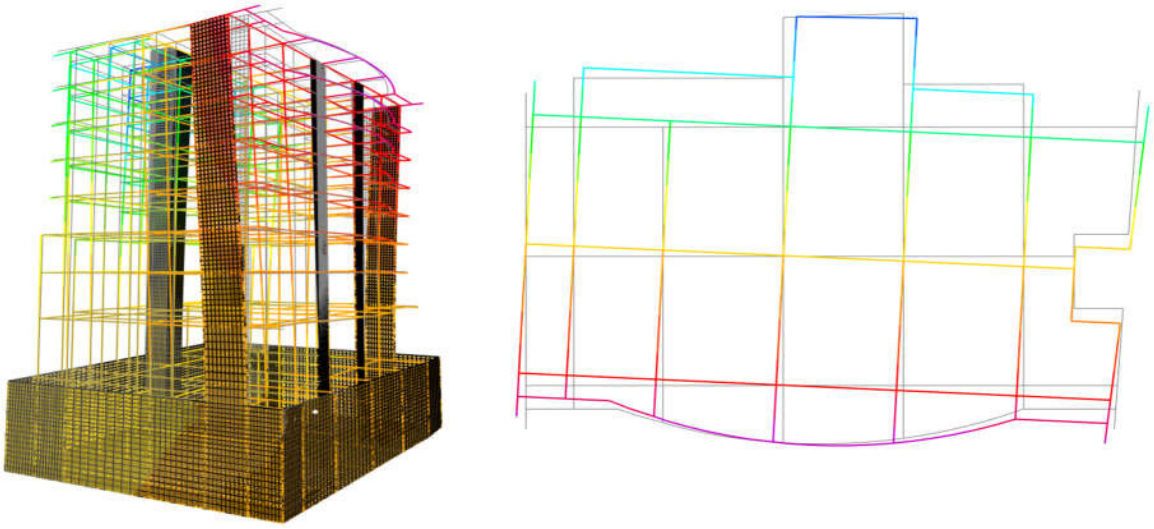

(c)

Figure 3.65 deformed shape of building (a) first mode; (b) second mode and (c) third mode

These deformed shapes are the same for all models.

Table 3.30. modal participating mass ratio of the model with h=31.675 m on wet clay

Mode	Modal participating mass ratio (%)			
	Period (s)	In x direction	In y direction	Around z
1	1.43	0.06	44.66	0.26
2	1.34	45.57	0.06	0.41
3	1.07	0.24	0.05	39.53
4	0.40	10.79	0.29	0.01
5	0.38	0.27	14.21	0.04
6	0.30	0.05	0.39	14.65
7	0.21	0.84	0.08	0.06
8	0.20	8.14	0.01	0.00
9	0.19	0.13	4.45	0.04
10	0.18	0.16	10.55	0.22
11	0.16	2.09	0.10	0.12
12	0.15	0.27	0.62	31.36
13	0.13	25.62	0.62	0.00
14	0.13	1.13	16.19	2.85
15	0.12	0.15	2.50	9.72
16	0.09	3.44	0.97	0.00
17	0.09	0.85	2.90	0.29
18	0.08	0.00	1.15	0.37

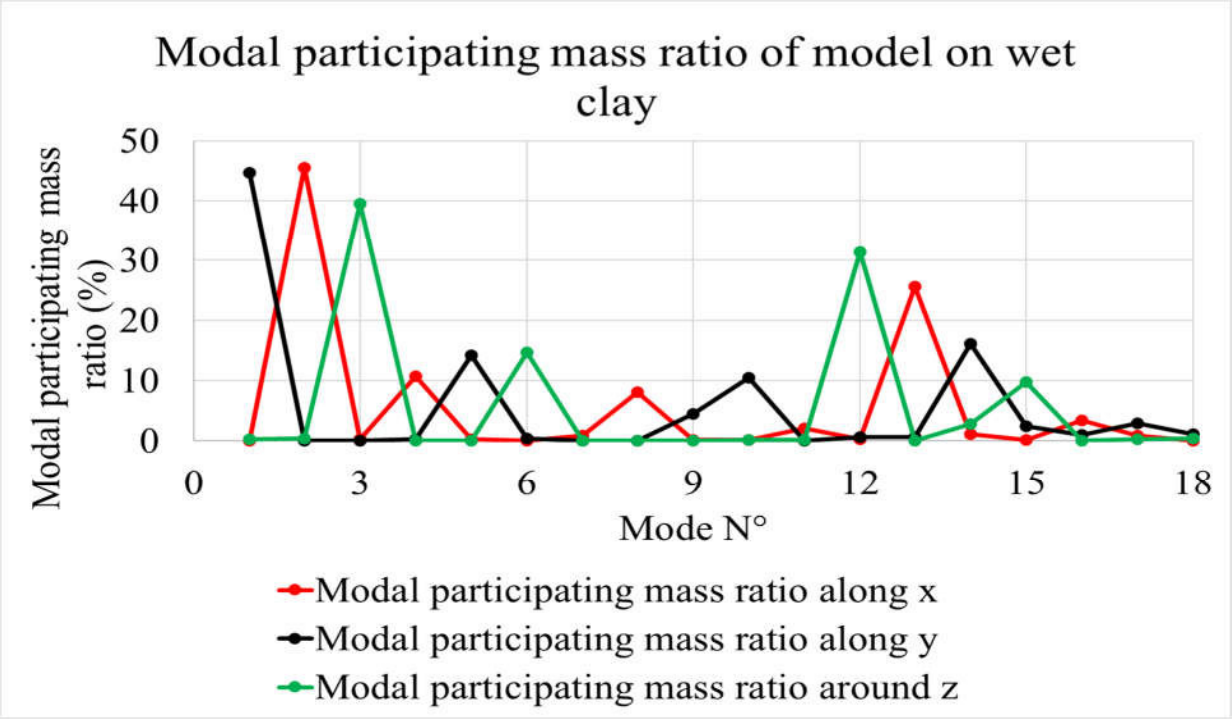

Figure 3.66. Modal Participating Mass Ratio of Model on wet clay

Table 3.31. modal participating mass ratio of the model with height h=31.675 m

Embankment of humus, sand and gravel

Mode	Modal participating mass ratio (%)			
	periode	in x direction	in y direction	around z
1	1.59	0.04	49.53	0.19
2	1.45	50.11	0.05	0.26
3	1.09	0.12	0.03	44.71
4	0.43	10.17	9.97	0.03
5	0.43	8.41	12.73	0.00
6	0.35	0.00	0.10	38.15
7	0.30	0.00	0.15	0.06
8	0.28	1.98	0.00	0.66
9	0.26	0.00	0.68	1.28
10	0.25	24.80	0.53	0.21
11	0.24	0.78	23.10	0.27
12	0.23	0.76	0.75	13.92
13	0.19	2.56	0.01	0.03
14	0.17	0.00	2.01	0.00
15	0.15	0.03	0.08	0.08
16	0.12	0.03	0.02	0.13
17	0.11	0.18	0.05	0.02
18	0.10	0.02	0.20	0.01

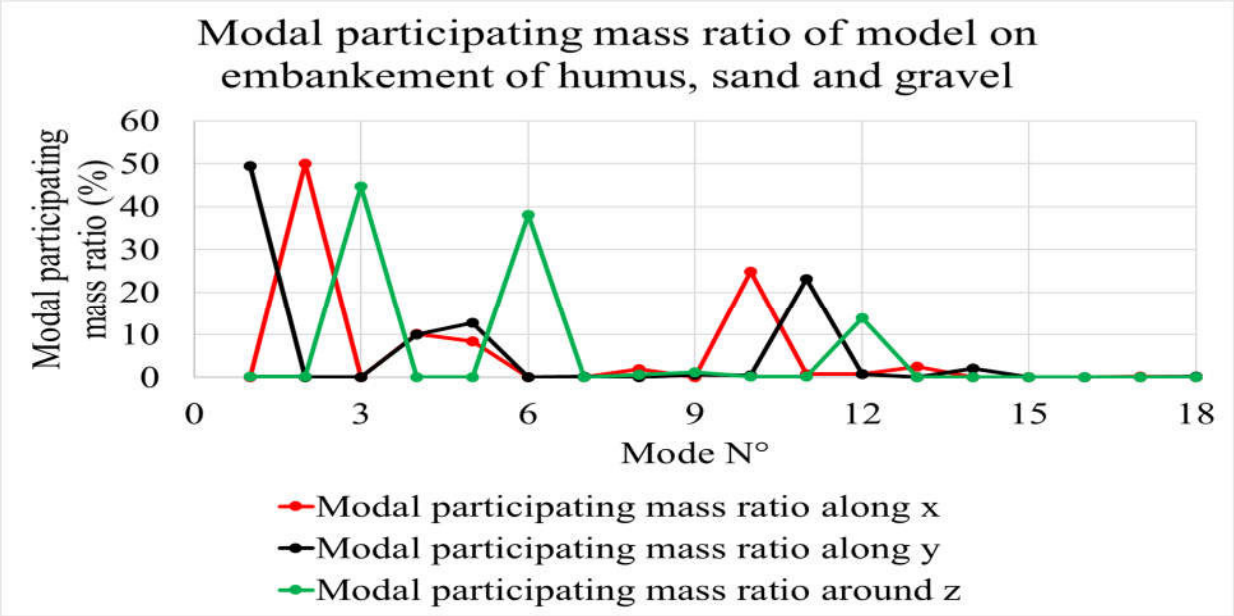

Figure 3.67. Modal Participating Mass Ratio of Model on embankment of humus, sand and gravel

Table 3.32. modal participating mass ratio of the model with height h=31.675 m on fixed base

Mode	Modal participating mass ratio (%)			
	Period (s)	in x direction	in y direction	around z
1	1.35	0.07	51.71	0.33
2	1.28	53.51	0.08	0.79
3	1.05	0.47	0.08	46.24
4	0.39	10.64	0.12	0.01
5	0.36	0.14	12.46	0.11
6	0.29	0.06	0.45	11.42
7	0.20	0.00	0.01	0.01
8	0.19	0.07	0.01	0.00
9	0.19	3.25	0.05	0.01
10	0.18	0.03	0.11	0.00
11	0.16	0.03	2.71	0.06
12	0.15	0.00	1.24	0.14
13	0.13	0.02	0.39	3.18
14	0.11	2.06	0.03	0.14
15	0.09	0.02	3.46	0.18
16	0.08	0.28	0.75	1.41
17	0.07	1.81	0.21	0.43
18	0.05	0.03	22.37	0.28
19	0.04	24.12	0.03	0.00
20	0.03	0.00	0.14	28.79

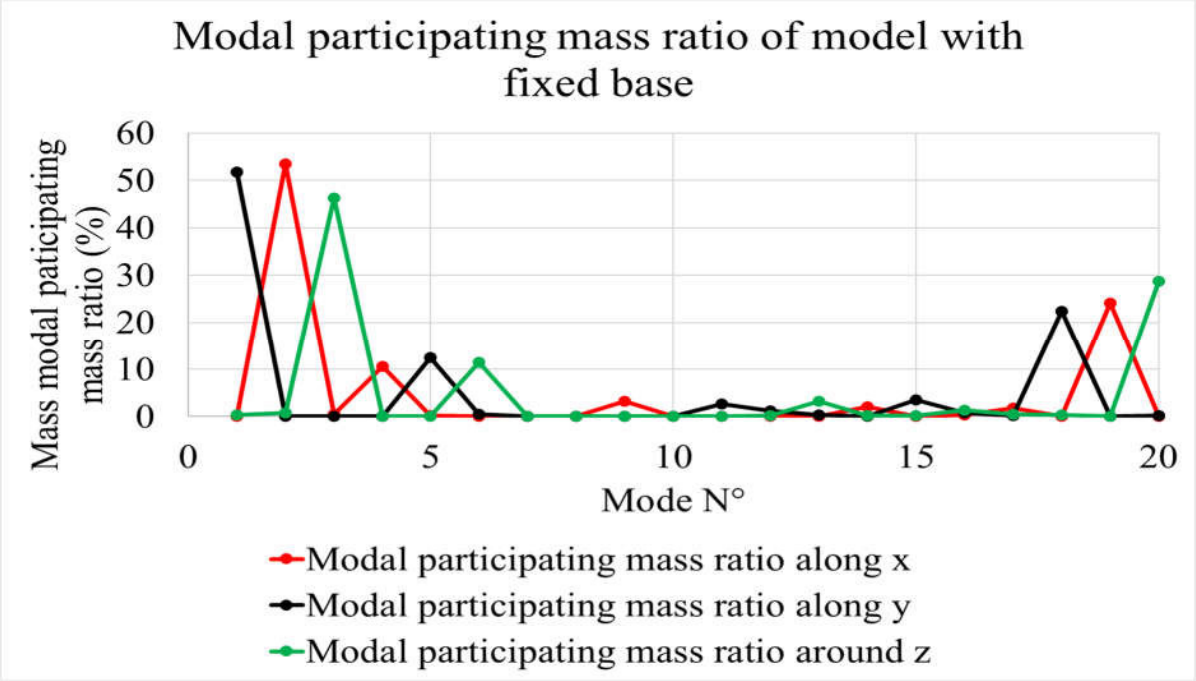

Figure 3.68 Modal Participating Mass Ratio of Model with fixed

From this data, the modes that will be used are selected based on the cumulative percentage of participating mass as describe in the paragraph above.

Table 3.33. Cumulative mass modal participating ratio of the model with height h= 31.675 m on wet clay

Mode	Cumulative mass modal participating ratio (%)			
	Period(s)	In x direction	In y direction	Around z
1	1.43	0.06	44.66	0.26
2	1.34	45.63	44.72	0.68
3	1.07	45.87	44.77	40.20
4	0.40	56.66	45.06	40.22
5	0.38	56.93	59.28	40.26
6	0.30	56.98	59.66	54.91
7	0.21	57.82	59.75	54.97
8	0.20	65.96	59.76	54.97
9	0.19	66.09	64.21	55.01
10	0.18	66.25	74.76	55.23
11	0.16	68.34	74.86	55.35
12	0.15	68.61	75.47	86.71
13	0.13	94.23	76.09	86.71
14	0.13	95.35	92.28	89.56
15	0.12	95.50	94.78	99.29

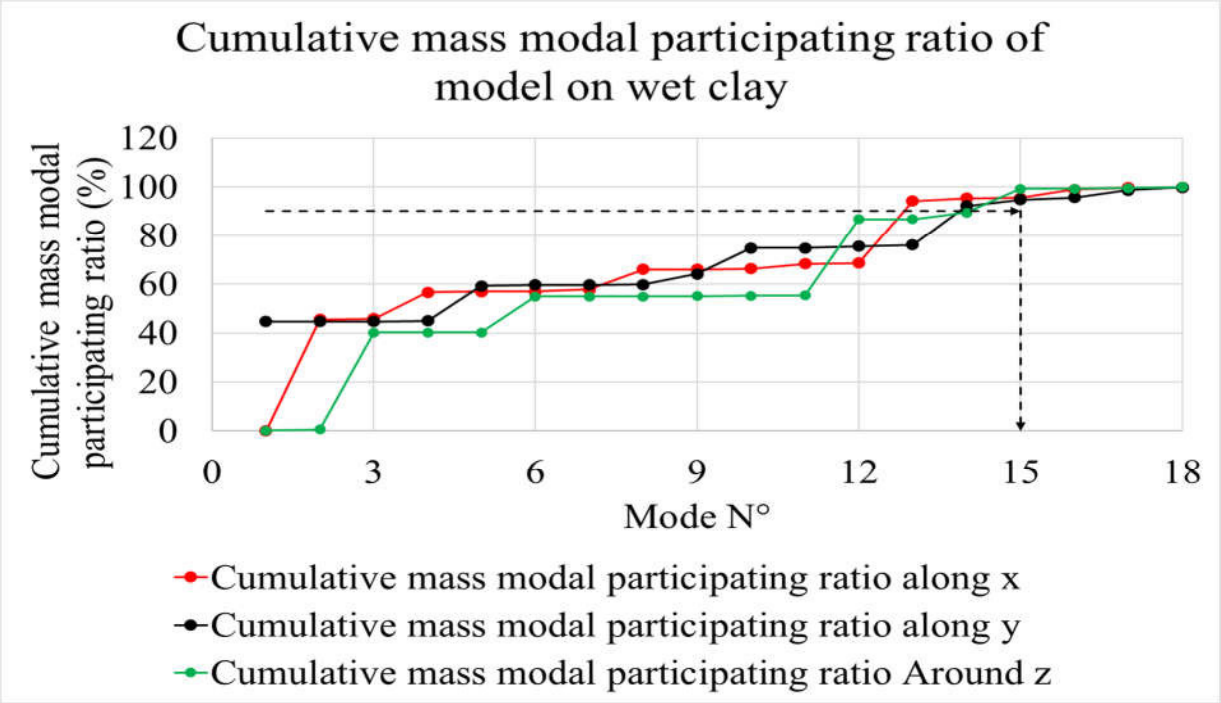

Figure 3.69. Cumulative Modal Participating Mass Ratio of Model on Wet clay

Table 3.34. Cumulative mass modal participating ratio of the model with height h= 31.675 m on Embankment of humus, sand and gravel

Mode	Modal participating mass ratio (%)			
	Period (s)	In x direction	In y direction	Around z
1	1.59	0.04	49.53	0.19
2	1.45	50.15	49.57	0.44
3	1.09	50.27	49.61	45.15
4	0.43	60.44	59.57	45.18
5	0.43	68.85	72.30	45.19
6	0.35	68.85	72.40	83.33
7	0.30	68.85	72.55	83.39
8	0.28	70.83	72.55	84.05
9	0.26	70.83	73.23	85.33
10	0.25	95.62	73.76	85.54
11	0.24	96.40	96.86	85.81
12	0.23	97.16	97.61	99.73

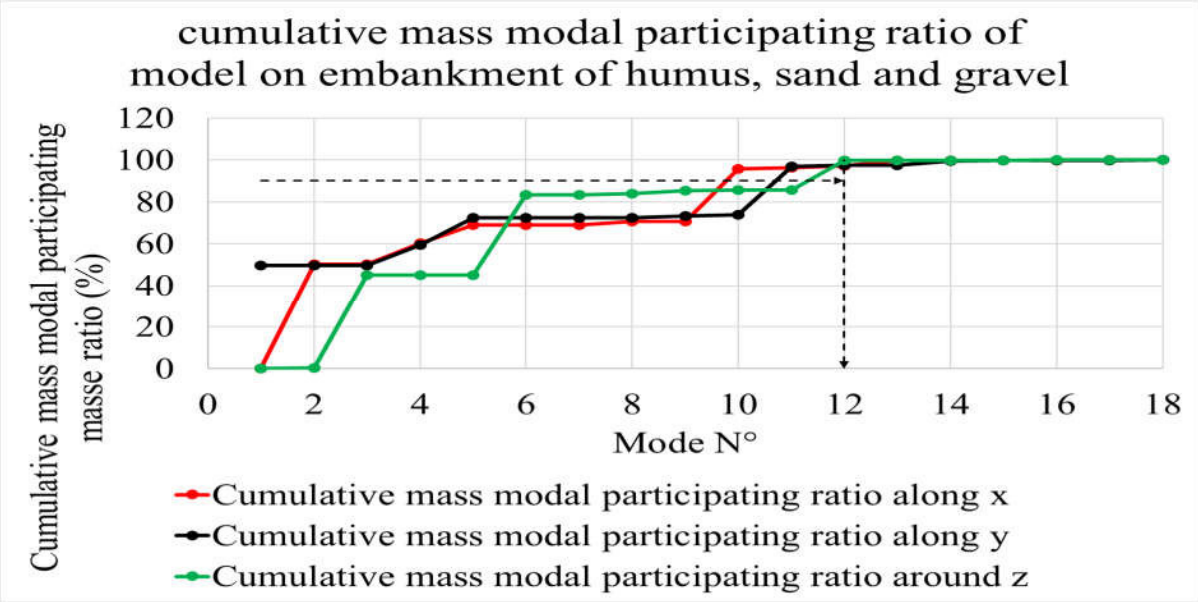

Figure 3.70. Cumulative Modal Participating Mass Ratio of Model on Embankment of humus, sand and gravel

Table 3.35. Cumulative mass modal participating ratio of the model with height h= 31.675 m fixed base

Mode	Modal participating mass ratio (%)			
	Period	In x direction	In y direction	Around z
1	1.35	0.07	51.71	0.33
2	1.28	53.58	51.80	1.12
3	1.05	54.05	51.88	47.36
4	0.39	64.69	52.00	47.36
5	0.36	64.82	64.46	47.47
6	0.29	64.88	64.91	58.89
7	0.20	64.88	64.92	58.90
8	0.19	64.95	64.93	58.91
9	0.19	68.20	64.97	58.91
10	0.18	68.23	65.08	58.91
11	0.16	68.26	67.79	58.97
12	0.15	68.26	69.03	59.11
13	0.13	68.28	69.42	62.29
14	0.11	70.34	69.44	62.43
15	0.09	70.36	72.90	62.62
16	0.08	70.64	73.65	64.03
17	0.07	72.45	73.86	64.46
18	0.05	72.48	96.23	64.74
19	0.04	96.60	96.26	64.74
20	0.03	96.61	96.40	93.53

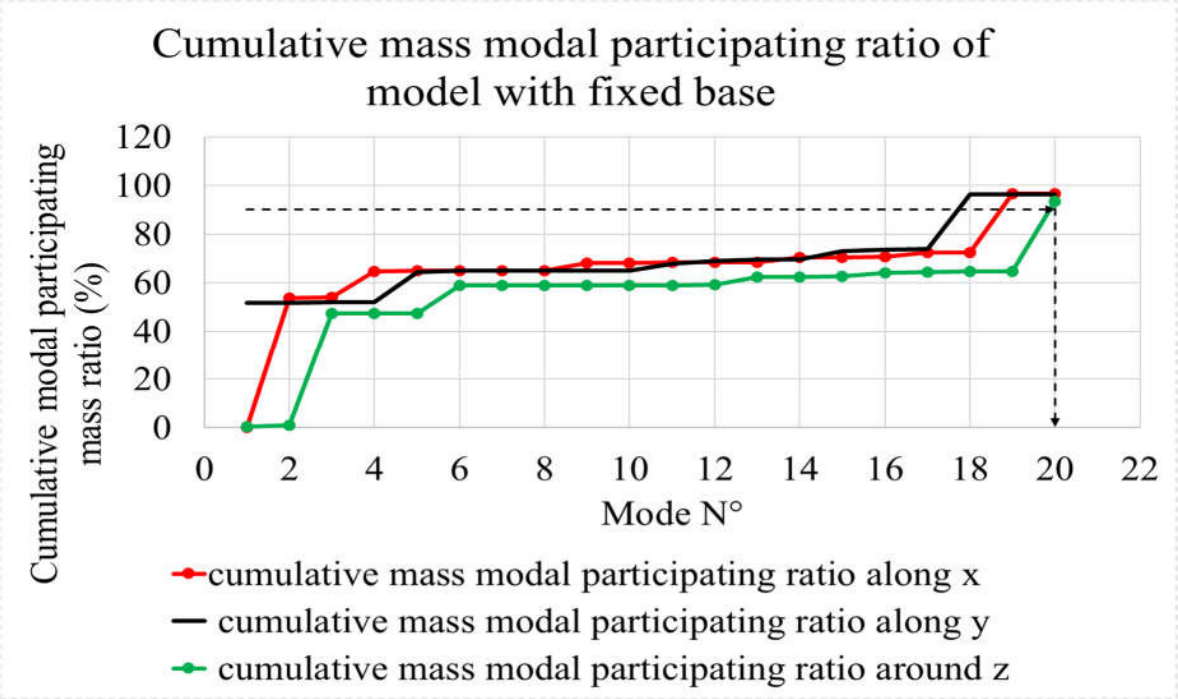

Figure 3.71. Cumulative Modal Participating Mass Ratio of Model with fixed base

according to tables 3.33 to 3.35, for the same number of modes considered, the percentage of participatory mass of the structure for the flexible base models is higher than for the fixed base models. this is explained by the fact that the fixed base model is much more rigid and therefore has more difficulty in moving.

Moreover, the flexible base models reach a percentage of about 99% of the participative mass around the z-axis contrary to the fixed base model which, caps at about 93% for a higher mode number than the one considered for the flexible bases. this difference is due to the flexibility of the system brought by the soil-structure interaction which strongly increases the displacement of the structure and increase.

3.5.2. Ground motion selection

As mentioned in section, this part consists of analyzing the structure under seismic loading and determine it responses.

The action of the earthquake is represented by its response spectrum which depend of the type of structure and the acceleration of ground motion on which the structure stand.

Soil investigations reveal that the soil consists of loose to medium cohesionless soil with soft clay layers and can be classify as soil type D. so, according to this information, the response

spectrum of Palermo earthquake can be used. Figure 3.72 show response spectrum use for design

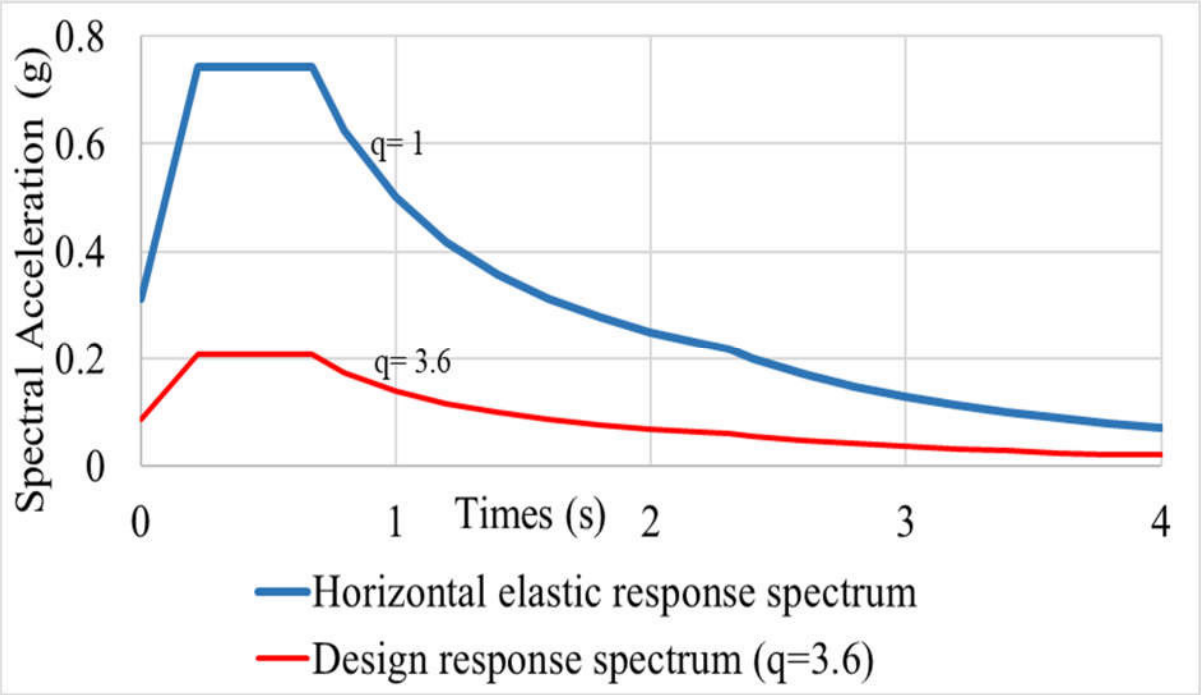

Figure 3.72. Response Spectrum used for the design.

3.5.2.1. Seismic load combination

Height combinations of actions were considered for seismic design

Seismic 1&2: $\sum_k \mathbf{G_k} + \mathbf{0.6}\sum_k \mathbf{Q_k} + \mathbf{E_x} \pm \mathbf{0.3E_y}$ 3.7

Seismic 3&4: $\sum_k \mathbf{G_k} + \mathbf{0.6}\sum_k \mathbf{Q_k} \pm \mathbf{E_x} + \mathbf{0.3E_y}$ 3.8

Seismic 5&6 $\sum_k \mathbf{G_k} + \mathbf{0.6}\sum_k \mathbf{Q_k} \pm \mathbf{E_y} - \mathbf{0.3E_x}$ 3.9

Seismic7&8: $\sum_k \mathbf{G_k} + \mathbf{0.6}\sum_k \mathbf{Q_k} + \mathbf{E_y} \pm \mathbf{0.3E_y}$ 3.10

3.5.3. Analysis criteria

3.5.3.1. Vibration period

The vibration period is an important parameter of a structure to estimate its seismic demand. Table 3.33 to3.35 above provides the vibration periods of the building models with height h=31.675 m. table 3.36 presents the summary of the periods of the first tree mode of the different models studied.

Table 3.36. period of the first three mode

Mode	Period (s)		
	Wet clay	Embankment of humus, sand and gravel	Fixed base
1	1.43	1.59	1.35
2	1.34	1.45	1.28
3	1.07	1.09	1.05

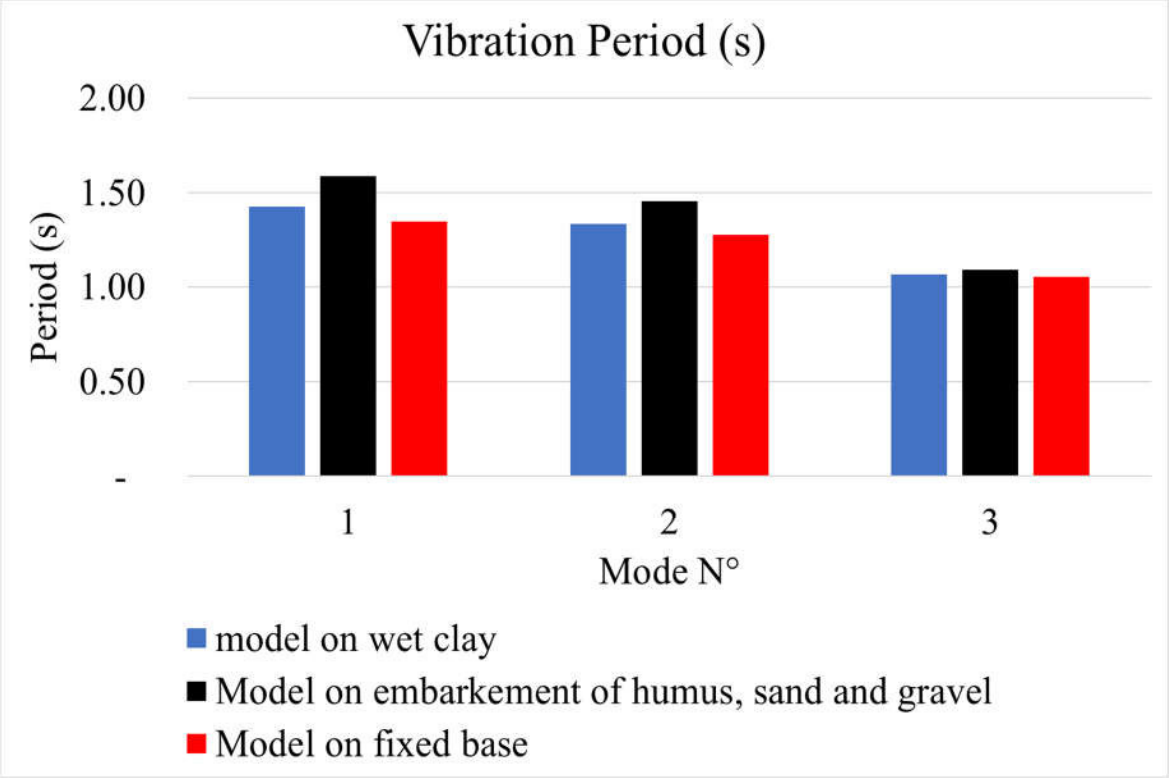

Figure 3.73. vibration period of the structure on different soil type

As expected, the results of the modal analysis show an increase in the period of vibration for each of the flexible base models studied compared to the fixed base models. This is due to the fact that the flexible base takes into account the deformations of the foundation system and the soil, thus reducing the stiffness of the system. This means that SSI affects the dynamic properties of the structure.

3.5.3.2. displacement of the structure

a. Lateral displacement

The results of the numerical analysis of the 3D model for the maximum lateral deflections of the structure supported by the fixed and flexible base are evaluated for each model in the x and y directions. The values of these deflections are presented in the tables 3.37 and 3.38 while the shape of these deflections are illustrated by the graphs in figures 3.74 and 3.75

Table 3.37. Maximum lateral displacement of the structure with height h=31.675 m on different soil type

Maximum lateral displacement of structure (mm)						
	Fixed base		Wet clay		embankment of humus, sand and gravel	
Floor heigth (m)	x direction	Y direction	x direction	Y direction	x direction	Y direction
-7	0	0	1.474	4.24	5.78	15.47
-3.85	0.14	0.694	1.668	7.43	7.14	22.6
0	0.365	1.5	2.275	10.25	8.45	28.964
5.075	12.065	33.74	14.076	45	21.35	67.468
8.675	23.5	68.462	25.575	80.451	33.31	105.018
11.675	33.104	99.678	35.234	111.881	42.712	138.15
14.675	43.204	132.924	45.307	145.167	51.785	172.943
17.675	52.74	165.95	54.812	178.21	60.104	207.451
20.675	61.23	197.7	63.313	210.3	68.409	240.92
23.675	68.49	227.53	70.7	240.9	77.162	272.976
26.675	74.6	255.4	76.97	269.7	85.65	303.46
29.675	74	275.77	76.45	292.86	87.54	328.85
31.675	73.2	290.145	78.77	309.4	92.95	346.216

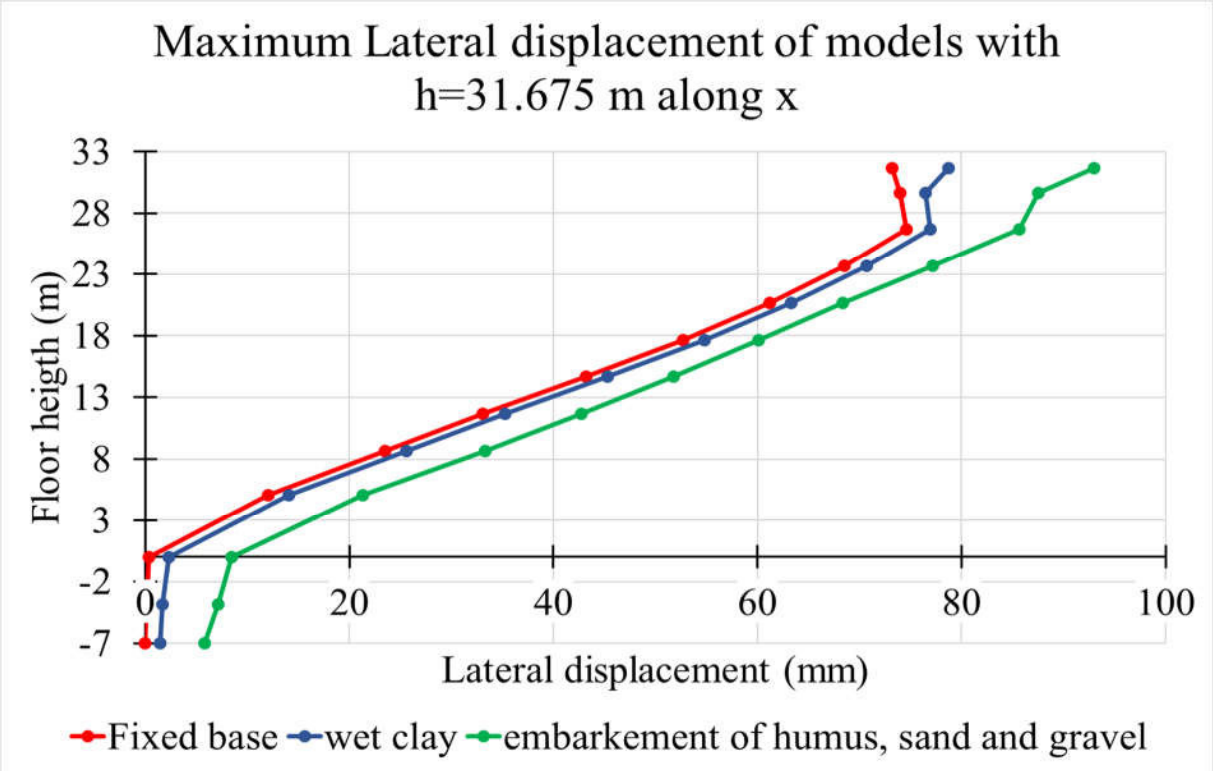

(a)

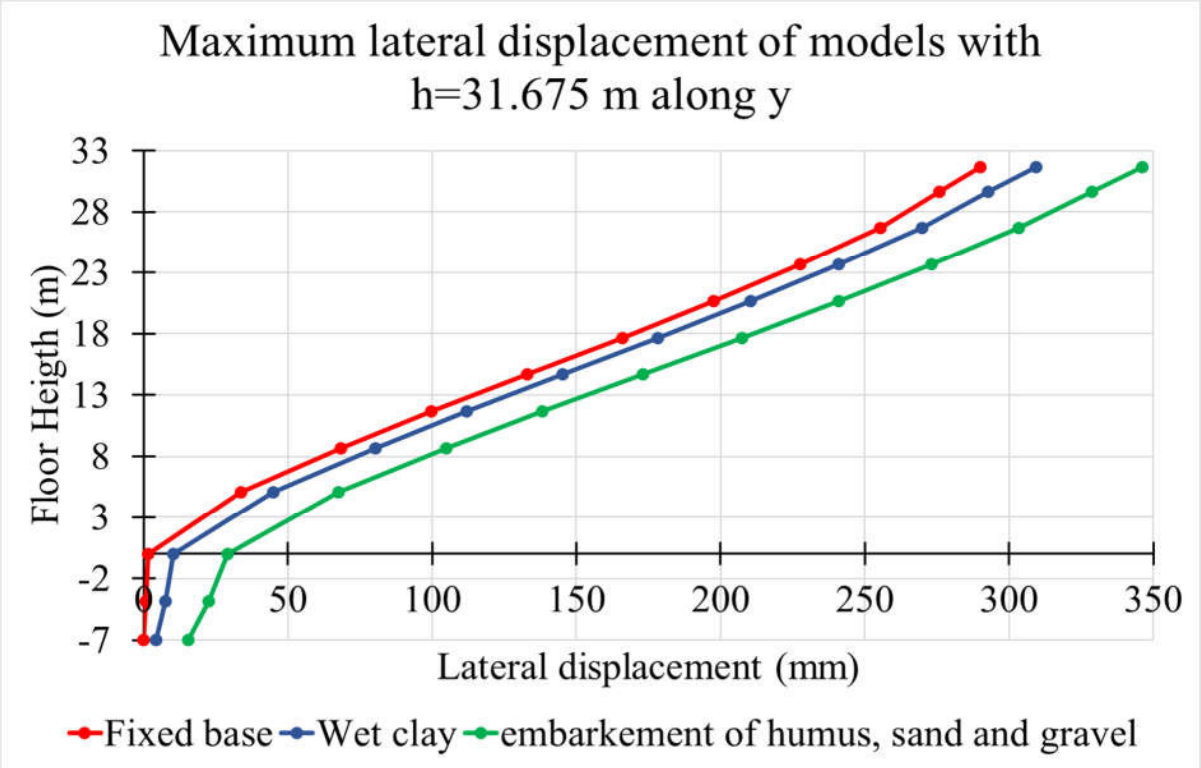

(b)

Figure 3.74. maximum lateral deformation of the structure with height h=31.675 m in: (a) x-direction and (b) y-direction.

Table 3.38. Maximum lateral displacement of the structure with height h=26.675 m on different soil type

Maximum lateral displacement of structure (mm)						
	Fixed base		Wet clay		Embankment of humus	
Floor heigth (m)	x direction	Y direction	x direction	Y direction	x direction	Y direction
-7	0	0	1.52	4.421	4.321	15.682
-3.85	0.155	0.722	1.74	7.73	6.007	23.973
0	0.394	1.553	2.34	10.61	7.588	24.572
5.075	14.299	35.909	15.12	47.205	20.629	72.064
8.675	27.579	72.153	27.384	83.919	32.108	110.265
11.675	38.099	103.903	37.405	115.76	41.057	142.7
14.675	47.918	136.638	47.421	148.535	50.335	176.278
17.675	56.713	168.09	56.426	180.146	58.926	208.882
20.675	64.743	197.459	64.178	209.884	66.584	239.895
23.675	56.837	209.071	63.505	225.663	65.309	261.444
25.675	60.23	212.764	62.563	233.492	70.308	274.444

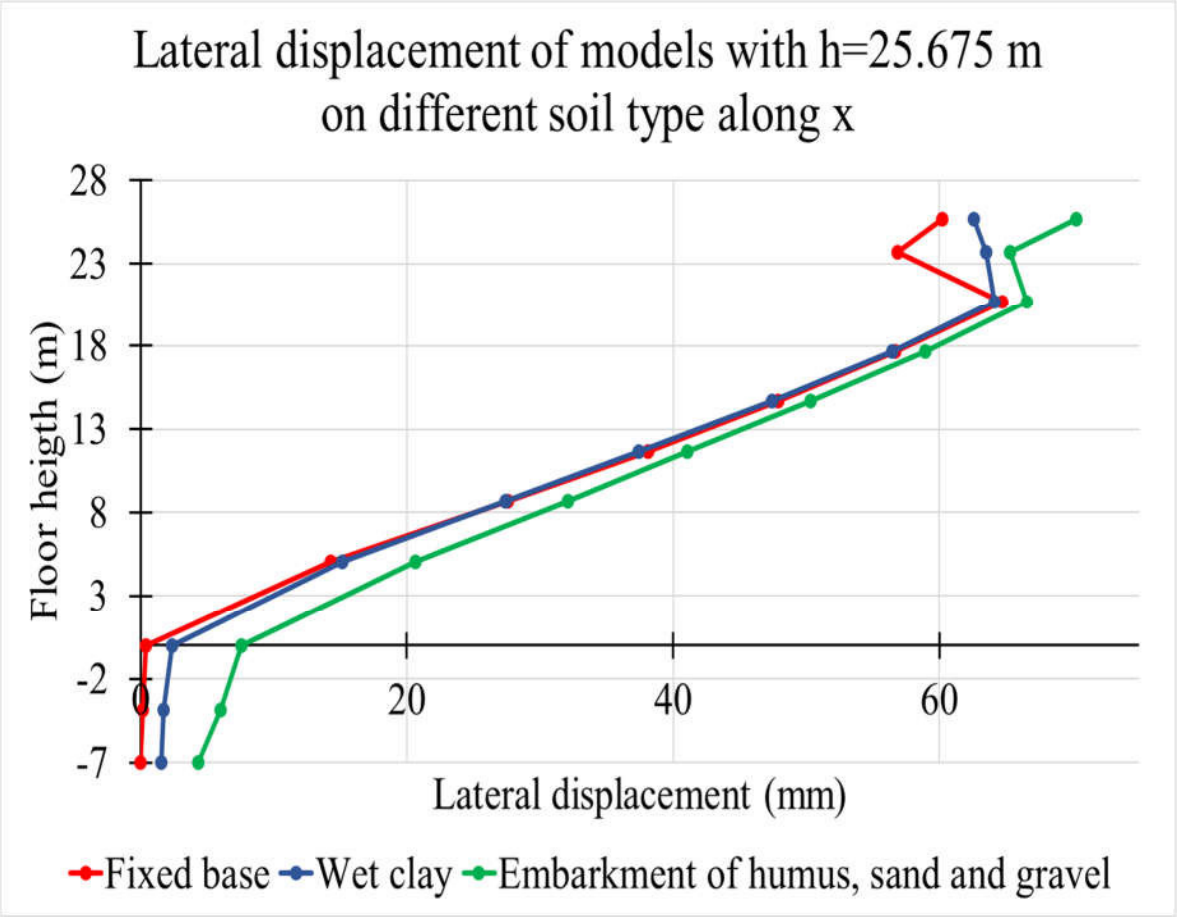

(a)

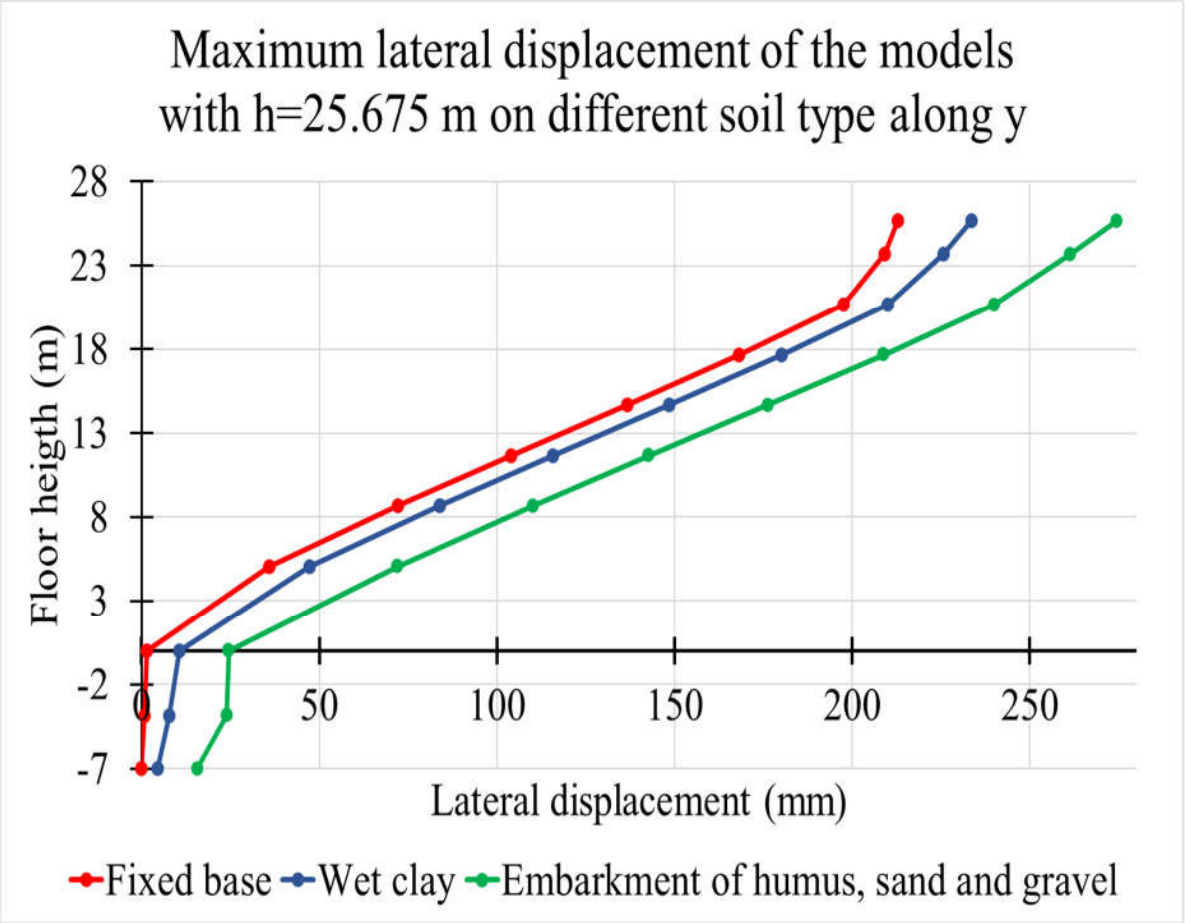

(b)

Figure 3.75. maximum lateral deformation of the structure with height h=25.675m in: (a) x-direction and (b) y-direction.

Referring to the graphs in the figures 3.74 and 3.75, it can be seen that taking into account the flexibility of the soil increases the lateral deformation of the structure as expected. The largest values of lateral deformation belong to the flexible foundation model.

For instance, the maximum lateral deflection of the model with a height of 31.675 m subjected to the Palermo earthquake is 73,2 mm for the fixed base, 78.77 mm and 92.95 mm for the flexible base model on wet clay and embankment of humus, sand and gravel respectively in x direction. this corresponds respectively to an increase of 7.6 % and 27% of the displacements of the flexible base model relative to the fixed base one. the same phenomenon happens for the models with a height of h=25.675 m. but here the variation is 3.87 % and 16,7%

In the y-direction, the same thing happens with a variation of 6.63% and 19,33 % for the models with height h=31.675 m. 9.74% and 28.99 % for the models with height h =25.675m.

in addition, as expected, the flexible base models show a lateral displacement in the foundation in comparison to the fixed base models which show a zero displacement These displacements are significantly greater in the models with a height of h=25.675 m. they represent the deformations of the soil supporting the structure under the seismic action and thus influence the response of the structure.

b. Vertical Displacement in foundation

As shown above, the seismic action causes lateral deformations in the foundation to which can be added vertical deformations as in the static case. Figures 3.76 and 3.77 show the vertical deformation of the foundations of the analyzed models according to the type of soil under seismic loading.

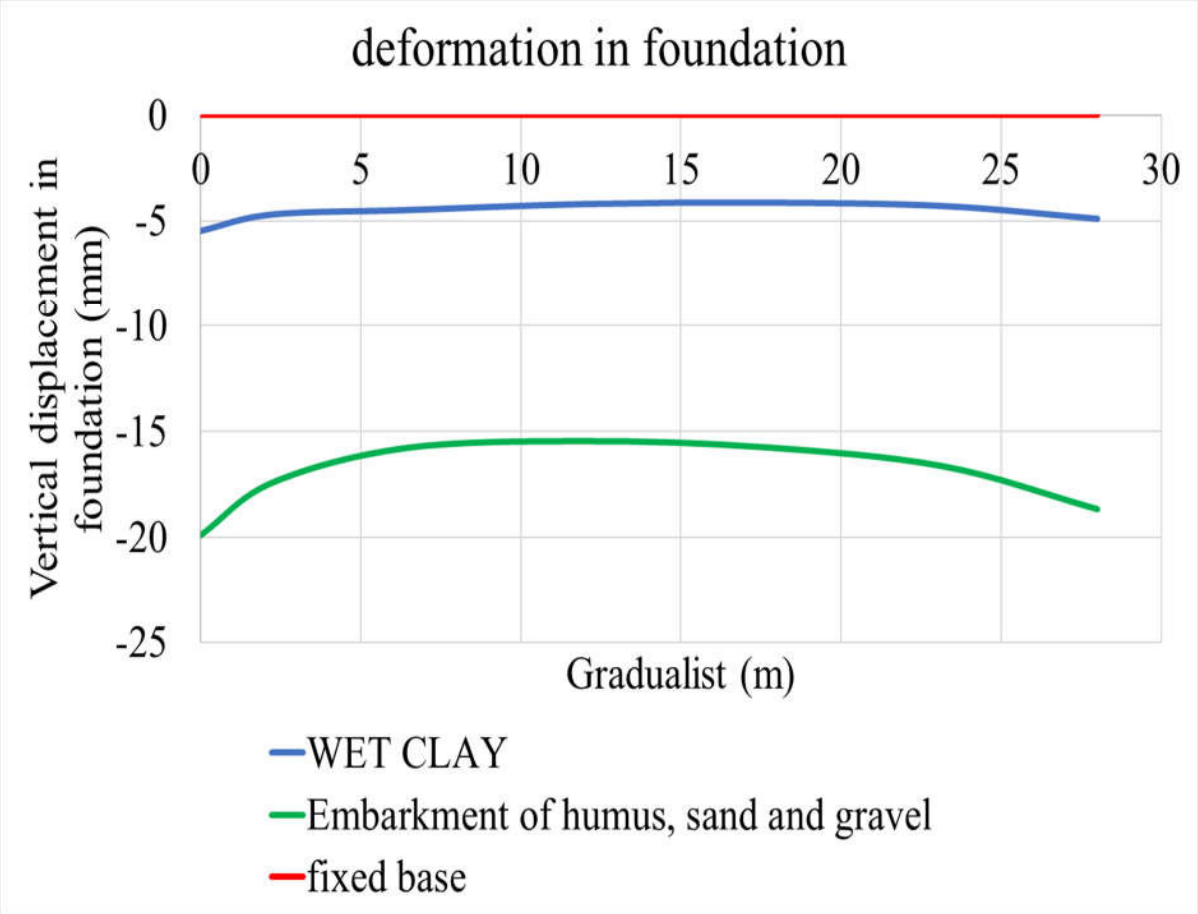

Figure 3.76. deformation in foundation of the model with h=31,675 m

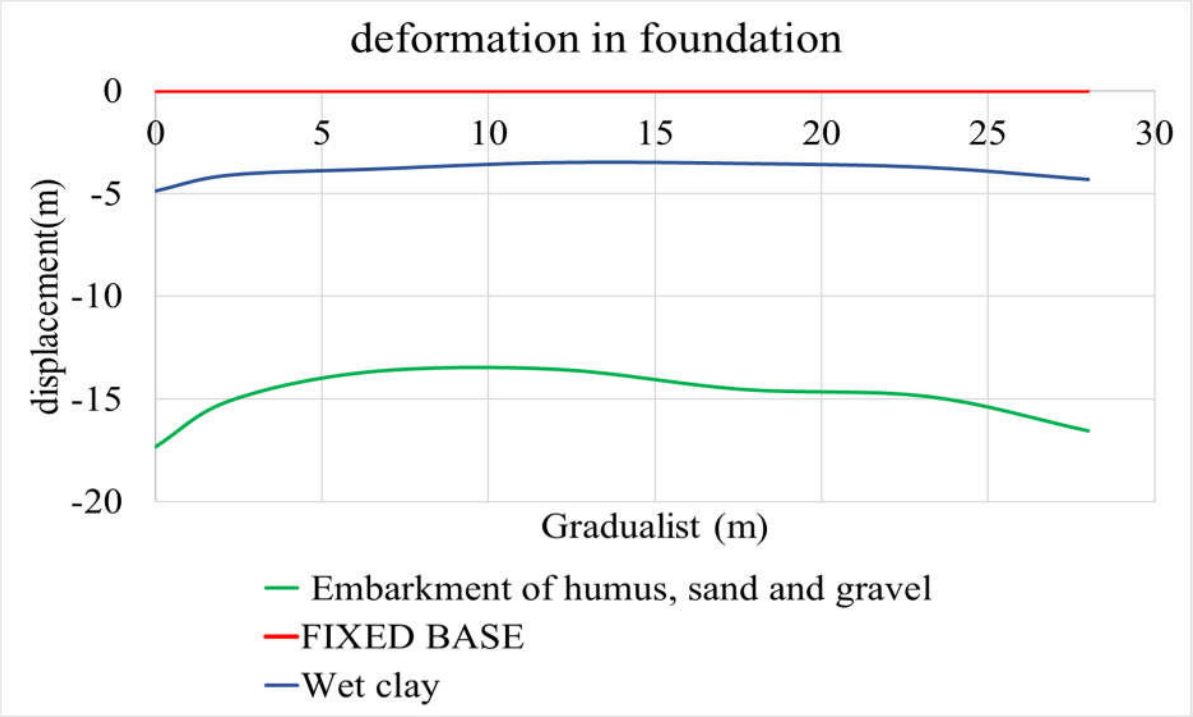

Figure 3.77. deformation in foundation of the model with h=26,675 m

As in section 3.4, figures 3.76 and 3.77 show the foundation deformations for the models with a flexible base, while the models with a fixed base have zero deformation regardless of the height of the structure. These curves show the evolution of the foundation deformations, which in this case can be confounded with foundation debonding.

3.5.3.3. Inter-storey drift Ratio

It is the difference between the lateral deflections of two adjacent stories divided by the height of that storey. For this class of building with brittle materials and a reduction factor ν = 0.4. using equation 2.59 and 2.60, the inter-story drift ratio are computed for all models and presented is table 3.39 and 3.40

Table 3.39. Maximum inter-story drift for model with h=31.675 m and different base

Floor heigth (m)	Fixed base		Wet clay		embankment of humus, sand and gravel	
	X direction	Y direction	X direction	Y direction	X direction	Y direction
-7	0.004	0.018	0.005	0.083	0.035	0.185
-3.15	0.007	0.026	0.019	0.090	0.042	0.202
0	0.231	0.635	0.233	0.685	0.254	0.759

5.075	0.318	0.961	0.319	0.985	0.332	1.043
8.675	0.320	1.044	0.322	1.048	0.313	1.104
11.675	0.337	1.141	0.336	1.110	0.303	1.160
14.675	0.318	1.068	0.316	1.101	0.277	1.150
17.675	0.283	1.058	0.283	1.070	0.277	1.116
20.675	0.242	0.994	0.247	1.020	0.292	1.069
23.675	0.204	0.929	0.209	0.960	0.283	1.016
26.675	- 0.020	0.679	- 0.017	0.772	0.063	0.846
29.675	- 0.020	0.479	0.077	0.551	0.180	0.579
31.675	- 0.020	0.479	0.077	0.551	0.180	0.579

These values permit to plot the graph presented in the figure 3.78

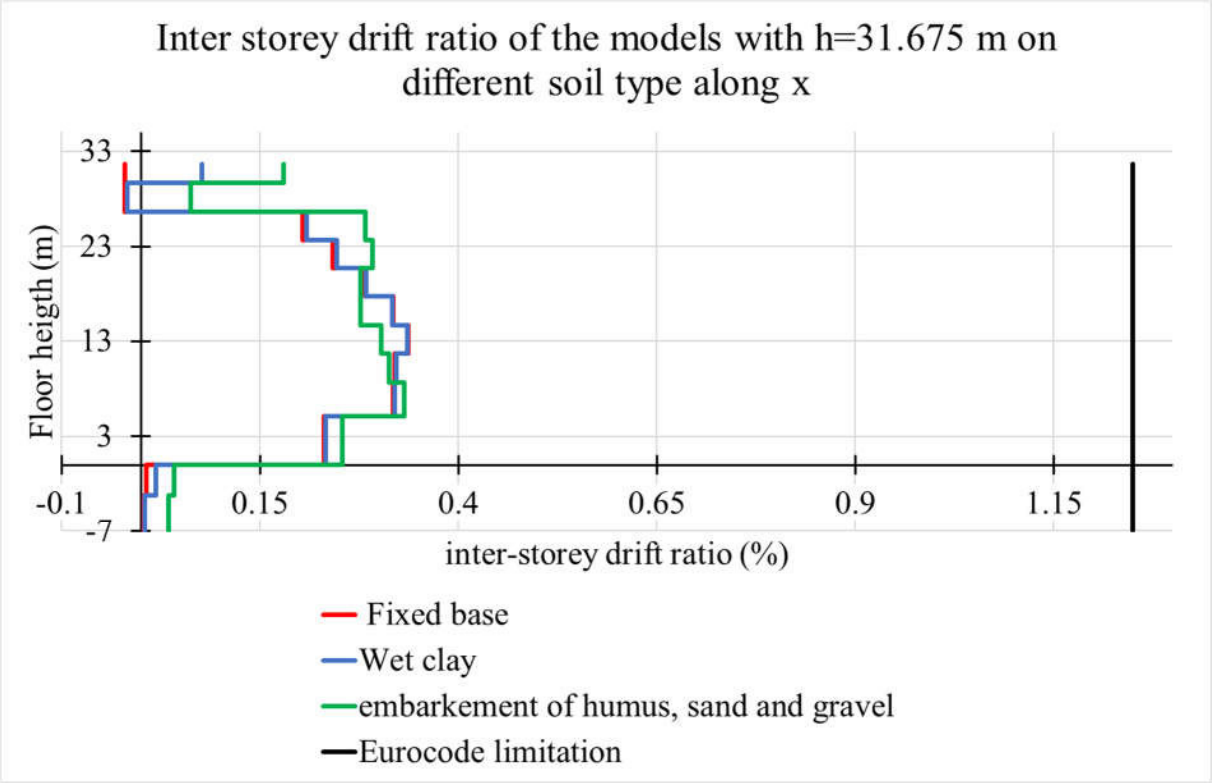

Figure 3.78. inter-story drift of the structure with height h=31.675 m resting on different soil type along x

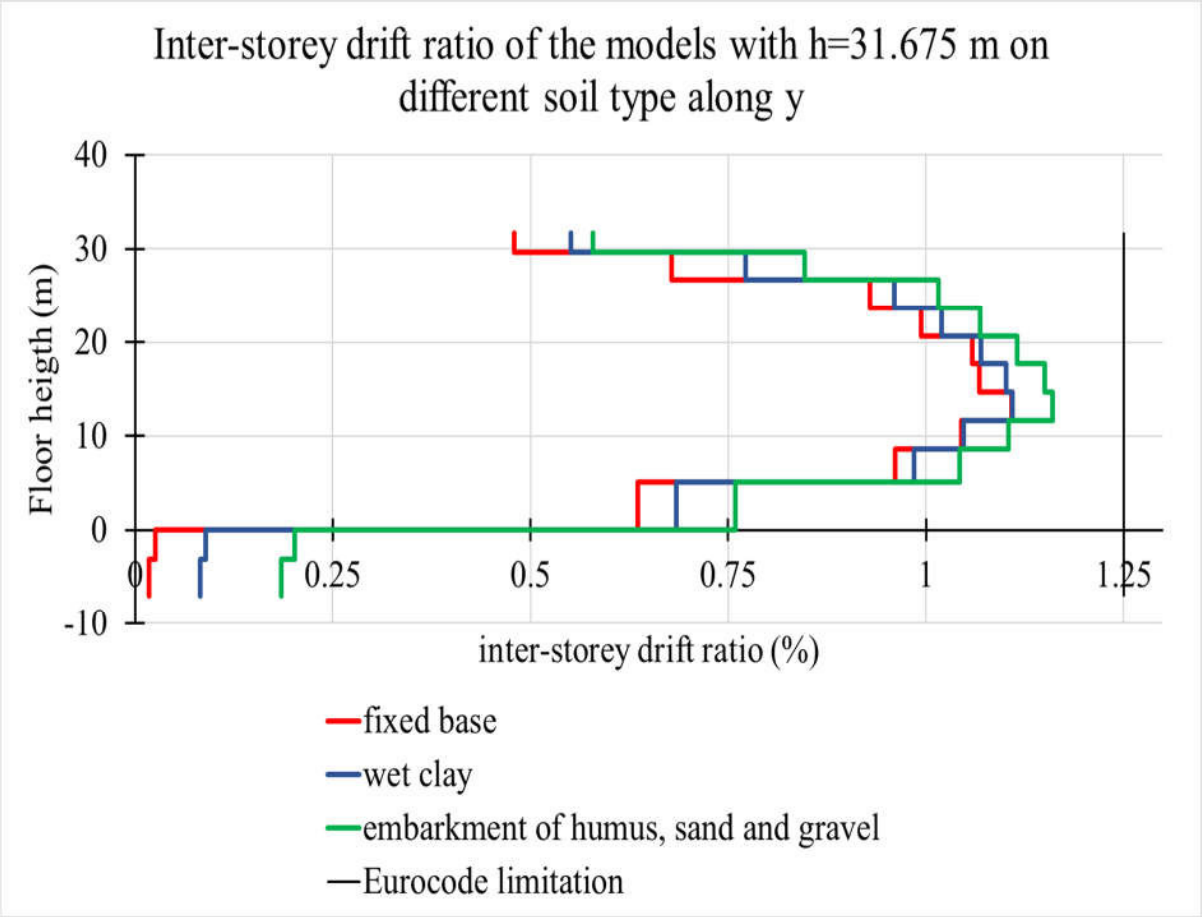

Figure 3.79. inter-story drift of the structure with height h=31.675 m resting on different soil type along y

Table 3.40. Maximum values of inter-storey drift of the models with h=31.675 m resting on different soil type

Maximum inter-storey drift (%)			
Direction	Fixed base	Wet clay	embarkment of humus and clay
X	0.337	0.336	0.332
Y	1.108	1.11	1.16

Figure 3.80. Maximum inter-story drift of the models with h=26.675 m resting on different soil type

Table 3.41. Maximum inter-story drift for model with h=26.675 m and different base

Floor heigth (m)	Fixed base		Wet clay		Embankment of humus, sand and gravel	
	x direction	Y direction	x direction	Y direction	x direction	Y direction
-7	0.004	0.019	0.006	0.086	0.044	0.215
-3.15	0.008	0.026	0.019	0.091	0.050	0.019
0	0.274	0.677	0.252	0.721	0.257	0.936
5.075	0.369	1.007	0.341	1.020	0.319	1.061
8.675	0.351	1.058	0.334	1.061	0.298	1.081
11.675	0.327	1.091	0.334	1.093	0.309	1.119
14.675	0.293	1.048	0.300	1.054	0.286	1.087
17.675	0.268	0.979	0.258	0.991	0.255	1.034
20.675	-0.264	0.387	-0.022	0.526	- 0.043	0.718
23.675	0.170	0.185	-0.047	0.391	0.250	0.650
26.675	0.170	0.185	-0.047	0.391	0.250	0.650

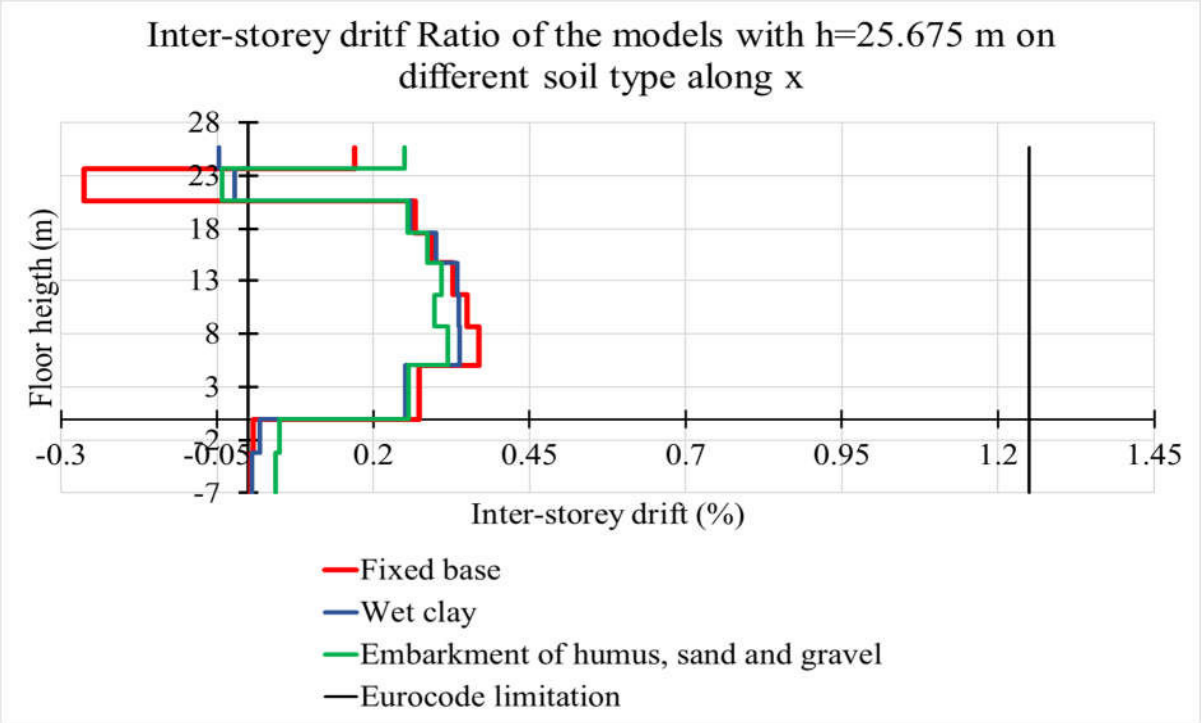

Figure 3.81. inter-story drift of the structure with height h=26.675 m resting on different soil type along x

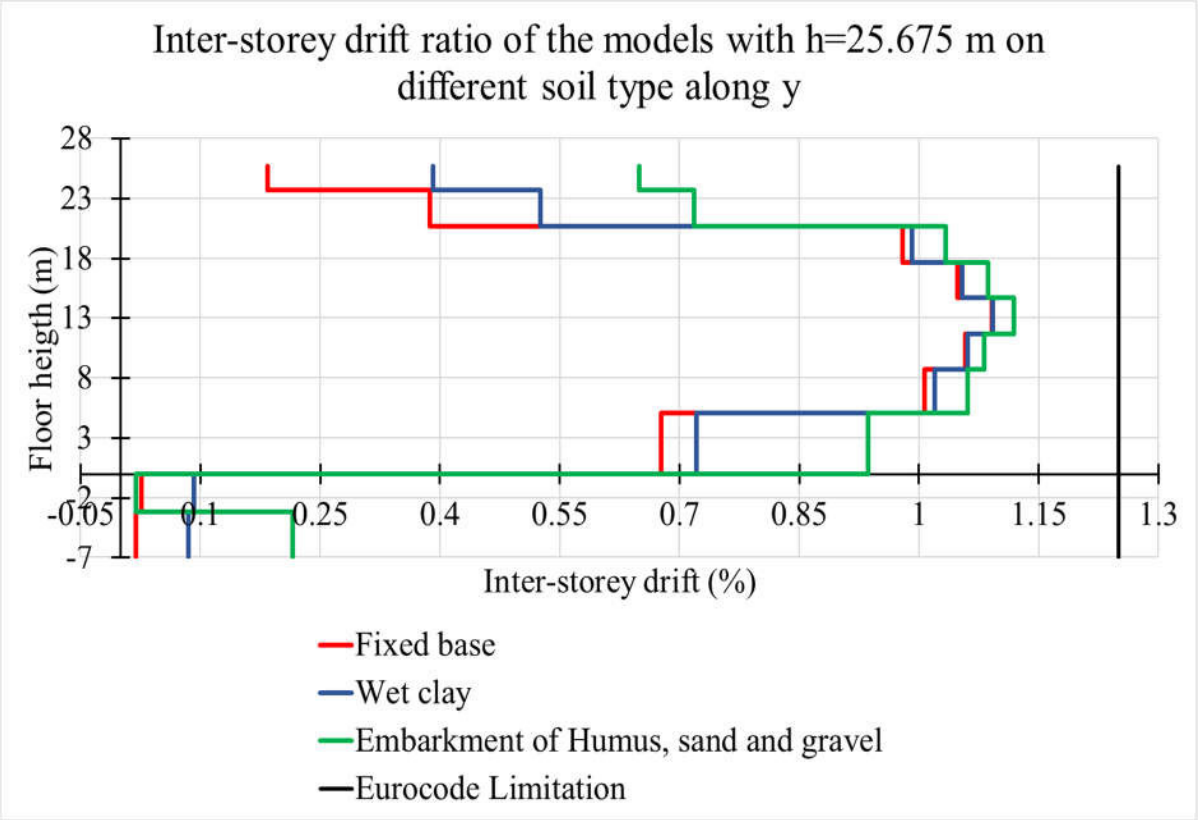

Figure 3.82. inter-story drift of the structure with height h=25.675 m resting on different soil type along y

Table 3.42. Maximum values of inter-storey drift of the models with h=26.675 m resting on different soil type

Maximum inter-storey drift (%)			
Direction	Fixed base	Wet Clay	embankment of humus, sand and gravel
X	0.351	0.334	0.319
Y	1.091	1.093	1.119

According to these figures, the SSI tends to increase the inter-storey drift of the superstructure in the y-direction and reduce it in the x-direction. This variation is best observed on the models of height h=25.675 m. In the y-direction, the inter-storey drift increases by about 1.8% and 4.7% respectively for the models of height 31.675 m on wet clay and embankment of humus, sand and gravel. on the other hand, it decreases in the x-direction by about 0.29% and 1.4% in

the same order as before compared to the fixed base model. the same phenomenon is observed for the models with height h=25.675 m but with much higher percentage reduction.

Thus, soil interaction can, depending on the characteristics of the structure and the soil, reduce or increase the inter-storey drift. its impact can vary depending on the height of the structure.

3.5.3.4. Base shear

The base shear which represents the total lateral seismic force is given for different base conditions for both axes in Table 3.31. The base shear for the two axes is given for different base conditions in Table 3.40. To show the difference between the base shear of each model, the diagrams in Figure 3.83 are plotted

Table 3.43. Base shear computed from response spectrum

Shear base (kN)			
	Wet clay	Embankment of humus, sand and gravel	Fixed base
X	11927.319	20304.009	9238.189
Y	46124.138	52605.389	42069.906

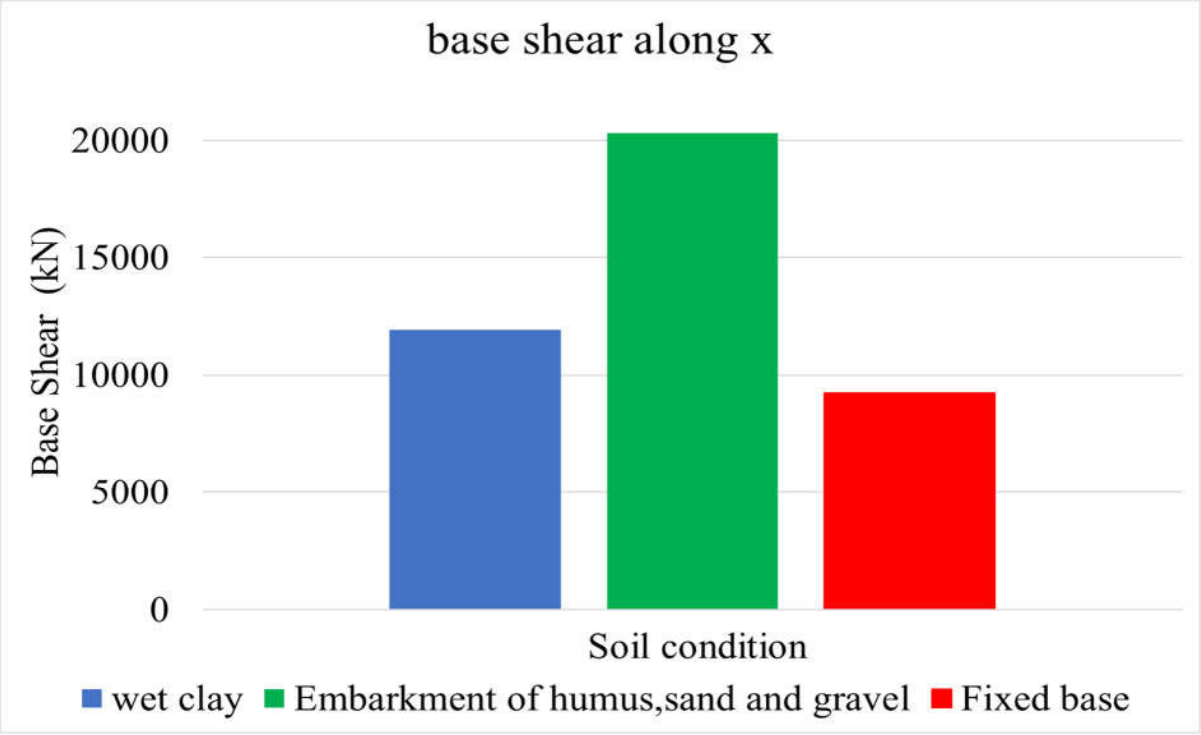

(a)

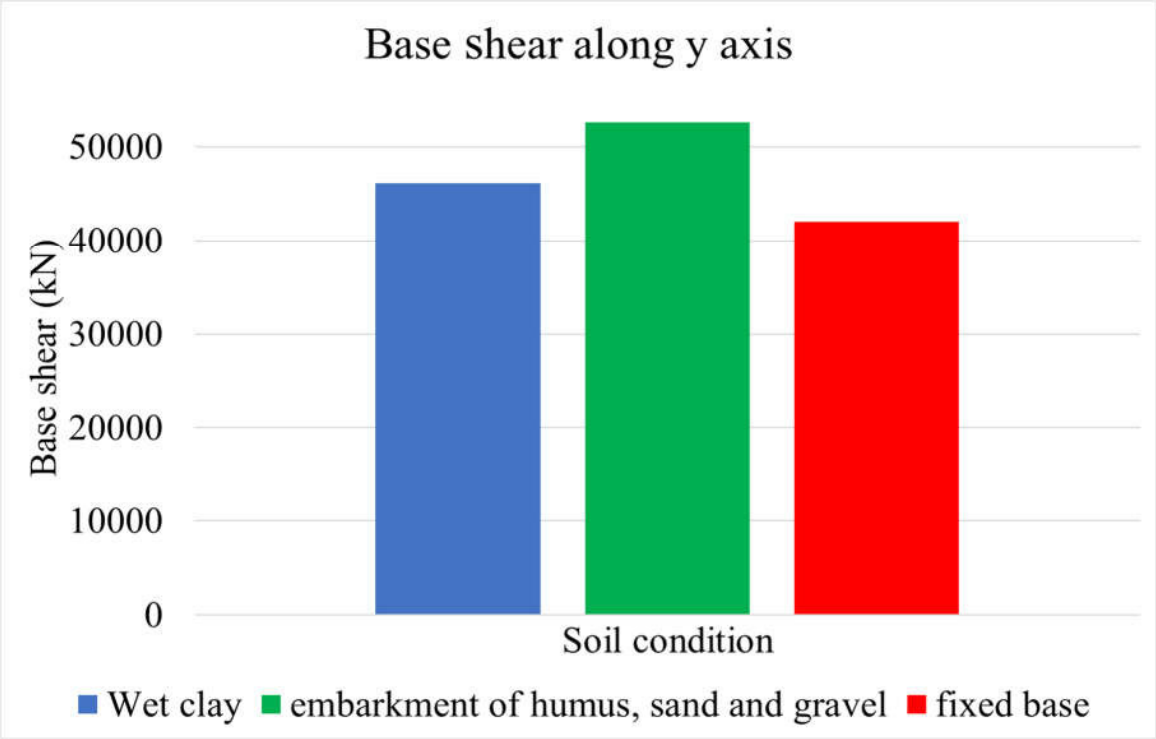

(b)

Figure 3.83. Shear base for the structure with h= 31.675 m resting on different soil type in the: (a) x-axis and (b) y-axis

From the comparative study carried out, it was observed that the ratio of the differences between the SSI numerical cases and the fixed base cases for the shear of are about 29,11% and 119% in x direction, 9.94 % and 25 % in y direction for the structure resting on wet clay, an embankment of humus, sand and gravel. Thus, according to the results of the current study, it can be concluded that the fixed base concept underestimates the response of structures based on these types of soil profiles under dynamic loading.

As the total base shear increases with the flexibility of the soil, this can lead to overloading and subsequent failure of structural elements. to avoid such situations, it is necessary to choose structural systems that are adapted to the anticipated forces.

3.5.3.5. New solicitation on the structure

As done previously with the static analysis, the new stresses on the structure are determined under seismic action and presented in the figures 3.84 and 3.85

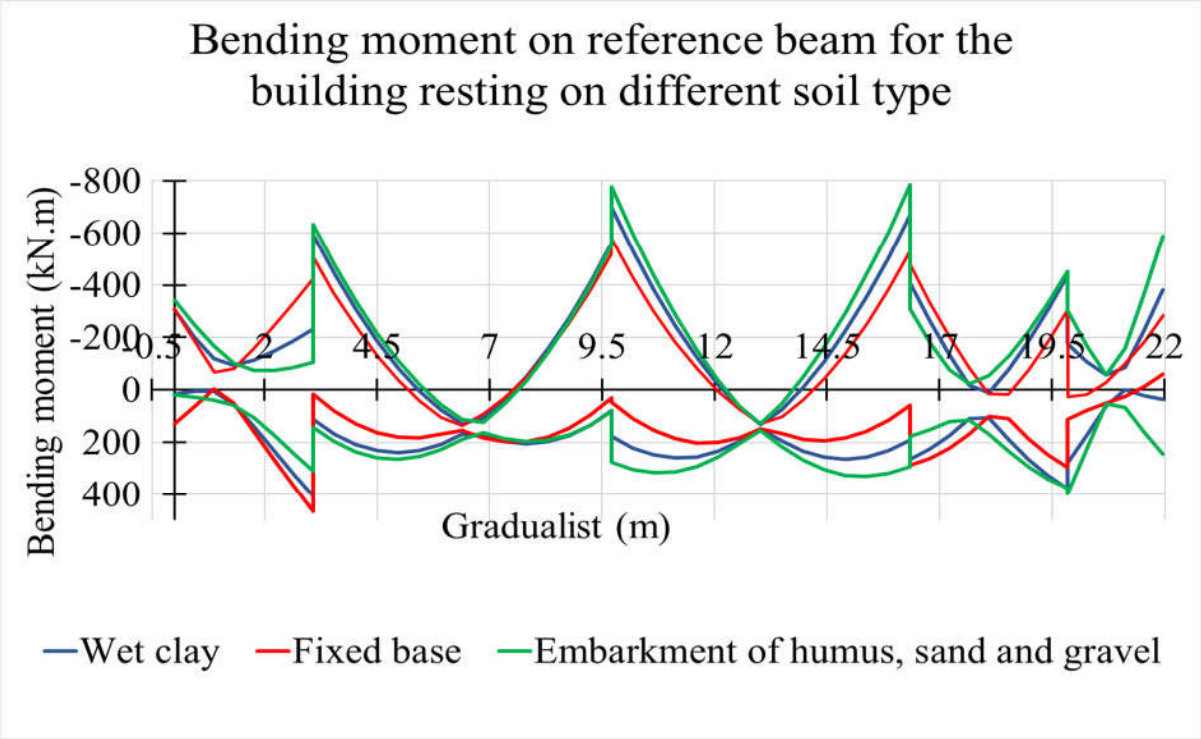

Figure 3.84. new bending moment curves on the reference beam of the structure resting on different soil types

As in section 3.4, figure 3.84 shows that the bending moment in this beam increases with the flexibility of the soil but in an even more pronounced way.

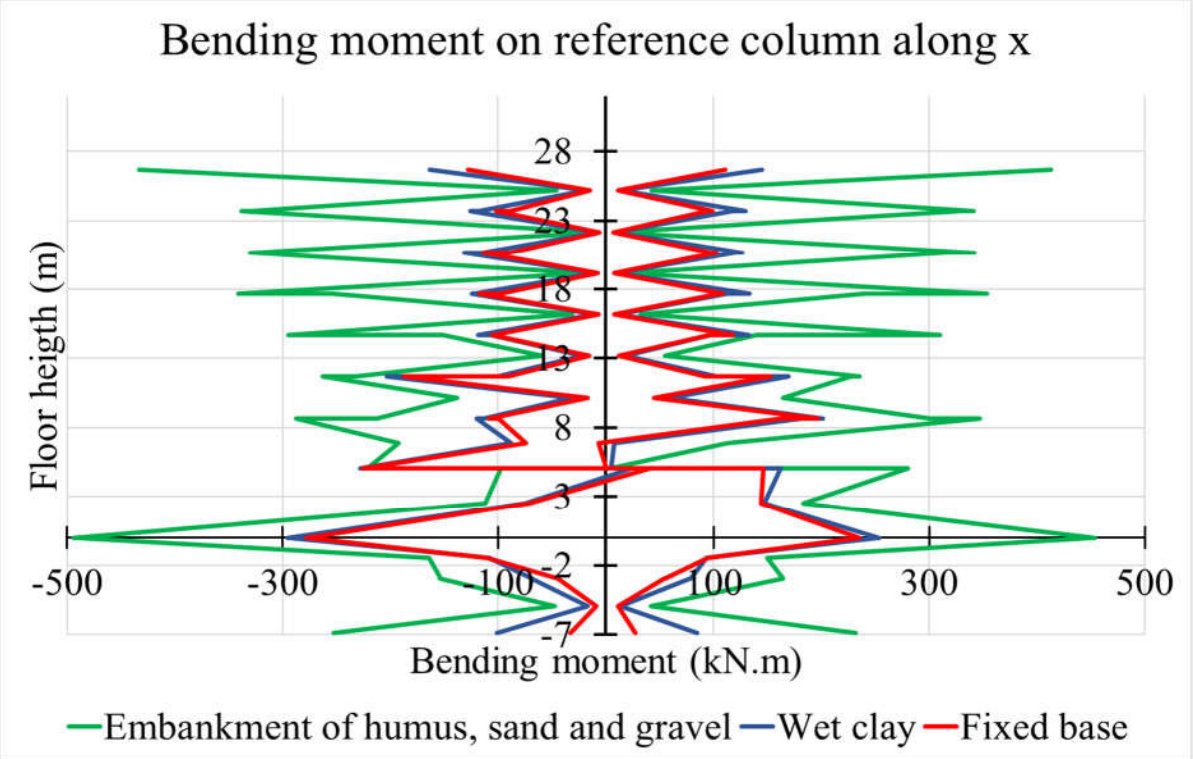

(a)

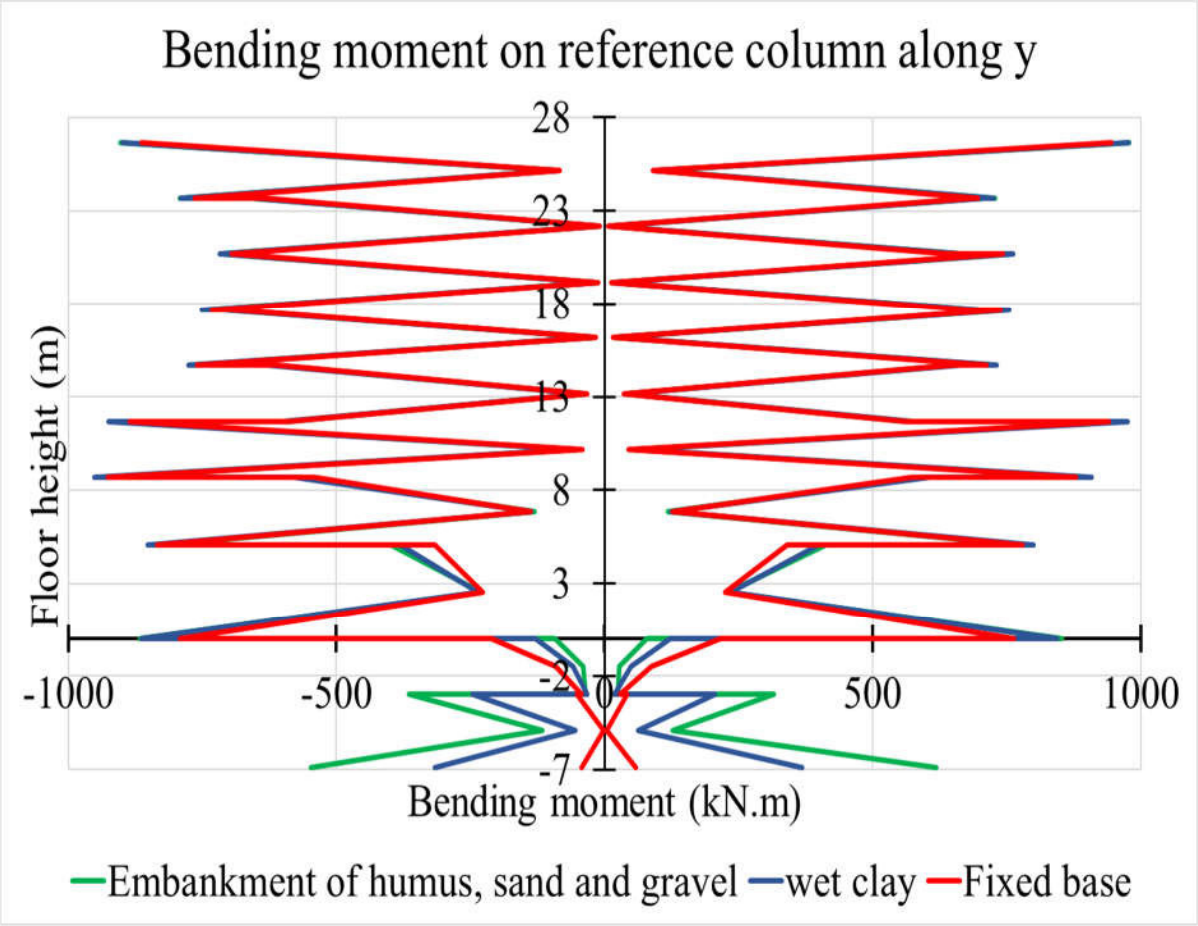

(b)

Figure 3.85. Bending moment on the reference column of the structure in :(a) in x-axis and (b) y-axis

Like the beam, Figure 3.85 shows that the bending moment in the column also increases with soil flexibility

Conclusion

The objective of this chapter was to present the case study, to carry out the analysis and design of the structural elements and to evaluate its behavior under static and dynamic action by varying its height and considering different types of soil. Finally, we obtain a section of 70 cm in height and 35 cm in width for the reference beam, a rectangular section of 50x80 cm for the most solicited column in the basement. The retaining wall of the designed retaining wall, which supports the lateral earth thrusts, is 40 cm thick. The foundation was designed as a raft foundation with reinforcing beams. The analysis of the building is done with a fixed base and an invert foundation, modelled according to the Winkler model where the soil is represented by

springs of stiffness Ks equivalent to the modulus of the soil reaction enabling in fact to simulate the elastic behavior of the soil. Following the results obtained, it was shown that the fixed base model minimizes the period of vibration of the structure, the lateral displacements, and the shear at the base compared to the flexible base models. It is also noted that, the solicitation also varies with the flexibility of the soil and are much more important in the structures resting on soft soils.

GENERAL CONCLUSION

The aim of this work was to show the influence of soil-structure interaction in the static and dynamic design of a mid-rise concrete structure. This study was first conducted through a literature review on soil-structure interaction, mid-rise structures, and dimensioning methods Subsequently, the methodology for the analysis and design of the structural and foundation elements was presented. The comparative criteria of the different models studied were also defined for the static and dynamic analysis. Following this methodology, a 4-storey plus mezzanine building with two basements that was raised to 6-storeys was studied. Six models were analyzed, two of which were on a fixed basis and the other four on a flexible basis. The analysis was carried out using the SAP 2000 software. The results obtained from the analysis revealed that (1) SSI Taking into account the flexibility of the soil increases the stresses in the structural elements, except for the axial force, which increases with the stiffness. This increase is amplified under dynamic action. (2) The SSI provides information on foundation deformations depending on the nature of the soil and the characteristics of the superstructure. (3) The SSI amplifies the lateral deflection of the building, and this amplification is inversely proportional to the stiffness of the ground in the sense that a soft ground gives the greatest value. This impact is also a function of the height of the structure given that the stiffness varies with the height and is amplified by the flexibility provided by the SSI. This work has drawbacks related to the neglect of the damping coefficient of the springs representing the soil and the assumption of linear behavior of the soil and the superstructure. To ensure continuity in the research, it is suggested to adopt a global analysis method where the soil is modelled as a solid finite element. It is also suggested to evaluate the impact of the damping of the soil-foundation system on the behaviour factor.

BIBLIOGRAPHY

BOOKS AND ARTICLE

Aubry, D. (1986). Sur une approche intégrée de l'interaction sismique sol-structure, journées communes fondations, propriétés des sols et impératifs sismiques, cfms-afps. *Revue française de Géotechnique, Presses ENPC(ed.), Paris*, pages 81–100.

Baumann, P. (1935). Analysis of sheet-pile bulkheads, Trans. ASCE, Vol. 100, pp. 707-797

Bielak, J. (1974). Dynamic behaviour of structures with pile-supported foundations. In *6th World Conference on Earthquake Engineering* (Vol. 3, Issue March 1974).

CEN. (2005). *Eurocode 8 : Calcul des structures pour leur résistance aux séismes. Partie 3 : Evaluation et renforcement des bâtiments. NF EN 1998-3, Bruxelles*. *33*(0).

Delattre, L. (2000). Un siécle d'écrans de souténements revue bibliographique sur l'évolution des techniques. *Bulletin Des Laboratoires Des Ponts et Chaussees*, *227*, 51–61.

Elan, L. (2018). # *LoiElan*. 1–12.

Filonenko-Borodich, M. M. (1940). *Some approximate theories of elastic foundation*. Uchenyie Zapiski Moskovskogo Gosudarstvennogo Universiteta. Mekhanica, 46, 3–18 (in Russian).

Forni, M. (sd). Fondations spéciales et reprise en sous-oeuvre. Eyrolles.

Gcr, N. (n.d.). *Soil-Structure Interaction for Building Structures*.

Ghalimath, A. G., A, M. S., A, H. M., A, J. C., & Solapur, A. G. P. I. T. (2015). *Analytical Approaches for Soil Structure Interaction*. 595–600.

Grange, S. (2008). *Modélisation simplifiée 3D de l ' interaction sol-structure : application au génie parasismique . To cite this version : HAL Id : tel-00306842 par Modélisation simplifiée 3D de l ' interaction sol-structure : application au génie parasismique Directeur de*.

Hetenyi, I. M. (1946). *Beam on Elastic Foundation*.

Housner, G. . (1955). DYNAMIC PRESSURES ON A C C E L E R A T E D F L U I D CONTAINERS By G. W. I-IovsI~'ER. *Bulletin of the Seismological Society of America*, 15–35.

Jeremi, B. (2004). *Soil – Foundation – Structure Interaction Simulations : Static and Dynamic Issues*. *May*, 1–45.

kerr. (1964). *A Study of a N e w Foundation Model* (Issue l).

Kramer, S. L. (1996). Geotechnical Earthquake Engineering. New Jersey, USA: Prentice Hall

Murugananthan, U. (2018). *IMPACT DE L ' INTERACTION SOL-STRUCTURE SUR LA CONCEPTION DES FONDATIONS SUPERFICIELLES DES CADRES CONCENTRIQUES EN ACIER*. *Génie Civil*.

NIST. (2012). *Soil-Structure Interaction for building structures.* USA: NEHRP Consultants JointVenture.

Pecker, A. (1984). *Dynamique des sols*. Presse, ENPC, Paris, France.

Poh'sie*, D. E. G. H., Guabiapsie, E. L. K. G., Nathou, E. G. L. D., Cardillo, E. G., & Majorana, P. C. (2021). Finite Element Method Analysis Applied to Different Foundations Structures Systems. *International Journal of Innovative Science and Modern Engineering*, *7*(3), 18–24. https://doi.org/10.35940/ijisme.c1289.087321

Section 3_ Performance Standards for Mid-Rise Buildings.pdf. (n.d.).

Stewart, J. P., Fenves, G. L., & Seed, R. B. (1999). Seismic Soil-Structure Interaction in Buildings. I: Analytical Methods. *Journal of Geotechnical and Geoenvironmental Engineering*, *125*(1), 26–37. https://doi.org/10.1061/(asce)1090-0241(1999)125:1(26)

Terzaghi, K. (1955). Evaluation of coefficients of subgrade reaction. *Geotechnique*, *5*(4), 297–326. https://doi.org/10.1680/geot.1955.5.4.297

Uildings, B., Stewart, B. J. P., Seed, R. B., & Fenves, G. L. (1999). *seismic s oil -s tructure i nteraction ii : e mpirical f indings in*. *January*, 38–48.

Veletsos, A. S. and Meek, J. W. (1974). Dynamic behavior of building-foundation systems. *Journal of earthquake engineering structure dynamics*, 3(2) :121–138

Wolf, J. P. (1989). Soil-structure-interaction analysis in time domain. *Nuclear Engineering and Design*, *111*(3), 381–393. https://doi.org/10.1016/0029-5493(89)90249-5

Zhang, X. (2012). *Modélisation physique et numérique des interactions sol-structure sous sollicitations dynamiques transverses To cite this version : HAL Id : tel-00767071 Modélisation physique et numérique des interactions sol- structure sous sollicitations*

dynamiques.

NORMS

Comité Européen de Normalisation. (2002). *Eurocode 0: Basis of structural design. Norm EN 1990.* Brussels: Comité Européen de Normalisation.

Comité Européen de Normalisation. (2002). *Eurocode 1: Actions on structures. Norm EN 1991.* Brussels: Comité Européen de Normalisation.

Comité Européen de Normalisation. (2002). *Eurocode 2: Design of concrete structures. Norm EN 1992.* Brussels: Comité Européen de Normalisation.

Comité Européen de Normalisation. (2002). *Eurocode 7: Geotechnical design. Norm EN 1997.* Brussels: Comité Européen de Normalisation.

Comité Européen de Normalisation. (2002). *Eurocode 8: Design of structures for earthquake resistance.* Brussels: Comité Européen de Normalisation.

THESIS

Moustapha Housseni. (2019). Influence of foundation type on the seismic response of buildings considering soil-structure interaction. *(Master Thesis). National Advanced School of Public Works.*

Djeukoua Nathou, G. L. (2019). *Compartive analysis of seismic protection system.(Master Thesis).* National Adavanced School of Public Works.

WEBOGRAPHY

https://scholar.google.com/scholar (Consuld on 18/06/22)

https://www.scirp.org (Consuld on 18/06/22)

ANNEXES

ANNEX A: Tables for the methodology

Table A1. Imposed loads on floors, balconies and stairs in buildings (EC 1 Part 1)

Categories of loaded areas	q_k [kN/m²]	Q_k [kN]
Category A		
- Floors	1,5 to2,0	2,0 to 3,0
- Stairs	2,0 to4,0	2,0 to 4,0
- Balconies	2,5 to 4,0	2,0 to 3,0
Category B	2,0 to 3,0	1,5 to 4,5
Category C		
- C1	2,0 to 3,0	3,0 to 4,0
- C2	3,0 to 4,0	2,5 to 7,0 (4,0)
- C3	3,0 to 5,0	4,0 to 7,0
- C4	4,5 to 5,0	3,5 to 7,0
- C5	5,0 to 7,5	3,5 to 4,5
category D		
- D1	4,0 to 5,0	3,5 to 7,0 (4,0)
- D2	4,0 to 5,0	3,5 to 7,0

Table A2. Recommended values of Ψ factors for buildings (EC 0 Part 1)

Action	ψ_0	ψ_1	ψ_2
Imposed loads in buildings, category (see EN 1991-1-1)			
Category A : domestic, residential areas	0,7	0,5	0,3
Category B : office areas	0,7	0,5	0,3
Category C : congregation areas	0,7	0,7	0,6
Category D : shopping areas	0,7	0,7	0,6
Category E : storage areas	1,0	0,9	0,8
Category F : traffic area, vehicle weight ≤ 30kN	0,7	0,7	0,6
Category G : traffic area, 30kN < vehicle weight ≤ 160kN	0,7	0,5	0,3
Category H : roofs	0	0	0
Snow loads on buildings (see EN 1991-1-3)*			
Finland, Iceland, Norway, Sweden	0,70	0,50	0,20
Remainder of CEN Member States, for sites located at altitude H > 1000 m a.s.l.	0,70	0,50	0,20
Remainder of CEN Member States, for sites located at altitude H ≤ 1000 m a.s.l.	0,50	0,20	0
Wind loads on buildings (see EN 1991-1-4)	0,6	0,2	0
Temperature (non-fire) in buildings (see EN 1991-1-5)	0,6	0,5	0
NOTE The ψ values may be set by the National annex. * For countries not mentioned below, see relevant local conditions.			

Table A3. Values of Minimum cover, $C_{min,dur}$, requirements with regard to durability for reinforcement steel (EC2)

Environmental Requirement for $c_{min,dur}$ (mm)							
Structural Class	**Exposure Class according to Table 4.1**						
	X0	XC1	XC2 / XC3	XC4	XD1 / XS1	XD2 / XS2	XD3 / XS3
S1	10	10	10	15	20	25	30
S2	10	10	15	20	25	30	35
S3	10	10	20	25	30	35	40
S4	10	15	25	30	35	40	45
S5	15	20	30	35	40	45	50
S6	20	25	35	40	45	50	55

Table A5. Values of subgrade modulus for different soil types (Forni, sd)

	Nature du sol	*C* (t/m³)
1	terrain légèrement tourbeux et marécageux	500- 1 000
2	terrain essentiellement tourbeux et marécageux	1 000- 1 500
3	sable fin	1 000- 1 500
4	remblais d'humus, sable et gravier	1 000- 2 000
5	sol argileux détrempé	2 000- 3 000
6	sol argileux humide	4 000- 5 000
7	sol argileux sec	6 000- 8 000
8	sol argileux très sec	10 000
9	terrain compacté contenant de l'humus du sable et peu de pierres	8 000-10 000
10	même nature que ci-dessus avec beaucoup de pierres	10 000-12 000
11	gravier fin et beaucoup de sable fin	8 000-10 000
12	gravier moyen et sable fin	10 000-12 000
13	gravier moyen et sable grossier	12 000-15 000
14	gros gravier et sable grossier	15 000-20 000
15	gros gravier et peu de sable	15 000-20 000
16	gros gravier et peu de sable mais très compacté	20 000-25 000

ANNEX B: Architectural plans of the building

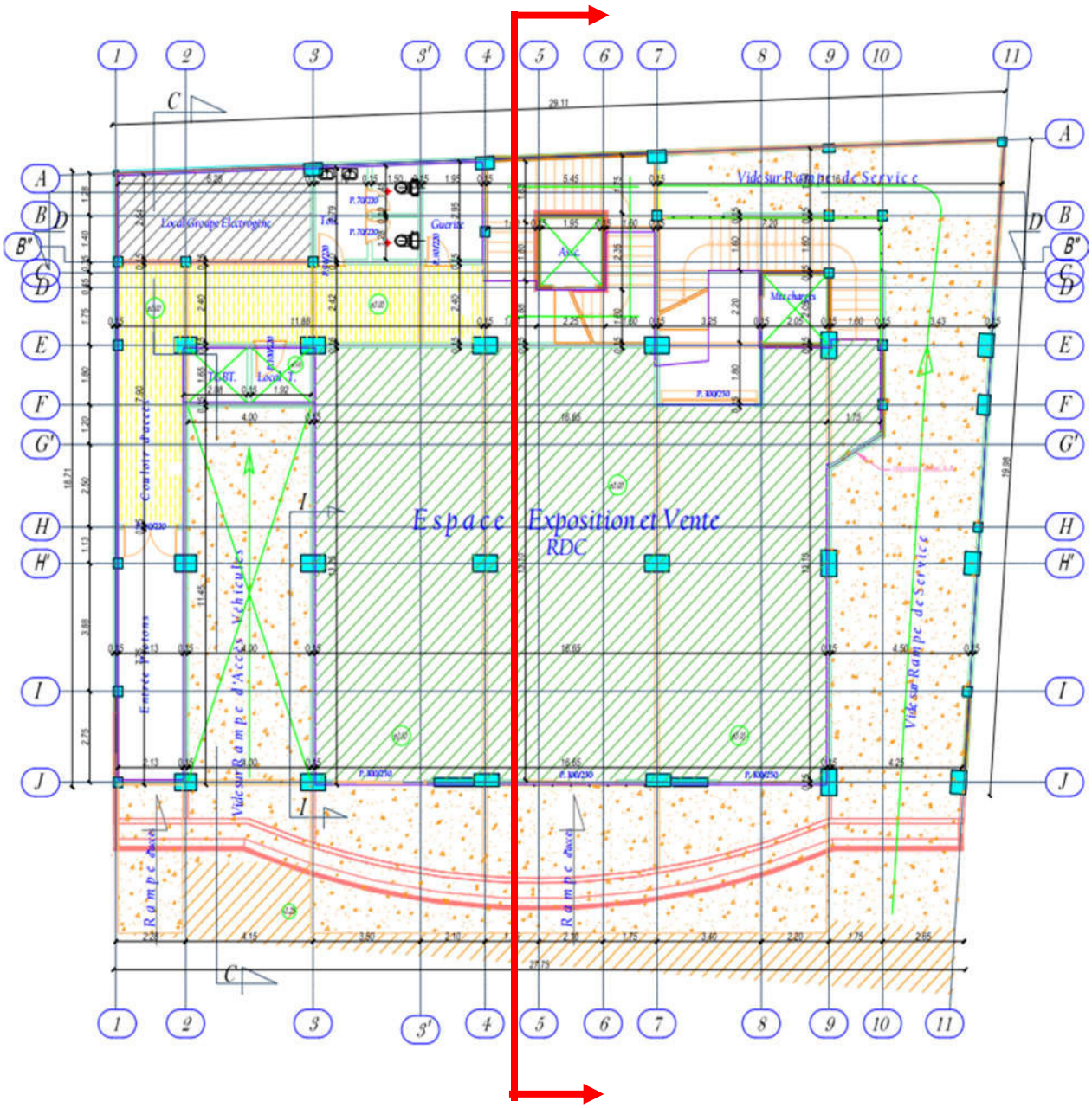

Ground floor

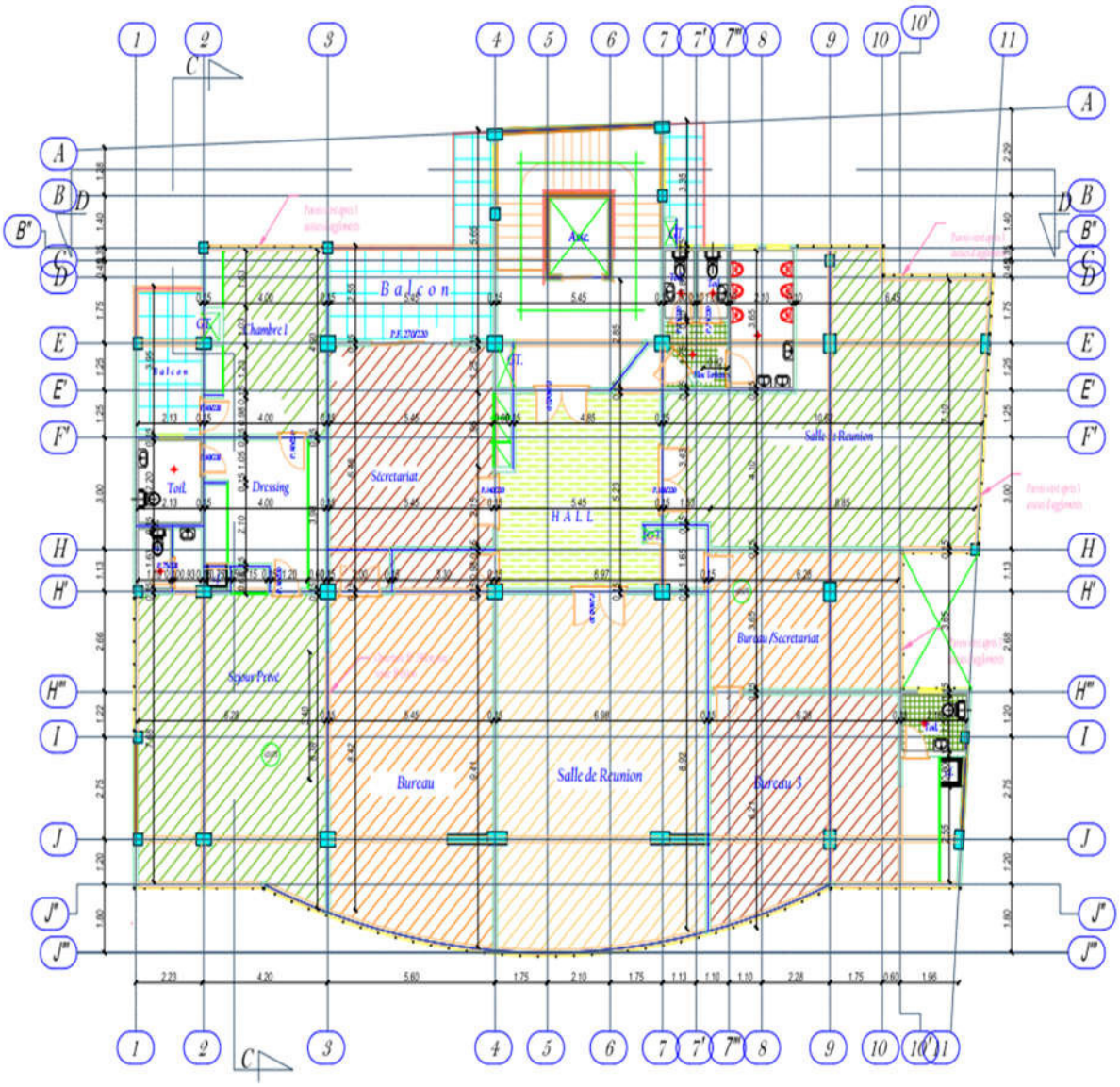
Balcon
Chambre I
Dressing
Secretariat
HALL
Salle de Reunion
Bureau
Bureau Secretariat
Bureau 3
Salle de Reunion
Asc.

Storey 5

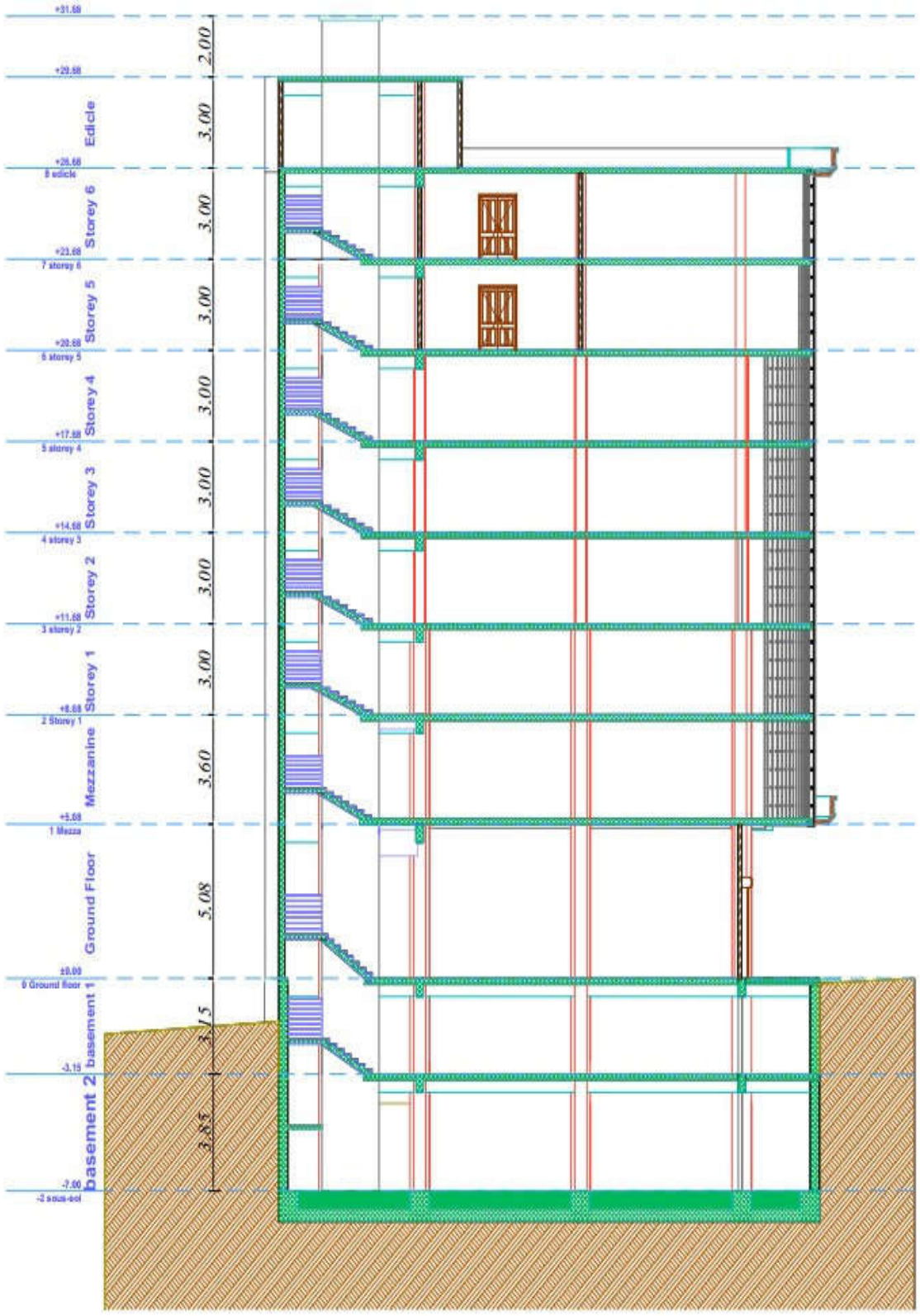

Cross-section of the building

Annex C: Detailing of structural elements

ANNEX C1: Detailing of the beam

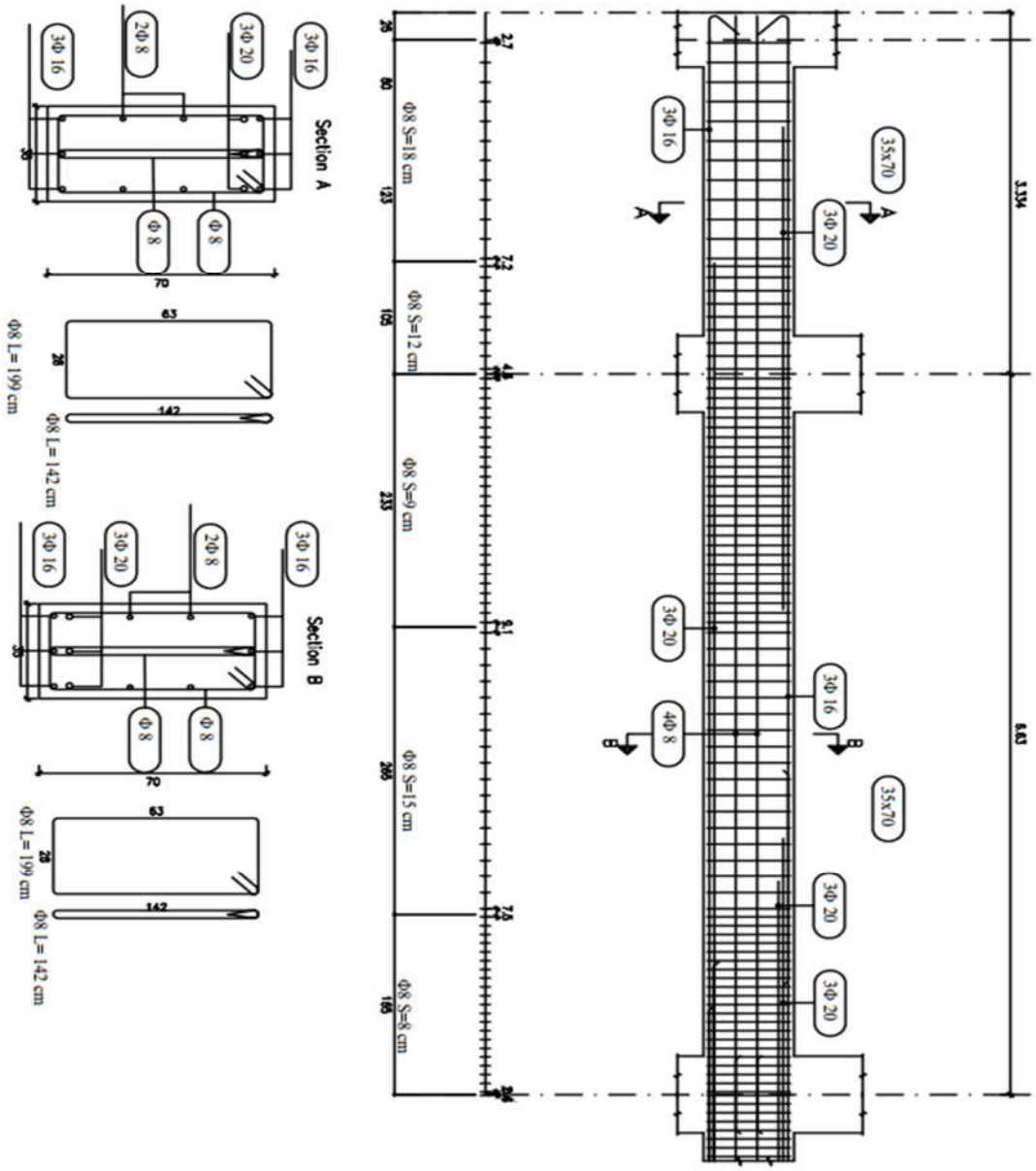

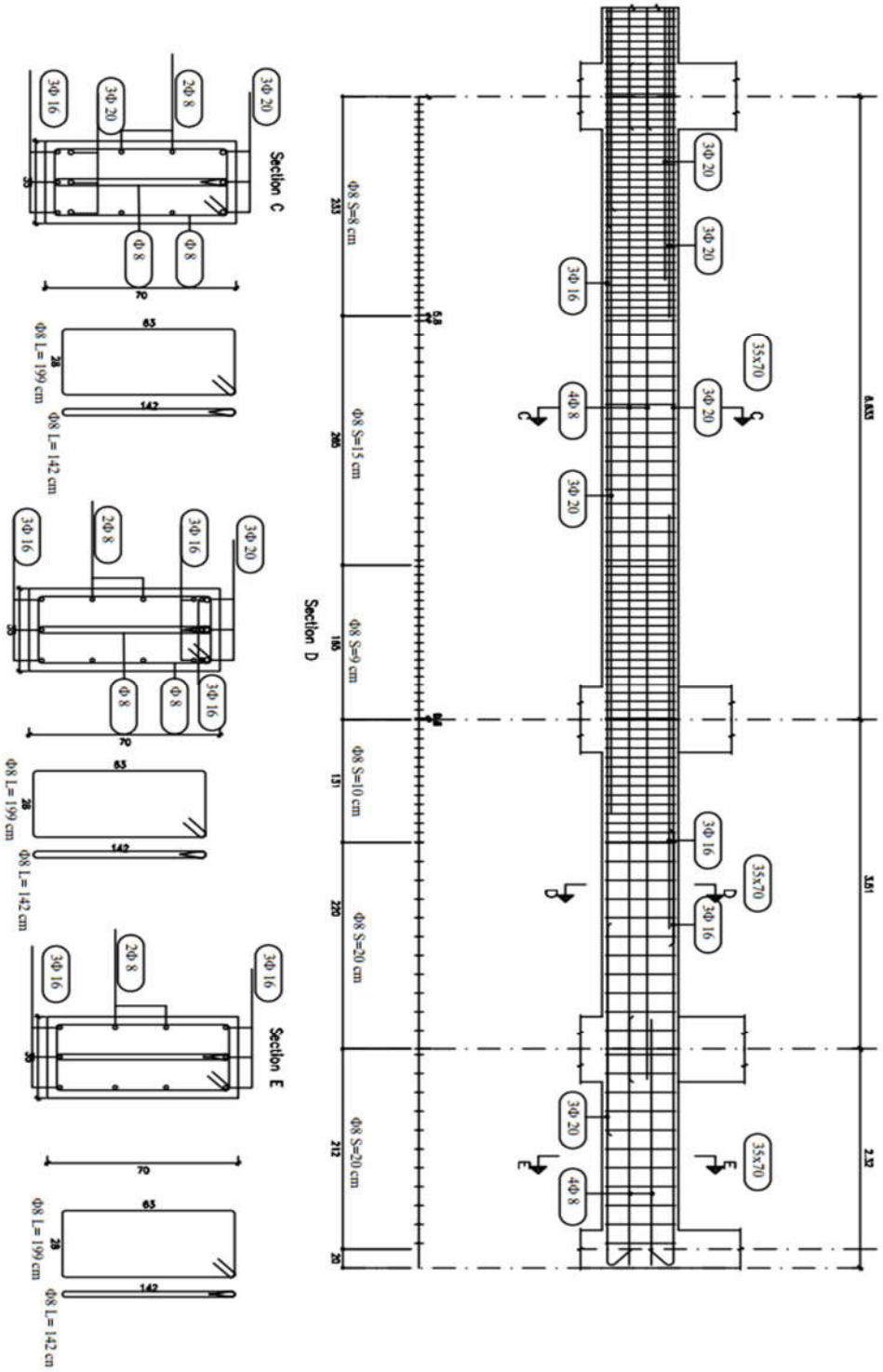

Annexe C2. Detailing of the column P1 and P2 at basement 2

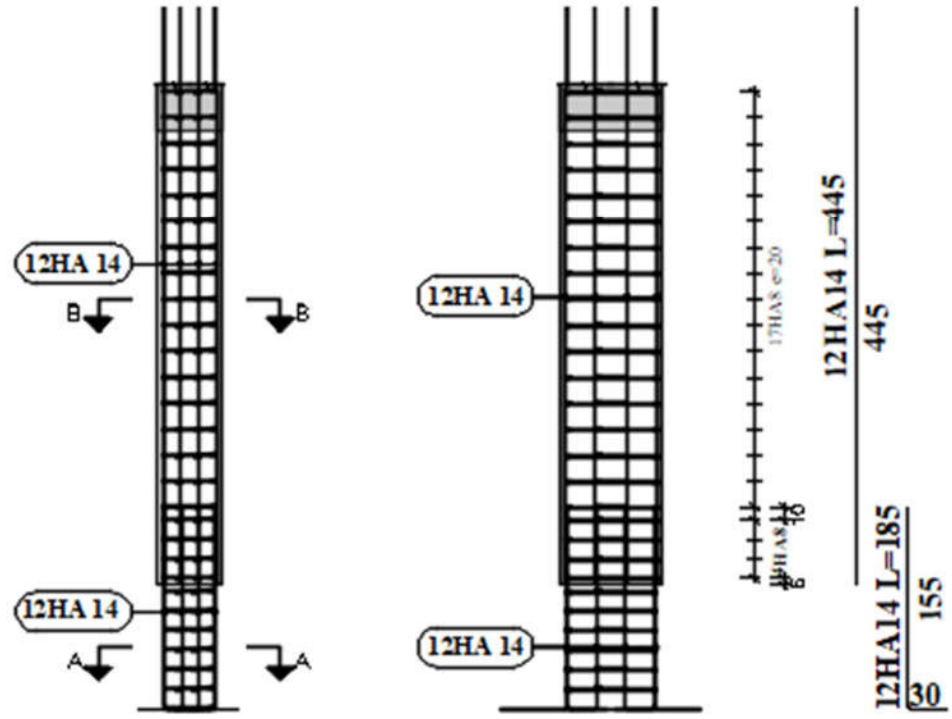
12HA 14
B
B
12HA 14
A
A
12HA 14
12HA 14
12HA14 L=445
445
12HA14 L=185
155
30

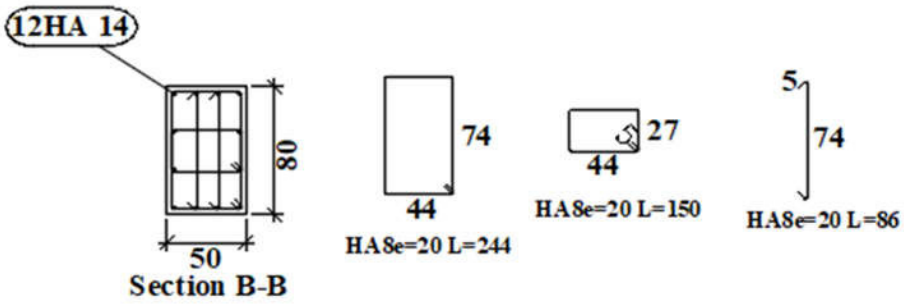
12HA 14
80
50
Section B-B
74
44
HA8e=20 L=244
27
44
HA8e=20 L=150
5
74
HA8e=20 L=86

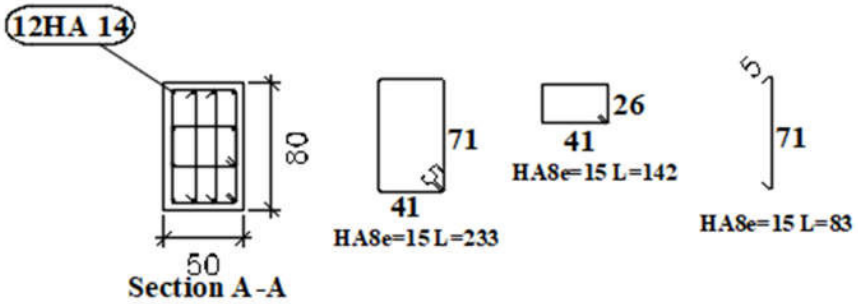
12HA 14
80
50
Section A-A
71
41
HA8e=15 L=233
26
41
HA8e=15 L=142
5
71
HA8e=15 L=83

Annexe C2. Detailing of Foundation